DISS. ETH NO. 24264

N-LINKED PROTEIN GLYCOSYLATION
Functional characterization of the eukaryotic oligosaccharyltransferases

A thesis submitted to attain the degree of

DOCTOR OF SCIENCES of ETH ZURICH

(Dr.sc. ETH Zurich)

presented by

KRISTINA POLJAK

MSc. in Molecular Biology, University of Zagreb, Croatia

MSc. in Bioindustrial Techniques, University of Orleans, France

born on 04.11.1987

citizen of Republic of Croatia

accepted on the recommendation of

Prof. Dr. Markus Aebi

Prof. Dr. Kaspar Locher

Prof. Dr. Yves Barral

2017

Acknowledgements

First and foremost, I would like to thank my thesis supervisor Prof. Dr. Markus Aebi for opening the doors of ETH Zurich by offering me an internship followed by an encouragement to do my PhD in his group as well. Not only could I profit highly from his guidance and extensive knowledge but I also appreciated greatly the freedom I enjoyed in pursuing the research described in this thesis as I saw fit.

I thank the members of my PhD committee, Prof. Dr. Kaspar Locher, Prof. Dr. Yves Barral and Prof. Dr. Reid Gilmore, for fruitful discussions and useful input into my research during our yearly meetings. I am especially thankful to Prof. Dr. Yves Barral and his group members for experimental support and providing valuable expertise when my experiments asked for it.

I would also like to thank all current and former members of the Aebi group for their help, discussions and generally a nice working atmosphere. Special thanks go to Elsy, Martina, Nathalie, Susanna and Julia for sharing the good and less good experiences throughout our joint time in the lab, Dr. Robert Gauss for his input and good discussions, Dr. Jörg Breitling for entrusting his *Trypanosoma brucei STT3* project to me, and Carole Grädel for the hard work during her semester project.

I owe gratitude to the Functional Genomics Center Zurich members, especially Dr. Nathalie Selevsek who taught me everything I know about mass spectrometry, patiently answered all my questions and supported me during the last two years of my thesis.

I would like to thank Melina, for her support, patience and understanding during difficult times and her cheers during the good ones. You indebt me to always be the best version of myself and I will always be grateful for that. Special thanks goes to my brother Mirko, who has never seized to amaze me ever since we were kids. Thank you for making me grow up with a love of science, you were and always will be an inspiration.

My deepest gratitude goes to the most basic source of my life, my parents to whom I dedicate this thesis. Their support and love has been unconditional, they have given up many things for me to be at ETH Zurich and I would like to thank them in Croatian now.

Dragi roditelji, dugujem vam svoju najdublju zahvalnost na ljubavi, razumijevanju i svakodnevnim odricanjima kroz koje ste omogućili ovaj rad kojeg posvećujem vama. Hvala vam na bezgraničnom ponosu i pouzdanju na mom putu od prvoškolske klupe do doktorata znanosti. Vaša bezuvjetna ljubav i podrška su me pratili u svim trenucima i bez vas sigurno ne bih bila tu gdje jesam. Volim vas puno.

Table of Contents

Summary

N-linked protein glycosylation is a highly conserved and an essential protein modification found throughout the three domains of life. In animal, plants and fungi the preassembled oligosaccharide consisting of two N-acetylglucosamines, nine mannoses and three glucoses is transferred *en bloc* from the lipid carrier to the asparagine side chains within N-X-S/T consensus sequences on nascent polypeptides in the lumen of the endoplasmic reticulum (ER). This transfer is catalysed by the central enzyme of the pathway, oligosaccharyltransferase (OST). After the transfer, the oligosaccharide is modified in a species, tissue and cell-specific manner, resulting in a vast array of different glycan structures.

The first chapter of this thesis offers an overview of the N-linked protein glycosylation pathway. The biosynthesis of the lipid-linked oligosaccharide (LLO) is described first followed by the description of the OST and the biological relevance of this modification. Furthermore, diverse analytical tools and methods used to help explore and characterize the pathway, with the emphasis on the quantitative mass spectrometric approaches, are discussed.

In the second chapter, we coupled parallel reaction monitoring (PRM) mass spectrometry method to stable isotope labelling (SILAC) to measure N-linked glycosylation occupancy of yeast glycoproteins. The OST from yeast *Saccharomyces cerevisiae* is a multi-subunit protein complex. Using our SILAC-PRM method, we further explored the roles of the two non-essential OST subunits, Ost3p and Ost6p, and provided insights into the mechanisms that regulate site-specific N-glycosylation by the OST.

The investigation of the substrate specificity of the single subunit OSTs from *Trypanosoma brucei* is reported in chapter three. The effect of different oligosaccharide substrate structures on the function of *Tb*OSTs was studied in yeast using genetic manipulations of the LLO biosynthesis. Additionally, structure to function coupled to SILAC-PRM analyses were performed to identify regions in the OST proteins that influence the specificity of different paralogues for the LLO as well as for the polypeptide substrate.

In order to functionally characterize WBP1, an essential subunit of yeast OST, we performed a mutagenesis study reported in the fourth chapter. We have used reverse genetics approach for generating point mutations in the conserved residues of Wbp1p and identified novel mutants that alter glycosylation by influencing complex assembly.

Concluding remarks and future perspectives complete the thesis in the fifth chapter.

Zusammenfassung

Die Glykosylierung von Asparaginen ist eine hoch konservierte und essentielle Modifikation von Proteinen, die in allen Domänen des Lebens gefunden wird. In Tieren, Pflanzen und Pilzen wird das zuvor gebildete Oligosaccharid, bestehend aus zwei N-Acetylglukosaminen, neun Mannosen und drei Glukosen, vom Lipidträger zu den Asparagin Seitenketten in N-X-S/T Sequenzmotiven auf Polypeptide im Lumen des Endoplasmatischen Retikulums (ER) übertragen. Diese Übertragung wird durch das zentrale Enzym der Asparagin-gebundenen Proteinglykosylierung, Oligosaccharyltransferase (OST) katalysiert. Nach der Übertragung wird das Oligosaccharid in einer spezies-, gewebe- und zell-spezifischen Weise modifiziert, was zu einer Vielzahl unterschiedlicher Glykanstrukturen führt.

Das erste Kapitel dieser Doktorarbeit bietet einen Überblick über die Asparagin-gebundene Proteinglykosylierung. Die Biosynthese des lipidgebundenen Oligosaccharids (LLO) wird zuerst geschildert, gefolgt von der Beschreibung der OST und der biologischen Relevanz dieser Modifikation. Darüber hinaus werden diverse analytische Instrumente und Methoden zur Erforschung und Charakterisierung der Asparagin-gebundenen Proteinglykosylierung diskutiert, mit Schwerpunkt der verschiedenen quantitativen Massenspektrometrie-Methoden.

Im zweiten Kapitel koppelten wir stabile Isotopen-Markierung von Aminosäuren in Zellkultur (SILAC) mit einer parallelen Reaktions-Monitoring (PRM) Methode, um die N-Glykosylierung von Hefe-glykoproteinen zu messen. Die OST der Hefe *Saccharomyces cerevisiae* ist ein Proteinkomplex mit mehreren Untereinheiten. Mit unserer SILAC-PRM Methode haben wir die Rollen der beiden nicht-katalytischen OST-Untereinheiten Ost3p und Ost6p weiter untersucht und Einblicke in die Mechanismen gegeben, welche die ortsspezifische N-Glycosylierung durch die OST regulieren.

Die Untersuchung der Substratsspezifität der einzelnen Untereinheiten der OSTs von *Trypanosoma brucei* wird in Kapitel drei beschrieben. Die Wirkung unterschiedlicher Oligosaccharid-strukturen auf die Funktion von *Tb*OSTs wurde in Hefe unter Verwendung genetischer Manipulationen der LLO-Biosynthese untersucht. Zusätzlich wurden Struktur und Funktionsanalysen, gekoppelt mit SILAC-PRM Analysen durchgeführt, um Bereiche in den OST-Proteinen zu identifizieren, die die Spezifität der verschiedenen Paralogen für das LLO sowie für das Polypeptidsubstrat beeinflussen.

Um WBP1, eine essenzielle Untereinheit der Hefe OST, funktionell zu charakterisieren, haben wir im vierten Kapitel eine Mutagenesestudie durchgeführt. Wir haben einen reversen Genetik-Ansatz zur Erzeugung von Punktmutationen in den konservierten Resten von Wbp1p verwendet und neue Allelen identifiziert, die die Glykosylierung durch Beeinflussung des OST Aufbaus verändern.

Schlussbemerkungen und Zukunftsperspektiven vervollständigen die Dissertation im fünften Kapitel.

Abbreviations

OST	oligosaccharyltransferase
LLO	lipid-linked oligosaccharide
Dol	dolichol
P	phosphate
PP	pyrophophate
Hex	hexose
HexNAc	N-acetylhexosamine
Glc	glucose
Gal	galactose
Man	mannose
GlcNAc	N-acetylglucosamine
EndoH	endo-β-N-acetylglucosaminidase
SRM	selected reaction monitoring
PRM	parallel reaction monitoring
SILAC	stable isotope labelling with amino acids in cell culture
HPLC	high-pressure liquid chromatography

Chapter 1

Introduction to N-linked Protein Glycosylation

1. Lipid linked oligosaccharide biosynthesis

N-linked glycosylation is a highly conserved posttranslational modification of proteins. The initial steps of N-linked protein glycosylation are carried out on the endoplasmic reticulum (ER) membrane in eukaryotes and periplasmic membrane in archaea and bacteria. The assembly of the lipid linked oligosaccharide (LLO) is the first step of N-linked glycosylation followed by the transfer of the oligosaccharide to the dedicated asparagine residues of nascent polypeptides in the ER. The LLO assembly is characterized by the use of dolichyl-pyrophosphate (Dol-PP) as a carrier for oligosaccharide assembly and the bipartite localisation of the pathway. The process is catalysed by a panel of membrane-bound glycosyltransferases belonging to the *ALG* family (asparagine-linked-glycosylation) leading to the assembly of a Dol-PP-linked precursor oligosaccharide. The LLO assembly is initiated at the cytoplasmic side of the ER membrane and only after the LLO intermediate has been flipped, continues at the lumenal side (Helenius & Aebi 2004; Breitling & Aebi 2013)(Figure 1).

1.1. Lipid carrier

The LLO biosynthesis is characterized by the participation of a special carrier lipid dolichol that belongs to a group of polyisoprenoid molecules with a saturated α-isoprene unit. The initial steps in dolichol biosynthesis are the same as for sterols and ubiquinones and start with the mevalonic acid pathway (Chojnacki & Dallner 1988). A precisely coordinated mechanism regulates the biosynthesis of the mevalonic acid pathway intermediates that are precursors in biosynthesis of many essential molecules such as sterols (especially ergosterol in yeast and cholesterol in animals) involved in membrane structure, and dolichol, required for glycoprotein synthesis (Goldstein & Brown 1990). The pathways diverge after the synthesis of farnesyl-pyrophosphate, which is a substrate of either *cis*-prenyltransferase that leads to dolichol biosynthesis, or squalene synthase that leads to ergosterol biosynthesis (Adair & Cafmeyer 1987; Robinson et al. 1993).

Farnesyl-pyrophosphate is elongated by *cis*-prenyltransferase that sequentially adds activated isopentenyl-pyrophosphate units in species-dependent manner, where different organisms have distinct dolichol chain length. Mammalian cells have dolichols that consist of 18-21 isoprene units, 15-16 isoprene units were described in dolichols from *Saccharomyces cerevisiae* while shorter dolichols with 11-12 isoprene units are found in the protozoan parasite *Trypanosoma brucei* (Jung & Tanner 1973; Rip et al. 1985; Adair & Cafmeyer 1987; Löw et al. 1991; Breitling & Aebi 2013). In the final steps of dolichol biosynthesis, the polyprenyl-pyrophosphate product is first dephosphorylated and then reduced by an NADPH dependent α-reductase, encoded by *DFG10* in yeast (Sagami et al. 1993;

Szkopińska et al. 1993; Schenk et al. 2001; Frank & Waechter 1998; Cantagrel et al. 2010). Since dolichol was detected in the cells deleted of *DFG10*, an alternative pathway for de novo synthesis of dolichol was suggested as well (Cantagrel et al. 2010). Dolichol is subsequently phosphorylated by CTP-dependent dolichol kinase, encoded by *SEC59* in yeast, to form dolichyl-phosphate (Dol-P) (Heller et al. 1992; Shridas & Waechter 2006). The Dol-P lipid carrier is then ready to serve as a carrier for sugar residues used in N-linked glycosylation, as well as O-mannosylation and glycosylphosphatidylinositol (GPI) anchor synthesis (Rip et al. 1985).

1.2. Sugar donors for LLO biosynthesis

The three main carbohydrate components of LLOs are N-acetylglucosamine (GlcNAc), mannose (Man) and glucose (Glc). These sugar residues are added to the LLO in a stepwise manner, starting at the cytoplasmic side of the ER membrane where sugar residues are added from soluble, nucleotide activated sugar donors, and continues in the lumen of the ER where Dol-P linked sugars serve as substrate donors in LLO biosynthesis.

The biosynthesis of GDP-Man, UDP-GlcNAc and UDP-Glc starts with Glc-6-phosphate. In the case of first two sugar donors, GDP-Man and UDP-GlcNAc, Glc-6-phosphate is enzymatically isomerized to form fructose-6-phosphate (Dickinson 1991). GDP-Man is then synthesized in three steps from fructose-6-phosphate while biosynthesis of UDP-GlcNAc includes four steps (Hashimoto et al. 1997; Milewski et al. 2006). In the biosynthesis of UDP-Glc Glc-6-phosphate is first converted to Glc-1-phosphate followed by formation of UDP-Glc (Boles et al. 1994; Daran et al. 1995).

Sugars bound to Dol-P serve as substrates for LLO assembly in the ER lumenal phase. Here, nucleotide activated sugars, GDP-Man and UDP-Glc, serve as donors for the biosynthesis of Dol-P-Man and Dol-P-Glc, respectively. Both reactions take place at the cytoplasmic side of ER membrane. Dol-P-Man is synthesized by the essential Dol-P-Man synthase, encoded by *DPM1* in budding yeast (Orlean 1990), while the fission yeast and mammalian enzymes are a complex of three proteins, where the homologue of Dpm1p is the catalytic subunit (Maeda et al. 1998; Maeda et al. 2000). Dol-P-Glc is generated by the non-essential Dol-P-Glc synthase, encoded by *ALG5* (te Heesen et al. 1994). As Dol-P bound sugars are synthesized on the cytoplasmic side, in order to participate in LLO assembly they need to be translocated to the lumenal side of the ER membrane. Although proteins responsible for translocation have not been identified so far, the Dol-P-Man flipping was characterized to be ATP-dependent and stereoselective (Sanyal & Menon 2010).

1.3. The assembly of the LLO

Fully assembled LLO contains two N-acetylglucosamine, nine mannose and three glucose residues. Asparagine linked glycosylation (*ALG*) pathway genes encode for a series of enzymes involved in LLO biosynthesis responsible for the stepwise build-up of the $GlcNAc_2Man_9Glc_3$ LLO (Figure 1).

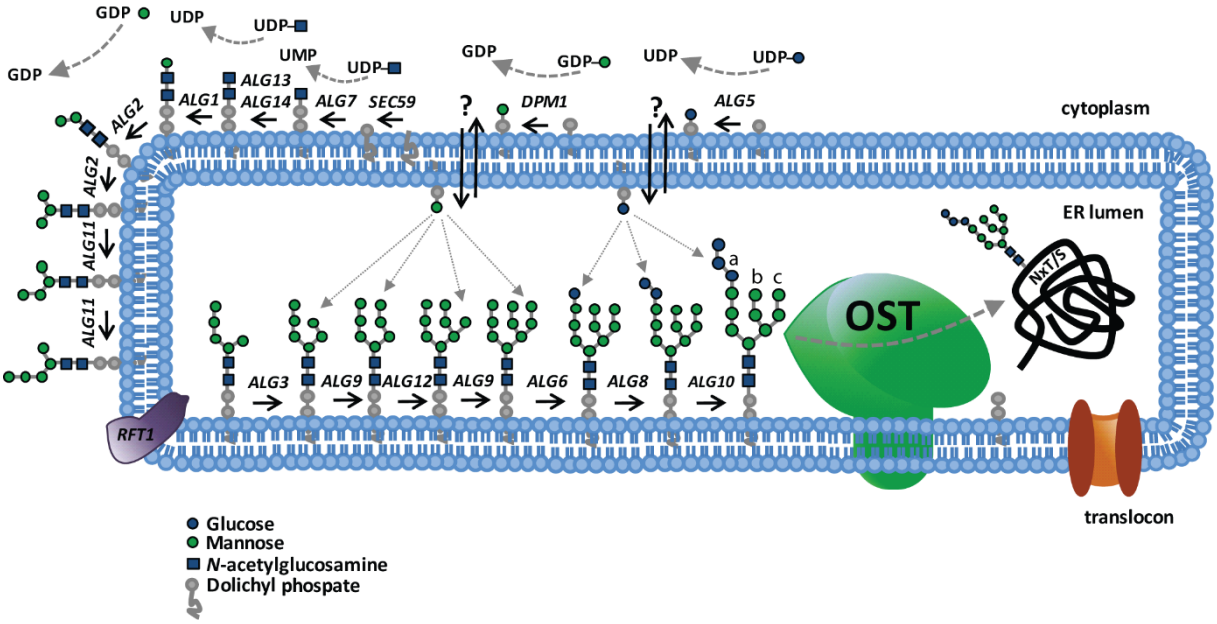

Figure 1. The N-linked glycosylation pathway.

Biosynthesis of the Dol-PP-$GlcNAc_2Man_9Glc_3$ LLO precursor is a sequential process catalysed by glycosyltransferases encoded by *ALG* genes. The assembly is initiated at the cytoplasmic side of the ER membrane, after the flipping of the intermediate Dol-PP-$GlcNAc_2Man_5$, it continues at the lumenal side. The final *en block* transfer of the fully assembled LLO to the asparagine within the N-X-S/T sequon of nascent polypeptide is catalysed by the OST.

The build-up of the LLO starts at the cytoplasmic side of the ER membrane and is catalysed by cytosolic enzymes that produce Dol-PP-$GlcNAc_2Man_5$ from the soluble nucleotide activated sugar donors (Figure 1). Enzymes involved in this stepwise cytoplasmic biosynthesis are organized into two functional complexes proposed to facilitate efficient glycosylation by permitting a flux of LLO intermediates between successive active sites (Noffz et al. 2009; Lu et al. 2012). The initial step of LLO assembly is catalysed by the UDP-GlcNAc utilizing Alg7/Alg13/Alg14 protein complex where the essential *ALG7* encoded N-acetylglucosaminyl phosphate transferase is responsible for the transfer of the GlcNAc-phosphate to the Dol-P lipid carrier to form Dol-PP-GlcNAc (Rine et al. 1983; Noffz et al. 2009). Alg7p is a known target of the drug tunicamycin, frequently used to study the effect of N-linked glycosylation

inhibition on biological processes (Takatsuki et al. 1971; Kukuruzinska & Robbins 1987). The second GlcNAc residue is added to Dol-PP-GlcNAc by Alg13p and Alg14p (Bickel et al. 2005; Chantret et al. 2005) where Alg14p coordinates the recruitments of both Alg7 and Alg13 proteins (Lu et al. 2012). The following steps of cytoplasmic LLO assembly are catalysed by GDP-Man dependent Alg1p/Alg2p/Alg11p complex (X. D. Gao et al. 2004). *ALG1* encoded β-1,4-mannosyltransferase adds the first mannose to Dol-PP-GlcNAc (Couto et al. 1984). Alg2p sequentially adds two branching mannoses, where α-1,3-linked mannose is added first followed by an addition of α-1,6-linked mannose residue (O'Reilly et al. 2006; Kampf et al. 2009). LLO is then elongated by two α-1,2-linked mannoses added by Alg11p to the α-1,3-linked branching mannose residue (Cipollo et al. 2001; O'Reilly et al. 2006). In order to be further elongated, the final product of the *ALG* pathway on the cytoplasmic side, Dol-PP-$GlcNAc_2Man_5$, of the ER membrane needs to be translocated into the ER lumen. Although not fully understood, the process is substrate specific and mediated by Rft1p in yeast, albeit *in vitro* experiments demonstrated Rft1p-independent flipping as well (Snider & Rogers 1984; Rush & Waechter 1995; Rush et al. 1998; Helenius et al. 2002; Sanyal et al. 2008; Sanyal & Menon 2009). The crystal structure of the LLO flippase PglK from *Campylobacter jejuni* revealed a whip-like mechanism where the lipid tail of the LLO interacts first with the flippase, followed by the pyrophosphate group that pulls along the oligosaccharide. Upon ATP hydrolysis, the conformational change of PglK results in the release of the polar pyrophosphate-oligosaccharide into the aqueous milieu and disengagement of the lipid tail from the PglK (Perez et al. 2015). Compared to bacterial LLOs that contain undecaprenyl-linked oligosaccharide, eukaryotic LLOs have longer polyisoprenoids and do not seem to require ATP in the flipping process; therefore, the flipping mechanism might not be the same (Jung and Tanner 1973; Rip et al. 1985; Adair and Cafmeyer 1987; Sanyal and Menon 2009).

After translocation of Dol-PP-$GlcNAc_2Man_5$, four mannosyltransferases and three glucosyltransferases are involved in the full assembly of the lipid-linked core oligosaccharide at the lumenal side of the ER membrane (Figure 1). Luminal enzymes differ from early *ALG* enzymes in three respects. First, they utilize lipid-bound activated sugars as donor substrates, Dol-P-Man and Dol-P-Glc. Second, they are grouped in GT-C superfamily of inverting enzymes, resulting in α configuration of the added sugar residue (Lairson et al. 2008). Third, the genes encoding for these transferases are not essential for vegetative growth of yeast cells at non permissive temperature, though deletions of late *ALG* genes result in hypoglycosylation of secretory proteins (Huffaker & Robbins 1983; Runge & Robbins 1986; Burda & Aebi 1999). Glycosylation of the LLO at the ER lumenal side is initiated by the Alg3, an α-1,3 mannosyltransferase that initiates the LLO b-branch (Figure 1) (Aebi et al. 1996; Sharma et al. 2001). The assembly of the b-branch is then completed by *ALG9* encoded α-1,2 mannosyltransferase (Cipollo & Trimble 2000; Frank & Aebi 2005). In the next step, LLO c-branch is initiated by Alg12 α-1,6 mannosyltransferase and is further elongated by Alg9p, adding the second α-1,2-linked Man residue

(Burda et al. 1999; Cipollo & Trimble 2002; Frank & Aebi 2005). Further steps involve the addition of three glucose residues to LLO a-branch. Alg6 and Alg8 glucosyltransferase transfer the first and the second α-1,3-linked glucose, respectively (Stagljar et al. 1994; Reiss et al. 1996). The final step in LLO synthesis, addition of a third glucose residue in α-1,2 linkage yielding the fully assembled core oligosaccharide, is catalysed by Alg10p (Burda & Aebi 1998).

High substrate specificity of the *ALG* encoded glycosyltransferases for the define LLO intermediates results in ordered built-up of the LLO described above. Therefore, deletions of individual *ALG* genes involved in the lumenal LLO assembly result in accumulation of define LLO intermediates allowing for the "genetic tailoring" of the OST substrate (Jakob et al. 1998).

1.4. The dolichol cycle

As mentioned before, Dol-P serves as substrate for the initiating step of N-linked glycosylation and for the biosynthesis of Dol-P bound sugars used in N-linked glycosylation, GPI-anchor biosynthesis and O-mannosylation reactions, and C-mannosylation reaction in mammalian cells. It is therefore not surprising that the availability of Dol-P represents a key factor in the assembly of the LLO in eukaryotes. There are several ways of Dol-P generation (Schenk et al. 2001). (1) Dol-P is generated *de novo* on the cytoplasmic side of the ER by the biosynthetic pathway described above. (2) Dol-P is a product of Dol-P-Man and Dol-P-Glc dependent glycosyltransferases in the lumen of the ER, where seven Dol-P molecules are produced during each round of protein N-linked glycosylation. (3) Additional five Dol-P molecules are also formed in the lumen of ER as a result of GPI-anchor synthesis (three molecules per one GPI anchor synthesized) and protein C- and O-mannosylation (one for each reaction) (4) Dol-PP, a product of the OST catalysed N-linked glycosylation reaction, can be dephosphorylated to form Dol-P as well. Consequently, the bipartite localization of N-linked protein glycosylation, GPI-anchor biosynthesis and C- and O-mannosylation, results in a transfer of Dol-P from the cytoplasmic to the lumenal side of the ER membrane. Lumenal Dol-PP phosphatase, encoded by *CWH8*, has been described to dephosphorylate Dol-PP into Dol-P (van Berkel et al. 1999; Fernandez et al. 2001). The current models suggest that lumenal Dol-P is then recycled and reused in glycosylation reactions. Since the phosphoryl group would prohibit free diffusion across the membrane, the rapid availability of Dol-P on the cytosolic side suggests active translocation across the membrane (McCloskey & Troy 1980; Sanyal & Menon 2010). The exact mechanism and proteins involved in the Dol-P recycling are to be further investigated.

2. Transfer of the LLO precursor to the polypeptide

Besides the use of Dol-PP as a carrier for LLO assembly, N-linked protein glycosylation is further characterized by the transfer of the fully assembled oligosaccharide from the Dol-PP carrier to the asparagine residues defined by the specific consensus sequence on nascent polypeptides in the ER lumen of eukaryotes or periplasm of bacteria and archaea. Oligosaccharyltransferase (OST) is the enzyme responsible for the catalysis of this glycosylation reaction.

2.1. Oligosaccharyltransferase (OST)

The central step of N-linked glycosylation is catalysed by the OST. In animals, plants and fungi the OST is a hetero-oligomeric complex composed of distinct membrane-bound subunits, involved in the *en bloc* transfer of a preassembled $GlcNAc_2Man_9Glc_3$ oligosaccharide to the asparagine side chain within the asparagine-X-serine/threonine consensus sequence (where X represents any amino acid except proline) of the nascent polypeptides as they enter the rough ER. The enzyme exist as a single subunit OST in certain unicellular eukaryotes and some archaeal and bacterial species (Wacker 2002; Kelleher and Gilmore 2006; Manthri et al. 2008; Nasab et al. 2008). Although the oligosaccharide structures transferred may differ, the formation of an N-glycosidic linkage between the amide nitrogen of the acceptor asparagine and C1 carbon of the first sugar residue on the LLO donor is evolutionary conserved (Bause & Legler 1981; Lizak et al. 2011).

2.1.1. *Saccharomyces cerevisiae* OST complex

OST has been most extensively studied in yeast. A combination of protein biochemistry and yeast genetics experiments has led to the identification of yeast OST as a complex of eight subunits encoded by *OST3/OST6*, *OST4*, *OST5*, *OST1*, *OST2*, *WBP1*, *SWP1* and *STT3*, where the last five are essential for survival (te Heesen et al. 1992; Stephan te Heesen et al. 1993; Kelleher & Gilmore 1994; Knauer & Lehle 1994; Zufferey et al. 1995; Chi et al. 1996; Karaoglu et al. 1997; Reiss, te Heesen, Gilmore, Zufferey & Aebi 1997; Spirig et al. 1997; Schwarz et al. 2005) (Figure 2). The complex exists in two isoforms, either containing Ost3p or Ost6p (Schwarz et al. 2005). Other organisms contain OSTs with distinct extent of structural complexity. The OST complex in mammalian cells encodes subunits homologous to those found in yeast: *N33*/*Tusc3* and *IAP3* (*OST3* and *OST6*), *DAD1* (*OST2*), *ribophorin I* (*OST1*), *OST48* (*WBP1*), *ribophorin II* (*SWP1*), where mammalian complex exists in two additional isoforms, containing either STT3A or STT3B (*STT3*) (Daniel J. Kelleher et al. 2003; Mohorko et al. 2011). Unicellular eukaryote *Cryptosporidium parvum* OST encodes for most of the subunits found in yeast except for *OST5* and

SWP1. Hetero-tetrameric OST complexes were described in *Trichomonas vaginalis*, *Entamoeba histolytica* and *Plasmodium falciparum* genomes where homologues encoding for *OST1*, *OST2*, *STT3* and *WBP1* were identified (Kelleher & Gilmore 2006).

Earlier studies demonstrated that yeast OST subunits have distinct interaction between each other and form three subcomplexes, the first subcomplex being described between Wbp1, Swp1 and Ost2 proteins, then Stt3p, Ost3/6p and Ost4p, and lastly between Ost1 and Ost5 proteins (Stephan te Heesen et al. 1993; Silberstein 1995; Karaoglu et al. 1997; Reiss, te Heesen, Gilmore, Zufferey & Aebi 1997). Recently, the work of Mueller and colleagues showed that the assembly of OST complex occurs in an ordered manner going through the formation of intermediate subcomplexes (Mueller et al. 2015). Taken together all the research, the order of the assembly of OST complex was proposed. It starts with the formation of the first subcomplex between Wbp1p, Swp1p and Ost2p. Similarly, Ost1p and Ost5p together with Stt3p form the second subcomplex. In the next step, the two subcomplexes interact and Ost4p subsequently binds to Stt3p and anchors Ost3/6p into the final active complex (Silberstein 1995; Karaoglu et al. 1997; Reiss, te Heesen, Gilmore, Zufferey & Aebi 1997; Spirig et al. 1997; Yan et al. 2003; Spirig et al. 2005; Mueller et al. 2015).

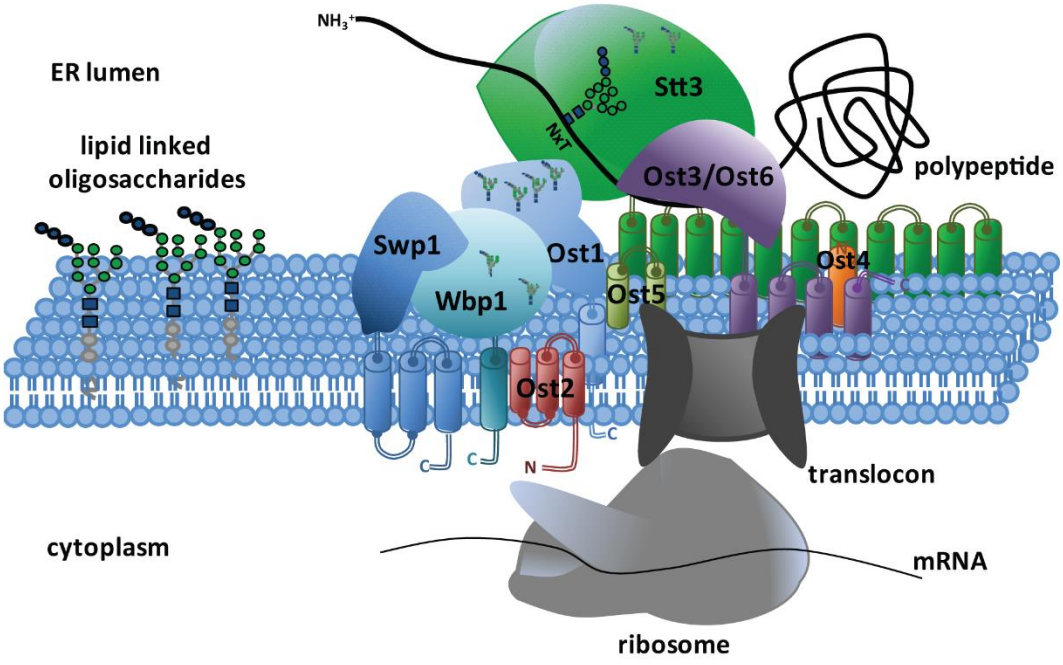

Figure 2. The oligosaccharyltransferase complex from yeast *Saccharomyces cerevisiae.*

The yeast OST complex is located in the ER lumen. It consists of eight subunits including Wbp1p, Ost2p, Swp1p, Ost1p, Ost5p, Stt3p, Ost4p and mutually exclusive Ost3p and Ost6p. OST catalyses the *en block* transfer of the $GlcNAc_2Man_9Glc_3$ LLO to the asparagine side chain within the N-X-S/T sequon of the polypeptide that has been translated and translocated into the ER by Sec61 translocon.

2.1.2. Function of distinct OST subunits

Stt3 subunit is the most conserved and is essential for the catalytic activity of the enzyme (Wacker 2002; Yan & Lennarz 2002; Daniel J. Kelleher et al. 2003; Nilsson et al. 2003). Homologues of Stt3p correspond to single subunit OSTs in unicellular eukaryotes (such as in kinetoplastids *Leishmania major* and *Trypanosoma brucei*), as well as archaeal and bacterial species (such as in *Campylobacter jejuni*) (Wacker 2002; Manthri et al. 2008; Nasab, Benjamin L. Schulz, et al. 2008). The overexpression of *L. major* Stt3p homologue in *S. cerevisiae* is sufficient to complement the deletion of *STT3* gene, even if they do not incorporate into the native complex (Nasab, Benjamin L. Schulz, et al. 2008; Hese et al. 2009). Therefore, cells with a non-functional yeast OST are viable in the presence of *Lm*Stt3D protein.

Some kinetoplastids, although having single subunit OSTs, encode several paralogues of *STT3*. Duplication and diversification of *STT3*, where the paralogues possess distinct preferences for LLO and polypeptide substrates, seems to represent an alternative approach to increase the number of protein substrates (Nasab, Benjamin L. Schulz, et al. 2008; Izquierdo et al. 2009; Schwarz & Aebi 2011). As mentioned above mammalian OST complex contains either Stt3A or Stt3B, where the two isoforms differ in their catalytic activity and selectivity for the LLO substrate (Daniel J. Kelleher et al. 2003). The STT3A isoform glycosylates substrate polypeptide chains cotranslationally, while STT3B isoform can posttranslationally glycosylate sites that were skipped by STT3A complexes. The presence of two OST complex isoforms with distinct properties and activities, similar to the presence of multiple paralogues of STT3 in kinetoplastids, was suggested to increase glycosylation occupancy on different polypeptide substrates (Ruiz-Canada et al. 2009). It is worthy to mention that *S. cerevisiae*, as well as *Saccharomyces pombe* and *Caenorhabditis elegans*, express a single OST catalytic subunit that is more closely related to the STT3B isoform responsible for posttranslational glycosylation (Shrimal et al. 2013).

The addition of non-catalytic subunits is regarded as a mean to promote the catalytically active Stt3 protein to glycosylate a more diverse range of substrate proteins. Two best characterized OST subunits are Ost3 and Ost6, two proteins that define two OST complex isoforms in yeast (Schwarz et al. 2005). Glycosylation occupancy analysis on various glycosylation sites on cell wall proteins revealed that Ost3p and Ost6p facilitate efficient glycosylation in a site-specific manner (Schulz & Aebi 2009). Structural and biochemical characterization led to a model proposing that Ost3/6p form mixed disulphides with the protein substrates and thus prevent certain substrate polypeptides to oxidatively fold (Mohd Yusuf et al. 2013). In addition, noncovalent binding of polypeptides to Ost6p was also demonstrated (Jamaluddin et al. 2011). The model then proposes that different OST isoforms assist in

the binding of specific polypeptide substrates, increasing the time for efficient glycosylation of sites, which could otherwise be inaccessible due to protein folding prior to glycosylation (Schulz et al. 2009). Function of all other OST subunits is less clear. Structure of the smallest subunit, Ost4p, consisting only of a short membrane stalk has been solved and its sole function was proposed to mediate interaction between Stt3p and Ost3/6p (Gayen & Kang 2011; Dumax-Vorzet et al. 2013). The lack of large luminal domain in Ost5p might indicate its function mainly as structural component as well. For Ost1p, studies suggested that its mammalian homolog ribophorin I associated with ribosomes and facilitated delivery of some integral membrane proteins to the catalytic centre of OST (Yu et al. 1990; Wilson & High 2007; Wilson et al. 2008). Disruption of Wbp1p, Ost2p and Swp1p subunits caused destabilization of OST suggesting an important function in complex stabilisation although no further role has been proposed for these subunits (Mueller et al. 2015). A possible role of non-catalytic subunits could be to allow for a subtler regulation of the OST as additional subunits could facilitate glycosylation of different proteins or might regulate the selection of specific LLO substrates (Kelleher et al. 2007; Schulz et al. 2009). Moreover, additional subunits might provide a higher concentration of substrates at the catalytic centre. Lastly, additional subunits might mediate coupling of the OST to the translocon complex at ER membrane, resulting in more efficient glycosylation of sites that would otherwise be inaccessible. Previously published results indicate that ribophorin I, a human homologue of Ost1p, might be involved in the translocation process (Yu et al. 1990). All of these arguments would lead to one outcome, increased glycosylation on different polypeptide substrates.

2.1.3. N-linked protein glycosylation reaction

In order to catalyse the transfer reaction OST Stt3 subunit must recognize two distinct substrates: the LLO and the nascent polypeptide chains. The optimal LLO substrate of the yeast OST is a highly conserved $GlcNAc_2Man_9Glc_3$ oligosaccharide. Here, the presence of glucose moieties, in particular the terminal α-1,2-linked glucose, is crucial for the efficient transfer (Burda & Aebi 1998). Truncated LLO precursors can still be transferred, although less effectively causing protein hypoglycosylation (Verosteks et al. 1993). The length of the lipid carrier, dolichol, does not play an important role as shorter carriers were effectively utilized by the OST enyzme (Grabińska & Palamarczyk 2002). I*n vitro* assays showed that the minimal oligosaccharide structure transferred by OST is Dol-PP-$GlcNAc_2$, while Dol-PP-$GlcNAc_2Man_3$ seems to be the minimal LLO structure that allows yeast cells to grow if the limiting translocation across the ER membrane is increased by Rft1p overexpression (Tai & Imperiali 2001; Helenius et al. 2002) (Figure 1). Thus, yeast cells with deletions of early *ALG* genes in the LLO biosynthetic pathway are not viable or display a severe growth phenotype (Albright & Robbins 1990; Jackson et al. 1993; Cipollo et al. 2001). Loss of lumenal *ALG* enzymes results in protein

hypoglycosylation, but does not give a growth phenotype of corresponding strains. Interestingly, glucosyltransferase defects were more severe in respect of protein hypoglycosylation as compared to the loss of lumenal mannosyltransferases, highlighting the importance of glucose residues in oligosaccharide recognition (Zacchi & BL. Schulz 2016). In summary, OST interacts with the LLO donor substrate in a highly specific way that favours the transfer of the mature LLO structure through the recognition of $GlcNAc_2$ core and the terminal α-1,2-linked glucose residue (Burda et al. 1999).

On the other hand, polypeptide substrates only seem to share the conserved N-X-T/S sequon. This strictly conserved property was found in eukaryotic and prokaryotic N-linked glycosylation (Marshall 1972; Wacker 2002; Abu-Qarn & Eichler 2007). The crystal structure of a bacterial single subunit OST, PglB, had provided the molecular basis for the understanding of N-linked protein glycosylation reaction (Lizak et al. 2011). The work of Lizak and colleagues revealed that the WWD motif (a diagnostic motif among Stt3 homologs) defines the OST sequon specificity, favouring a threonine or serine at +2 position. Earlier studies have shown that sequons containing threonine at the +2 position are glycosylated more efficiently compared to N-X-S sequons (Bause 1984; Breuer et al. 2001). The structure of PglB with bound acceptor peptide explained that this effect is due to stabilizing interaction of the PglB with the threonine residue, which is absent when serine is present at the +2 position. Furthermore, it revealed that the catalytic centre of the OST requires a polypeptide to bind in a loop, which almost completes a 180° turn, suggesting that the glycosylation sequons have to be located in flexible, surface exposed loops. This explained why proline residues are not present at the +1 position of the consensus sequon. The authors proposed a three-stage catalytic cycle for the single subunit OST glycosylation. Upon binding of the peptide substrate, the flexible external loop 5 (EL5) is engaged in restricting the movement of the peptide. This results in the formation of the catalytic centre and glycosylation. In the last stage, the EL5 is disengaged from the catalytic centre resulting in the release of glycosylated peptide (Lizak et al. 2011). Although the model proposed that the binding of acceptor peptide precedes that of the LLO, there is no experimental evidence to support this.

Earlier work has demonstrated that less than 65% of the overall glycosylation sequons are actually glycosylated (Petrescu et al. 2004). Hence, there are additional factors besides the consensus sequon that influence whether a certain glycosylation site is to be occupied or not. It has been shown that the nature of amino acids in the X position within the sequon, as well as in the regions surrounding the sequon may influence glycosylation (Shakin-Eshleman et al. 1996). The location of the sequon within the glycoprotein plays a role as well: if located near transmembrane regions or the carboxyl terminus the glycosylation efficiency may be decreased, although this effect may be protein specific (Nilsson & Von Heijne 2000). Protein secondary structure seems to be important as consensus sequons are required to be flexible in order to be accessible to the OST catalytic site. Such requirement explains

why in the eukaryotic systems N-glycans are attached preferentially to polypeptides before the protein folds into its native conformation. Although polypeptide substrates only seem to share the conserved N-X-T/S sequon, it is clear that this is not the sole determinant of whether a protein will be N-glycosylated. With the rest of the polypeptide being very diverse, OST needs to adopt a broad spectrum of interactions to successfully glycosylated multiple polypeptide substrates.

2. Functional roles of N-linked glycosylation

Once oligosaccharides have been transferred onto respective glycoproteins they partake diverse set of roles on, both, newly synthetized and mature glycoproteins. In the ER, glycan structures on newly synthesized glycoproteins contribute to quality control and influence protein folding (Aebi et al. 2010). N-linked glycans mediate transfer through the secretory pathway by providing signals for the intracellular transport and targeting (Ni et al. 2006). Once a glycoprotein has reached the final destination, N-glycans can provide different cell surface profiles or mediate interactions with extracellular environment, but can also be directly involved in the function of mature glycoproteins (Moremen et al. 2012). Lastly, the importance of N-linked glycans on proteins is underlined by congenital disorders of glycosylation (CDGs) in humans, a series of diseases correlated with defects in the N-linked glycosylation pathway (Hennet 2012).

2.1. ER quality control and unfolded protein response

N-linked glycans effect the properties of the newly synthetized glycoproteins where the presence of hydrophilic oligosaccharides facilitates protein folding, as well as the overall stability of glycoproteins (Hanson et al. 2009; Braakman & Hebert 2013).

N-linked glycans have a role in the ER quality control (ERQC), where the function of the ERQC machinery is to allow only properly folded proteins to reach their final destinations through the secretory pathway. The ERQC mechanism relies on two major ER resident chaperone systems: the classical chaperones and the carbohydrate-binding chaperones, both being able to promote the efficient folding, but also have the ability to evaluate the conformational state of their substrates (Aebi et al. 2010; Braakman & Hebert 2013). The classical chaperones, belonging to the ER primary quality control mechanisms that apply to all proteins regardless of their glycosylation status, are capable of identifying their substrates based on the presence of exposed hydrophobic regions normally buried in the native proteins (Ellgaard & Helenius 2003). The second chaperone system consists of the

carbohydrate-binding chaperones that are specialized for recognition of specific oligosaccharide structures on the glycoproteins. Modifications of the N-linked glycan structure occurring inside the ER, after the oligosaccharide has been transferred, help the quality control system to distinguish between folding intermediates, fully folded or misfolded proteins (Aebi et al. 2010). After the OST transfers the $GlcNAc_2Man_9Glc_3$ to the nascent polypeptide, glucosidase I and II sequentially remove the glucose residues. The N-linked glycan is then re-glucosylated by an UDP-Glc:glycoprotein glycosyltransferase (UGT1) that adds α-1,3-linked glucose residue to glycan a branch. UGT1 is a sensor of glycoprotein conformation as it is specific for unglucosylated glycans on unfolded but not native polypeptides. Monoglucosylated N-linked glycan is specifically recognised by the lectin chaperones calnexin and calreticulin that help the polypeptide to fold correctly. It has been shown that both lectins form a complex with ERp57, a thiol-disulphide oxidoreductase known to form native disulphide bonds in folding polypeptides. Glucosidase II is then responsible for dissociation of glycoprotein substrate from calnexin or calreticulin by removing the terminal glucose. If the glycoprotein still has not reached its native conformation it will be re-glucosylated by UGT1 and the whole cycle starts again (Ellgaard & Helenius 2003; Aebi et al. 2010).

Ultimately, if a polypeptide is not able to fully fold in appropriate time, even after cycles of glucosylation and de-glucosylation, the N-linked glycan structure will target the respective glycoprotein at the ER-associated degradation pathway (ERAD) (Thibault & Ng 2012; Christianson & Ye 2014). The unfolded glycoprotein is diverted for the degradation upon the action of ER resident α-1,2 mannosidase I, encoded by *MNS1* in yeast, that trims the terminal b branch mannose from the N-linked glycan. The glycoprotein is still able to properly fold and additional chaperons like Pdi1p and Kar2p assist in this process. At this stage, if the folding is successful, the native glycoprotein will exit the ER carrying $GlcNAc_2Man_8$ N-linked glycan. On contrary, the trimming of the b branch mannose leads to an association with ER degradation enhancing 1,2 mannosidase like protein (EDEM), encoded by *HTM1* in yeast, that removes the terminal c branch mannose and exposes the terminal α-1,6-linked mannose residue that serves as the N-glycan degradation signal. Htm1p was found in complex with Pdi1p, here serving to identify unfolded substrates for Htm1p (Gauss et al. 2011). The N-linked glycan with the exposed α-1,6-linked mannose is ligand for yeast ERAD lectin Yos9p. In combination with Hrd3p that detects misfolded stretches on the glycoprotein, Yos9p recognition will target the protein for ubiquitination by Hrd1p, followed by degradation (Quan et al. 2008; Zattas & Hochstrasser 2015).

Alternatively, a second mean of coping with unfolded proteins in the ER is the unfolded protein response (UPR) machinery. In the UPR, the accumulation of unfolded ER proteins leads to transcriptional induction of UPR target genes (Chapman et al. 1998). Many of the UPR target genes have been identified by now, where most encode ER-resident chaperones that bind to misfolded

proteins, prevent aggregation, and promote folding. In addition, components of the phospholipid and different glycosylation biosynthetic pathways are targets as well, together with proteins involved in vesicular transport and ERAD (Travers et al. 2000). It is believed that activation of N-linked glycosylation enzymes would assist in the folding of proteins that require carbohydrate modification to attain their proper conformation. Interestingly, UPR induction in mammalian cells was shown to accelerate synthesis of the dolichol-oligosaccharides employed in N-linked glycosylation (Doerrler & Lehrman 1999). Regulation of gene expression by the UPR allows the cell to cope with folding stress and adjust the capacity of protein folding in the ER according to the need, although how N-linked glycosylation components are directly involved in this regulation needs to be further investigated.

2.3. Congenital disorders of glycosylation

Many proteins are modified by glycans that can be crucial for protein function, localization, transport and/or protein stability (Larkin & Imperiali 2011). The essentiality of the correct assembly of the N-linked glycan and its attachment to different protein substrates was further highlighted with the discovery of CDG syndromes in humans. Although clinically heterologous, most types of CDGs are associated with neurological impairments ranging from severe psychomotor retardation to moderate intellectual disabilities, and in worst cases, to infantile lethality (Haeuptle & Hennet 2009). CDG patients were identified using serum transferrin isoelectric focusing, although in the last years, sequencing techniques are commonly used. By now, CDG patients with mutations in all genes involved in LLO biosynthesis (except *ALG10*) were described, where some of these genes were associated with congenital myasthenic syndromes or impaired neuromuscular transmission as well (Freeze 2006; Haeuptle & Hennet 2009; Timal et al. 2012; Cossins et al. 2013). CDGs have also been identified for mutations affecting different OST subunits and subsequent modification steps of the N-glycans (Hennet 2012). Insects and plants are also affected by defects in the N-linked glycosylation pathway which can lead to developmental alterations and hypersensitivity to stress conditions (Haecker et al. 2008; Pattison & Amtmann 2009; Farid et al. 2011; Shaik et al. 2011). Further identification and investigation of CDGs and similar diseases might improve our understanding of glycosylation pathways and their complex regulation.

3. Analytical tools for the analysis of N-linked glycosylation

Considering the importance of N-linked glycosylation discussed above, it is not surprising that this process has been extensively studied over the years. This section will be discussing the analytical tools used to examine OST complex stability and the enzyme activity in respect of glycosylation occupancy, a term describing the presence or absence of glycans on glycoprotein substrates.

3.1. Genetic and biochemical analysis of N-linked protein glycosylation

Although the genetic analysis of N-linked glycosylation pathway has been performed in many model organisms, including bacteria, yeast and mammalian cells, the ease of genetic manipulation makes the yeast *Saccharomyces cerevisiae* the best eukaryotic model organisms for the analysis of this pathway (Frazer & O'Keefe 2007). The facility of transformation and homologous recombination, including the possibility of complementation with different auxotrophy marker genes, have enabled the isolation of many mutants that helped understand the function of the pathway as well as the distinct roles of OST subunits. Yeast genetic techniques have enabled the identification of all loci required in the assembly of LLO. In brief, *ALG1*, *ALG2* and *ALG11* loci were cloned by complementation of the temperature-sensitive phenotype of the corresponding mutants; *ALG13* and *ALG14* were identified based on *in silico* search; *ALG3, ALG9, ALG12, ALG6, ALG8* and *ALG10* were isolated through a synthetic lethal screen or through sensitivity or resistance to different toxins, or mannose-suicide selection (Burda & Aebi 1999; Breitling & Aebi 2013). Furthermore, isolation of OST mutants and high copy number suppression of the temperature-sensitive phenotype of these mutants led to identification of all OST complex subunits. Shortly, *SWP1* and *OST2* loci were isolated as high copy number suppressors of *wbp1* mutants, *OST5* was a suppressor of *ost1* mutant and Ost3p overexpression suppressed the *ost4* deletion phenotype while *OST3* and *OST4* are high copy number suppressors of *stt3* mutants (Kelleher & Gilmore 2006). As majority of genes involved in N-linked glycosylation pathway have been identified, genetic manipulation of the genes involved facilitates further investigation of the pathway.

Biochemical methods, such as co-immunoprecipitation and chemical cross-linking, have been used to investigate the interaction between OST subunits as well as the role of WWDYG motif of Stt3p in peptide recognition (Yan & Lennarz 2002; Nilsson et al. 2003; Yan et al. 2003). Chromatographic and immunoaffinity methods have been used to purify OST from various organisms later used for *in vitro* activity assays (Kumar et al. 1994). Earlier, OST activity assays were often conducted using radiolabelled LLOs and isotopically labelled or biotinylated peptides (Xu & Coward 1997; Srinivasan & Coward 2002). Current assays use fluorophore labelled synthetic peptides that are electrophoretically separated and detected by fluorescence gel imagining, offering an easier, faster and less hazardous

approach compared to the previous one (Kohda et al. 2007; Gerber et al. 2013; Lizak et al. 2013). Most common way of OST *in vivo* activity investigation uses Western blot analysis followed by immunodetection of specific glycoproteins where the extent of protein hypoglycosylation is evident from a ladder like appearance of faster moving, hypoglycosylated protein species. Broadly used model glycoprotein in glycosylation occupancy analysis is a vacuolar protease CPY that harbours four glycosylation sites. Although quite swift and easy, this type of analysis is low throughput since only a few glycoproteins can be monitored per experiment. Recent approaches use mass spectrometry offering precise, reproducible and high throughput workflows for the analysis of glycosylation occupancy. The following pages will be focusing on different mass spectrometry techniques used for the investigation of N-linked protein glycosylation.

3.2. Mass spectrometry analysis of N-linked protein glycosylation

Mass spectrometry (MS) is an analytical method that allows identification and quantification of molecules based on their mass and charge. Every mass spectrometer includes an ion source, a mass analyser and a detector. For each part of the instrument, different types of devices are available and their combination allows a number of different applications. In proteomics, mass spectrometry is used either to identify the overall protein content of a sample using shotgun proteomics, or to focus on quantification of specific analytes using targeted proteomics. The two targeted techniques discussed below are Selected Reaction Monitoring (SRM) MS and Parallel Reaction Monitoring (PRM) MS. An alternative technique that combines shotgun with targeted data analysis is Sequential Window Acquisition of all Theoretical mass spectra (SWATH) MS (Figure 3). In all cases a standard proteomics workflow includes: (1) protein extraction, (2) digestion into peptides, (3) separation using liquid chromatography (LC), (4) ionization before entering the mass analyser where ionized peptides, also called precursor ions, are resolved according to their mass-to-charge (m/z) ratio and MS^1 (or MS) spectrum is recorded, (5) selection of particular precursor ions and their fragmentation in a process termed collision-induced dissociation (CID) and (6) record of fragment ions of a single peptide in MS^2 (or MS/MS) spectrum (Figure 3) (Steen & Mann 2004).

Glycoproteomics, the global analysis of glycoproteins, is a field of proteomics for the systematic identification and quantification of glycoproteins in complex biological samples. While glycomics analysis focuses on characterization of the glycan structure attached to proteins, the emerging techniques in glycoproteomics are focused on the identification of protein glycosylation sites and quantification of glycosylation site occupancy.

3.2.1. Supporting techniques for the analysis of glycoproteins by MS

Although ubiquitous, the glycoproteome is overshadowed by the complicated cellular environment, due to the relative low abundance and low MS properties of glycosylated peptides additional steps are usually required for the analysis of glycoproteins by MS. In order to reduce sample complexity a basic workflow was established for the analysis of glycoproteins by MS following adequate sample preparation often including the cell fractionation, glycoprotein or glycopeptide enrichment and trimming of the glycan moiety.

Many enrichment methods on glycoprotein and/or glycopeptide level have been developed that can be divided into affinity approach and chemical approach (Pasing et al. 2012). The affinity approach relies on the interaction of glycans and stationary phase such as lectin affinity chromatography, titanium dioxide (TiO_2) affinity chromatography and hydrophilic interaction liquid chromatography (HILIC). The chemical approach is based on immobilization of glycoproteins or glycopeptides relying on the chemical interaction of glycans and specific functional groups, such as hydrazine chemistry, reductive amination chemistry and boronic acid chemistry. Probably the most renowned method for glycoprotein or glycopeptide enrichment is lectin affinity chromatography with the advantage of broad spectrum of available specificities. Commonly used lectins are: wheat germ agglutinin (WGA) prefers dimers and trimers of GlcNAc and sialic acid-bearing glycans; concanavalin A (ConA) binds core α-mannose residues and is therefore preferentially used for the enrichment of N-glycopeptides; and galactosyl(-1,3)-GalNAc and O-glycoprotein specific jacalin (JAC) (Baenzigers 1979; Chatterjee et al. 1985; Debray et al. 2005). Despite the advantage of their specificity, the use of lectins has drawbacks, such as secondary specificity and low binding efficiency in protein mixtures (Lee et al. 2010). A broad range of glycoproteins and glycopeptides can be enriched by solid-phase extraction method used in hydrazine chemistry (Zhang et al. 2003). Although the method has been successfully used to investigate many complex biological samples, it requires careful optimization and extensive preparation. Recently, the application of HILIC has been used in glycoproteomics. This non-modifying technique relies on the hydrophilic interaction between the glycan moiety and the stationary phase separating the glycopeptides from the rest of the non-glycosylated peptides that are washed out with an organic solvent. The newest strategy combines HILIC with zwitterionic materials (ZIC-HILIC) creating a column of high ionic strength for polar interaction with glycans. This strategy has been successfully used for the enrichment and identification of glycopeptides in different studies (Hägglund et al. 2004; Neue et al. 2011).

After enrichment of the glycopeptides, most workflows proceed with the trimming of the glycan moiety before MS analysis. Two most commonly enzymes used are N-glycosidase F (PNGaseF) and endo-β-N-acetylglucosaminidase (EndoH). PNGase F cleaves all N-glycans between the reducing end

GlcNAc and the asparagine residue, except those carrying an α-1,3-linked fucose attached to GlcNAc, as observed in plants and some insects (Tarentino et al. 1985; Tretter et al. 1991). Glycan digestion with PNGase F results in a deamination of asparagine to aspartic acid at the former glycosylation site. The resulting mass shift of 0.98 Da can be detected by MS and can be used as an indirect assignment of former glycosylation sites (Zhang et al. 2003). However, deaminations can occur naturally within a cell or during sample preparation resulting in false positive results. The use of ^{18}O-water during PNGaseF digestion helps to rule out natural deamination and increases mass difference, although it does not exclude the possibility of spontaneous deamination during sample preparation (Beck et al. 2011). The use of Endo H, which cleaves between the two first GlcNAc residues of high-mannose and some hybrid oligosaccharides of N-linked glycoproteins leaving a remnant GlcNAc residue, unambiguously marks the glycosylation site during MS analysis (Tarentino et al. 1974; Hägglund et al. 2004). However, a neutral loss of the labile GlcNAc can occur during the fragmentation of the peptide in the mass spectrometer, although this can be avoided using appropriate fragmentation technique (such as electron-transfer dissociation (ETD) or electron-capture dissociation (ECD)) (Wiesner et al. 2008).

In order to facilitate and improve quantification of complex biological samples label-based approached have been developed where the ratios of mass spectrometry intensities between the "light" and "heavy" samples are calculated. Various approaches include metabolic incorporation, stable isobaric or isotopic labelling using chemical reactions, use of spiked synthetic peptide standards and enzymatic reactions using ^{18}O labelling mentioned above (Bantscheff et al. 2007). Metabolic incorporation or Stable Isotope Labelling by Amino acids in Cell culture (SILAC) is a simple, straightforward and most accurate labelling approach where non-radioactive, stable isotope-containing amino acids are incorporated *in vivo* into proteins (Ong 2002). It involves growing the cells in growth medium where natural amino acids are replaced by "heavy" amino acids, usually arginine and lysine, that are then being incorporated into newly synthesized proteins. This way the label is introduced in the earliest possible point and hence it excludes all sources of quantification error introduced by biochemical and MS procedures. However, the approach is costly and sometimes not feasible for the metabolic labelling in higher eukaryotes (Ong & Mann 2006).

In the following part, we will be discussing current existing MS technologies utilized for the characterization and identification of N-glycoproteins as well as for the understanding of N-linked glycosylation pathway.

3.2.2. Shotgun MS for the identification of glycoproteins

In the shotgun proteomics, all precursor ions are detected, resulting in MS1 spectra acquired over the whole LC gradient, and the most intense ions present in MS^1 spectra will sequentially be isolated, fragmented and recorded in MS^2 spectrum. This results in the "fingerprint" of each peptide's fragmentation mass spectrum. To identify the peptides and proteins, the MS^2 spectra are searched against a database (with commercially available software such as Mascot or Sequest) containing the theoretical spectra of the whole proteome of interest, enabling the identification of thousands of proteins in a single experiment, while requiring only minimal prior knowledge about the sample (Wu & MacCoss 2002).

Shotgun proteomics have proved to be a powerful tool to investigate the extent of glycoproteome in various organisms. Using shotgun proteomics, Zielinska and colleagues have identified 516 glycosylation sites in yeast *Saccharomyces cerevisiae*, 425 in the fission yeast *Schizosacharomyces pombe*, 1794 in *Caenorahbditis elegans*, 2186 in plant *Arabidopsis italiana*, 2229 in fly *Drosophila melanogaster*, 2254 in zebrafish *Danio rerio* and 6367 in four mouse tissues (Zielinska et al. 2010; Dorota F. Zielinska et al. 2012). Furthermore, shotgun method was used for the identification and semi-quantification of salivary N-glycoproteins (Xu et al. 2014). Although relevant when it comes to identification of distinct glycoproteins, due to the selection of only the most intense ions, shotgun proteomics approach offers low or failed identification of low abundant proteins, making the quantification of those proteins challenging. For the reproducible and sensitive quantification of proteins, other proteomics approaches have been successfully used.

3.2.3. SWATH MS for the analysis of N-linked glycosylation occupancy

SWATH MS is a recently developed method where all precursor ions within a defined mass windows or swaths, covering the entire m/z range are sent for fragmentation and full MS^2 spectra are then obtained, allowing for higher quantification accuracy and precision compared to shotgun (Gillet et al. 2012). The spectra are then analysed in a targeted way using sophisticated software, such as Skyline, PeakView or OpenSWATH, to group the fragment ions based on their retention time and the precursor ion mass window (MacLean et al. 2010; Röst et al. 2014).

SWATH MS method has been used for automated measurement of site-specific glycosylation in yeast cell wall preparations, human saliva and in human plasma (Liu et al. 2013; Xu et al. 2015). Additionally, using SWATH MS Zacchi and Schulz have studied how mutations in N-linked glycosylation pathway lead to changes in glycosylation occupancy as well as in the structure of glycans at a specific site in yeast

cell wall glycoproteins (Zacchi & BL. Schulz 2016). They have shown that mutations in earlier mannosylation or glucosylation steps of LLO biosynthesis had stronger phenotypes, although glucosylation defects were in general more severe as compared to mannosylation defects. Furthermore, the study provided insight into the role of the non-essential OST subunits. Loss of non-essential subunits affected glycosylation in site-specific manner, where the deletion of *OST3* led to most severe hypoglycosylation. The deletion in *OST5* had a less severe effect as compared to loss of Ost3p, while *OST6* deletion had a minor hypoglycosylation phenotype (Zacchi & BL. Schulz 2016).

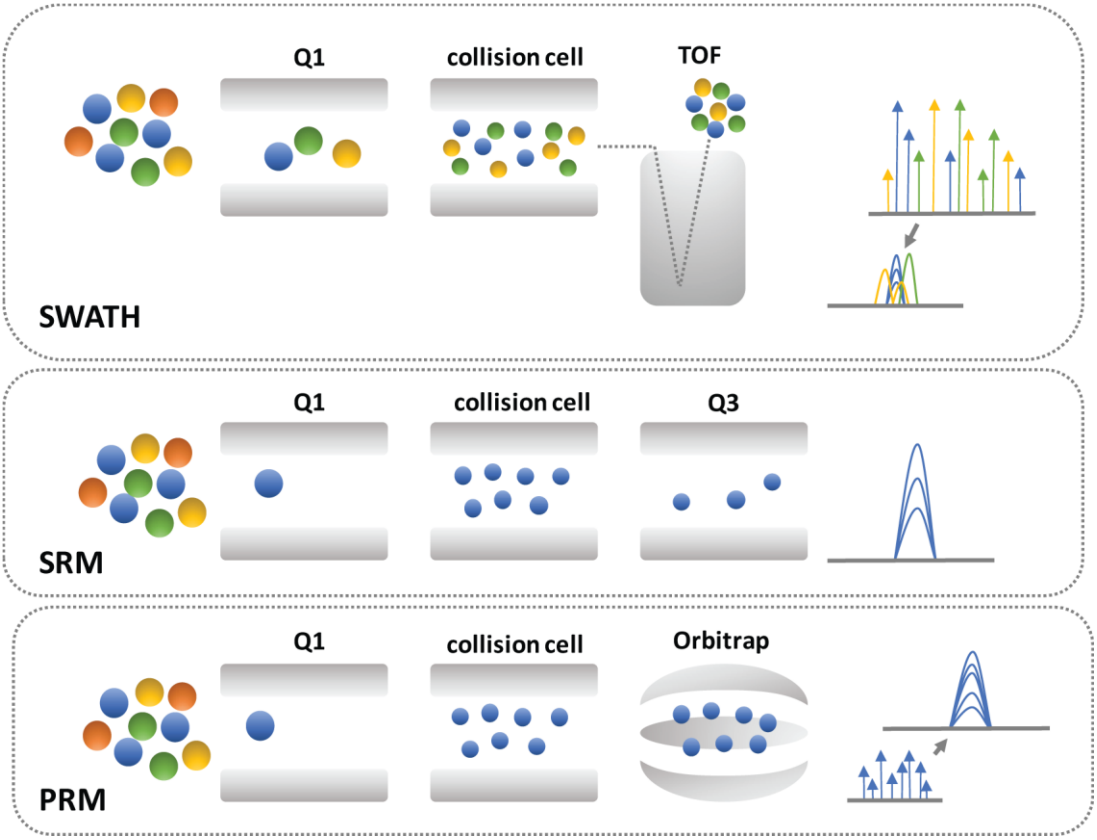

Figure 3. Schematic representation of different MS techniques.

From the proteins of interest defined in the context of a biological question, a set of peptides are generated that can be analysed by various MS analyses. In SWATH, all peptide ions within a defined mass windows or swaths are sent for fragmentation and all possible fragment ion transitions are analysed. The obtained spectra are then analysed in a targeted way. Q1 refers to the first mass-resolving quadrupole while the second mass analyser is commonly a time-of-flight (TOF) mass analyser. In SRM, only selected peptide ions are sent for fragmentation and only selected fragment ion transitions are serially monitored one at a time. Q1 and Q3 refer to the first and third mass-resolving quadrupoles. In PRM, only selected peptide ions are sent for fragmentation but all possible fragment ion transitions are analysed in one high resolution and high mass accuracy mass analysis. Q1 refers to the first mass-resolving quadrupole while the second mass analyser is commonly an Orbitrap.

3.2.4. SRM MS for the analysis of OST complex stability

Although SWATH experiments are well suited for quantification studies, the sensitivity and selectivity of this approach is not good enough for the analysis of low abundant compounds in complex samples. Therefore, targeted methods were developed that involve the selection of predetermined set of peptide ions of interest and their respective fragment ions prior to MS analysis. SRM, often called Multiple Reaction Monitoring (MRM), is a common targeted MS technique where predefined pairs of peptide/fragment ions (called transitions) of interest are monitored, resulting in increased sensitivity of measurements (Picotti et al. 2009). SRM assays require prior knowledge about the peptide ion m/z, elution time and characteristic high-intensity fragment ions. This information is entered into the instrument software as a transition list. Sophisticated software (such as Skyline) are used for the data analysis where the peptide ion and a specific fragment ion are grouped into a transition and all transitions are assembled into a peak (MacLean et al. 2010). Although SRM offers precise quantification over a wide dynamic range, the low resolution of both mass analysers and the number of targeted peptides can result in low selectivity and limit the measurement specificity.

Some studies describe the use of SRM MS for the quantification of glycosylation occupancy focused on the investigation of a small number of glycoproteins in human samples (Kim et al. 2012; Hong et al. 2013). Using yeast genetic methods to individually affect OST subunits with SILAC based SRM approach, Mueller and colleagues have analysed OST subunit protein degradation rates and relative amounts in steady state (Mueller et al. 2015). They showed that deleting essential subunits destabilized the OST complex while the overexpression of individual subunits resulted in degradation of the excess subunit without perturbing the complex. Using relative quantification of subunit levels in steady state, they have deduced the order of assembly of OST complex subunits discussed earlier.

3.2.5. PRM MS for the analysis of N-linked glycosylation occupancy

PRM is a novel targeted MS technique implemented on high resolution/accurate mass (HRAM) instruments resulting in improved sensitivity and selectivity allowing for reliable quantification of low abundant proteins (Gallien et al. 2012; Peterson et al. 2012). During PRM measurement the peptide precursor ion is selected in the first mass analyser, fragmented in the second and unlike SRM, all generated fragments are monitored in parallel with a full scan mass spectrometer. The time spent to analyse the ions in the last mass analyser, called transient time, is determined by the predefined operating resolving power. Similar to SRM, the data processing is done by sophisticated software (such as Skyline) although the post-acquisition analysis of PRM assay is more flexible and selective. The general advantages of PRM are higher specificity, sensitivity and no prior knowledge of the target transitions is required hence less time is needed for assay development.

We applied PRM MS technique for the quantification of N-linked glycosylation occupancy on numerous glycoproteins from membrane preparations of yeast *Saccharomyces cerevisiae* (see Chapter 2; Poljak et al. unpublished).

4. Concluding Remarks

Asparagine-linked protein glycosylation in the lumen of the endoplasmic reticulum is a ubiquitous, essential and evolutionary highly conserved protein modification, important for protein folding and stability as well as for distinct cellular functions. The pathway is characterized by the use of Dol-PP as a carrier for LLO assembly, a bipartite localization and the transfer of the completely assembled $GlcNAc_2Man_9Glc_3$ oligosaccharide from the Dol-PP carrier to the asparagine residues defined by the specific consensus N-X-S/T sequence. The last and key step of the pathway is catalyzed by the hetero-oligomeric OST complex in *Saccharomyces cerevisiae*. Five of OST subunits in yeast, Wbp1, Swp1, Ost2, Ost1, and Stt3, are essential for viability of the cell, whereas Ost4, Ost5, Ost3, and Ost6 are not essential but are required for maximal OST activity. The essential Stt3p is the catalytic subunit of OST and is responsible for the transfer of the oligosaccharide. There are organisms that contain only some of the OST subunits or only encode *STT3* homologues that serve as single subunits OST, but in all of these organisms, the basic mechanisms of N-linked glycosylation are conserved. Besides their importance for complex stability, the specific function of the non-catalytic subunits is largely unknown. The work described in the following chapters is trying to illuminate the mechanism of action of the multi-subunit OST complex from yeast *Saccharomyces cerevisiae* as well as of the single subunit *STT3* paralogues from *Trypanosoma brucei*.

References

Abu-Qarn, M. & Eichler, J., 2007. An analysis of amino acid sequences surrounding archaeal glycoprotein sequons. *Archaea (Vancouver, B.C.)*, 2(2), pp.73–81.

Adair, W.L. & Cafmeyer, N., 1987. Characterization of the Saccharomyces cerevisiae cis-prenyltransferase required for dolichyl phosphate biosynthesis. *Archives of biochemistry and biophysics*, 259(2), pp.589–96.

Aebi, M. et al., 1996. Cloning and characterization of the ALG3 gene of Saccharomyces cerevisiae. *Glycobiology*, 6(4), pp.439–444.

Aebi, M. et al., 2010. N-glycan structures: recognition and processing in the ER. *Trends in Biochemical Sciences*, 35(2), pp.74–82.

Albright, C.F. & Robbins, P.W., 1990. The sequence and transcript heterogeneity of the yeast gene ALG1, an essential mannosyltransferase involved in N-glycosylation. *Journal of Biological Chemistry*, 265(12), pp.7042–7049.

Baenzigers, U., 1979. Structural Determinants Oligosaccharides * of Concanavalin A Specificity for. , 254(7), pp.2400–2407.

Bantscheff, M. et al., 2007. Quantitative mass spectrometry in proteomics: a critical review. *Analytical and bioanalytical chemistry*, 389(4), pp.1017–31.

Bause, E., 1984. Model studies on N -glycosylation of proteins. *Biochemical Society Transactions*, 12(3), pp.514–517.

Bause, E. & Legler, G., 1981. The role of the hydroxy amino acid in the triplet sequence Asn-Xaa-Thr(Ser) for the N-glycosylation step during glycoprotein biosynthesis. *The Biochemical journal*, 195(3), pp.639–44.

Beck, F. et al., 2011. The good, the bad, the ugly: validating the mass spectrometric analysis of modified peptides. *Proteomics*, 11(6), pp.1099–109.

van Berkel, M.A. et al., 1999. The Saccharomyces cerevisiae CWH8 gene is required for full levels of dolichol-linked oligosaccharides in the endoplasmic reticulum and for efficient N-glycosylation. *Glycobiology*, 9(3), pp.243–253.

Bickel, T. et al., 2005. Biosynthesis of lipid-linked oligosaccharides in Saccharomyces cerevisiae: Alg13p and Alg14p form a complex required for the formation of GlcNAc 2-PP-dolichol. *Journal of Biological Chemistry*, 280(41), pp.34500–34506.

Boles, E. et al., 1994. A family of hexosephosphate mutases in Saccharomyces cerevisiae. *European journal of biochemistry*, 220(1), pp.83–96.

Braakman, I. & Hebert, D.N., 2013. Protein folding in the endoplasmic reticulum. *Cold Spring Harbor perspectives in biology*, 5(5), p.a013201.

Breitling, J. & Aebi, M., 2013. *N* -Linked Protein Glycosylation in the Endoplasmic Reticulum. *Cold Spring Harbor Perspectives in Biology*.

Breuer, W. et al., 2001. Oligosaccharyltransferase is highly specific for the hydroxy amino acid in Asn-Xaa-Thr/Ser. *FEBS Letters*, 501, pp.106–110.

Burda, P. et al., 1999. Ordered assembly of the asymmetrically branched lipid-linked oligosaccharide in the endoplasmic reticulum is ensured by the substrate specificity of the individual glycosyltransferases. *Glycobiology*, 9(6), pp.617–625.

Burda, P. & Aebi, M., 1998. The ALG10 locus of Saccharomycescerevisiae encodes the alpha-1,2 glucosyltransferase of the endoplasmic reticulum: the terminal glucose of the lipid-linked oligosaccharide is required for efficient N-linked glycosylation. *Glycobiology*, 8(5), pp.455–462.

Burda, P. & Aebi, M., 1999. The dolichol pathway of N-linked glycosylation. *Biochimica et Biophysica Acta -*

General Subjects, 1426(2), pp.239–257.

Cantagrel, V. et al., 2010. SRD5A3 Is Required for Converting Polyprenol to Dolichol and Is Mutated in a Congenital Glycosylation Disorder. *Cell*, 142(2), pp.203–217.

Chantret, I. et al., 2005. Two proteins homologous to the N- and C-terminal domains of the bacterial glycosyltransferase Murg are required for the second step of dolichyl-linked oligosaccharide synthesis in Saccharomyces cerevisiae. *The Journal of biological chemistry*, 280(10), pp.9236–42.

Chapman, R., Sidrauski, C. & Walter, P., 1998. Intracellular signaling from the endoplasmic reticulum to the nucleus. *Annual review of cell and developmental biology*, 14, pp.459–485.

Chatterjee, B.P. et al., 1985. Jackfruit (Artocarpus integrifolia) and the Agaricus mushroom lectin fit also to the so-called peanut receptor. *Behring Institute Mitteilungen*, (78), pp.148–58.

Chojnacki, T. & Dallner, G., 1988. The biological role of dolichol. *The Biochemical journal*, 251(1), pp.1–9.

Christianson, J.C. & Ye, Y., 2014. Cleaning up in the endoplasmic reticulum: ubiquitin in charge. *Nature structural & molecular biology*, 21(4), pp.325–35.

Cipollo, J.F. et al., 2001. *The Yeast ALG11 Gene Specifies Addition of the Terminal α-1,2-Man to the Man5GlcNAc2-PP-dolichol N-Glycosylation Intermediate Formed on the Cytosolic Side of the Endoplasmic Reticulum*,

Cipollo, J.F. & Trimble, R.B., 2000. The accumulation of man6GlcNAc2-PP-dolichol in the Saccharomyces cerevisiae δalg9 mutant reveals a regulatory role for the Alg3p α1,3-Man middle-arm addition in downstream oligosaccharide-lipid and glycoprotein glycan processing. *Journal of Biological Chemistry*, 275(6), pp.4267–4277.

Cipollo, J.F. & Trimble, R.B., 2002. The Saccharomyces cerevisiae alg12 Δ mutant reveals a role for the middle-arm α 1 , 2Man- and upper-arm α 1 , 2Man α 1 , 6Man- residues of Glc 3 Man 9 GlcNAc 2 -PP-Dol in regulating glycoprotein glycan processing in the endoplasmic reticulum and Golgi app. , 12(11), pp.749–762.

Cossins, J. et al., 2013. Congenital myasthenic syndromes due to mutations in ALG2 and ALG14. *Brain*, 136(3), pp.944–956.

Couto, J.R., Huffaker, T.C. & Robbins, P.W., 1984. Cloning and expression in Escherichia coli of a yeast mannosyltransferase from the asparagine-linked glycosylation pathway. *The Journal of biological chemistry*, 259(1), pp.378–82.

Daran, J.M. et al., 1995. Genetic and biochemical characterization of the UGP1 gene encoding the UDP-glucose pyrophosphorylase from Saccharomyces cerevisiae. *European journal of biochemistry*, 233(2), pp.520–30.

Debray, H. et al., 2005. Specificity of Twelve Lectins Towards Oligosaccharides and Glycopeptides Related to N-Glycosylproteins. *European Journal of Biochemistry*, 117(1), pp.41–51.

Dickinson, J.R., 1991. Biochemical and genetic studies on the function of, and relationship between, the PGI1- and CDC30-encoded phosphoglucose isomerases in Saccharomyces cerevisiae. *Journal of general microbiology*, 137(4), pp.765–70.

Doerrler, W.T. & Lehrman, M. a, 1999. Regulation of the dolichol pathway in human fibroblasts by the endoplasmic reticulum unfolded protein response. *Proceedings of the National Academy of Sciences of the United States of America*, 96(23), pp.13050–5.

Dumax-Vorzet, A., Roboti, P. & High, S., 2013. OST4 is a subunit of the mammalian oligosaccharyltransferase required for efficient N-glycosylation. *Journal of cell science*, 126(Pt 12), pp.2595–606.

Ellgaard, L. & Helenius, A., 2003. Quality control in the endoplasmic reticulum. *Nature reviews.Molecular cell biology*, 4(3), pp.181–191.

Farid, A. et al., 2011. Arabidopsis thaliana alpha1,2-glucosyltransferase (ALG10) is required for efficient N-glycosylation and leaf growth. *The Plant journal : for cell and molecular biology*, 68(2), pp.314–25.

Fernandez, F. et al., 2001. The CWH8 Gene Encodes a Dolichyl Pyrophosphate Phosphatase with a Luminally

Oriented Active Site in the Endoplasmic Reticulum of Saccharomyces cerevisiae. *Journal of Biological Chemistry*, 276(44), pp.41455–41464.

Frank, C.G. & Aebi, M., 2005. ALG9 mannosyltransferase is involved in two different steps of lipid-linked oligosaccharide biosynthesis. *Glycobiology*, 15(11), pp.1156–1163.

Frank, D.W. & Waechter, C.J., 1998. Purification and characterization of a polyisoprenyl phosphate phosphatase from pig brain. Possible dual specificity. *The Journal of biological chemistry*, 273(19), pp.11791–8.

Frazer, L.N. & O'Keefe, R.T., 2007. A new series of yeast shuttle vectors for the recovery and identification of multiple plasmids from Saccharomyces cerevisiae. *Yeast (Chichester, England)*, 24(9), pp.777–89.

Freeze, H.H., 2006. Genetic defects in the human glycome. *Nature reviews. Genetics*, 7(7), pp.537–51.

Gallien, S. et al., 2012. Targeted proteomic quantification on quadrupole-orbitrap mass spectrometer. *Molecular & cellular proteomics : MCP*, 11(12), pp.1709–23.

Gao, X.D., Nishikawa, A. & Dean, N., 2004. Physical interactions between the Alg1, Alg2, and Alg11 mannosyltransferases of the endoplasmic reticulum. *Glycobiology*, 14(6), pp.559–570.

Gauss, R. et al., 2011. A complex of Pdi1p and the mannosidase Htm1p initiates clearance of unfolded glycoproteins from the endoplasmic reticulum. *Molecular cell*, 42(6), pp.782–93.

Gayen, S. & Kang, C., 2011. Solution structure of a human minimembrane protein Ost4, a subunit of the oligosaccharyltransferase complex. *Biochemical and biophysical research communications*, 409(3), pp.572–6.

Gerber, S. et al., 2013. Mechanism of bacterial oligosaccharyltransferase: in vitro quantification of sequon binding and catalysis. *The Journal of biological chemistry*, 288(13), pp.8849–61.

Gillet, L.C. et al., 2012. Targeted data extraction of the MS/MS spectra generated by data-independent acquisition: a new concept for consistent and accurate proteome analysis. *Molecular & cellular proteomics : MCP*, 11(6), p.O111.016717.

Goldstein, J.L. & Brown, M.S., 1990. Regulation of the mevalonate pathway. *Nature*, 343, pp.425–430.

Grabińska, K. & Palamarczyk, G., 2002. Dolichol biosynthesis in the yeast *Saccharomyces cerevisiae*: An insight into the regulatory role of farnesyl diphosphate synthase. *FEMS Yeast Research*, 2, pp.259–265.

Haecker, A. et al., 2008. Wollknauel is required for embryo patterning and encodes the Drosophila ALG5 UDP-glucose:dolichyl-phosphate glucosyltransferase. *Development (Cambridge, England)*, 135(10), pp.1745–9.

Haeuptle, M.A. & Hennet, T., 2009. Congenital disorders of glycosylation: An update on defects affecting the biosynthesis of dolichol-linked oligosaccharides. *Human Mutation*, 30(12), pp.1628–1641.

Hägglund, P. et al., 2004. A New Strategy for Identification of N-Glycosylated Proteins and Unambiguous Assignment of Their Glycosylation Sites Using HILIC Enrichment and Partial Deglycosylation. *Journal of Proteome Research*, 3(3), pp.556–566.

Hanson, S.R. et al., 2009. The core trisaccharide of an N-linked glycoprotein intrinsically accelerates folding and enhances stability. *Proceedings of the National Academy of Sciences of the United States of America*, 106(9), pp.3131–6.

Hashimoto, H. et al., 1997. Saccharomyces cerevisiae VIG9 encodes GDP-mannose pyrophosphorylase, which is essential for protein glycosylation. *Journal of Biological Chemistry*, 272(26), pp.16308–16314.

te Heesen, S. et al., 1994. Isolation of the ALG5 locus encoding the UDP-glucose:dolichyl-phosphate glucosyltransferase from Saccharomyces cerevisiae. *European Journal of Biochemistry*, 224(1), pp.71–79.

te Heesen, S. et al., 1993. Yeast Wbp1p and Swp1p form a protein complex essential for oligosaccharyl transferase activity. , 12(1), pp.279–284.

Helenius, A. & Aebi, M., 2004. Roles of N-linked glycans in the endoplasmic reticulum. *Annual review of biochemistry*, 73, pp.1019–49.

Helenius, J. et al., 2002. Translocation of lipid-linked oligosaccharides across the ER membrane requires Rft1 protein. *Nature*, 415(6870), pp.447–50.

Heller, L., Orlean, P. & Adair, W.L., 1992. Saccharomyces cerevisiae sec59 cells are deficient in dolichol kinase activity. *Proceedings of the National Academy of Sciences of the United States of America*, 89(15), pp.7013–6.

Hennet, T., 2012. Diseases of glycosylation beyond classical congenital disorders of glycosylation. *Biochimica et Biophysica Acta - General Subjects*, 1820(9), pp.1306–1317.

Hese, K. et al., 2009. The yeast oligosaccharyltransferase complex can be replaced by STT3 from Leishmania major. *Glycobiology*, 19(2), pp.160–171.

Hong, Q. et al., 2013. Absolute quantitation of immunoglobulin G and its glycoforms using multiple reaction monitoring. *Analytical chemistry*, 85(18), pp.8585–93.

Huffaker, T.C. & Robbins, P.W., 1983. Yeast mutants deficient in protein glycosylation. *Proceedings of the National Academy of Sciences of the United States of America*, 80(24), pp.7466–70.

Izquierdo, L. et al., 2009. Distinct donor and acceptor specificities of Trypanosoma brucei oligosaccharyltransferases. *The EMBO journal*, 28(17), pp.2650–61.

Jackson, B.J., Kukuruzinska, M.A. & Robbins, P., 1993. Biosynthesis of asparagine-linked oligosaccharides in Saccharomyces cerevisiae: the alg2 mutation. *Glycobiology*, 3(4), pp.357–64.

Jakob, C.A. et al., 1998. Genetic tailoring of N-linked oligosaccharides: the role of glucose residues in glycoprotein processing of Saccharomyces cerevisiae in vivo. *Glycobiology*, 8(2), pp.155–64.

Jamaluddin, M.F.B. et al., 2011. Polypeptide binding specificities of saccharomyces cerevisiae oligosaccharyltransferase accessory proteins Ost3p and Ost6p. *Protein Science*, 20(5), pp.849–855.

Jung, P. & Tanner, W., 1973. Identification of the Lipid Intermediate in Yeast Mannan Biosynthesis. *European Journal of Biochemistry*, 37(1), pp.1–6.

Kampf, M. et al., 2009. Biochemical characterization and membrane topology of Alg2 from Saccharomyces cerevisiae as a bifunctional a-1,3- and 1,6-mannosyltransferase involved in lipid-linked oligosaccharide biosynthesis. *Journal of Biological Chemistry*, 284(18), pp.11900–11912.

Karaoglu, D., Kelleher, D.J. & Gilmore, R., 1997. The Highly Conserved Stt3 Protein Is a Subunit of the Yeast Oligosaccharyltransferase and Forms a Subcomplex with Ost3p and Ost4p. *Journal of Biological Chemistry*, 272(51), pp.32513–32520.

Kelleher, D.J. et al., 2007. Dolichol-linked oligosaccharide selection by the oligosaccharyltransferase in protist and fungal organisms. *Journal of Cell Biology*, 177(1), pp.29–37.

Kelleher, D.J. et al., 2003. Oligosaccharyltransferase isoforms that contain different catalytic STT3 subunits have distinct enzymatic properties. *Molecular Cell*, 12(1), pp.101–111.

Kelleher, D.J. & Gilmore, R., 2006. An evolving view of the eukaryotic oligosaccharyltransferase. *Glycobiology*, 16(4), pp.47–62.

Kim, Y.J. et al., 2012. Mass spectrometry-based detection and quantification of plasma glycoproteins using selective reaction monitoring. *Nature protocols*, 7(5), pp.859–71.

Kohda, D. et al., 2007. New oligosaccharyltransferase assay method. *Glycobiology*, 17(11), pp.1175–82.

Kukuruzinska, M. a & Robbins, P.W., 1987. Protein glycosylation in yeast: transcript heterogeneity of the ALG7 gene. *Proceedings of the National Academy of Sciences of the United States of America*, 84(8), pp.2145–9.

Kumar, V., Heinemann, F.S. & Ozols, J., 1994. Purification and characterization of avian oligosaccharyltransferase. Complete amino acid sequence of the 50-kDa subunit. *The Journal of biological chemistry*, 269(18), pp.13451–7.

Lairson, L.L. et al., 2008. Glycosyltransferases: Structures, Functions, and Mechanisms. *Annual Review of*

Biochemistry, 77(1), pp.521–555.

Larkin, A. & Imperiali, B., 2011. The expanding horizons of asparagine-linked glycosylation. *Biochemistry*, 50(21), pp.4411–26.

Lee, A. et al., 2010. The lectin riddle: glycoproteins fractionated from complex mixtures have similar glycomic profiles. *Omics : a journal of integrative biology*, 14(4), pp.487–99.

Liu, Y. et al., 2013. Quantitative measurements of N-linked glycoproteins in human plasma by SWATH-MS. *Proteomics*, 13(8), pp.1247–56.

Lizak, C. et al., 2013. Unexpected reactivity and mechanism of carboxamide activation in bacterial N-linked protein glycosylation. *Nature communications*, 4, p.2627.

Lizak, C. et al., 2011. X-ray structure of a bacterial oligosaccharyltransferase. *Nature*, 474(7351), pp.350–355.

Löw, P. et al., 1991. The mevalonate pathway in the bloodstream form of Trypanosoma brucei: Identification of dolichols containing 11 and 12 isoprene residues. *Journal of Biological Chemistry*, 266(29), pp.19250–19257.

Lu, J. et al., 2012. Alg14 organizes the formation of a multiglycosyltransferase complex involved in initiation of lipid-linked oligosaccharide biosynthesis. *Glycobiology*, 22(4), pp.504–516.

MacLean, B. et al., 2010. Skyline: An open source document editor for creating and analyzing targeted proteomics experiments. *Bioinformatics*, 26(7), pp.966–968.

Maeda, Y. et al., 1998. DPM2 regulates biosynthesis of dolichol phosphate-mannose in mammalian cells: Correct subcellular localization and stabilization of DPM1, and binding of dolichol phosphate. *EMBO Journal*, 17(17), pp.4920–4929.

Maeda, Y., Tanaka, S. & Hino, J., 2000. Maeda_y et al 2001. , 19(11), pp.2475–2482.

Manthri, S. et al., 2008. Deletion of the TbALG3 gene demonstrates site-specific N-glycosylation and N-glycan processing in Trypanosoma brucei. *Glycobiology*, 18(5), pp.367–383.

Marshall, R., 1972. Glycoproteins. *Annu. Rev. Biochem*, 41(34), pp.673–702.

Milewski, S., Gabriel, I. & Olchowy, J., 2006. Enzymes of UDP-GlcNAc biosynthesis in yeast. *Yeast*, 23(1), pp.1–14.

Mohd Yusuf, S.N.H. et al., 2013. Mixed disulfide formation in vitro between a glycoprotein substrate and yeast oligosaccharyltransferase subunits Ost3p and Ost6p. *Biochemical and Biophysical Research Communications*, 432(3), pp.438–443.

Mohorko, E., Glockshuber, R. & Aebi, M., 2011. Oligosaccharyltransferase: The central enzyme of N-linked protein glycosylation. *Journal of Inherited Metabolic Disease*, 34(4), pp.869–878.

Moremen, K.W., Tiemeyer, M. & Nairn, A. V, 2012. Vertebrate protein glycosylation: diversity, synthesis and function. *Nature reviews. Molecular cell biology*, 13(7), pp.448–462.

Mueller, S. et al., 2015. Protein degradation corrects for imbalanced subunit stoichiometry in OST complex assembly. *Molecular Biology of the Cell*, 26(14), pp.2596–2608.

Nasab, F.P. et al., 2008. All in One: Leishmania major STT3 Proteins Substitute for the Whole Oligosaccharyltransferase Complex in Saccharomyces cerevisiae. *Molecular Biology of the Cell*, 19, pp.3758–3768.

Neue, K. et al., 2011. Elucidation of glycoprotein structures by unspecific proteolysis and direct nanoESI mass spectrometric analysis of ZIC-HILIC-enriched glycopeptides. *Journal of proteome research*, 10(5), pp.2248–60.

Ni, X., Canuel, M. & Morales, C.R., 2006. The sorting and trafficking of lysosomal proteins. *Histology and Histopathology*, 21(7–9), pp.899–913.

Nilsson, I. et al., 2003. Photocross-linking of nascent chains to the STT3 subunit of the oligosaccharyltransferase complex. *The Journal of cell biology*, 161(4), pp.715–25.

Nilsson, I. & Von Heijne, G., 2000. Glycosylation efficiency of Asn-Xaa-Thr sequons depends both on the distance from the C terminus and on the presence of a downstream transmembrane segment. *Journal of Biological Chemistry*, 275(23), pp.17338–17343.

Noffz, C., Keppler-Ross, S. & Dean, N., 2009. Hetero-oligomeric interactions between early glycosyltransferases of the dolichol cycle. *Glycobiology*, 19(5), pp.472–8.

O'Reilly, M.K., Zhang, G. & Imperiali, B., 2006. In vitro evidence for the dual function of Alg2 and Alg11: Essential mannosyltransferases in N-linked glycoprotein biosynthesis. *Biochemistry*, 45(31), pp.9593–9603.

Ong, S.-E., 2002. Stable Isotope Labeling by Amino Acids in Cell Culture, SILAC, as a Simple and Accurate Approach to Expression Proteomics. *Molecular & Cellular Proteomics*, 1(5), pp.376–386.

Ong, S. & Mann, M., 2006. A practical recipe for stable isotope labeling by amino acids in cell culture (SILAC). *Nature protocols*, 1(6), pp.2650–2660.

Orlean, P., 1990. Dolichol phosphate mannose synthase is required in vivo for glycosyl phosphatidylinositol membrane anchoring, O mannosylation, and N glycosylation of protein in Saccharomyces cerevisiae. *Molecular and Cellular Biology*, 10(11), pp.5796–805.

Pasing, Y., Sickmann, A. & Lewandrowski, U., 2012. N-glycoproteomics: Mass spectrometry-based glycosylation site annotation. *Biological Chemistry*, 393(4), pp.249–258.

Pattison, R.J. & Amtmann, A., 2009. N-glycan production in the endoplasmic reticulum of plants. *Trends in plant science*, 14(2), pp.92–9.

Perez, C. et al., 2015. Structure and mechanism of an active lipid-linked oligosaccharide flippase. *Nature*, 524(7566), pp.433–438.

Peterson, A.C. et al., 2012. Parallel reaction monitoring for high resolution and high mass accuracy quantitative, targeted proteomics. *Molecular & cellular proteomics : MCP*, 11(11), pp.1475–88.

Petrescu, A.-J. et al., 2004. Statistical analysis of the protein environment of N-glycosylation sites: implications for occupancy, structure, and folding. *Glycobiology*, 14(2), pp.103–14.

Picotti, P. et al., 2009. Full dynamic range proteome analysis of S. cerevisiae by targeted proteomics. *Cell*, 138(4), pp.795–806.

Quan, E.M. et al., 2008. Defining the glycan destruction signal for endoplasmic reticulum-associated degradation. *Molecular cell*, 32(6), pp.870–7.

Reiss, G. et al., 1997. A specific screen for oligosaccharyltransferase mutations identifies the 9 kDa OST5 protein required for optimal activity in vivo and in vitro. *The EMBO journal*, 16(6), pp.1164–72.

Reiss, G. et al., 1996. Isolation of the ALG6 locus of Saccharomyces cerevisiae required for glucosylation in the N-linked glycosylation pathway. *Glycobiology*, 6(5), pp.493–498.

Rine, J. et al., 1983. Targeted selection of recombinant clones through gene dosage effects (Sacchwromyce cerevisiae/recombinant DNA/metabolic inhibitors/UDP-N-acetylglucosamine-l-P transferase/ 3-hydroxy-3-methy glutaryl CoA reductase). *Biochemistry*, 80(November), pp.6750–6754.

Rip, J.W. et al., 1985. Distribution, metabolism and function of dolichol and polyprenols. *Progress in Lipid Research*, 24(4), pp.269–309.

Robinson, G.W. et al., 1993. Conservation between human and fungal squalene synthetases: similarities in structure, function, and regulation. *Molecular and cellular biology*, 13(5), pp.2706–2717.

Röst, H.L. et al., 2014. OpenSWATH enables automated, targeted analysis of data-independent acquisition MS data. *Nature biotechnology*, 32(3), pp.219–23.

Ruiz-Canada, C., Kelleher, D.J. & Gilmore, R., 2009. Cotranslational and Posttranslational N-Glycosylation of Polypeptides by Distinct Mammalian OST Isoforms. *Cell*, 136(2), pp.272–283.

Runge, K.W. & Robbins, P.W., 1986. A new yeast mutation in the glucosylation steps of the asparagine-linked

glycosylation pathway. Formation of a novel asparagine-linked oligosaccharide containing two glucose residues. *Journal of Biological Chemistry*, 261(33), pp.15582–15590.

Rush, J.S. et al., 1998. Transbilayer movement of Glc-P-dolichol and its function as a glucosyl donor: Protein-mediated transport of a water-soluble analog into sealed ER vesicles from pig brain. *Glycobiology*, 8(12), pp.1195–1205.

Rush, J.S. & Waechter, C.J., 1995. Transmembrane movement of a water-soluble analogue of mannosylphosphoryldolichol is mediated by an endoplasmic reticulum protein. *The Journal of cell biology*, 130(3), pp.529–36.

Sagami, H., Kurisaki, A. & Ogura, K., 1993. Formation of dolichol from dehydrodolichol is catalyzed by NADPH-dependent reductase localized in microsomes of rat liver. *The Journal of biological chemistry*, 268(14), pp.10109–13.

Sanyal, S., Frank, C.G. & Menon, A.K., 2008. Distinct flippases translocate glycerophospholipids and oligosaccharide diphosphate dolichols across the endoplasmic reticulum. *Biochemistry*, 47(30), pp.7937–7946.

Sanyal, S. & Menon, A.K., 2009. Specific transbilayer translocation of dolichol-linked oligosaccharides by an endoplasmic reticulum flippase. *Proceedings of the National Academy of Sciences of the United States of America*, 106(3), pp.767–72.

Sanyal, S. & Menon, A.K., 2010. Stereoselective transbilayer translocation of mannosyl phosphoryl dolichol by an endoplasmic reticulum flippase. *Proc Natl Acad Sci USA*, 107(25), pp.11289–11294.

Schenk, B., Fernandez, F. & Waechter, C.J., 2001. The ins(ide) and out(side) of dolichyl phosphate biosynthesis and recycling in the endoplasmic reticulum. *Glycobiology*, 11(5), p.61R–70R.

Schulz, B.L. et al., 2009. Oxidoreductase activity of oligosaccharyltransferase subunits Ost3p and Ost6p defines site-specific glycosylation efficiency. *Proceedings of the National Academy of Sciences of the United States of America*, 106(27), pp.11061–6.

Schulz, B.L. & Aebi, M., 2009. Analysis of glycosylation site occupancy reveals a role for Ost3p and Ost6p in site-specific N-glycosylation efficiency. *Molecular & cellular proteomics : MCP*, 8(18), pp.357–364.

Schwarz, F. & Aebi, M., 2011. Mechanisms and principles of N-linked protein glycosylation. *Current Opinion in Structural Biology*, 21(5), pp.576–582.

Schwarz, M., Knauer, R. & Lehle, L., 2005. Yeast oligosaccharyltransferase consists of two functionally distinct sub-complexes, specified by either the Ost3p or Ost6p subunit. *FEBS Letters*, 579(29), pp.6564–6568.

Shaik, K.S. et al., 2011. The Alg5 ortholog Wollknäuel is essential for correct epidermal differentiation during Drosophila late embryogenesis. *Glycobiology*, 21(6), pp.743–56.

Shakin-Eshleman, S.H., Spitalnik, S.L. & Kasturi, L., 1996. The Amino Acid at the X Position of an Asn- X -Ser Sequon Is an Important Determinant of N -Linked Core-glycosylation Efficiency *. *The Journal of Biological Chemistry*, 271(11), pp.6363–6366.

Sharma, C.B., Knauer, R. & Lehle, L., 2001. Biosynthesis of lipid-linked oligosaccharides in yeast: The ALG3 gene encodes the Dol-P-Man:Man5GlcNAc2-PP-Dol Mannosyltransferase. *Biological Chemistry*, 382(2), pp.321–328.

Shridas, P. & Waechter, C.J., 2006. Human Dolichol Kinase, a Polytopic Endoplasmic Reticulum Membrane Protein with a Cytoplasmically Oriented CTP-binding Site. *Journal of Biological Chemistry*, 281(42), pp.31696–31704.

Shrimal, S., Trueman, S.F. & Gilmore, R., 2013. Extreme C-terminal sites are posttranslocationally glycosylated by the STT3B isoform of the OST. *Journal of Cell Biology*, 201(1), pp.81–95.

Silberstein, S., 1995. The essential OST2 gene encodes the 16-kD subunit of the yeast oligosaccharyltransferase, a highly conserved protein expressed in diverse eukaryotic organisms. *The Journal of Cell Biology*, 131(2), pp.371–383.

Snider, M.D. & Rogers, O.C., 1984. Transmembrane movement of oligosaccharide-lipids during glycoprotein synthesis. *Cell*, 36(3), pp.753–761.

Spirig, U. et al., 2005. The 3.4-kDa Ost4 protein is required for the assembly of two distinct oligosaccharyltransferase complexes in yeast. *Glycobiology*, 15(12), pp.1396–1406.

Spirig, U. et al., 1997. The STT3 protein is a component of the yeast oligosaccharyltransferase complex. *Molecular & general genetics : MGG*, 256(6), pp.628–37.

Srinivasan, A. & Coward, J.K., 2002. A Biotin Capture Assay for Oligosaccharyltransferase. *Analytical Biochemistry*, 306(2), pp.328–335.

Stagljar, I., te Heesen, S. & Aebi, M., 1994. New phenotype of mutations deficient in glucosylation of the lipid-linked oligosaccharide: cloning of the ALG8 locus. *Proc Natl Acad Sci USA*, 91(13), pp.5977–5981.

Steen, H. & Mann, M., 2004. The ABC's (and XYZ's) of peptide sequencing. *Nature reviews. Molecular cell biology*, 5(9), pp.699–711.

Szkopińska, A. et al., 1993. The deficiency of sterol biosynthesis in Saccharomyces cerevisiae affects the synthesis of glycosyl derivatives of dolichyl phosphates. *FEMS microbiology letters*, 112(3), pp.325–328.

Tai, V.W.F. & Imperiali, B., 2001. Substrate specificity of the glycosyl donor for oligosaccharyl transferase. *Journal of Organic Chemistry*, 66(19), pp.6217–6228.

Takatsuki, A., Arima, K. & Tamura, G., 1971. Tunicamycin, a new antibiotic: 1. Isolation and characterization of tunicamycin. *The Journal of Antibiotics*, 24(4), pp.215–223.

Tarentino, A.L., Gomez, C.M. & Plummer, T.H., 1985. Deglycosylation of asparagine-linked glycans by peptide:N-glycosidase F. *Biochemistry*, 24(17), pp.4665–4671.

Tarentino, A.L., Plummer, T.H. & Maley, F., 1974. The release of intact oligosaccharides from specific glycoproteins by endo ?? N acetylglucosaminidase H. *Journal of Biological Chemistry*, 249(3), pp.818–824.

Thibault, G. & Ng, D.T.W., 2012. The endoplasmic reticulum-associated degradation pathways of budding yeast. *Cold Spring Harbor perspectives in biology*, 4(12), pp.a013193–a013193.

Timal, S. et al., 2012. Gene identification in the congenital disorders of glycosylation type i by whole-exome sequencing. *Human Molecular Genetics*, 21(19), pp.4151–4161.

Travers, K.J. et al., 2000. Functional and genomic analyses reveal an essential coordination between the unfolded protein response and ER-associated degradation. *Cell*, 101(3), pp.249–258.

Tretter, V., Altmann, F. & Marz, L., 1991. Peptide-N4-(N-acetyl-beta-glucosaminyl)asparagine amidase F cannot release glycans with fucose attached alpha1 3 to the asparagine-linked N-acetylglucosamine residue. *European Journal of Biochemistry*, 199(3), pp.647–652.

Verosteks, M.F. et al., 1993. Glycoprotein Biosynthesis in the alg3 Saccharomyces cerevisiae Mutant. *The Journal of Biological Chemistry*, 268(16), pp.12095–12103.

Wacker, M., 2002. N-Linked Glycosylation in Campylobacter jejuni and Its Functional Transfer into E. coli. *Science*, 298(5599), pp.1790–1793.

Wiesner, J., Premsler, T. & Sickmann, A., 2008. Application of electron transfer dissociation (ETD) for the analysis of posttranslational modifications. *Proteomics*, 8(21), pp.4466–83.

Wilson, C.M. & High, S., 2007. Ribophorin I acts as a substrate-specific facilitator of N-glycosylation. *Journal of cell science*, 120(Pt 4), pp.648–657.

Wilson, C.M., Roebuck, Q. & High, S., 2008. Ribophorin I regulates substrate delivery to the oligosaccharyltransferase core. *Proceedings of the National Academy of Sciences of the United States of America*, 105(28), pp.9534–9.

Wu, C.C. & MacCoss, M.J., 2002. Shotgun proteomics: tools for the analysis of complex biological systems. *Current opinion in molecular therapeutics*, 4(3), pp.242–50.

Xu, T. & Coward, J.K., 1997. 13C- and 15N-labeled peptide substrates as mechanistic probes of oligosaccharyltransferase. *Biochemistry*, 36(48), pp.14683–9.

Xu, Y. et al., 2014. Identification of salivary N-glycoproteins and measurement of glycosylation site occupancy by boronate glycoprotein enrichment and liquid chromatography/electrospray ionization tandem mass spectrometry. *Rapid communications in mass spectrometry : RCM*, 28(5), pp.471–82.

Xu, Y., Bailey, U.M. & Schulz, B.L., 2015. Automated measurement of site-specific N-glycosylation occupancy with SWATH-MS. *Proteomics*, 15(13), pp.2177–2186.

Yan, A. et al., 2003. New findings on interactions among the yeast oligosaccharyl transferase subunits using a chemical cross-linker. *The Journal of biological chemistry*, 278(35), pp.33078–87.

Yan, Q. & Lennarz, W.J., 2002. Studies on the function of oligosaccharyl transferase subunits. Stt3p is directly involved in the glycosylation process. *The Journal of biological chemistry*, 277(49), pp.47692–700.

Yu, Y., Sabatini, D.D. & Kreibich, G., 1990. Antiribophorin antibodies inhibit the targeting to the ER membrane of ribosomes containing nascent secretory polypeptides. *Journal of Cell Biology*, 111(4), pp.1335–1342.

Zacchi, L. & Schulz, B.L., 2016. SWATH-MS glycoproteomics reveals consequences of defects in the glycosylation machinery. *Molecular & Cellular Proteomics*, 15, pp.2435–2447.

Zattas, D. & Hochstrasser, M., 2015. Ubiquitin-dependent Protein Degradation at the Yeast Endoplasmic Reticulum and Nuclear Envelope. *Crit Rev Biochem Mol Biol.*, 50(1), pp.1–17.

Zhang, H. et al., 2003. Identification and quantification of N-linked glycoproteins using hydrazide chemistry, stable isotope labeling and mass spectrometry. *Nature biotechnology*, 21(6), pp.660–6.

Zielinska, D.F. et al., 2012. Mapping N-Glycosylation Sites across Seven Evolutionarily Distant Species Reveals a Divergent Substrate Proteome Despite a Common Core Machinery. *Molecular Cell*, 46(4), pp.542–548.

Zielinska, D.F. et al., 2010. Precision mapping of an in vivo N-glycoproteome reveals rigid topological and sequence constraints. *Cell*, 141(5), pp.897–907.

Chapter 2

Quantitative Profiling of N-linked Glycosylation Machinery in Yeast *Saccharomyces cerevisiae*

Kristina Poljak, Nathalie Selevsek, Jonas Grossmann, Elsy Ngwa, Marie Estelle, and Markus Aebi

Contributions:

Setting up SILAC-PRM method.

Construction of strains

Preparation of samples for mass spectrometry.

PRM and shotgun MS measurements.

Data analysis.

Writing the manuscript.

Summary

Asparagine-linked glycosylation is a common posttranslational protein modification regulating the structure, stability and function of many proteins. N-linked glycosylation machinery involves enzymes responsible for the assembly of the lipid-linked oligosaccharide (LLO), which is then transferred to the asparagine residues on the polypeptides by the enzyme oligosaccharyltransferase (OST). A major goal in the study of protein glycosylation is the establishment of quantitative methods for the analysis of site-specific extent of glycosylation. Here, we developed a sensitive approach to examine glycosylation site occupancy in *Saccharomyces cerevisiae* by coupling stable isotope labelling (SILAC) approach to parallel reaction monitoring (PRM) mass spectrometry (MS). Combined with genetic tools, this analysis allowed identification of novel glycosylation sites dependent on the Ost3p and Ost6p regulatory subunits of OST. Furthermore, we applied this approach to show that the glycosylation efficiency of the OST is influenced by the preceding binding of the LLO donor substrate and the folding speed of protein substrates. We also demonstrated the utility of our approach for the quantitative assessment of additional networks directly or indirectly connected to protein glycosylation.

Introduction

Glycosylation is a fundamental part of life whose impact and intricacy increase with the complexity of the organism (Dorota F Zielinska et al. 2012). Glycans affect protein folding, stability and degradation, they mediate interactions of all cells and regulate essential biological, chemical and physical processes (Varki 1993). Asparagine linked N-glycosylation is an essential modification of proteins conserved between eukaryotes, archaea and some bacteria (Szymanski & Wren 2005). In eukaryotes, the reaction is catalysed by oligosaccharyltransferase (OST) in the lumen of the endoplasmic reticulum (ER) (Kelleher & Gilmore 2006). Upon arrival of protein substrate to the lumen of the ER, the preassembled oligosaccharide is transferred, co-translationally or post-translationally, en bloc from the lipid carrier dolichol pyrophosphate (Dol-PP) to asparagines in selected glycosylation sequons (N-X-S/T; X≠P) (Kelleher & Gilmore 2006; Kelleher et al. 2007). After the oligosaccharide has been transferred, the N-linked glycan structure influences protein folding and helps ER quality control (ERQC) machinery to distinguish between folding intermediates, where only properly folded proteins are allowed to reach their final destinations through the secretory pathway (Aebi et al. 2010). Eventually if a polypeptide is not able to reach its native conformation, the misfolded glycoprotein will be recycled in the ER-associated degradation (ERAD) pathway (Zattas & Hochstrasser 2015). Alternatively, accumulation of unfolded proteins in the ER will lead to ER stress and activation of an unfolded protein response (UPR) pathway, where transcriptional induction of UPR target genes allows the cell to adjust the capacity of protein folding in the ER (Chapman et al. 1998; Travers et al. 2000). Many proteins are modified by glycans that can be crucial for protein folding, stability, transport, localization and/or function, hence the study of correct assembly of the N-linked glycans and its attachment to different protein substrates has been of great interest since (Larkin & Imperiali 2011).

In yeast, the N-linked glycosylation pathway starts with the assembly of the $Glc_3Man_9GlcNAc_2$ lipid-linked oligosaccharide (LLO) on a Dol-PP carrier on the ER membrane (Helenius & Aebi 2004; Breitling & Aebi 2013). The LLO is synthesized in a defined, stepwise manner by a series of enzymes belonging to the ALG (Asparagine-Linked Glycosylation) family (Burda & Aebi 1999). The process starts on the cytoplasmic side of the ER membrane, where $Man_5GlcNAc_2$ heptasaccharide is assembled on the Dol-PP by sequential action of the Alg7/Alg13/Alg14 and the Alg1/Alg2/Alg11 enzyme complexes (X.-D. Gao et al. 2004; Lu et al. 2012). These glycosyltransferases use nucleotide-activated sugars as donors. The LLO is then flipped onto the luminal side of the ER by a process requiring Rft1p (Helenius et al. 2002). The LLO is further elongated by the action of Alg3p, Alg9p, Alg12p, and again Alg9p that add four additional mannosyl residues. The LLO structure is completed by the action of three glucosyltransferases Alg6, Alg8 and Alg10. Unlike the cytoplasmic glycosyltransferases, lumenal ALG enzymes utilize Dol-P-bound sugars as donors and have a high LLO substrate specificity that ensures

an assembly of an optimal OST LLO substrate that exposes the terminal α-1,2-linked glucose (Lairson et al. 2008). As a result, Alg12p will only be able to add the α-1,6-linked Man residue to the α-1,2-linked Man, once α-1,2-linked Man has been attached by Alg9p (Jakob et al. 1998). Due to sequential nature of LLO biosynthesis, deficiencies in ALG enzymes result in accumulation of LLO intermediates. Truncated LLO structures will still be transferred by the OST though will a lower efficiency, resulting in the appearance of hypoglycosylated protein substrates (Karaoglu et al. 2001).

In higher eukaryotes, OST is a multiprotein complex consisting of different subunits (Stt3p, Ost1p, Ost5p, Wbp1p, Ost2p, Swp1p, Ost3p/Ost6p and Ost4p in yeast *S. cerevisiae*). Some protozoan, archaeal, and bacterial species have a single protein OST, homologous with Stt3p, the catalytic protein subunit of the eukaryotic OST (Kelleher & Gilmore 2006). From the phylogenetic analysis yeast STT3 is proposed to be a B type STT3 that is not associated with the translocon (Ruiz-Canada et al. 2009). As consensus sequons are required to be flexible in order to be accessible to the OST catalytic site, there is a competition between folding and glycosylation (Lizak et al. 2011). Consequently, OST has evolved ways of competing with protein folding. In yeast, the presence of either Ost3p or Ost6p results in two alternative OST complexes (Spirig et al. 2005). Both subunits have thioredoxin-like ER lumenal domains that transiently capture stretches of OST protein substrates in the ER through noncovalent or mixed disulfide bonds (Fetrow et al. 2001; Jamaluddin et al. 2011; Mohd Yusuf et al. 2013). The proposed role of these subunits is to increase the efficiency at particular glycosylation sites by guiding the catalytic site of OST to nearby sequons and inhibiting local polypeptide folding (Schulz et al. 2009; Jamaluddin et al. 2014). The roles of the additional subunits in the eukaryotic OST are mostly unknown but may be necessary for directing the glycosylation toward particular protein substrates and glycans.

Mass spectrometry (MS) has become the method of choice for the identification and quantification of N-linked glycoproteins (Zhang et al. 2003; Lazar et al. 2013; Liu et al. 2013; Parker et al. 2013; Song et al. 2013; Pan 2014; Xu et al. 2015; Yeo et al. 2016; Zacchi & Schulz 2016). MS assays relay on the elution time and precursor mass of the modified peptides, as well as the mass-to-charge ratio and relative intensity of specific fragment ions that indicate the sequence position of modified asparagine residues. Several MS techniques for measuring N-linked glycosylation site occupancy in yeast have been described utilizing different modes of operation for targeted glyco-peptide analysis, such as SRM (Selected Reaction Monitoring), SWAT (Sequential Window Acquisition of Targeted fragment ions) and data-independent techniques, such as SWATH (Sequential Window Acquisition of all Theoretical fragment ion spectra) (Xu et al. 2015; Zacchi & Schulz 2016; Yeo et al. 2016). These techniques have used isolation of the glycoprotein rich cell wall fraction for sample simplification. However, cell wall fractionation can introduce analytical bias as proteins that are inefficiently glycosylated in the ER tend to fold incorrectly and are prevented from trafficking out of the ER by ERQC mechanism (Aebi et al.

2010; Zattas & Hochstrasser 2015). In this paper, we describe a novel method for the identification and relative quantification of N-linked glycosylation occupancy and protein abundance of yeast membrane and luminal proteins using SILAC (Stable Isotope Labelling by Amino acids in Cell culture) strategy combined with PRM (Parallel Reaction Monitoring) based MS method. The PRM technique is currently the most powerful mode of targeted proteomics analyses for quantitative measurements in biological samples and this is the first time it is being exploited for quantitative analysis of N-linked glycosylation. We took advantage of the latest generation HRAM (High Resolution Accurate Mass) analysers usually utilized in PRM analyses, which dramatically increase the selectivity of measurements by reducing the signal interference in complex samples, and the accurate mass measurement capability, which enhances the confidence in the assignment of the fragment ions. Both qualities improve the analysis of low abundance peptides and enable us to successfully detect N-GlcNAc peptides, resulting from endoglycosidase H glycan release used in the sample preparation, without a prior glycoprotein and/or glyco-peptide enrichment. Furthermore, we used the SILAC strategy based on stable isotopes being incorporated into cellular proteome by *in vivo* metabolic labelling and mixing at the cellular level to achieve higher quantitative accuracy, thus minimizing handling bias (Ong 2002; Ong & Mann 2006). Heavy isotopes of arginine and lysine amino acids are added to yeast cultures and using tryptic digestion, which results in peptides containing either one lysine or one arginine residue, ratios of each peptide could be determined accurately in the SILAC samples. We decided to perform our analysis on yeast microsomal fractions, thus enriching for membrane and luminal proteins as those are the most abundant glycoproteins in yeast cells and by doing so are able to monitor glycosylation occupancy of all OST glycoproteins and several glycoproteins whose structures have been solved. This type of analysis provides us with quantitative results of increased precision and allows us to monitor an extended list of novel glycosylation sites, as compared to SRM, SWATH, SWAT or other proteomics approaches utilized before (Schulz & Aebi 2009; Xu et al. 2015; Zacchi & BL Schulz 2016; Yeo et al. 2016). We implemented newly developed SILAC PRM MS method, together with yeast genetic approaches, to analyse glycosylation occupancy as well as cellular abundance, since these have profound physiological effects and may fluctuate independently, of many glycoproteins in multiple yeast mutants. By simultaneous analysis of protein levels we are able to study the effect of glycosylation on protein folding and UPR activation. Finally, we exploited the ease of developing a directed PRM assay to quantify protein levels of a majority of proteins involved in mevalonate and ergosterol pathway, which enabled us to investigate the intricate connection between dolichol and ergosterol biosynthetic pathways.

Results

SILAC based PRM MS for quantitative profiling of N-glycoproteins in yeast

To design targeted MS assays for site-specific quantification of N-linked glycosylation site occupancy in yeast *Saccharomyces cerevisiae*, we focused on glycoproteins originating from microsomal fractions (Mueller et al. 2015). A schematic overview of our assay development and workflow is presented in Figure 1. In a discovery phase, glyco-peptides originating from microsomal fractions were enriched after proteinase digestion (Figure 1). Glycoproteins originating from microsomal fractions were digested sequentially with LysC and trypsin proteinase. The use of both proteinases, compared to the use of trypsin proteinase alone, has been shown to result in higher yields, higher reproducibility and more accurate quantification (McDonald et al. 2002). We enriched for glyco-peptides by solid-phase extraction (SPE) using zwitterionic hydrophilic interaction chromatography (ZIC-HILIC) to ensure high coverage of hydrophilic N-linked glyco-peptides as described previously (Neue et al. 2011). Glycans were released with endoglycosidase H leaving previously glycosylated asparagine residues tagged with a single GlcNAc residue and identified by shotgun-MS. The use of Endo H offers an additional advantage over other analyses that have used PNGase F for deglycosylation, as measurements of tryptic peptides deglycosylated by PNGase F failed to robustly differentiate nonglycosylated from deglycosylated versions of the same peptide (Xu et al. 2015). We were able to identify 170 high confidence glycosylation sites corresponding to 103 glycoproteins, of which four were novel glycoproteins (Gpi12o, Chs7p, Heh2p and Osw7p) (Supplementary Table 1). Most of glycoproteins were represented with either one or two glyco-peptides, the exception were glycoproteins like Pdi1p, Ape3p, Fet3p, Plb1p, Ero1p, Plb2p and Rax2p that were represented with four or more glyco-peptides. These results were the basis for a PRM-based approach, where glyco-peptides were monitored together with the peptides without glycosylation sequon belonging to the same glycoprotein.

To test whether we are able to target the peptides identified in the shotgun analysis but omitting the glyco-peptide enrichment step, we mixed yeast wild type cells grown in medium with heavy arginine and lysine isotopes with cells grown in medium with light arginine and lysine isotopes in an equal ratio and performed targeted PRM analysis (Figure 1). Samples enriched for microsomal fractions were digested with LysC and Trypsin proteinases and EndoH was used to generate single GlcNAc glycopeptides. Of 170 glyco-peptides corresponding to 103 glycoproteins measured in the enriched samples we were able to detect 62 belonging to 43 glycoproteins in the unenriched samples from three biological replicates with high confidence (i.e. co-elution of light and heavy peaks, good correlation of relative intensity of specific fragment ions with the reference library, reproducible retention times across different samples) (Table 1).

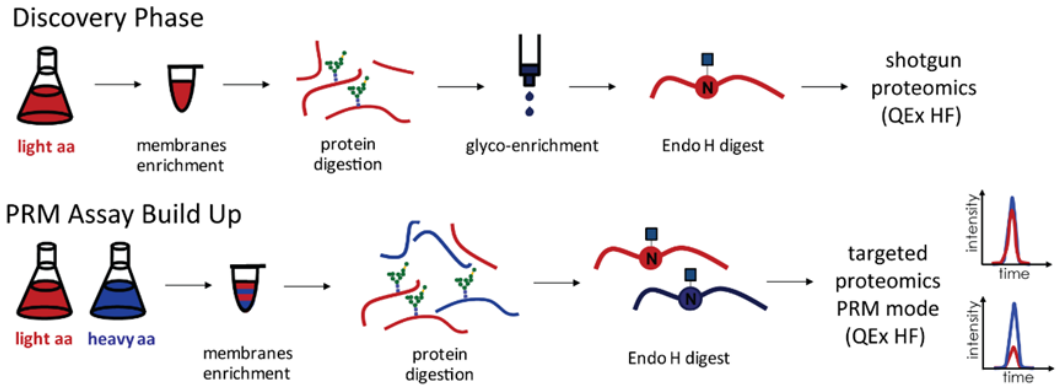

Figure 1. Schematic representation of SILAC PRM MS assay development.

During discovery phase yeast cells were grown in light medium, microsomal fractions were prepared using previously published method (Mueller et al. 2015) and proteins digested with LysC and trypsin proteinases. Glycan containing peptides were enriched using SPE ZIC-HILIC method (Neue et al. 2011) prior to glycan release with Endo H endoglycosidase. Glyco-peptides containing previously glycosylated asparagine residues tagged with a single GlcNAc residue were identified using shotgun proteomics. Obtained data was used for PRM assay build up where yeast cells were grown in light medium and mixed 1:1 with the cells grown in heavy medium. Membrane derived peptides were prepared as described above, glycans were released with EndoH and targeted PRM analysis was performed.

As it is known that changes in glycosylation can have an impact on glycoprotein steady-state levels, we determined the relative protein abundance as well (Helenius & Aebi 2004; Molinari 2007). In order to quantify protein abundance of each targeted glycoprotein in our analysis, we extended the target list by adding up to two peptides without glycosylation sequon for each glycoprotein analysed. In the final set-up, the full analytical list consisted of 62 glyco-peptides and 74 peptides without glycosylation sequon corresponding to 43 glycoproteins (Appendix Table 1). Furthermore, to account for any variance during mixing of light and heavy cells we also targeted peptides belonging to the ribosomal proteins Rpl5 and Rsp1, respectively. To ensure high-quality quantification of low abundance proteins and proteins containing peptides with poor MS properties, such proteins were analysed using a PRM method with higher resolution (Appendix Table 1). The simultaneous accurate quantification of modified peptides as well as peptides that do not contain a glycosylation sequon enabled us to follow changes in the occupancy of the glycosylation sites analysed as well as relative glycoprotein abundance.

Table 1. List of all glycoproteins and the corresponding glycosylated peptides used in the SILAC PRM-MS analysis of N-linked glycosylation occupancy.

UniProt ID	Protein	Glycosylation Site	Modified Peptide Sequence	Protein Description
P00729	CPY	N124	ILGIDPN[HexNAc]VTQYTGYLDVEDEDK	Carboxypeptidase Y
P00729	CPY	N479	VRN[HexNAc]WTASITDEVAGEVK	Carboxypeptidase Y
P12684	HMG2	N150	IPTELVSEN[HexNAc]GTK	3-hydroxy-3-methylglutaryl-coenzyme A reductase 2
P17967	PDI	N425	LAPTYQELADTYAN[HexNAc]ATSDVLIAK	Protein disulfide-isomerase
P17967	PDI	N117	NSDVN[HexNAc]NSIDYEGPR	Protein disulfide-isomerase
P17967	PDI	N82	N[+203.1]ITLAQIDC[+57]TENQDLC[+57]M[+16]EHNIPGFPSLK	Protein disulfide-isomerase
P17967	PDI	N174	IDADFN[HexNAc]ATFYSMANK	Protein disulfide-isomerase
P17967	PDI	N155	QSQPAVAVVADLPAYLAN[HexNAc]ETFVTPVIVQSGK	Protein disulfide-isomerase
P22146	GAS1	N40	FFYSNN[HexNAc]GSQFYIR	1,3-beta-glucanosyltransferase
P23797	GPI12	N110	VRELN[HexNAc]ESAALLLHNER	GlcANc-phosphatidylinositol de-N-acetylase
P27810	KTR1	N120	N[HexNAc]VTSALVSGTTK	Alpha-1,2 mannosyltransferase
P27825	CNE1	N416	N[HexNAc]VTEAQIIGNK	Calnexin homolog
P31382	PMT2	N403	GLPSWSEN[HexNAc]ETDIEYLKPGTSYR	Dol-P-Man-protein mannosyltransferase 2
P32353	ERG3	N40	LLGLNSGFSN[HexNAc]STILQETLNSK	C-5 sterol desaturase
P32623	CRH2	N310	N[HexNAc]GTSAYVYTSSSEFLAK	Probable glycosidase CRH2
P32623	CRH2	N233/N237	N[HexNAc]ETYN[HexNAc]ATTQK	Probable glycosidase CRH2
P33302	PDR5	N734	GPAYAN[HexNAc]ISSTESVCTVVGAVPGQDYVLGDDFIR	Pleiotropic ABC efflux transporter of multiple drugs
P33754	SEC66	N12	FSN[HexNAc]NGTFFETEEPIVETK	Translocation protein
P33767	WBP1	N332	LTLSPSGN[HexNAc]DSETQYYTTGEFILPDR	Oligosaccharyltransferase subunit WBP1
P33767	WBP1	N60	LEYLDIN[HexNAc]STSTTVDLYDK	Oligosaccharyltransferase subunit WBP1
P36016	LHS1	N458	LSN[HexNAc]ESELYDVFTR	Heat shock protein 70 homolog
P36051	MCD4	N90	SLVMNN[HexNAc]ATYGISHTR	GPI ethanolamine phosphate transferase 1
P36051	MCD4	N198	HLDQLFHN[HexNAc]STLNSTLDYEIR	GPI ethanolamine phosphate transferase 1
P36091	DCW1	N203	YTGN[HexNAc]QTYVDWAEK	Mannan endo-1,6-alpha-mannosidase
P37302	APE3	N96	LAN[HexNAc]YSTPDYGHPTR	Aminopeptidase Y
P37302	APE3	N150	IISFN[HexNAc]LSDAETGK	Aminopeptidase Y
P37302	APE3	N162	SFAN[HexNAc]TTAFALSPPVDGFVGK	Aminopeptidase Y
P37302	APE3	N85	IKVDDLN[HexNAc]ATAWDLYR	Aminopeptidase Y
P38244	PFF1	N121	SILFQQQDPFN[HexNAc]ESSR	Probable zinc metalloprotease YBR074W
P38248	ECM33	N304	VQTVGGAIEVTGN[HexNAc]FSTLDLSSLK	Cell wall protein ECM33
P38843	CHS7	N31	THLILSN[HexNAc]STIIHDFDPLNLNVGVLPR	Chitin synthase export chaperone
P38875	GPI16	N184	SYASDIGAPLFN[HexNAc]STEK	GPI transamidase component
P38993	FET3	N244	N[HexNAc]VTDMLYITVAQR	Iron transport multicopper oxidase FET3
P38993	FET3	N359	NGVNYAFFNN[HexNAc]ITYTAPK	Iron transport multicopper oxidase FET3
P39007	STT3	N539	TTLVDNNTWN[HexNAc]NTHIAIVGK	Oligosaccharyltransferase subunit STT3
P39105	PLB1	N215	DAGFN[HexNAc]ISLADVWGR	Lysophospholipase 1
P39105	PLB1	N489	N[HexNAc]LTDLEYIPPLIVYIPNSR	Lysophospholipase 1
P40345	PDAT	N439	SSSEDALNN[HexNAc]NTDTYGNFIR	Phospholipid:diacylglycerol acyltransferase
P40533	TED1	N266	DNYWIEYETN[HexNAc]TTHPWR	Protein TED1
P40557	EPS1	N299	FPN[HexNAc]ITEGELEK	ER-retained PMA1-suppressing protein 1
P40557	EPS1	N264	VALVLPN[HexNAc]K	ER-retained PMA1-suppressing protein 1
P41543	OST1	N217	FSSN[HexNAc]ETLAIVYSHNAPLNQVVNLR	Oligosaccharyltransferase subunit OST1
P43561	FET5	N364	YAFFNN[HexNAc]ITYVTPK	Iron transport multicopper oxidase FET5
P43561	FET5	N24	LN[HexNAc]YTASWVTANPDGLHEK	Iron transport multicopper oxidase FET5
P43611	OSW7	N297	NLDDLN[HexNAc]TTVNEQLVFLDSK	Uncharacterized protein YFR039C
P46982	MNN5	N136	LN[HexNAc]FSIPQR	Alpha-1,2-mannosyltransferase MNN5
P46992	YJR1	N219	N[HexNAc]SSSIGYYDLPAIWLLNDHIAR	Cell wall protein YJL171C
P52911	EXG2	N50	FASYYAN[HexNAc]DTITVK	Glucan 1,3-beta-glucosidase 2
P52911	EXG2	N157	NLYIDN[HexNAc]ITFNDPYVSDGLQLK	Glucan 1,3-beta-glucosidase 2
P53379	MKC7	N286	STAYSLFAN[HexNAc]DSDSK	Aspartic proteinase MKC7
P54003	SUR7	N47	FYWVQGN[HexNAc]TTGIPNAGDETR	Protein SUR7
Q03103	ERO1	N458	YTIENIN[HexNAc]STK	Endoplasmic oxidoreductin-1
Q03281	HEH2	N520	SN[HexNAc]NTNYIYR	Inner nuclear membrane protein
Q03674	PLB2	N193	SIVNPGGSN[HexNAc]LTYTIER	Lysophospholipase 2
Q03674	PLB2	N217	SDAGFN[HexNAc]ISLSDLWAR	Lysophospholipase 2
Q03691	ROT1	N139	YN[HexNAc]QTETFK	Protein ROT1
Q06689	YL413	N429	ILNSAVN[HexNAc]MTTITPEQLK	Cell membrane protein YLR413W
Q06689	YL413	N49	IN[HexNAc]VTK	Cell membrane protein YLR413W
Q07830	GPI13	N411	N[HexNAc]ISNTPPTSDPEK	GPI ethanolamine phosphate transferase 3
Q12465	RAX2	N88	EIGPETSSHGLVYYSN[HexNAc]NTYIQLEDASDDTR	Bud site selection protein
Q12465	RAX2	N677	N[HexNAc]QTIQGDVHGITK	Bud site selection protein
Q12465	RAX2	N640	N[HexNAc]SSLYADIYDNK	Bud site selection protein

Evaluation of the functional studies of the glycosylation machinery

To validate the newly developed SILAC PRM MS method, we investigated the roles of the Ost3 and Ost6 subunits in OST function *in vivo.* It has been described previously that these subunits with oxidoreductase activity facilitate glycosylation in a site-specific manner (Schulz et al. 2009; Xu et al. 2015; Yeo et al. 2016). As yeast OST contains either Ost3p or Ost6p, we generated strains where either the OST3 or OST6 loci were deleted. Overexpression of plasmid-encoded OST3 or OST6 ensured normal levels of uniform OST (Spirig et al. 2005). This allowed us to compare the phenotype of strains expressing either Ost3p- or Ost6p-containing OST complexes at equal levels. Equal amounts of wild type reference cells grown in heavy medium and of cells with a deletion in one OST subunit grown in light medium were pooled. Cells were lysed, membranes collected, proteins prepared for MS, and light-to-heavy ratios for all peptides measured by PRM. Glyco-peptide abundance relative to wild type was calculated. Values were normalized to the average of two control proteins, Rps1 and Rpl5 and to the average of peptides without glycosylation sequon belonging to the same glycoproteins (Supplementary Table 2).

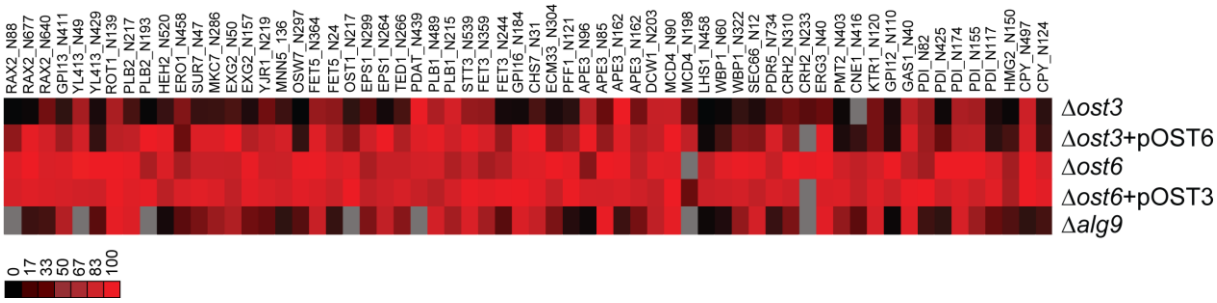

Figure 2. Glycosylation occupancy analysis at different glycosylation sites of various OST mutant strains and Δ*alg9* strain compared to wild type cells.

OST mutant cells, Δ*ost3*, Δ*ost3* complemented with OST6, Δ*ost6* and Δ*ost6* complemented with OST3, and cells deleted in ALG9 loci were grown in light medium, mixed 1:1 with the wild type reference strain grown in heavy medium and membrane derived peptides were prepared. Peptide abundance was measured by PRM MS. Intensity ratios of glycosylated light to heavy peptides were normalized for expression differences in mutant cells and wild type cells. The resulting ratios represent the site occupancy for the mutant cells relative to the wild type reference strain presented in a heatmap. Data is the mean ± SE of biological triplicates. Colour is mapped from black (0%) to red (100%), grey is for data not being obtained. Data from Supplementary Table 2.

SILAC PRM MS analysis revealed that 84% of the glycosylation sites were hypoglycosylated (where the glycosylation occupancy ratio compared to wild type reference strain was lower than 0.75) in the strain

lacking Ost3 protein, whereas less severe hypoglycosylation was observed in the strain with OST6 being overexpressed with 39% of the glycosylation sites being hypoglycosylated (Figure 2). Severe hypoglycosylation in Δ*ost3* strain was therefore a combination of a reduced level of fully assembled OST and the lack of OST3 function. These results highlight the importance of using yeast strains expressing normal amounts of fully assembled OST, but lacking either Ost3p or Ost6p for the functional analysis of these subunits. The extent of hypoglycosylation is only mild in strains lacking Ost6p, where only 2% of the glycosylation sites were hypoglycosylated in combination with overexpressed OST3. These results indicated that Ost3p-containing complex has a broader substrate specificity as compared to Ost6p-containing complex (Figure 2). The data are in agreement with previously published work demonstrating that Ost3p has a more evident role in N-linked glycosylation compared to Ost6p (Schulz & Aebi 2009; Schulz et al. 2009; Jamaluddin et al. 2014; Yeo et al. 2016). Ost3p affects polypeptide substrate specificity, as in a strain with Ost6p-containing OST only a hypoglycosylation on a subset of glycosylation sites (24 out of 62 sites analysed, corresponding to 21 out of 43 glycoproteins) was observed (Supplementary Table 2). We detected 17 novel Ost3p substrates (Supplementary Table 2, in bold italic), where the glycosylation of these protein substrates was dependent on the presence of the Ost3 subunit. Interestingly, when we examined Ost3p substrates with available structure or structural model, the majority of these proteins required oxidative folding (disulfide bond formation) (data not shown). These results are in accordance with previously proposed function of Ost3 protein to transiently form mixed disulfide bonds with OST polypeptide substrates (Schulz et al. 2009; Mohd Yusuf et al. 2013).

An alternative way to affect OST activity *in vivo* is to prevent complete synthesis of the lipid-linked oligosaccharide substrate (Burda & Aebi 1999). Yeast Alg9p has a dual role in LLO biosynthesis. It is responsible for the addition of two α-1,2-linked Man residues, whereby the assembly of b-branch is a requirement for the assembly of c-branch (Frank & Aebi 2005). We generated a strain where ALG9 loci was deleted, resulting in the accumulation of $Man_6GlcNAc_2$ LLO and determined site-specific glycosylation efficiencies. As expected, in the *alg* mutant strain many sequons were not efficiently glycosylated and the level of hypoglycosylation was increased as compared to the strain lacking Ost3p complemented with OST6 (Figure 2). Absence of Alg9p resulted in hypoglycosylation (glycosylation lower than 0.75) of 64% of the sites analysed, whereas the lack of Ost3p complemented with OST6 resulted in hypoglycosylation of 39% of the sites analysed (Supplementary Table 2). Although more severe as compared to the loss of Ost3p complemented with OST6, the effect of suboptimal glycan donor appears to have a site specific effect on the OST activity as more than one third of the sites in our analysis were not affected when the *ALG9* loci was deleted.

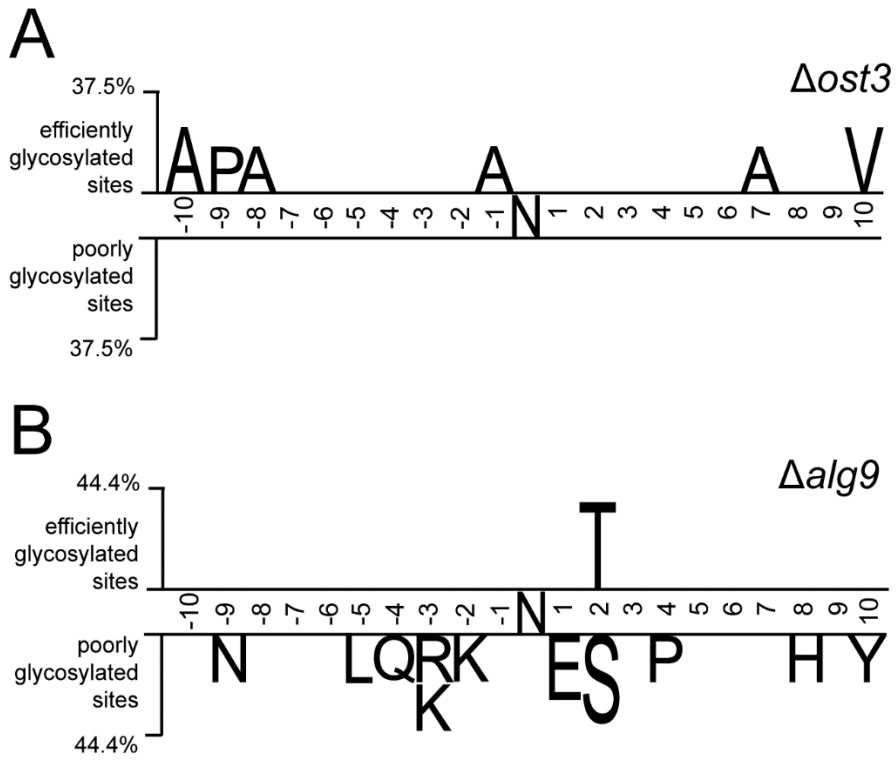

Figure 3. N-glycosylation efficiency is influenced by the primary protein sequence surrounding the glycosylation site.

Two sample logo analysis (Vacic et al. 2006) was used to calculate and visualize residues surrounding glycosylation sites that are significantly enriched in either efficiently or poorly glycosylated sites in Δ*ost3* complemented with OST6 (A) and Δ*alg9* (B) strains. Sequence size analysed contained ten amino acids upstream and downstream from the glycosylation site. Efficiently glycosylated sites are considered where glycosylation occupancy ratio compared to wild type is more than 0.75 and poorly glycosylated sites are considered where glycosylation occupancy ratio compared to wild type is less than 0.25.

In order to examine if the presence of specific amino acids in the local environment of the glycosylation sites influenced N-glycosylation efficiency, sequence analysis was performed on glycosylation sequons plus ten residues upstream and downstream from the glycosylation sites. Two sample logo analysis (Vacic et al. 2006) was used to visualize differences between efficiently and poorly glycosylated sequences surrounding the glycosylation sites. Glycosylation efficiency of Ost6-containing OST (in Δ*ost3* strain complemented with OST6) was not dependent on the presence of specific amino acids in the local surrounding of the glycosylation site (Figure 3A). In contrast, poorly glycosylated sites in Δ*alg9* strain were enriched in N-X-S sequons, as compared to the more efficiently modified N-X-T sequons (Figure 3B). Sequons that contain glutamic acid at +1 position are also less likely to be efficiently glycosylated. Furthermore, sites that are surrounded by basic arginine and lysine residues and polar amino acids appear to be disfavoured when OST is presented with a suboptimal glycan donor. When

we examined the localization of efficiently glycosylated sites in respect to their structural environment, for the substrates with available structure or structural model, we discovered that the glycosylation efficiency was not dependent on the type of secondary structures glycosylation sites were placed on in Δ*ost3* strains nor Δ*alg9* strain (data not shown).

Based on our results, we concluded that the SILAC PRM MS method was a reproducible, sensitive and useful approach for determining the efficiency of the N-linked glycosylation machinery in yeast.

Protein structural domains influence protein specific glycosylation efficiency

Our novel analytical approach allowed us to analyse the N-glycosylation process of defined proteins in more detail. In particular, we followed the modifications of the ER resident protein disulfide isomerase, Pdi1p that carries five N-linked glycans. Pdi1p is composed of four thioredoxin folds termed a, b, b' and a' that can fold independently (Tian et al. 2006). The a and a' domains contain two and one disulfide bonds, respectively, one per domain is directly involved in the catalytic activity of the isomerase. The five glycosylation sites are located in domain a (2 sites), b (2 sites) and a' (1 site), all of them in structured area of the protein: site 1 (N82, domain a) and site 2 (N117, domain a) are placed in structured loops, site 3 (N155, domain b), site 4 (N174, domain b) and site 5 (N425, domain a') are in α-helices (Tian et al. 2006) (Figure 4).

Glycosylation occupancy of any of the five sites was not severely affected in strains lacking Ost6p, except for site one (N82) being hypoglycosylated in Δ*ost6* strain. This hypoglycosylation was rescued by overexpression of OST3. However, absence of the OST3 component had strong, but site-specific effects on Pdi1p glycosylation. In the Δ*ost3*+pOST6 strain, sites one (N82), two (N117) and five (N425) were hypoglycosylated in the absence of Ost3p (with 0.70, 0.20 and 0.47 glycosylation occupancy, respectively). We noted that these three sites are located in the a and a' domains of the protein that contain disulfide bonds (Tian et al. 2006). Sites three (N155) and four (N174), located in the b domain, were not hypoglycosylated (Figure 4). Pdi1p glycosylation occupancy analysis in Δ*alg9* strain revealed similar results as in Δ*ost3*+pOST6 strain, where the glycosylation of sites one (N82), two (N117) and five (N425) was more severely affected as compared to sites three (N155) and four (N174) (Figure 4).

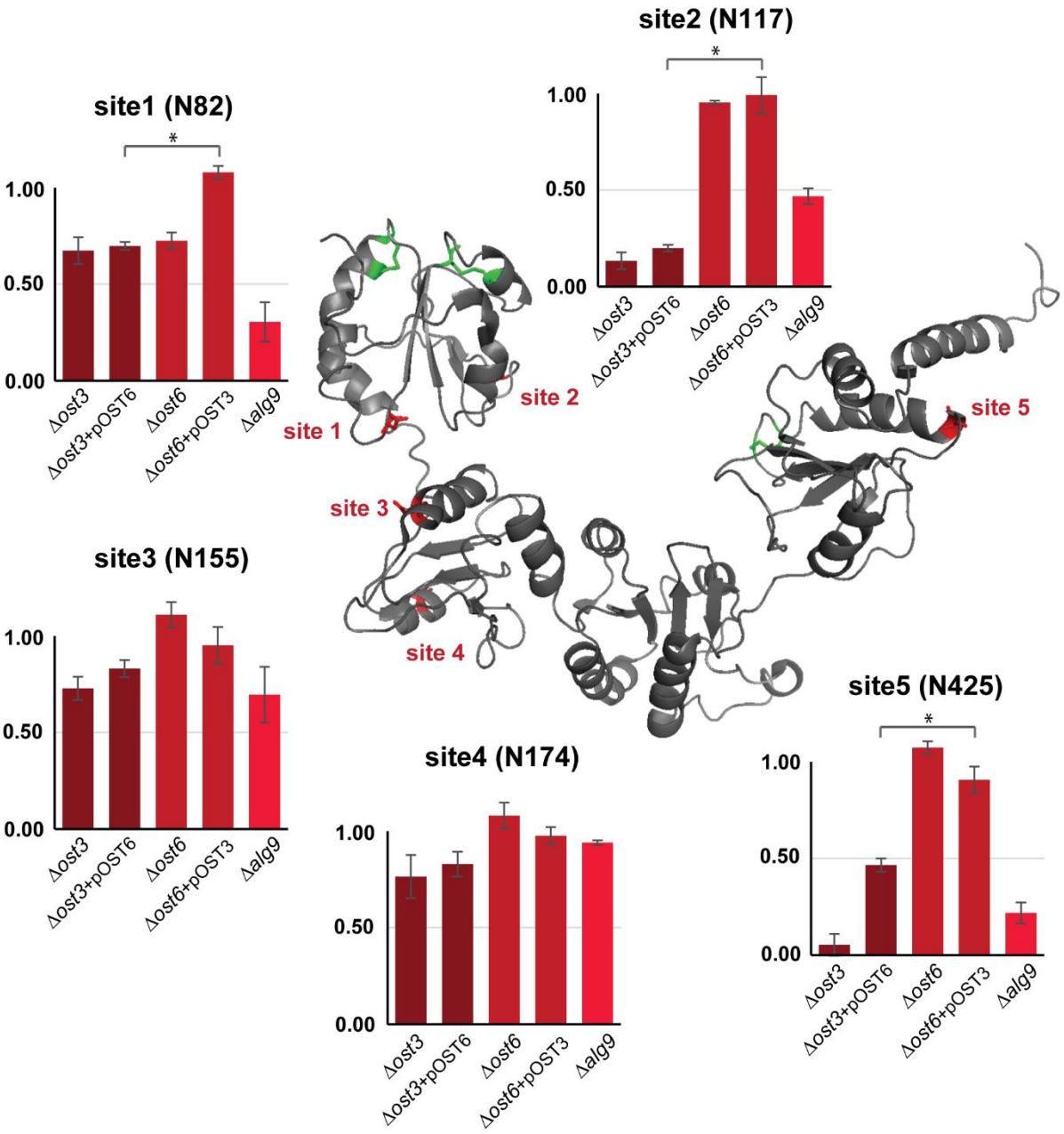

Figure 4. Site-specific glycosylation occupancy of Pdi1p is influenced by the localization of glycosylation sites in respect of distinct protein domains.

Glycosylation occupancy ratio compared to wild type at five N-linked glycosylation sites (N82, N117, N155, N174 and N425) of Pdi1p in Δ*ost3*, Δ*ost3* complemented with OST6, Δ*ost6*, Δ*ost6* complemented with OST3 and Δ*alg9* cells. Values are a mean of biological triplicates. Error bars show SEM.*$p < 0.05$. Pdi1p protein structure is modified from Tian et al. 2001 Cell. Data from Supplementary Table 3.

Defects in LLO biosynthesis lead to changes in ergosterol pathway

We determined the relative protein abundance of glycoproteins across different strains and measured by PRM MS peptides without glycosylation sequon belonging to 62 glycoproteins (Supplementary Table 3). We noted a correlation between hypoglycosylation and unfolded protein response: Δ*ost3* strains and Δ*alg9* strain displayed the most significant increase of six proteins known to be controlled by this regulatory network (Ero1p, Rot1p, Lhs1p, Pdi1p, Mcd4p and Eps1p). The majority of these proteins act as molecular chaperons and are involved in either ERAD or UPR (Travers et al. 2000; Masato et al. 2008). However, one particular protein, ERG3 C-5 sterol desaturase, involved in ergosterol biosynthesis, showed a 4-fold increase in abundance in Δ*alg9* strain only and not in strains with mutations affecting OST components (Figure 5A and 5B; Supplementary Table 3).

Because the initial steps in dolichol (the lipid involved in LLO biosynthesis) and ergosterol biosynthesis are connected, we investigated whether defects in LLO assembly affect other proteins involved in sterol biosynthesis (Chojnacki & Dallner 1988). PRM assays were developed to analyse the abundance of enzymes required in the mevalonate, ergosterol or dolichol pathways (Appendix Table 2). Peptides belonging to 20 out of the 26 proteins were identified and quantified (Figure 5A, black). We also included an *alg3* mutant strain in the analysis. Yeast Alg3p is a α-1,3 mannosyltransferase responsible for the initiation of glycosylation on the LLO b-branch at the ER lumenal side, which is then subsequently elongated by Alg9p (Burda & Aebi 1999). Protein abundance of Erg3p protein showed a 3 to 3.5-fold increase in both Δ*alg3* and Δ*alg9* strains, suggesting that the changes in protein levels of this protein are a result of general defects in LLO assembly (Figure 5C). Moreover, the abundance of three other proteins (Erg11, Erg25 and Erg5, respectively), all acting in ergosterol biosynthetic pathway, showed an increased protein level ratio compared to wild type cells in both Δ*alg3* and Δ*alg9* strains. Additionally, Erg1p was significantly increased in Δ*alg3* strain (Figure 5C). Both defects in LLO assembly resulted in a 3- to 4-fold increase in protein amounts of Erg11p, Erg25p and Erg3p and 1-to 2-fold increase of Erg5p. Earlier measurements using promoter fusions and mutations that alter sterol biosynthesis found upregulation of genes encoding for the same proteins in various genetic backgrounds (Smith et al. 1996; Kennedy et al. 1999; Henry et al. 2002). Furthermore, exposure of yeast cells to sterol inhibitors upregulated the expression of the same genes as well (Bammert & Fostel 2000). To examine if the same phenotype was observed using our proteomic setup, we treated wild type yeast cells with miconazole, an inhibitor of lanosterol 14-α-demethylase Erg11p (Figure 5A) (Joseph-Horne & Hollomon 2006). Equal amounts of wild type cells grown in heavy medium and of cells treated with miconazole or DMSO were pooled and processed as described above. The protein levels were normalized to the ones of the control cells treated with DMSO (Supplementary Table 4).

Similar to strains defective in LLO assembly, the same proteins displayed a significant increase in protein level ratio compared to cells, including proteins Erg11, Erg25, Erg3 and Erg5 (Figure 5C).

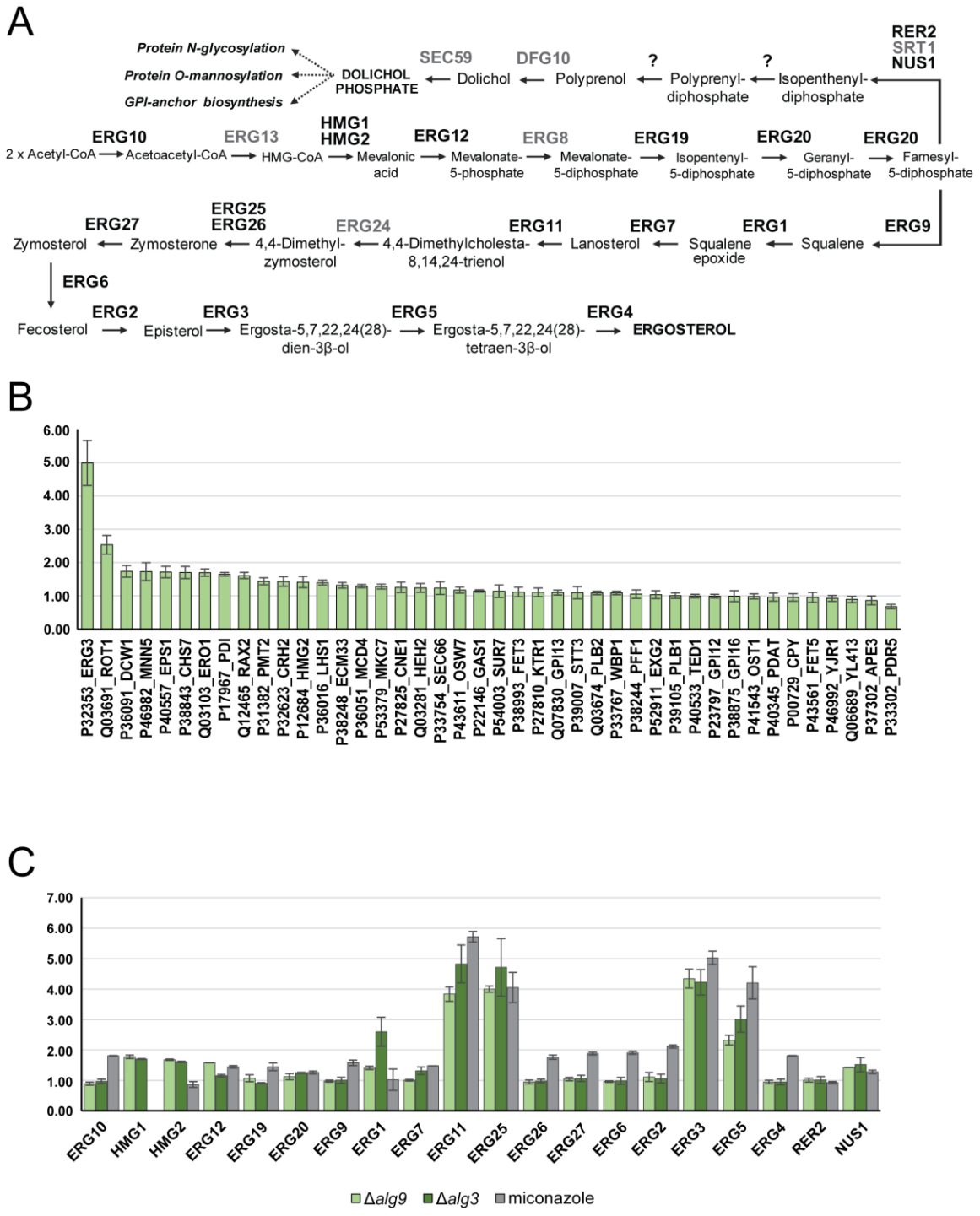

Figure 5. Protein abundance of several ergosterol pathway proteins is influenced by defects in dolichol pathway.

(A.) Schematic representation of mevalonate, ergosterol and dolichol pathway (adapted from Grabińska & Palamarczyk 2002; Liang et al. 2009). (B.) Deletion of *ALG9* loci results in increased abundance of several proteins involved in UPR as well as Erg3p. Δ*alg9* cells were grown in light medium, mixed 1:1 with the wild type reference strain grown in heavy medium and membrane derived peptides were prepared. Peptide abundance was

measured by SILAC PRM. Intensity ratios of light to heavy peptides were normalized for expression differences in mutant cells and wild type cells. The resulting ratios represent the protein abundance for the mutant cells relative to the wild type reference strain. Data is the mean ± SE of biological triplicates. Data from Supplementary Table 3. (C.) Deletion of *ALG9* and *ALG3* loci, as well as treatment of cells with sterol inhibitor miconazole results in increased protein abundance of multiple ERG proteins. Δ*alg9*, Δ*alg3*, cells treated with miconazole or DMSO were grown in light medium, mixed 1:1 with the wild type reference strain grown in heavy medium and membrane derived peptides were prepared. Peptide abundance was measured by PRM MS with an inclusion list containing peptides belonging to mevalonate, ergosterol and dolichol pathway proteins. Data was normalized to the data obtained for control cells treated with DMSO. Data is the mean ± SE of three biological triplicates. Data from Supplementary Table 4.

Discussion

N-linked glycosylation machinery, with OST as the central enzyme, modifies many proteins with glycans that can be fundamental in many different ways for cell viability, yet the crucial mechanisms responsible for the regulation of N-linked glycosylation are not well understood. To increase the resolution of measurement of OST function *in vivo*, we developed a novel analytical tool to quantify relative N-glycosylation occupancy at many glycosylation sites in different membrane and lumenal proteins. We have shown that its sensitivity and consistency make PRM MS especially suitable for the analysis of N-linked glycoproteins, sometimes present in medium to low amounts in the cell. Coupled with SILAC our approach offers a powerful analytical tool to study the efficiency of N-linked glycosylation machinery in a sensitive, effective and reproducible way providing results that were in agreement with previously published data. Our method is a complementary analytical approach to the recently reported methods where SWATH and SWAT MS were used to quantify relative glycosylation occupancy of a lower number of predefined glycosylation sites in glycoproteins extracted from yeast cell wall (Xu et al. 2015; Yeo et al. 2016; Zacchi & BL Schulz 2016). Compared to other approaches, the analysis of yeast membrane and luminal glycoproteins eliminates the analytical bias present in the complementary approaches where only mature, successfully secreted proteins from yeast cell wall extracts are analysed (Schulz & Aebi 2009). We are now able to investigate the glycosylation extent of glycoproteins involved in N-linked glycosylation, ERQC and UPR, in a resolved, quantifiable and reproducible way. Simultaneous analysis of protein abundance allows us to examine distinct influence of glycosylation on steady-state levels of individual substrate proteins or a global influence evident in ERQC and UPR activation.

We have used this approach to investigate protein substrate specificities of OST isoforms containing either Ost3p or Ost6p. In agreement with other reports, both isoforms affected OST substrates specifically and displayed site-specific preferences for a subset of glycosylation sites. This effect was not caused by a general reduction in OST activity as distinct sites were affected in the absence of Ost3p or Ost6p (Schwarz et al. 2005; Schulz et al. 2009). Furthermore, Ost3p was required for efficient glycosylation of more than a third of glycosylation sites analysed here, compatible with a broader substrate array as compared to Ost6p isoform (Schulz & Aebi 2009; Xu et al. 2015; Yeo et al. 2016; Zacchi & BL Schulz 2016). We were able to detect novel Ost3p substrates and a majority of these protein substrates required oxidative folding. It has been demonstrated that both Ost3 and Ost6 subunits have thioredoxin-like domains that transiently interact with their protein substrates through mixed disulfide bonds (Mohorko et al. 2014). However, the importance of noncovalent interactions has been demonstrated as well, explaining why Ost3p influenced glycosylation at asparagines in

substrate proteins that do not contain disulfide bonds (Fetrow et al. 2001; Schwarz et al. 2005; Schulz et al. 2009; Jamaluddin et al. 2011; Mohd Yusuf et al. 2013; Jamaluddin et al. 2014).

In the process of N-linked glycosylation the OST enzyme displays a preference for both the polypeptide substrate and LLO donor, where suboptimal LLO structures are utilized, although will lower efficiency (Burda & Aebi 1999). We have examined the effect of the $Man_6GlcNAc_2$ suboptimal glycan donor generated in Δ*alg9* strain on the glycosylation efficiency of OST *in vivo*. Absence of Alg9p resulted in a more severe hypoglycosylation phenotype as compared to the loss of Ost3p complemented with OST6. Furthermore, the presence of a suboptimal glycan donor had a site-specific effect on the OST activity. This effect was not dependent on the protein secondary structure, e.g. the folding of the acceptor protein. However, glycosylation efficiency was sensitive to the primary sequence of the OST substrate: in Δ*alg9* strain, poorly glycosylated sites were enriched in N-X-S sequons as compared to the more efficiently modified N-X-T sequons. Crystal structure of PglB, a single subunit OST from *Campylobacter jejuni*, a homolog of the STT3 subunit of multi-subunit OSTs revealed that the WWD domain, not directly involved in the catalysis, bound the N-X-T sequon more efficiently (Lizak et al. 2011). We propose that the combination of a suboptimal LLO substrate and the low affinity sequon N-X-S is the cause for the reduced glycosylation of these sites. Similarly, our analysis revealed that sites that have a negative charge at X position and sites that are adjacent to basic and polar amino acids were disfavoured when OST was presented with a suboptimal glycan donor. Therefore, the analysis of site-specific N-glycosylation in *alg* mutant strains revealed a peptide substrate preference of the OST. Importantly, this preference was not observed in *ost3* or *ost6* mutant strains. Glycosylation efficiency of Ost3/Ost6p-containing OSTs did not reveal a site specificity indicating that Ost3 and Ost6 subunits are not involved in defining the general polypeptide binding affinity of OST. Kinetic experiments with yeast OST have revealed that there is a single binding site for the polypeptide substrate while the LLO substrate is bound in a cooperative manner (Karaoglu et al. 2001; Daniel J Kelleher et al. 2003; Kelleher et al. 2007). A substrate activation model suggests that the binding of the LLO donor substrate to the regulatory LLO binding site is a prerequisite for the binding of both the polypeptide substrate and second LLO donor substrate to the catalytic site (Karaoglu et al. 2001). We have shown that the accumulation of suboptimal LLO donor substrate in Δ*alg9* strain influenced the polypeptide preference of OST, which is in agreement with this model.

The possibility to investigate the status of all glycosylation sites of Pdi1p, an ER-resident protein whose protein structure is known, allowed us to analyse the N-glycosylation process in more detail. N-linked glycosylation of sites located in two domains of Pdi1p that also contain disulfide bonds (a and a' respectively) were Ost3p dependent, where the site closest to the non-active disulfide bond (site two, N117) was the one most affected in the cells lacking Ost3p. We conclude that the formation of a mixed

disulfide between Ost3p and Pdi1p slows down the folding and increases the glycosylation efficiency of this sequon. Protein folding is a critical competitor of N-linked glycosylation and indeed, the N117 site of Pdi1p is located in a protein sequence with secondary structure not competitive with N-glycosylation. The same site of Pdi1p is also hypoglycosylated in Δ*alg9* strain, supporting our hypothesis that reducing OST activity affects sites where folding is in competition with glycosylation. On the other hand, glycosylation of sites three (N155) and four (N174) was not affected as compared to other sites in *ost3/6* or *alg9* cells even though sites three and four are located in α-helices. Folding of the b domain might be slower than the folding of the a and a' domains, leaving an OST with enough time to efficiently glycosylate sequons present in this regions. Alternatively, additional OST components might prevent rapid folding of this domain.

Glycosylation and folding of proteins in the ER co-evolved and suboptimal glycosylation can affect the folding of specific proteins. In a system where not properly folded proteins are degraded this leads to an altered steady-state level of glycoproteins (Varki 1993; Larkin & Imperiali 2011; Zattas & Hochstrasser 2015). In addition, the unfolded protein response (UPR) can be activated (Chapman et al. 1998; Travers et al. 2000). We observed reduced steady-state level upon reduced glycosylation (Δ*alg9*) for only a few glycoproteins tested (Yjr1p, Yl413p, Ape3p, Pdr5p) but we detected an upregulation of the know UPR proteins such as Rot1p, Ero1p, Pdi1p (Figure 5). The largest increase in abundance was observed for Erg3p in the Δ*alg9* strain, which was not a result of UPR activation nor hypoglycosylation as the level of this protein was not altered in any other mutant strain, such as Δ*ost3* or Δ*ost6*, tested. We showed that the deficiency in LLO assembly affected several other enzymes involved in the ergosterol but not mevalonate pathway. Genes encoding for the upregulated proteins were found previously to be upregulated upon mutations that altered sterol biosynthesis or upon exposure to sterol inhibitors and we were able to increase the steady-state levels when cells were treated with the sterol biosynthesis inhibitor miconazole. We postulate a regulatory mechanism that links the LLO biosynthetic pathway with ergosterol biosynthesis. In view of the topology of the different pathways involved, we postulate that dolichyl pyrophosphate might act as a mediator in this regulation process. However, more experiments have to be performed to confirm this hypothesis.

In summary, the SILAC PRM MS method provided adequate selectivity and sensitivity for the quantitative analysis of a large number of glycosylation sites on yeast N-glycoproteins. Compared to other analytical methods, our assay allowed detection of novel Ost3p and Ost6p glycoprotein substrates and made it possible to target specific substrates such as Pdi1p for a more detailed analysis. The targeted analytical approach, in combination with a time resolved SILAC approach, will be instrumental for a detailed description of the role of N-glycosylation in the *in vivo* protein maturation at a molecular level.

Materials and Methods

Yeast strains and growth conditions

All yeast strains and plasmids used in this study are listed in Supplementary Table 5 and 6. Standard yeast genetic techniques were used (Güldener et al. 1996; Knop et al. 1999). All yeast strains were grown in an orbital shaker at 30°C and 180rpm to exponential phase (OD_{600nm} 1.0).

For MS assay, cells were grown in appropriate synthetic drop-out (SD) medium (0.67% (w/v) yeast nitrogen base, 2% (w/v) glucose with appropriate amino acid supplements) containing either 20 mg/L of light or heavy isotopes of arginine (13C6) and lysine (13C6-15N2) (Cambridge Isotope Laboratories). Cells were collected, frozen in liquid nitrogen and stored at -80°C.

For sterol inhibition assay, mid-log phase cultures of the wild type yeast cells in light SD medium were exposed to miconazole (0.3 µg/mL, dissolved in DMSO; Janseen Geel) while the controls received an equivalent amount of DMSO. After 2.5 hours, cells were washed once with ice cold 50 mM sodium acetate, 10 mM EDTA buffer (pH 4.5) before they were collected, frozen in liquid nitrogen and stored at -80°C.

Sample preparation for mass spectrometry

Membrane proteins were prepared as described (Mueller et al. 2015). In brief, yeast cells were lysed at 4°C using glass beads, and the microsomal fraction was pelleted by centrifugation (16000 x g; 20 min), resuspended in 0.1 M Na_2CO_3, 1 mM EDTA, pH 11.3 buffer and pelleted again. Samples were resuspended in SDS buffer (2% SDS (w/v), 50 mM DTT, 0.1 M Tris HCl pH 7.6) and processed using the filter assisted sample preparation protocol (Wiśniewski et al. 2009). Membrane proteins were digested first with endopeptidase LysC (20 µg/ml; Wako Pure Chemical, Richmond, VA) at room temperature for 16 h followed by digestion with trypsin (20 µg/ml; Promega) at 37°C for 4 h. For shotgun experiments in the discovery phase of PRM assay development, sample was enriched for glyco-peptides using SPE ZIC-HILIC (SeQuant) column as described before (Neue et al. 2011). For PRM experiments protein digestion was directly followed by digestion of N-glycans with endo-β-N-acetylglucosaminidase H (EndoH; 500 U; New England Biolabs) in sodium citrate buffer (50 mM, pH 5.5) at 37°C with agitation for 40 h. Peptides were desalted using Sep Pak C18 classic (Waters) and dried using speed vacuum. Desalted peptides were resuspended in ACN/H_2O (3:97 (v/v)) with formic acid (FA; 0.1% (v/v)) and analysed by LC-ESI-MS/MS.

Shotgun and targeted proteomics analysis

Mass spectrometric analysis

Samples were subjected to a Q Exactive HF mass spectrometer (Thermo Scientific) coupled to a nano EasyLC 1000 (Thermo Fisher Scientific) system and to an Acquity UPLC M-class System (Waters). Samples were loaded onto a self-made column (75 µm × 150 mm) packed with reverse-phase C18 material (ReproSil-Pur 120 C18-AQ, 1.9 µm, Dr. Maisch GmbH) when the EasyLC 1000 was coupled. ACQUITY UPLC M-Class column (75 µm × 150 mm) packed with reverse-phase C18 material (Waters HSS T3 100 C18, 1.8 µm) was used when the Acquity UPLC M-class system was coupled. Peptides were separated at a flow rate of 300 nL/min using a linear gradient of 1% to 35% solvent B (0.1% formic acid in acetonitrile) over 90 min, followed by an increase to 98 % B over 2 min and held at 98 % B for 5 min before returning to initial conditions of 1% B.

In shotgun-MS, the mass spectrometer was set to acquire full-scan MS spectra (300-1700 m/z) at a resolution of 60000 after accumulation to an automated gain control (AGC) target value of $3e^6$ and a maximum injection time of 15 ms. Charge state screening was enabled and unassigned charge states and single charged precursors were excluded. Ions were isolated using a quadrupole mass filter with a 1.2 m/z isolation window. A maximum injection time of 45 ms was set. HCD fragmentation was performed at a normalized collision energy (NCE) of 28 %. Selected ions were dynamically excluded for 20 sec.

For PRM measurements, the Q Exactive HF performed MS1 scans (400-1200 m/z) followed by 12 MS/MS acquisitions in PRM mode. The full scan event was collected at a resolution of 60 000 (at m/z 400) and a AGC value of $3e^6$ and a maximum injection time of 120 ms. The PRM scan events used an Orbitrap resolution of 30 000 or 60 000, maximum fill time of 55 ms or 110 ms respectively, with an isolation width of 2 m/z and an AGC value of $2e^5$. HCD fragmentation was performed at a normalized collision energy (NCE) of 28 % and MS/MS scans were acquired with a starting mass of m/z 120. Scan windows were set to 10 min for each peptide in the final PRM method to ensure the measurement of 6–10 points per LC peak per transition. All samples were analysed using two PRM methods based on scheduled inclusion lists containing the 175 target precursor ions, including Biognosys iRT standard peptides, at an Orbitrap resolution of 30 000 and two PRM methods based on scheduled inclusion lists containing the 128 target precursor ions, including Biognosys iRT standard peptides, at an Orbitrap resolution of 60 000 (Appendix Table 1).

Protein identification and spectral library building

MS and MS/MS spectra generated from enriched and non-enriched glycopeptides extracts were converted to Mascot generic format (MGF) using Proteome Discoverer, v2.1 (Thermo Fisher Scientific, Bremen, Germany). The MGFs were searched with Mascot Server v.2.4.1 (www.matrixscience.com) using the following parameters: a precursor ion mass tolerance of 15 ppm, product ion mass tolerance of 0.05 Dalton, and as variable modifications methionine oxidation, carbamidomethylation of cysteine and asparagine N-linked HexNAc (CID/HCD) glycosylation for the glyco-enriched samples. Searches were made against the *Saccharomyces cerevisiae* reference proteome database, concatenated to a reversed decoyed FASTA database and 260 common protein contaminants. The Mascot search results (dat. files) were imported into the Skyline software (v2.6.0) (MacLean et al. 2010) and spectral libraries were built using the BiblioSpec algorithm (Frewen & MacCoss 2007). Additionally published spectral libraries (Selevsek et al. 2015) were used to populate the final PRM assays. For glyco-peptides where ion libraries could not be obtained at the time, fragment ions were manually selected based on MS2 spectra obtained directly from the mascot search results.

Data processing and analysis

Skyline software (v2.6.0) with standard settings was used for data processing (MacLean et al. 2010). The abundance of peptides was analysed by summing the integrated areas of at least four fragment ions per peptide. Peptide peaks were analysed manually, and correct identification was assigned on the basis of the following criteria: (i) retention time matching to spectral library within 5% of the gradient length, (ii) co-elution of light and heavy peptides, (iii) dot product between light peptide precursor ion isotope distribution intensities and theoretical, (iv) dot product between library spectrum intensities and light peptides, and (v) matching peak shape for precursor and product ions from light and heavy peptides. The reported light to heavy intensity ratios (L/H) were normalized for proportionate mixing of heavy labelled with light labelled cells, by dividing the L/H intensity ratio of all measured peptides by the median of L/H intensity reported for four peptides belonging to two control proteins, Rps1a and Rpl5. L/H ratio for glyco-peptides modified with HexNAc was used to calculate the relative site occupancy for the given peptide/ glycosylation site compared to the wild type reference strain. The relative site occupancy was normalized for expression differences between heavy labelled wild type reference strain (H) and the mutant light strains (L) by dividing the L/H intensity ratio for the occupied glyco-peptide by the median of L/H intensity ratios reported for all peptides that do not containing a NxT/S sequon from the same protein. Protein level quantification was calculated as the median of L/H intensity ratios reported for all peptides without glycosylation sequon belonging to the

same protein, normalized for proportionate mixing of heavy labelled with light labelled cells as described above.

PRM MS quantification of ergosterol pathway protein abundance

SWATH-MS data published earlier (Selevsek et al. 2015) was used as ion library source to build a PRM assay for targeted analysis of ergosterol pathway proteins. Ion library information for peptides belonging to 20 from 26 proteins known to be involved in mevalonate, ergosterol and dolichol pathway were extracted and targeted PRM analysis was performed on Q Exactive HF mass spectrometer as described before. Scheduled inclusion list contained 100 target precursor ions, including Biognosys iRT standard peptides (Appendix Table 2).

The abundance of peptides was analysed using Skyline software with standard settings, where peptide peaks were analysed manually as described above. The reported L/H intensity ratios where normalized for proportionate mixing of heavy labelled with light labelled cells, by dividing the L/H intensity ratio of all measured peptides by the median of L/H intensity reported for peptides belonging to two control proteins, Rps1a and Rpl5. Protein level quantification was calculated as the median of L/H intensity ratios reported for all peptides belonging to the same protein. In the case of sterol inhibition assay, resulting protein abundance was further normalized to the protein abundance of the control samples treated with DMSO.

References

Aebi, M. et al., 2010. N-glycan structures: recognition and processing in the ER. *Trends in Biochemical Sciences*, 35(2), pp.74–82.

Bammert, G.F. & Fostel, J.M., 2000. Genome-Wide Expression Patterns in Saccharomyces cerevisiae : Comparison of Drug Treatments and Genetic Alterations Affecting Biosynthesis of Ergosterol Genome-Wide Expression Patterns in Saccharomyces cerevisiae : Comparison of Drug Treatments and Geneti. *Antimicrobial Agents and Chemotherapy*, 44(5), pp.1255–1265.

Bause, E., 1984. Model studies on N -glycosylation of proteins. *Biochemical Society Transactions*, 12(3), pp.514–517.

Breitling, J. & Aebi, M., 2013. *N* -Linked Protein Glycosylation in the Endoplasmic Reticulum. *Cold Spring Harbor Perspectives in Biology*.

Burda, P. & Aebi, M., 1999. The dolichol pathway of N-linked glycosylation. *Biochimica et Biophysica Acta - General Subjects*, 1426(2), pp.239–257.

Chapman, R., Sidrauski, C. & Walter, P., 1998. Intracellular signaling from the endoplasmic reticulum to the nucleus. *Annual review of cell and developmental biology*, 14, pp.459–485.

Chojnacki, T. & Dallner, G., 1988. The biological role of dolichol. *The Biochemical journal*, 251(1), pp.1–9.

Fetrow, J.S. et al., 2001. Genomic-scale comparison of sequence- and structure-based methods of function prediction: does structure provide additional insight? *Protein science : a publication of the Protein Society*, 10(5), pp.1005–14.

Frank, C.G. & Aebi, M., 2005. ALG9 mannosyltransferase is involved in two different steps of lipid-linked oligosaccharide biosynthesis. *Glycobiology*, 15(11), pp.1156–1163.

Frewen, B. & MacCoss, M.J., 2007. Using BiblioSpec for creating and searching tandem MS peptide libraries. *Current protocols in bioinformatics / editoral board, Andreas D. Baxevanis ... [et al.]*, Chapter 13, p.Unit 13.7.

Gao, X.-D., Nishikawa, A. & Dean, N., 2004. Physical interactions between the Alg1, Alg2, and Alg11 mannosyltransferases of the endoplasmic reticulum. *Glycobiology*, 14(6), pp.559–70.

Grabińska, K. & Palamarczyk, G., 2002. Dolichol biosynthesis in the yeast *Saccharomyces cerevisiae*: An insight into the regulatory role of farnesyl diphosphate synthase. *FEMS Yeast Research*, 2, pp.259–265.

Güldener, U. et al., 1996. A new efficient gene disruption cassette for repeated use in budding yeast. *Nucleic acids research*, 24(13), pp.2519–24.

Helenius, A. & Aebi, M., 2004. Roles of N-linked glycans in the endoplasmic reticulum. *Annual review of biochemistry*, 73, pp.1019–49.

Helenius, J. et al., 2002. Translocation of lipid-linked oligosaccharides across the ER membrane requires Rft1 protein. *Nature*, 415(6870), pp.447–50.

Henry, K.W., Nickels, J.T. & Edlind, T.D., 2002. ROX1 and ERG regulation in Saccharomyces cerevisiae: Implications for antifungal susceptibility. *Eukaryotic Cell*, 1(6), pp.1041–1044.

Jakob, C.A. et al., 1998. Genetic tailoring of N-linked oligosaccharides: the role of glucose residues in glycoprotein processing of Saccharomyces cerevisiae in vivo. *Glycobiology*, 8(2), pp.155–64.

Jamaluddin, M.F.B. et al., 2011. Polypeptide binding specificities of saccharomyces cerevisiae oligosaccharyltransferase accessory proteins Ost3p and Ost6p. *Protein Science*, 20(5), pp.849–855.

Jamaluddin, M.F.B., Bailey, U.-M. & Schulz, B.L., 2014. Oligosaccharyltransferase subunits bind polypeptide substrate to locally enhance N-glycosylation. *Mol Cell Proteomics*, pp.1–31.

Joseph-Horne, T. & Hollomon, D.W., 2006. Molecular mechanisms of azole resistance in fungi. *FEMS Microbiology Letters*, 149(2), pp.141–149.

Karaoglu, D., Kelleher, D.J. & Gilmore, R., 2001. Allosteric regulation provides a molecular mechanism for preferential utilization of the fully assembled dolichol-linked oligosaccharide by the yeast oligosaccharyltransferase. *Biochemistry*, 40(40), pp.12193–12206.

Kelleher, D.J. et al., 2007. Dolichol-linked oligosaccharide selection by the oligosaccharyltransferase in protist and fungal organisms. *Journal of Cell Biology*, 177(1), pp.29–37.

Kelleher, D.J. et al., 2003. Oligosaccharyltransferase isoforms that contain different catalytic STT3 subunits have distinct enzymatic properties. *Molecular cell*, 12(1), pp.101–11.

Kelleher, D.J. & Gilmore, R., 2006. An evolving view of the eukaryotic oligosaccharyltransferase. *Glycobiology*, 16(4), pp.47–62.

Kennedy, M. a, Barbuch, R. & Bard, M., 1999. Transcriptional regulation of the squalene synthase gene (ERG9) in the yeast Saccharomyces cerevisiae. *Biochimica et biophysica acta*, 1445(1), pp.110–122.

Knop, M. et al., 1999. Epitope tagging of yeast genes using a PCR-based strategy: more tags and improved practical routines. *Yeast (Chichester, England)*, 15(10B), pp.963–72.

Lairson, L.L. et al., 2008. Glycosyltransferases: Structures, Functions, and Mechanisms. *Annual Review of Biochemistry*, 77(1), pp.521–555.

Larkin, A. & Imperiali, B., 2011. The expanding horizons of asparagine-linked glycosylation. *Biochemistry*, 50(21), pp.4411–26.

Lazar, I.M., Lee, W. & Lazar, A.C., 2013. Glycoproteomics on the rise: established methods, advanced techniques, sophisticated biological applications. *Electrophoresis*, 34(1), pp.113–25.

Liang, R. et al., 2009. 2-Amino-nonyl-6-methoxyl-tetralin muriate inhibits sterol C-14 reductase in the ergosterol biosynthetic pathway. *Acta Pharmacologica Sinica*, 30(12), pp.1709–1716.

Liu, Y. et al., 2013. Quantitative measurements of N-linked glycoproteins in human plasma by SWATH-MS. *Proteomics*, 13(8), pp.1247–56.

Lizak, C. et al., 2011. X-ray structure of a bacterial oligosaccharyltransferase. *Nature*, 474(7351), pp.350–355.

Lu, J. et al., 2012. Alg14 organizes the formation of a multiglycosyltransferase complex involved in initiation of lipid-linked oligosaccharide biosynthesis. *Glycobiology*, 22(4), pp.504–516.

MacLean, B. et al., 2010. Skyline: An open source document editor for creating and analyzing targeted proteomics experiments. *Bioinformatics*, 26(7), pp.966–968.

Masato, T., Yukio, K. & Kenji, K., 2008. Saccharomyces cerevisiae Rot1 Is an Essential Molecular Chaperone in the Endoplasmatic Reticulum. *Molecular biology of the cell*, 19(1), pp.3514–3525.

McDonald, W.H. et al., 2002. Comparison of three directly coupled HPLC MS/MS strategies for identification of proteins from complex mixtures: single-dimension LC-MS/MS, 2-phase MudPIT, and 3-phase MudPIT. *International Journal of Mass Spectrometry*, 219(1), pp.245–251.

Mohd Yusuf, S.N.H. et al., 2013. Mixed disulfide formation in vitro between a glycoprotein substrate and yeast oligosaccharyltransferase subunits Ost3p and Ost6p. *Biochemical and Biophysical Research Communications*, 432(3), pp.438–443.

Mohorko, E. et al., 2014. Structural basis of substrate specificity of human oligosaccharyl transferase subunit N33/Tusc3 and its role in regulating protein N-glycosylation. *Structure*, 22(4), pp.590–601.

Molinari, M., 2007. N-glycan structure dictates extension of protein folding or onset of disposal. *Nature chemical biology*, 3(6), pp.313–20.

Mueller, S. et al., 2015. Protein degradation corrects for imbalanced subunit stoichiometry in OST complex assembly. *Molecular Biology of the Cell*, 26(14), pp.2596–2608.

Neue, K. et al., 2011. Elucidation of glycoprotein structures by unspecific proteolysis and direct nanoESI mass spectrometric analysis of ZIC-HILIC-enriched glycopeptides. *Journal of proteome research*, 10(5), pp.2248

Ong, S.-E., 2002. Stable Isotope Labeling by Amino Acids in Cell Culture, SILAC, as a Simple and Accurate Approach to Expression Proteomics. *Molecular & Cellular Proteomics*, 1(5), pp.376–386.

Ong, S. & Mann, M., 2006. A practical recipe for stable isotope labeling by amino acids in cell culture (SILAC). *Nature protocols*, 1(6), pp.2650–2660.

Pan, S., 2014. Quantitative glycoproteomics for N-glycoproteome profiling. *Methods in molecular biology (Clifton, N.J.)*, 1156, pp.379–88.

Parker, B.L. et al., 2013. Site-specific glycan-peptide analysis for determination of N-glycoproteome heterogeneity. *Journal of proteome research*, 12(12), pp.5791–800.

Ruiz-Canada, C., Kelleher, D.J. & Gilmore, R., 2009. Cotranslational and Posttranslational N-Glycosylation of Polypeptides by Distinct Mammalian OST Isoforms. *Cell*, 136(2), pp.272–283.

Schulz, B.L. et al., 2009. Oxidoreductase activity of oligosaccharyltransferase subunits Ost3p and Ost6p defines site-specific glycosylation efficiency. *Proceedings of the National Academy of Sciences of the United States of America*, 106(27), pp.11061–6.

Schulz, B.L. & Aebi, M., 2009. Analysis of glycosylation site occupancy reveals a role for Ost3p and Ost6p in site-specific N-glycosylation efficiency. *Molecular & cellular proteomics : MCP*, 8(18), pp.357–364.

Schwarz, M., Knauer, R. & Lehle, L., 2005. Yeast oligosaccharyltransferase consists of two functionally distinct sub-complexes, specified by either the Ost3p or Ost6p subunit. *FEBS Letters*, 579(29), pp.6564–6568.

Selevsek, N. et al., 2015. Reproducible and consistent quantification of the Saccharomyces cerevisiae proteome by SWATH-MS. *Molecular & Cellular Proteomics*, (716), pp.1–16.

Smith, S.J., Crowley, J.H. & Parks, L.W., 1996. Transcriptional regulation by ergosterol in the yeast Saccharomyces cerevisiae. *Molecular and cellular biology*, 16(10), pp.5427–32.

Song, W. et al., 2013. N-glycan occupancy of Arabidopsis N-glycoproteins. *Journal of proteomics*, 93, pp.343–55.

Spirig, U. et al., 2005. The 3.4-kDa Ost4 protein is required for the assembly of two distinct oligosaccharyltransferase complexes in yeast. *Glycobiology*, 15(12), pp.1396–1406.

Szymanski, C.M. & Wren, B.W., 2005. Protein glycosylation in bacterial mucosal pathogens. *Nature reviews. Microbiology*, 3(3), pp.225–237.

Tian, G. et al., 2006. The crystal structure of yeast protein disulfide isomerase suggests cooperativity between its active sites. *Cell*, 124(1), pp.61–73.

Travers, K.J. et al., 2000. Functional and genomic analyses reveal an essential coordination between the unfolded protein response and ER-associated degradation. *Cell*, 101(3), pp.249–258.

Vacic, V., Iakoucheva, L.M. & Radivojac, P., 2006. Two Sample Logo: A graphical representation of the differences between two sets of sequence alignments. *Bioinformatics*, 22(12), pp.1536–1537.

Varki, a, 1993. Biological roles of oligosaccharides: all of the theories are correct. *Glycobiology*, 3(2), pp.97–130.

Wiśniewski, J.R. et al., 2009. Universal sample preparation method for proteome analysis. *Nature methods*, 6(5), pp.359–62.

Xu, Y., Bailey, U.M. & Schulz, B.L., 2015. Automated measurement of site-specific N-glycosylation occupancy with SWATH-MS. *Proteomics*, 15(13), pp.2177–2186.

Yeo, K.Y.B. et al., 2016. High-performance targeted mass spectrometry with precision data-independent acquisition reveals site-specific glycosylation macroheterogeneity. *Analytical Biochemistry*, 510, pp.106–113.

Zacchi, L. & Schulz, B., 2016. SWATH-MS glycoproteomics reveals consequences of defects in the glycosylation machinery. *Molecular & Cellular Proteomics*, 15, pp.2435–2447.

Zacchi, L. & Schulz, B., 2016. SWATH-MS glycoproteomics reveals consequences of defects in the glycosylation machinery. *Molecular & Cellular Proteomics*, 15(7), pp.2435–47.

Zattas, D. & Hochstrasser, M., 2015. Ubiquitin-dependent Protein Degradation at the Yeast Endoplasmic Reticulum and Nuclear Envelope. *Crit Rev Biochem Mol Biol.*, 50(1), pp.1–17.

Zhang, H. et al., 2003. Identification and quantification of N-linked glycoproteins using hydrazide chemistry, stable isotope labeling and mass spectrometry. *Nature biotechnology*, 21(6), pp.660–6.

Zielinska, D.F. et al., 2012. Mapping N-glycosylation sites across seven evolutionarily distant species reveals a divergent substrate proteome despite a common core machinery. *Molecular cell*, 46(4), pp.542–8.

Chapter 2b

Supplementary Information to Chapter 2

Supplementary Table 1. The list of all glycosylation sites identified after ZIC-HILIC enrichment.

UniProt ID	Protein	Modified Peptide Sequence	Protein Description	Mascot pep_score	Mascot pep_expect
P00729	CPY	ILGIDPN[HexNAc]VTQYTGYLDVEDEDK	Carboxypeptidase Y	77.35	5.6E-08
P00729	CPY	VRN[HexNAc]WTASITDEVAGEVK	Carboxypeptidase Y	57.18	0.0000043
P09620	KEX1	YDRN[HexNAc]LTFVSVYNASHMVPFDK	Pheromone-processing carboxypeptidase	39.96	0.00018
P12684	HMG2	DN[HexNAc]STTLPSLDDVIYSVDHTR	3-hydroxy-3-methylglutaryl-coenzyme A reductase 2	63.96	0.0000018
P12684	HMG2	IPTELVSEN[HexNAc]GTK	3-hydroxy-3-methylglutaryl-coenzyme A reductase 2	47.48	0.000035
P17967	PDI	LAPTYQELADTYAN[HexNAc]ATSDVLIAK	Protein disulfide-isomerase	72.38	0.00000025
P17967	PDI	NSDVN[HexNAc]NSIDYEGPR	Protein disulfide-isomerase	65.09	0.00000079
P17967	PDI	N[+203.1]ITLAQIDC[+57]TENQDLC[+57]M[+16]EHNIPGFPSLK	Protein disulfide-isomerase	58.24	0.0000014
P17967	PDI	IDADFN[HexNAc]ATFYSMANK	Protein disulfide-isomerase	40.11	0.00017
P17967	PDI	QSQPAVAVVADLPAYLAN[HexNAc]ETFVTPVIVQSGK	Protein disulfide-isomerase	55.18	0.0000025
P18962	DAP2	TFIHNGQN[HexNAc]LTVESITASPDLK	Dipeptidyl aminopeptidase B	64.59	0.00000088
P18962	DAP2	YMHTPQENFDGYVESSVHN[HexNAc]VTALAQANR	Dipeptidyl aminopeptidase B	49.26	0.000024
P20840	SAG1	LLN[HexNAc]SSQTATISLADGTEAFK	Alpha-agglutinin	68.11	0.000005
P21375	OSM1	VYEN[HexNAc]YTNNINFYMSK	Osmotic growth protein 1	33.15	0.00078
P22023	KRE5	DITATLN[HexNAc]FTK	Killer toxin-resistance protein 5	50.07	0.00002
P22023	KRE5	N[HexNAc]STDNLTELK	Killer toxin-resistance protein 5	46.76	0.00011
P22146	GAS1	TVVDTFAN[HexNAc]YTNVLGFFAGNEVTNNYTNTDASAFVK	1,3-beta-glucanosyltransferase	91.28	6.1E-09
P22146	GAS1	FFYSNN[HexNAc]GSQFYIR	1,3-beta-glucanosyltransferase	78.05	4.8E-08
P22804	BET1	GSN[HexNAc]QTIDQLGDTFHNTSVK	Protein transport protein	51.8	0.000038
P23797	GPI12	VRELN[HexNAc]ESAALLLHNER	N-acetylglucosaminyl-phosphatidylinositol de-N-acetylase	81.54	2.3E-08
P25334	CYPR	LAMAYFGPDSN[HexNAc]TSEFIITTK	Peptidyl-prolyl cis-trans isomerase	26	0.0036
P25574	EMC1	LSN[HexNAc]SSDN[HexNAc]FSYDPLTGHINKPQFQTK	ER membrane protein complex subunit 1	36.29	0.00056
P25577	YCE9	SIAPAIVN[HexNAc]SSVIFHDVSR	Uncharacterized protein YCL049C	62.52	0.0000014
P25577	YCE9	N[HexNAc]ATTLEPLR	Uncharacterized protein YCL049C	20.2	0.017
P25580	PBN1	HLN[HexNAc]STTLLVPIPRPDTK	Protein PBN1	23.01	0.0069
P25619	HSP30	MN[HexNAc]DTLSSFLNR	30 kDa heat shock protein	65.51	0.00000072
P26725	YUR1	EN[HexNAc]ATILMLVR	Probable mannosyltransferase	31.95	0.001
P26725	YUR1	NSYDDYTLN[HexNAc]YTR	Probable mannosyltransferase	30.54	0.0042
P27810	KTR1	N[HexNAc]VTSALVSGTTK	Alpha-1,2 mannosyltransferase	68.4	0.00000086
P27825	CNE1	N[HexNAc]VTEAQIIGNK	Calnexin homolog	33.01	0.0008
P31382	PMT2	GLPSWSEN[HexNAc]ETDIEYLKPGTSYR	Dolichyl-phosphate-mannose--protein mannosyltransferase	65.9	0.0000023
P32353	ERG3	LLGLNSGFSN[HexNAc]STILQETLNSK	C-5 sterol desaturase	91.4	3E-09
P32474	EUG1	GQINFIALN[HexNAc]STMFPHHVR	Protein disulfide-isomerase	66.65	0.0000033
P32621	GDA1	FGDEN[HexNAc]YTLYQFSHLGYGLK	Guanosine-diphosphatase	26.59	0.0038
P32623	CRH2	N[HexNAc]GTSAYVYTSSSEFLAK	Probable glycosidase CRH2	102.52	2.4E-10
P32623	CRH2	N[HexNAc]ETYN[HexNAc]ATTQK	Probable glycosidase CRH2	40.67	0.00015
P32791	FRE1	NIYLN[HexNAc]ASNYLR	Ferric/cupric reductase transmembrane component	49.37	0.000023
P32802	TMN1	FN[HexNAc]ESATSWATR	Transmembrane 9 superfamily member 1	52.02	0.00000041
P32906	MNS1	MLGGLLSAYHLSDVLEVGN[HexNAc]K	ER mannosyl-oligosaccharide 1,2-alpha-mannosidase	27.85	0.0024
P33302	PDR5	GPAYAN[HexNAc]ISSTESVCTVVGAVPGQDYVLGDDFIR	Pleiotropic ABC efflux transporter of multiple drugs	20.81	0.02
P33550	KTR2	EN[HexNAc]ATLLMLVR	Probable mannosyltransferase KTR2	31.95	0.001
P33754	SEC66	FSN[HexNAc]NGTFFETEEPIVETK	Translocation protein	75.73	7.9E-08
P33767	WBP1	LTLSPSGN[HexNAc]DSETQYYTTGEFILPDR	Oligosaccharyltransferase subunit WBP1	105.86	1.4E-10
P33767	WBP1	LEYLDIN[HexNAc]STSTTVDLYDK	Oligosaccharyltransferase subunit WBP1	105.49	1.3E-10
P33894	STE13	FN[HexNAc]DTSVDDIR	Dipeptidyl aminopeptidase A	86.27	0.00000003
P36016	LHS1	LSN[HexNAc]ESELYDVFTR	Heat shock protein 70 homolog	96.38	9.2E-10
P36044	MNN4	SMN[HexNAc]QTTLDQVTK	Protein MNN4	83.01	1.6E-08
P36044	MNN4	HLQLLSQYFN[HexNAc]QSLILEDPR	Protein MNN4	21.2	0.026
P36051	MCD4	SLVMNN[HexNAc]ATYGISHTR	GPI ethanolamine phosphate transferase 1	79.51	4.3E-08
P36051	MCD4	HLDQLFHN[HexNAc]STLNSTLDYEIR	GPI ethanolamine phosphate transferase 1	33.28	0.00076
P36091	DCW1	YTGN[HexNAc]QTYVDWAEK	Mannan endo-1,6-alpha-mannosidase	45.75	0.00000012
P36096	TUL1	TEHNTFVN[HexNAc]MTYTDSFR	Transmembrane E3 ubiquitin-protein ligase 1	65.36	0.00000074
P36096	TUL1	LSYQDMLNNPLQN[HexNAc]ATYPLPGK	Transmembrane E3 ubiquitin-protein ligase 1	46.94	0.00004
P36112	FCJ1	TGNPSN[HexNAc]ATDFDSVYAR	Formation of crista junctions protein 1	76.28	0.0000001
P37302	APE3	LAN[HexNAc]YSTPDYGHPTR	Aminopeptidase Y	57.97	0.0000037
P37302	APE3	IISFN[HexNAc]LSDAETGK	Aminopeptidase Y	57.63	0.0000039
P37302	APE3	AHHLN[HexNAc]YTLVPFDGR	Aminopeptidase Y	35.53	0.00047
P37302	APE3	SFAN[HexNAc]TTAFALSPPVDGFVGK	Aminopeptidase Y	48.86	0.000092
P37302	APE3	IKVDDLN[HexNAc]ATAWDLYR	Aminopeptidase Y	104.98	6.5E-10
P38138	GLU2A	MPTN[HexNAc]SSGLLISSQR	Glucosidase 2 subunit alpha	90.53	3.2E-09
P38138	GLU2A	NNLQHN[HexNAc]ITLK	Glucosidase 2 subunit alpha	21.19	0.029
P38244	PFF1	VLEITGN[HexNAc]SSFASVSDDK	Probable zinc metalloprotease YBR074W	111.66	3.4E-11
P38244	PFF1	SILFQQQDPFN[HexNAc]ESSR	Probable zinc metalloprotease YBR074W	102.82	2.3E-10
P38248	ECM33	VQTVGGAIEVTGN[HexNAc]FSTLDLSSLK	Cell wall protein ECM33	92.23	2.3E-09

UniProt ID	Protein	Modified Peptide Sequence	Protein Description	Mascot pep_score	Mascot pep_expect
P38248	ECM33	AAFSN[HexNAc]LTTVGGGFIIANNTQLK	Cell wall protein ECM33	89.16	2.9E-08
P38616	YGP1	LFNSSSALN[HexNAc]ITELYNVAR	Protein YGP1	37.65	0.00033
P38813	BIG1	GN[HexNAc]NTEDFQPFIDSEK	Protein BIG1	55.62	0.0000061
P38836	ECM14	FTSDN[HexNAc]YSTLVR	Putative metallocarboxypeptidase	60.08	0.00001
P38843	CHS7	THLILSN[HexNAc]STIIHDFDPLNLNVGVLPR	Chitin synthase export chaperone	49.66	0.000022
P38875	GPI16	SYASDIGAPLFN[HexNAc]STEK	GPI transamidase component	40.22	0.00017
P38928	AXL2	FQSSN[HexNAc]LTLAGEVPK	Axial budding pattern protein 2	85.48	3.2E-08
P38928	AXL2	VN[HexNAc]ESFTFQISNDTYK	Axial budding pattern protein 2	61.64	0.0000017
P38928	AXL2	LDPNEVFN[HexNAc]VTFDR	Axial budding pattern protein 2	45.86	0.00005
P38992	SUR2	NVTSN[HexNAc]ATAAGSFPLAFGLK	Sphingolipid C4-hydroxylase SUR2	58.47	0.0000035
P38993	FET3	VPTLMTVLSSGDQAN[HexNAc]NSEIYGSNTHTFILEK	Iron transport multicopper oxidase	101.34	4.9E-10
P38993	FET3	N[HexNAc]VTDMLYITVAQR	Iron transport multicopper oxidase FET3	96.16	9.6E-10
P38993	FET3	NGVNYAFFNN[HexNAc]ITYTAPK	Iron transport multicopper oxidase FET3	37.27	0.00032
P38993	FET3	FDDTMLDVIPSDLQLN[HexNAc]ATSYMVYNK	Iron transport multicopper oxidase FET3	27.09	0.0029
P39007	STT3	TTLVDNNTWN[HexNAc]NTHIAIVGK	Oligosaccharyltransferase subunit STT3	80.11	9.4E-08
P39012	GAA1	EMVN[HexNAc]MTSMER	GPI transamidase component GAA1	34.58	0.00035
P39105	PLB1	ATSN[HexNAc]FSDTSLLSTLFGSNSSNMPK	Lysophospholipase 1	53.46	0.0000097
P39105	PLB1	DAGFN[HexNAc]ISLADVWGR	Lysophospholipase 1	51.3	0.000026
P39105	PLB1	EASGLSDN[HexNAc]ETEWLK	Lysophospholipase 1	88.22	1.8E-08
P39105	PLB1	N[HexNAc]LTDLEYIPPLIVYIPNSR	Lysophospholipase 1	47.18	0.000045
P39106	MNN1	TLN[HexNAc]ATFPNYDPDNFK	Alpha-1,3-mannosyltransferase MNN1	28.37	0.0028
P39106	MNN1	MFPFINN[HexNAc]FTTETFHEMVPK	Alpha-1,3-mannosyltransferase MNN1	20.92	0.011
P39543	SOP4	LDLAASN[HexNAc]ITGFVSTR	Protein SOP4	94.39	1.4E-09
P39543	SOP4	GRLDLAASN[HexNAc]ITGFVSTR	Protein SOP4	88.83	8.4E-09
P39685	PO152	IN[HexNAc]STEEIEYIELEYR	Nucleoporin POM152	93.59	8.8E-09
P39685	PO152	IMN[HexNAc]VTTDSLTK	Nucleoporin POM152	58.71	0.0000057
P39928	SLN1	N[HexNAc]DTFISSAFR	Osmosensing histidine protein kinase SLN1	69.64	0.0000003
P39928	SLN1	DALQSSLTSYVAGN[HexNAc]K	Osmosensing histidine protein kinase SLN1	53.18	0.00001
P40345	PDAT	SSSEDALNN[HexNAc]NTDTYGNFIR	Phospholipid:diacylglycerol acyltransferase	94.34	1.4E-09
P40345	PDAT	EEDDSSALN[HexNAc]LTIDYESK	Phospholipid:diacylglycerol acyltransferase	76.51	6.7E-08
P40358	JEM1	IVFN[HexNAc]ETYK	DnaJ-like chaperone JEM1	22.84	0.0072
P40504	KTR7	MN[HexNAc]ASFVMLTR	Probable mannosyltransferase KTR7	48.8	0.000027
P40514	YIG7	N[HexNAc]ETVSIDVLR	Uncharacterized protein YIL067C	61.52	0.000017
P40514	YIG7	MENPALAQMMDDALDASN[HexNAc]GTIDLYLR	Uncharacterized protein YIL067C	21.39	0.013
P40533	TED1	FN[HexNAc]GSTVLLTHVPFYK	Protein TED1	46.22	0.000048
P40533	TED1	DNYWIEYETN[HexNAc]TTHPWR	Protein TED1	26.7	0.0095
P40557	EPS1	FPN[HexNAc]ITEGELEK	ER-retained PMA1-suppressing protein 1	59.26	0.000011
P40557	EPS1	VALVLPN[HexNAc]K	ER-retained PMA1-suppressing protein 1	24.29	0.01
P40557	EPS1	NLIN[HexNAc]LSR	ER-retained PMA1-suppressing protein 1	22.75	0.023
P40985	HUL4	N[HexNAc]ITIR	Probable E3 ubiquitin-protein ligase HUL4	27.36	0.00041
P40986	CDC1	TNPN[HexNAc]VSR	Cell division control protein 1	35.63	0.0018
P41543	OST1	FSSN[HexNAc]ETLAIVYSHNAPLNQVVNLR	Oligosaccharyltransferase subunit OST1	83.64	1.4E-08
P43561	FET5	YAFFNN[HexNAc]ITYVTPK	Iron transport multicopper oxidase FET5	55.05	0.000013
P43561	FET5	LN[HexNAc]YTASWVTANPDGLHEK	Iron transport multicopper oxidase FET5	44.56	0.00024
P43561	FET5	SPGFHVDEAYDESEQDEMTVPYN[HexNAc]ESAPLQPFPERPMVR	Iron transport multicopper oxidase FET5	32.97	0.00081
P43571	BST1	WHLNIIN[HexNAc]K	GPI inositol-deacylase	32.74	0.0025
P43571	BST1	SLDINMHNVAPFIPLN[HexNAc]ESEPR	GPI inositol-deacylase	28.78	0.002
P43611	OSW7	NLDDLN[HexNAc]TTVNEQLVFLDSK	Uncharacterized protein YFR039C	35.99	0.00053
P46950	SNG1	FGTTN[HexNAc]STEIDR	Nitrosoguanidine resistance protein SNG1	101.93	1.3E-09
P46950	SNG1	EYLPSLMSN[HexNAc]ITSNDR	Nitrosoguanidine resistance protein SNG1	72.25	0.00000059
P46950	SNG1	FGTTN[HexNAc]STEIDRK	Nitrosoguanidine resistance protein SNG1	47.83	0.000033
P46982	MNN5	LN[HexNAc]FSIPQR	Alpha-1,2-mannosyltransferase MNN5	40.3	0.0019
P46992	YJR1	N[HexNAc]SSSIGYYDLPAIWLLNDHIAR	Cell wall protein YJL171C	45.12	0.000087
P52867	PMT5	WIIELAEHPNEN[HexNAc]VTSFQNLTDGTIIK	Dolichyl-phosphate-mannose--protein mannosyltransferase	47.98	0.000032
P52911	EXG2	FASYYAN[HexNAc]DTITVK	Glucan 1,3-beta-glucosidase 2	64.26	0.000001
P52911	EXG2	NLYIDN[HexNAc]ITFNDPYVSDGLQLK	Glucan 1,3-beta-glucosidase 2	39	0.00044
P53012	SCS3	N[HexNAc]VTASAAAAINTFIHDQMHR	FIT family protein SCS3	65.22	0.00000077
P53058	VEL1	LTTIASN[HexNAc]ETK	Protein VEL1	50.33	0.000019
P53059	MNT2	GIVISASDVQLN[HexNAc]ETIR	Alpha-1,3-mannosyltransferase MNT2	20.78	0.011
P53089	YGV4	MN[HexNAc]GTDILR	Putative uncharacterized protein YGL204C	33.83	0.0015
P53379	MKC7	GDKEDN[HexNAc]LTTLTTTK	Aspartic proteinase MKC7	100.32	3.9E-10
P53379	MKC7	STAYSLFAN[HexNAc]DSDSK	Aspartic proteinase MKC7	70.41	0.00000025
P53746	FRE4	AGIN[HexNAc]ITYPIR	Ferric reductase transmembrane component 4	30.07	0.0019
P53983	ASI3	DVFSFFHN[HexNAc]K	Protein ASI3	38.65	0.00024
P54003	SUR7	FYWVQGN[HexNAc]TTGIPNAGDETR	Protein SUR7	58.47	0.0000035
P54070	KTR6	SYGGN[HexNAc]ETTLGFMVPSYINHR	Mannosyltransferase KTR6	50.98	0.000017
P54070	KTR6	N[HexNAc]ATVNAIK	Mannosyltransferase KTR6	35.18	0.0017
P54730	UBX4	NKKPLNN[HexNAc]ASQER	UBX domain-containing protein 4	28.56	0.000024
Q03103	ERO1	TN[HexNAc]NSQSHVFDDLK	Endoplasmic oxidoreductin-1	84.3	5.3E-08
Q03103	ERO1	YTIENIN[HexNAc]STK	Endoplasmic oxidoreductin-1	58.96	0.000003
Q03103	ERO1	AEIVPRPSN[HexNAc]GTVNK	Endoplasmic oxidoreductin-1	43.79	0.00027
Q03281	HEH2	SN[HexNAc]NTNYIYR	Inner nuclear membrane protein	61.12	0.0000048

UniProt ID	Protein	Modified Peptide Sequence	Protein Description	Mascot pep_score	Mascot pep_expect
Q03465	RPN4	LN[HexNAc]VTK	Protein RPN4	32.53	0.011
Q03674	PLB2	ATSN[HexNAc]FSDTSLLSTLFSSNSSNVPK	Lysophospholipase 2	58.37	0.0000094
Q03674	PLB2	SIVNPGGSN[HexNAc]LTYTIER	Lysophospholipase 2	53.08	0.000011
Q03674	PLB2	SDAGFN[HexNAc]ISLSDLWAR	Lysophospholipase 2	51.12	0.000047
Q03674	PLB2	MNYN[HexNAc]VTER	Lysophospholipase 2	36.07	0.0013
Q03691	ROT1	YN[HexNAc]QTETFK	Protein ROT1	48.28	0.00003
Q04399	YD506	IHVLEFN[HexNAc]ASSEYTLDK	Putative multicopper oxidase YDR506C	34.04	0.00064
Q05031	DFG5	GDANAGMN[HexNAc]SSTTNVLQNNLNIK	Mannan endo-1,6-alpha-mannosidase	63	0.0000014
Q06325	YPS7	HPSYLMN[HexNAc]DSTSSVPVSPGQIYEISFIDGR	Aspartic proteinase yapsin-7	51.81	0.000014
Q06325	YPS7	GNYYVN[HexNAc]STFGTPGQR	Aspartic proteinase yapsin-7	50.33	0.000019
Q06681	YSP2	GN[HexNAc]GTVQNSVLSNHIK	GRAM domain-containing protein YSP2	59.81	0.0000026
Q06689	YL413	ILNSAVN[HexNAc]MTTITPEQLK	Cell membrane protein YLR413W	64.89	0.00000082
Q06689	YL413	IN[HexNAc]VTK	Cell membrane protein YLR413W	32.53	0.011
Q07830	GPI13	HVLDN[HexNAc]ISSQNETSK	GPI ethanolamine phosphate transferase 3	68.85	0.00000035
Q07830	GPI13	N[HexNAc]ISNTPPTSDPEK	GPI ethanolamine phosphate transferase 3	37.69	0.0023
Q07895	YL001	SNSEGTSVSVN[HexNAc]NSDYSPISNR	FAS1 domain-containing protein YLR001C	49.13	0.000025
Q07895	YL001	IVGSQN[HexNAc]LTK	FAS1 domain-containing protein YLR001C	31.57	0.005
Q08108	PLB3	ATAN[HexNAc]FSDSSEVLSK	Lysophospholipase 3	68.71	0.00000036
Q08108	PLB3	IN[HexNAc]STHLPSFITR	Lysophospholipase 3	25.18	0.0043
Q08912	YO389	DIDFDN[HexNAc]STAIFNSIR	Uncharacterized protein YOR389W	27.1	0.0048
Q12096	GNT1	LLVFN[HexNAc]QTEFDR	Glucose N-acetyltransferase 1	54.99	0.000007
Q12096	GNT1	TLDNDGNDIPVGLN[HexNAc]DSVAYSK	Glucose N-acetyltransferase 1	39.11	0.00021
Q12200	NPC1	APYSTALVYN[HexNAc]ETSVSASVFR	Niemann-Pick type C-related protein 1	69.31	0.00000032
Q12200	NPC1	FVN[HexNAc]ITK	Niemann-Pick type C-related protein 1	32.7	0.005
Q12465	RAX2	EIGPETSSHGLVYYSN[HexNAc]NTYIQLEDASDDTR	Bud site selection protein	75.62	0.0000002
Q12465	RAX2	NLTMIAN[HexNAc]ETLGSNAR	Bud site selection protein	73.04	0.00000022
Q12465	RAX2	VGN[HexNAc]TTLNLFPVK	Bud site selection protein	72.31	0.0000011
Q12465	RAX2	N[HexNAc]QTIQGDVHGITK	Bud site selection protein	53.26	0.00001
Q12465	RAX2	N[HexNAc]SSLYADIYDNK	Bud site selection protein	42.23	0.00011
Q12465	RAX2	SN[HexNAc]FTSTR	Bud site selection protein	32.88	0.00083
Q12465	RAX2	LGSFN[HexNAc]LTN[HexNAc]STMIPLLSGSEGK	Bud site selection protein	32.3	0.0042
Q99234	DFG16	AYN[HexNAc]YTLNYPSFLIR	Protein DFG16	24.5	0.005
Q99316	MPD2	N[HexNAc]DSYTMIK	Protein disulfide isomerase	31.67	0.0011

Supplementary Table 2. Site-specific N-glycosylation occupancy analysis of various OST mutant strains and Δ*alg9* strain compared to wild type cells. Data for Figure 2.

UniProt ID	Protein	Glycosylation Site	Δost3	Δost3+pOST6	Δost6	Δost6+pOST3	Δalg9
P00729	*CPY*	N124	19.29 ± 3.68	29.27 ± 0.04	94.29 ± 6.26	100.11 ± 5.69	33.04 ± 13.09
P00729	*CPY*	N479	89.9 ± 11.06	94.18 ± 3.23	105.43 ± 4.56	107.89 ± 0.44	21.53 ± 10.06
P12684	**HMG2**	N150	3.3 ± 2.05	33.37 ± 9.94	73.01 ± 8.4	75.67 ± 9.36	37.76 ± 0.01
P17967	**PDI**	N117	13.45 ± 4.35	20.06 ± 1.7	95.36 ± 1.03	99.2 ± 9.31	46.8 ± 4.13
P17967	**PDI**	N155	72.91 ± 6.02	83.64 ± 4.43	111.08 ± 6.57	95.22 ± 9.47	69.62 ± 14.49
P17967	**PDI**	N174	76.59 ± 11.17	82.93 ± 6.44	108.09 ± 6.67	97.56 ± 4.56	94.09 ± 1.13
P17967	**PDI**	N425	5.39 ± 5.68	46.64 ± 3.46	107.44 ± 3.23	90.73 ± 6.88	21.81 ± 5.41
P17967	**PDI**	N82	67.5 ± 6.95	69.86 ± 2.07	72.49 ± 4.31	107.95 ± 3.31	30.51 ± 10.22
P22146	GAS1	N40	83.44 ± 5.59	96.7 ± 3.14	84.82 ± 1.79	103.73 ± 1.01	97.9 ± 7.68
P23797	**GPI12**	N110	11.51 ± 2.15	13.95 ± 0.53	104.43 ± 4.92	89.25 ± 7.49	3.86 ± 2.74
P27810	**KTR1**	N120	53.26 ± 4.43	53.45 ± 1.16	92.77 ± 0.99	98.32 ± 3.21	93.22 ± 9.81
P27825	**CNE1**	N416	N/A	27.5 ± 2.09	85.43 ± 1.25	86.67 ± 11.83	41.97 ± 14.87
P31382	**PMT2**	N403	4.77 ± 4.48	11.83 ± 0.38	91.64 ± 0.5	96.97 ± 9.5	65.35 ± 3.45
P32353	ERG3	N40	48.01 ± 8.81	102.21 ± 3.06	109.13 ± 5.35	95.6 ± 3.31	99.64 ± 7.85
P32623	*CRH2*	N233/N237	41.08 ± 13.57	N/A	102.13 ± 7.52	0 ± 0	N/A
P32623	*CRH2*	N310	50.57 ± 6.28	68.22 ± 4.06	105.93 ± 2.15	90.61 ± 7.87	55.3 ± 9.11
P33302	PDR5	N734	39.71 ± 8.12	94.65 ± 4.88	87.12 ± 0.24	94.74 ± 6.4	27.33 ± 10.89
P33754	**SEC66**	N12	13.17 ± 0.48	59.13 ± 3.37	101.25 ± 1.68	85.88 ± 11.36	92.73 ± 8.93
P33767	*WBP1*	N332	24.9 ± 6.36	61.64 ± 6.42	103.42 ± 1.51	92.73 ± 1.94	65.08 ± 14.79
P33767	*WBP1*	N60	4.4 ± 3.94	32.54 ± 8.34	99.01 ± 0.57	90.83 ± 6.28	12.84 ± 5.05
P36016	**LHS1**	N458	0.38 ± 1.56	5.5 ± 4.91	84.83 ± 4.39	89.18 ± 11.22	4.73 ± 3.05
P36051	**MCD4**	N198	39.75 ± 16.9	85.29 ± 3.57	N/A	47.95 ± 8.33	N/A
P36051	**MCD4**	N90	87.95 ± 9.28	106.62 ± 1.66	98.43 ± 0.12	105.68 ± 4.93	100.98 ± 8.24
P36091	DCW1	N203	87.52 ± 11.14	86.9 ± 4.86	99.08 ± 3.96	86 ± 1.58	84.68 ± 11.98
P37302	**APE3**	N150	52.91 ± 11.54	81.13 ± 4.36	84.99 ± 7.04	90.64 ± 11.42	52.53 ± 8.71
P37302	**APE3**	N162	107.35 ± 6.74	98.5 ± 10.61	103.27 ± 9.71	95.19 ± 8.87	29.59 ± 10.22
P37302	**APE3**	N85	47.72 ± 1.83	65.85 ± 6.25	109.52 ± 2.65	93.52 ± 4.38	102.58 ± 11.08
P37302	**APE3**	N96	82.18 ± 8.16	104.05 ± 2.42	59.81 ± 7.83	93.82 ± 6.01	5.02 ± 4.67
P38244	**PFF1**	N121	19.74 ± 5.78	73.63 ± 3.1	100.54 ± 13.07	103.76 ± 7.58	16.6 ± 3.61
P38248	*ECM33*	N304	10.34 ± 7.84	63.23 ± 4.48	108.15 ± 6.07	87.17 ± 1.07	55.37 ± 16.56
P38843	CHS7	N31	34.83 ± 4.32	104.88 ± 1.61	98.51 ± 1.01	99.97 ± 8.25	87.25 ± 6.8
P38875	GPI16	N184	6.87 ± 1.76	99.3 ± 9.93	97.36 ± 6.52	104.43 ± 3.53	95.52 ± 9.03
P38993	**FET3**	N244	8.69 ± 2.29	66.67 ± 1.51	79.97 ± 7.76	103.74 ± 12.75	40.52 ± 9.09
P38993	**FET3**	N359	64.51 ± 4.08	94.36 ± 4.94	72.94 ± 12.37	100.55 ± 10.6	72.7 ± 13.97
P39007	STT3	N539	66.68 ± 11.55	102.21 ± 5.5	89.18 ± 7.88	103.61 ± 4.28	95.22 ± 10.08
P39105	PLB1	N215	93.52 ± 4.38	90.36 ± 5.46	78.04 ± 7.36	93.1 ± 6.83	73.29 ± 6.06
P39105	PLB1	N489	76.92 ± 2.9	101.69 ± 3.65	93.94 ± 3.43	81.76 ± 1.73	92.46 ± 7.03
P40345	PDAT	N439	103.31 ± 0.13	98.13 ± 1.84	93.1 ± 6.83	88.05 ± 9.77	N/A
P40533	TED1	N266	34.18 ± 3.81	78.45 ± 1.32	87.97 ± 1.07	94.34 ± 0.36	60.37 ± 6.62
P40557	EPS1	N264	7.53 ± 3.1	108.27 ± 8.03	87.91 ± 3.6	90.04 ± 8.2	85.27 ± 6.25
P40557	EPS1	N299	40.37 ± 19	90.71 ± 9.52	75.86 ± 15.22	85.34 ± 3.58	56.07 ± 0.13
P41543	*OST1*	N217	22.19 ± 5.98	59.19 ± 0.88	98.58 ± 6.44	104.58 ± 6.74	N/A
P43561	FET5	N24	63.27 ± 16.13	78.26 ± 9.3	94.58 ± 2.7	89.3 ± 0.25	25.95 ± 7.39
P43561	FET5	N364	66.96 ± 0.37	97.89 ± 7.22	103.5 ± 3.96	96.16 ± 6.1	88.24 ± 12.25
P43611	**OSW7**	N297	0.13 ± 7.23	24.45 ± 9.38	103.23 ± 1.55	99.58 ± 4.67	39.4 ± 6.82
P46982	MNN5	N136	29.66 ± 7	93.32 ± 5.1	89.4 ± 5.08	92.41 ± 10.92	21.9 ± 0.98
P46992	YJR1	N219	50.14 ± 8.37	87.88 ± 1.37	89.87 ± 7.09	95.07 ± 4.66	44.3 ± 10.17
P52911	EXG2	N157	12.88 ± 1.05	80.59 ± 10.41	102.84 ± 4.52	100.04 ± 7.43	50.23 ± 12.71
P52911	EXG2	N50	35.06 ± 6.25	106.87 ± 5.12	88.11 ± 9.93	85.14 ± 5.77	78.55 ± 14.79
P53379	MKC7	N286	28.41 ± 11.05	96.74 ± 6.56	88.69 ± 13.07	96.01 ± 1.36	68.19 ± 10.36
P54003	SUR7	N47	28.16 ± 5.8	96.54 ± 3.85	88.39 ± 3.1	98.93 ± 1.42	53.97 ± 4.47
Q03103	**ERO1**	N458	58.06 ± 13.22	48.29 ± 4.07	74.07 ± 9.39	94.94 ± 2.27	41.26 ± 6.33
Q03281	HEH2	N520	27.3 ± 12.33	101.28 ± 3.38	96.09 ± 7.03	83.06 ± 10.2	8.12 ± 3.54
Q03674	PLB2	N193	2.11 ± 0.27	105.66 ± 4.32	76.22 ± 0.19	102.12 ± 0.84	N/A
Q03674	PLB2	N217	33.69 ± 7.84	85.64 ± 9.61	102.54 ± 7.69	98.66 ± 4.15	97.06 ± 6.47
Q03691	ROT1	N139	75.96 ± 15	82.94 ± 1.65	106.94 ± 1.91	104.16 ± 0.57	101.63 ± 4.83
Q06689	**YL413**	N429	10.52 ± 2.79	25.63 ± 14.09	105.59 ± 2.77	90.98 ± 11.19	40.78 ± 13.13
Q06689	**YL413**	N49	74.13 ± 11.88	92.56 ± 3.09	112.57 ± 12.49	91.95 ± 8.07	N/A
Q07830	**GPI13**	N411	22.18 ± 8.07	71.24 ± 6.77	96.53 ± 14.64	94.37 ± 5.33	79.6 ± 7.76
Q12465	**RAX2**	N640	51.16 ± 0.74	92.91 ± 6.76	94.94 ± 2.27	95.91 ± 10.74	32.91 ± 9.91
Q12465	**RAX2**	N677	3.73 ± 2.18	101.59 ± 1.19	106.04 ± 6.39	98.63 ± 6.26	29.25 ± 7.96
Q12465	**RAX2**	N88	1.44 ± 0.24	63.72 ± 12.38	96.74 ± 6.56	94.26 ± 6.12	N/A

Bold and italic - Ost3p substrates. Italic - novel Ost3 substrates.

Supplementary Table 3. Protein levels of glycoproteins in various OST mutant strains and Δ*alg9* strain compared to wild type cells. Data for Figure 5B.

UniProt ID	Protein	Δost3	Δost3+pOST6	Δost6	Δost6+pOST3	Δalg9
P00729	CPY	123.44 ± 7.14	93.91 ± 1.76	85.59 ± 8.94	109.36 ± 14.09	95.59 ± 10.99
P12684	HMG2	120.25 ± 1.71	88.6 ± 8.98	124.2 ± 18.72	158.37 ± 17.55	141.5 ± 16.93
P17967	PDI	182.48 ± 26.59	121.57 ± 9.45	91.2 ± 7.34	118.45 ± 9.76	164.86 ± 5.39
P22146	GAS1	55.04 ± 7.93	80.67 ± 1.8	93.4 ± 12.41	85.6 ± 2.67	114.75 ± 3.58
P23797	GPI12	84.9 ± 1.88	99.18 ± 7.71	85.39 ± 10	99.01 ± 7.47	99.27 ± 5.53
P27810	KTR1	130.97 ± 5.58	99.22 ± 0.5	119.8 ± 6	90.17 ± 5.43	110.93 ± 12.84
P27825	CNE1	N/A	217.01 ± 12.78	68.77 ± 0.45	111.94 ± 21.65	125.67 ± 15.71
P31382	PMT2	128.04 ± 9.51	106.33 ± 2.18	96.38 ± 5.46	99.32 ± 5.15	143.82 ± 10.64
P32353	ERG3	104.47 ± 9.87	110.61 ± 9.13	85.79 ± 4.45	105.3 ± 19.91	498.58 ± 67.42
P32623	CRH2	79.04 ± 1.08	96.3 ± 2.81	90.48 ± 6.3	123.64 ± 13.24	143.27 ± 14.61
P33302	PDR5	70.8 ± 4.22	92.75 ± 4.94	51.16 ± 3.76	92.6 ± 7.63	67.92 ± 6.8
P33754	SEC66	114.55 ± 4.35	102.87 ± 0.56	92.7 ± 8.84	94.46 ± 3.79	123.3 ± 18.98
P33767	WBP1	106.87 ± 7.81	105.13 ± 5.96	99.99 ± 8.85	98.57 ± 5.1	108.65 ± 5.29
P36016	LHS1	193.98 ± 16.49	121.16 ± 7.75	161.95 ± 39.58	122.5 ± 9.18	140.02 ± 7.5
P36051	MCD4	172.67 ± 1.55	88.52 ± 6.38	97.81 ± 0.36	105.07 ± 1.26	129.16 ± 4.98
P36091	DCW1	108.61 ± 26.26	89 ± 0.56	109.7 ± 4.2	91.73 ± 9.65	173.78 ± 17.35
P37302	APE3	88.38 ± 18.93	97.32 ± 14.92	83.88 ± 6.31	103.98 ± 6.31	86.58 ± 13.3
P38244	PFF1	65.06 ± 13.84	95.42 ± 11.24	97.27 ± 8.36	84.28 ± 6.19	105.28 ± 12.64
P38248	ECM33	66.16 ± 13.1	80.4 ± 3.99	70.91 ± 3.59	93.68 ± 8.47	131.78 ± 8.31
P38843	CHS7	95.76 ± 2.17	121.37 ± 9.43	91.85 ± 5.2	117.97 ± 8.35	170.38 ± 18.28
P38875	GPI16	105.61 ± 4.13	107.53 ± 2.55	N/A	104.17 ± 7.08	99.25 ± 16.36
P38993	FET3	70.65 ± 4.64	76.43 ± 8.74	61.09 ± 8.11	76.5 ± 6.24	111.72 ± 14.39
P39007	STT3	96.63 ± 8.97	99.91 ± 2.23	98.51 ± 6.21	97.44 ± 4.81	109.56 ± 18.32
P39105	PLB1	66.03 ± 8.86	55.34 ± 0.34	85.22 ± 5.29	122.38 ± 11.25	100.69 ± 8.04
P40345	PDAT	82.04 ± 5.24	94.83 ± 7.31	N/A	80.26 ± 4.47	96.34 ± 11.97
P40533	TED1	100.29 ± 15.62	90.77 ± 7.12	87.23 ± 7.12	91.79 ± 10.22	99.41 ± 5.26
P40557	EPS1	152.92 ± 26.91	87.06 ± 1.17	100.04 ± 11.86	89.92 ± 12.69	171.64 ± 17.28
P41543	OST1	109.59 ± 7.89	107.89 ± 3.71	103.7 ± 3.12	109.41 ± 5.65	98.51 ± 7.57
P43561	FET5	51.68 ± 16.13	85.01 ± 5.37	75.45 ± 0.91	102.93 ± 9.23	95.38 ± 14.97
P43611	OSW7	107.6 ± 15.79	82.79 ± 5.7	76.03 ± 0.41	65.74 ± 16.86	117.24 ± 8.98
P46982	MNN5	79.93 ± 6.04	84.56 ± 0.83	108.41 ± 16.77	90.21 ± 6.67	172.91 ± 26.82
P46992	YJR1	116.54 ± 8.14	105.36 ± 0.8	91.81 ± 4.08	113.65 ± 4.19	92.74 ± 8.75
P52911	EXG2	95.66 ± 10.65	85.09 ± 6.27	96.63 ± 6.16	104.43 ± 4.38	103.77 ± 11.87
P53379	MKC7	70.21 ± 5.56	92.72 ± 1.76	90.13 ± 7.89	93.14 ± 9.59	127.83 ± 7.15
P54003	SUR7	95.44 ± 3.04	87.64 ± 5.8	87.62 ± 8.67	84.71 ± 4.01	114.09 ± 18.67
Q03103	ERO1	216.12 ± 23.43	127.29 ± 2.12	104.01 ± 7.87	117.14 ± 4.44	169.75 ± 10.81
Q03281	HEH2	119.35 ± 3.68	95.9 ± 9.41	85.36 ± 8.13	86.45 ± 0.05	124.06 ± 13.24
Q03674	PLB2	59.09 ± 12.06	77.46 ± 6.42	94.82 ± 8.56	128.16 ± 12.06	108.76 ± 5.22
Q03691	ROT1	208.75 ± 54.58	102.99 ± 10.04	108.83 ± 3.22	120.52 ± 0.18	253.45 ± 28.11
Q06689	YL413	60 ± 6.16	101.91 ± 2.62	80.25 ± 5.64	94.06 ± 10.68	89.49 ± 9.57
Q07830	GPI13	140.93 ± 21.19	93.74 ± 3.4	102.16 ± 6.34	98.09 ± 4.3	109.92 ± 7.42
Q12465	RAX2	90.71 ± 6.22	91.81 ± 8.65	81.17 ± 3.25	94.58 ± 10.37	161.21 ± 9.23

Supplementary Table 4. Protein levels of different mevalonate, ergosterol and dolichol pathway proteins in strains deleted of *ALG3* or *ALG9* gene, or treated with sterol inhibitor miconazole. Data for Figure 5C.

UniProt ID	Protein	Δ*alg3*	Δ*alg9*	miconazole
P41338	ERG10	96.38 ± 7.34	89.06 ± 4.96	180.77 ± 0.75
P12683	HMG1	169.9 ± 1.34	177.27 ± 5.73	N/A
P12684	HMG2	160.84 ± 2.05	167.73 ± 2.38	86.34 ± 9.44
P07277	ERG12	114.77 ± 4.36	158.25 ± 0.63	144.2 ± 3.99
P32377	ERG19	90.48 ± 1.87	106.74 ± 11.52	144.51 ± 12.79
P08524	ERG20	124.35 ± 2.06	111.88 ± 10.25	125.67 ± 4.87
P29704	ERG9	100.18 ± 9.74	97.34 ± 3.22	157.37 ± 8.93
P32476	ERG1	259.71 ± 47.38	140.98 ± 5.53	102 ± 35.18
P38604	ERG7	131.31 ± 12.47	100.18 ± 2.36	147.58 ± 0.03
P10614	ERG11	482.55 ± 62.26	383.42 ± 23.58	571.84 ± 17.43
P53045	ERG25	471.15 ± 94.77	399.78 ± 10.2	404.82 ± 49.68
P53199	ERG26	97.68 ± 5.76	94.57 ± 6.31	175.91 ± 6.89
Q12452	ERG27	106.5 ± 10.12	103.92 ± 5.58	188.25 ± 4.68
P25087	ERG6	98.46 ± 11.23	95.85 ± 2.43	190.6 ± 5.05
P32352	ERG2	105.56 ± 14.6	110.93 ± 14.97	211.25 ± 5.04
P32353	ERG3	422.12 ± 41.84	434.27 ± 30.95	502.72 ± 21.75
P54781	ERG5	301.25 ± 43.12	232.19 ± 15.94	420.38 ± 52.99
P25340	ERG4	94.81 ± 9.23	94.53 ± 5.75	180.77 ± 0.75
P35196	RER2	100.92 ± 11.4	100.32 ± 6.39	92.23 ± 3.85
Q12063	NUS1	151.58 ± 23.59	142.06 ± 0.21	127.52 ± 5.66

Supplementary Table 5. Yeast strains used in this study. Related to Experimental Procedures.

Name	Genotype	Source
WT	*MATα his3Δ1 leu2Δ0 lys2Δ0 ura3Δ0 Δarg4Δ0*	This study
Δ*ost3*	*MATα his3Δ1 leu2Δ0 lys2Δ0 ura3Δ0 Δarg4Δ0 Δost3::LEU2MX6*	This study
Δ*ost3*+p*OST6*	*MATα his3Δ1 leu2Δ0 lys2Δ0 ura3Δ0 Δarg4Δ0 Δost3::LEU2MX6 + pOST3*	This study
Δ*ost6*	*MATα his3Δ1 leu2Δ0 lys2Δ0 ura3Δ0 Δarg4Δ0 Δost6::LEU2MX6*	This study
Δ*ost6*+p*OST3*	*MATα his3Δ1 leu2Δ0 lys2Δ0 ura3Δ0 Δarg4Δ0 Δost6::LEU2MX6 + pOST6*	This study
Δ*alg9*	*MATα his3Δ1 leu2Δ0 lys2Δ0 ura3Δ0 Δarg4Δ0 Δalg9::NATNT2*	This study
Δ*alg3*	*MATα his3Δ1 leu2Δ0 lys2Δ0 ura3Δ0 Δarg4Δ0 Δalg3::NATNT2*	This study

Supplementary Table 6. Plasmids used in this study. Related to Experimental Procedures.

Name	Gene	Souce
pOST3	*OST3*	(Schwarz et al., 2005)
pOST6	*OST6*	(Knauer and Lehle, 1999)

Chapter 3

Analysis of Substrate Specificity of *Trypanosoma brucei* OST by Functional Expression in Yeast

Kristina Poljak , Jörg Breitling, Robert Woodward, Amirreza Faridmoayer, Rober Gauss, George Rugarabamu, Mauro Pellanda, and Markus Aebi

Contributions:

Preparation of samples for mass spectrometry.

PRM MS measurements.

Data analysis.

Writing the manuscript.

Note:

The first part of this chapter, regarding LLO specificity of different *Tb*STT3 enzymes, has already been published in the PhD thesis of Jörg Breitling. The manuscript has been further extended by Kristina Poljak.

Summary

N-linked protein glycosylation is an essential and highly conserved post-translational modification in eukaryotes. The transfer of a glycan from a lipid-linked oligosaccharide (LLO) donor to asparagine residues of nascent polypeptide chains is catalysed by the oligosaccharyltransferase (OST) in the lumen of the endoplasmic reticulum. *Trypanosoma brucei* encodes three paralogue single protein OSTs called *Tb*STT3A, *Tb*STT3B and *Tb*STT3C that can functionally complement the *Saccharomyces cerevisiae* OST. We characterised the LLO specificity of all three OST isoforms in the heterologous expression host *S. cerevisiae* and demonstrated that *Tb*STT3A accepted LLO substrates ranging from $Man_5GlcNAc_2$ to $Man_7GlcNAc_2$. In contrast, *Tb*STT3B required $Man_6GlcNAc_2$ to $Glc_3Man_9GlcNAc_2$ structures while *Tb*STT3C did not display any LLO preference. Besides this substrate specificity *in vivo,* we show that all *T. brucei* OST transfer the short substrate $GlcNAc_2$ with equal affinity. We identified regions within different OST proteins that influence the specificity towards the LLO and polypeptide substrate.

Introduction

Asparagine-linked protein glycosylation (N-glycosylation) is a highly conserved posttranslational modification in eukaryotes. N-glycosylation is an essential process and plays important roles in protein folding quality control, cell-cell interactions and developmental processes (Lowe and Marth 2003; Helenius and Aebi 2004). The glycans transferred to nascent polypeptide chains in the endoplasmic reticulum (ER) are built on the lipid carrier dolichylphoshpate (Dol-P) to yield the lipid-linked oligosaccharide (LLO) substrate for OST. The biosynthesis of the LLO is an ordered, stepwise process conducted by the concerted action of specific glycosyltransferases that are encoded by the asparagine-linked glycosylation (*ALG*) genes. LLO biosynthesis is initiated by the addition of N-acetylglucosaminyl-phosphate and N-acetylglucosamine (GlcNAc) to the lipid carrier on the cytosolic face of the ER membrane using nucleotide activated UDP-GlcNAc as donor to form Dol-PP-$GlcNAc_2$. Subsequently the LLO is elongated by five mannose (Man) residues. The $Man_5GlcNAc_2$ LLO is then translocated into the ER lumen. There, Dol-P bound Man serves as donor for the further elongation of the LLO with Man until a $Man_9GlcNAc_2$ structure is built up. In most of the fungi and animal species the addition of three glucose (Glc) residues on the a-branch from Dol-P-Glc terminates LLO biosynthesis (Burda and Aebi 1999).

The mature $Glc_3Man_9GlcNAc_2$ LLO is used as donor substrate by the oligosaccharyltransferase (OST) that transfers the oligosaccharide from the lipid carrier *en bloc* to an asparagine residue of a nascent polypeptide chain. In eukaryotes, the acceptor asparagine residue is located within a conserved sequon consisting of three amino acids: asparagine, a second amino acid (any, but proline) and threonine or serine (NxT/S) (Gavel and von Heijne 1990). In multicellular eukaryotes the OST is a complex assembled from eight different proteins with *STT3* encoding the catalytic subunit (Yan and Lennarz 2002; Kelleher et al. 2003; Nilsson et al. 2003). Other subunits of the heterooligomeric complex were suggested to influence OST substrate interactions and complex assembly (Pathak et al. 1995; Spirig et al. 2005; Wilson et al. 2008; Schulz et al. 2009; Roboti and High 2012).

The genomes of the kinetoplastids *Trypanosoma* and *Leishmania* only encode homologues of the yeast *STT3* gene (Kelleher and Gilmore 2006). All other subunits found in heterooligomeric OST complexes of *S. cerevisiae* or mammals are missing in *T. brucei*, *T. cruzi* and *L. major*, suggesting that these proteins function as single subunit OSTs similar to enzymes known from bacterial and archaeal N-glycosylation systems (Wacker et al. 2002; Calo et al. 2010). *S. cerevisiae* has proven to be a suitable heterologous *in vivo* system to functionally express and characterize kinetoplastid OSTs. The yeast cells used in these studies lacked the essential yeast STT3 subunit or other essential OST subunits. This deleterious loss of a functional yeast OST is complemented by expression of different STT3 proteins

from *Trypanosoma cruzi*, *Trypanosoma brucei and Leishmania major*, demonstrating that these STT3s function as single protein OSTs (Castro et al. 2006; Parsaie Nasab et al. 2008; Hese et al. 2009; Izquierdo et al. 2009).

Trypanosoma brucei is a protozoan parasite causing African sleeping sickness in humans and nagana in cattle. *T. brucei* cells encounter two hosts during their life cycle. The parasite exists as the procyclic form in an insect vector (the tsetse fly) whereas it is referred to as bloodstream form when afflicting the mammalian host. The surface of *T. brucei* cells is covered by glycoproteins termed variant surface glycoprotein (VSG) in the bloodstream form and procyclins in its procyclic life stage. N-linked glycosylation epitopes on VSG play an important role in *T. brucei* virulence (Castillo-Acosta et al. 2016). Furthermore, a possible immune evasion strategy has been proposed where *T. brucei* genetically recombined its N-linked glycosylation machinery, resulting in the change of the glycosylation status of VSG (Castillo-Acosta et al. 2013). The *T. brucei* genome encodes three paralogues of *STT3* termed *Tb*STT3A, *Tb*STT3B and *Tb*STT3C (Samuelson et al. 2005; Izquierdo et al. 2009). In contrast to multicellular eukaryotes, trypanosomatids are incapable of synthesising Dol-P-Glc and therefore lack the three capping Glc residues found in yeast and higher eukaryotes (Parodi et al. 1981; de la Canal and Parodi 1987; Samuelson et al. 2005).

The three paralogue STT3s encoded by the *T. brucei* genome display distinct preferences for the LLO donor as well as for the acceptor polypeptide substrate. While *Tb*STT3A was shown to preferentially transfer $Man_5GlcNAc_2$ glycans to acceptor polypeptide chains, both *Tb*STT3B and *Tb*STT3C glycosylated acceptor sites with $Man_9GlcNAc_2$ glycans (Izquierdo et al. 2009). A recent study performed in *T. brucei* cells extended these findings, reporting that both *Tb*STT3A and *Tb*STT3B transfer $Man_7GlcNAc_2$ and $Man_5GlcNAc_2$ glycans to a VSG protein (Izquierdo et al. 2012). The authors suggest that the substrate specificity of *Tb*STT3A and *Tb*STT3B is promoted by the presence or absence of the LLO substrate c-branch. The LLO specificity of *Tb*STT3C was not addressed because this paralogue is not expressed in *T. brucei* cells used for the experiments (Izquierdo et al. 2009). Analysis of the OST protein products revealed that *Tb*STT3A and *Tb*STT3C preferentially glycosylate sequons with acidic amino acids in the sequon's vicinity. By contrast *TbSTT3*B did not display a particular preference for glycosylation sequons and the amino acids surrounding them (Izquierdo et al. 2009).

In this study, we used the functional expression of *T. brucei* STT3 proteins in yeast to analyse their function in detail. We took advantage of the "genetic tailoring" (Jakob et al. 1998) of the OST substrate and the quantitative analysis of glycosylation site occupancy (Poljak et al.; in preparation) to characterise *T. brucei* OST function. Domain-swap experiments made it possible to assign functional properties to specific regions of the STT3 proteins.

Results

*Tb*STT3A, *Tb*STT3B and *Tb*STT3C display differential preferences for LLO substrates from $Man_5GlcNAc_2$ to Glc3Man9GlcNAc2

In vivo analysis of the *Tb*STT3 LLO specificity revealed that *Tb*STT3B transfers primarily $Man_9GlcNAc_2$ oligosaccharides, while *Tb*STT3A transfers $Man_5GlcNAc_2$ glycans to its preferred glycosylation site of VSG221. Data acquired in the *Δstt3 S. cerevisiae* strain suggested that *Tb*STT3B and *Tb*STT3C both accept $Glc_3Man_9GlcNAc_2$ as LLO substrate, while *Tb*STT3A cannot utilise the $Glc_3Man_9GlcNAc_2$ LLO substrate (Izquierdo et al. 2009). We therefore further investigated the LLO specificity of all three *Tb*STT3 paralogues using the heterologous yeast expression system. We combined the *STT3* deletion with different deletions in the LLO biosynthesis pathway (*ALG* genes) in yeast. The *Δstt3Δalg* strains harbouring the yeast *STT3* (*ScSTT3*) *URA3*-plasmid and a second, *LEU2*-marked plasmid, encoding either *ScSTT3* or the different *TbSTT3* paralogues, were subjected to plasmid shuffling using 5-FOA. In this approach survival of the cells on 5-FOA depended on the ability of the different *TbSTT3* genes, encoded on the *LEU2* plasmids, to complement the yeast *STT3* deletion.

In the *Δstt3Δalg3* double mutant strain (accumulation of the $Man_5GlcNAc_2$ oligosaccharide), only *Tb*STT3A and *Tb*STT3C complemented the *STT3* deletion (Figure 1A). This result is in accordance with the finding that *Tb*STT3A can utilise the Man5GlcNAc2 LLO substrates in *T. brucei* (Izquierdo et al. 2009). Interestingly in both the Δ*stt3*Δ*alg9* and the Δ*stt3*Δ*alg12* strains, all three *TbSTT3* paralogues complemented the deletion of endogenous OST activity (Figure 1B and 1C). In the Δ*stt3* strain only *Tb*STT3B and *Tb*STT3C complement the *STT3* deletion, while *Tb*STT3A expressing cells did not survive plasmid shuffling (Figure 1E) (Izquierdo et al. 2009). The inability of *Tb*STT3A to complement *Δstt3* in the presence of $Glc_3Man_9GlcNAc_2$ LLOs was independent of the three terminal glucose residues on the LLO substrate since growth of *Δstt3Δalg6* cells expressing *Tb*STT3A was also not rescued (Figure 1D).

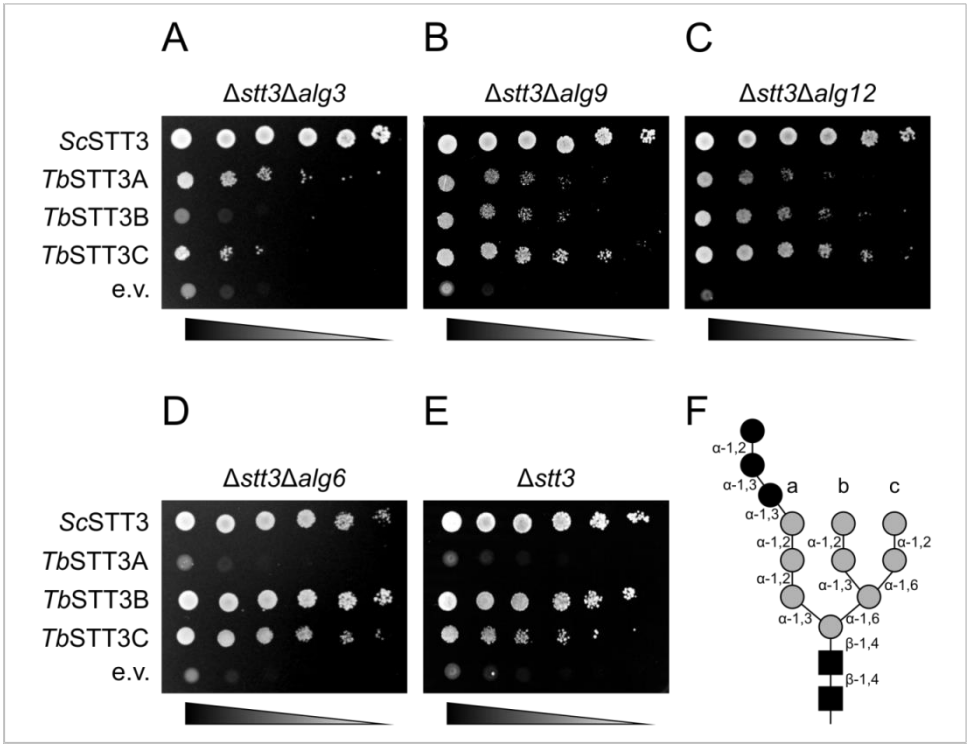

Figure 1. LLO specificity of *Tb*STT3 paralogues.

Strains deleted for genomic *STT3* (*Δstt3*) were complemented by a *URA3*-plasmid encoding yeast *STT3* (*Sc*STT3). The strains harboured a second, *LEU2*-marked plasmid encoding *Tb*STT3A, *Tb*STT3B, *Tb*STT3C, *Sc*STT3 or no STT3 gene (e.v.). Serial dilutions of (A) *Δstt3Δalg3*, (B) *Δstt3Δalg9*, (C) *Δstt3Δalg12*, (D) *Δstt3Δalg6* and (E) *Δstt3* were spotted on 5-FOA containing medium and incubated at 23°C for different times to select for ura- cells. STT3s encoded on the *LEU2*-plasmid complementing the genomic *Δstt3* deletion support growth on 5-FOA containing medium. LLO structures of the respective strains were depicted schematically. (F) The yeast LLO structure is represented by two GlcNAc (black squares), nine Man (grey circles) and three Glc (black circles) residues with the respective linkages indicated and LLO branches are labelled by a, b and c.

Our data confirm that the complementary activity of the different *T. brucei* STT3 proteins depended on the oligosaccharide structures of the substrate LLO. In particular, the observation that *Tb*STT3A was able to utilise LLO substrates from $Man_5GlcNAc_2$ up to $Man_7GlcNAc_2$ but did not accept LLOs with nine Man residues (i.e. in *Δstt3Δalg6* and *Δstt3*) suggested that c-branch Man residues reduced the use by *Tb*STT3A.

We tested this hypothesis by using *Δstt3Δalg9* cells complemented with *Tb*STT3 paralogues and overexpressing the yeast *ALG12* gene (p*ALG12*). Overexpression of *ALG12* in *Δalg9* cells resulted in a mixed LLO population consisting of $Man_6GlcNAc_2$ and $Man_7GlcNAc_2$ which contains the first c-branch α-1,6 Man residue added by *ALG12* (Figure 1F) (Burda et al. 1999). Protein-linked oligosaccharides (NLOs) were isolated to test whether the *ALG12*-generated triantennary $Man_7GlcNAc_2$ (Man7-ALG)

LLO can serve as a substrate for the three *Tb*STT3 paralogues to glycosylate substrate proteins. NLOs were enzymatically released from proteins, labelled with 2-AB and analysed by HPLC (Figure2A to 2D).

The first peak in the HPLC profile of NLOs obtained from the vector control strains corresponded to a $Man_6GlcNAc_2$ glycan (Figure 2A to 2D, e.v.). This oligosaccharide represented the $Man_6GlcNAc_2$ produced in *Δalg9* cells and transferred to proteins by OST. Higher mannose structures resolved in the chromatogram profile ($Man_7GlcNAc_2$ up to $Man_{11}GlcNAc_2$) reflected the subsequent addition of Man residues to the protein linked $Man_6GlcNAc_2$ by Golgi-resident mannosyltransferases (Munro 2001). Overexpression of *ALG12* in an *Δalg9* cell altered the LLO composition (Burda et al. 1999) and this was reflected by the altered NLO composition on N-glycoproteins. In all *Δalg9* control cells, small amounts of N-glycans larger than $Man_6GlcNAc_2$ were detected; they represent $Man_6GlcNAc_2$ structures modified in the Golgi (Munro 2001). Overexpression of the *ALG12* mannosyltransferase results in the generation of the triantennary $Man_7GlcNAc_2$ LLO substrate (Burda et al. 1999) and in an subsequent increase of the N-linked $Man_7GlcNAc_2$ glycans. However, this increase was dependent on the OST present: the endogenous OST (Figure 2A), *Tb*STT3B (Figure 2C) and *Tb*STT3C (Figure 2D) supported this transfer of $Man_7GlcNAc_2$ to protein, whereas expression of *Tb*STT3A led to minor alterations of N-glycan composition upon Alg12p overexpression (Figure 2B and 2E). We concluded that the α-1,3 Man added by *ALG12* mannosyltransferase reduced the affinity of *Tb*STT3A towards the lipid-linked oligosaccharide.

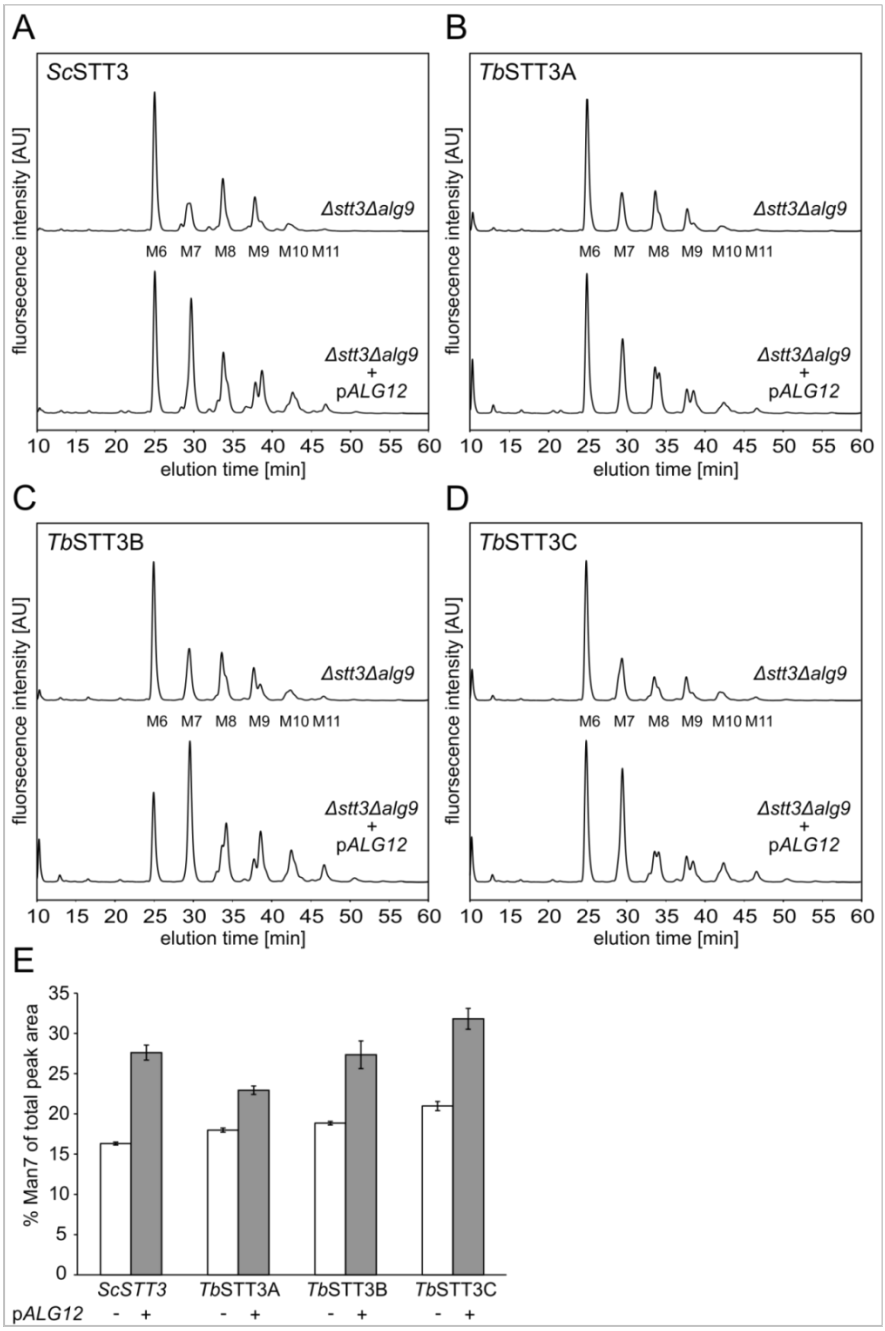

Figure 2. Analysis of NLOs isolated from *Δstt3Δalg9* cells complemented by *Tb*STT3 paralogues with or without overexpression of *ALG12.*

2-AB labelled NLOs were isolated from *Δstt3Δalg9* cells complemented by (A) *Sc*STT3, (B) *Tb*STT3A, (C) *Tb*STT3B or (D) *Tb*STT3C with (+ p*ALG12*) or without overexpression of *ALG12.* Labelled NLOs were separated by HPLC and fluorescence of the 2-AB label was detected (displayed as arbitrary units [AU]). In the resulting NLO profiles $Man_6GlcNAc_2$ (M6) up to $Man_{11}GlcNAc_2$ (M11) glycans were observed using NLOs from RNaseB to assign peak identities. (E) The $Man_7GlcNAc_2$ (Man7) NLO fraction in cells with (+) or without (-) *ALG12* overexpression were calculated and expressed as % of the total peak area of all NLO peaks (M6 to M11) of the individual strains (A-D) ± standard deviation from three independent experiments (error bars). Values of all peak areas can be found in Supplementary Table 1.

All TbSTT3 paralogues transfer GlcNAc2 LLOs to a peptide in vitro

Based on the experiments described above, we concluded that mannosyl residues present on the LLO substrate can alter the substrate specificity of the *T. brucei* OST. We therefore tested the activity of these enzymes towards the minimal $GlcNAc_2$ (chitobiose) substrate. Due to the lethal phenotype of *Δalg1* mutant strains (Albright and Robbins 1990), we turned to an in vitro assay and used tamra-labelled DANYTK peptide and microsomes from yeast cells deleted for endogenous *STT3* and expressing *Tb*STT3A, *Tb*STT3B or *Tb*STT3C. As LLO substrate we used a chemically synthesized $GlcNAc_2$ LLO whose lipid component is truncated compared to dolichol of yeast (Supplementary Figure 1A). Activity of the different enzymes was monitored by a shift in peptide mobility upon SDS-PAGE (Figure 3). We demonstrated *in vitro* activity in all cell extracts. For all three *Tb*STT3s activity was dependent on the presence of LLO and microsomes and the reaction was inhibited by EDTA, indicating cation dependence (Supplementary Figure 1B). We used the conversion of the peptide substrate at different LLO concentrations to roughly approximate the apparent k_m values for the LLO substrate and found them to be at the same order of magnitude for all OSTs (approximately 2.5-10 µM). Interestingly microsomes prepared from yeast wild type cells did not show any activity with the $GlcNAc_2$ LLO substrate under the conditions used (Supplementary Figure 1C).

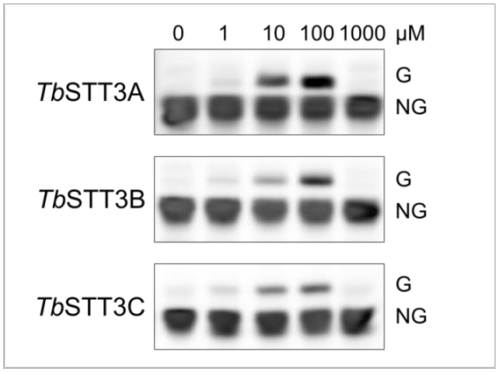

Figure 3. *In vitro* glycosylation assay with *Tb*STT3A, *Tb*STT3B and *Tb*STT3C using $GlcNAc_2$ LLO donor substrate. *Tb*STT3A, *Tb*STT3B and *Tb*STT3C were expressed in yeast cells with *Sc*STT3 deletion and microsomes were prepared from these cells. Microsomes were incubated with tamra-labelled peptide substrate and increasing $GlcNAc_2$ LLO concentrations (0-1000 µM). Subsequently non-glycosylated (NG) and glycosylated (G) peptides were separated by tricine SDS-PAGE and fluorescence of the tamra-label was detected.

Two distinct protein regions influence LLO specificity of *Tb*STT3B and *Tb*STT3C

*Tb*STT3B and *Tb*STT3C protein sequences are ~95% identical and sequence differences cluster in three distinct regions (Figure 4) but the OSTs differ significantly with respect to their LLO substrate specificity: *Tb*STT3B does not accept $Man_5GlcNAc_2$ LLOs, in contrast to *Tb*STT3C. We therefore reasoned that one or a combination of these regions would account for different LLO specificities of *Tb*STT3B and *Tb*STT3C.

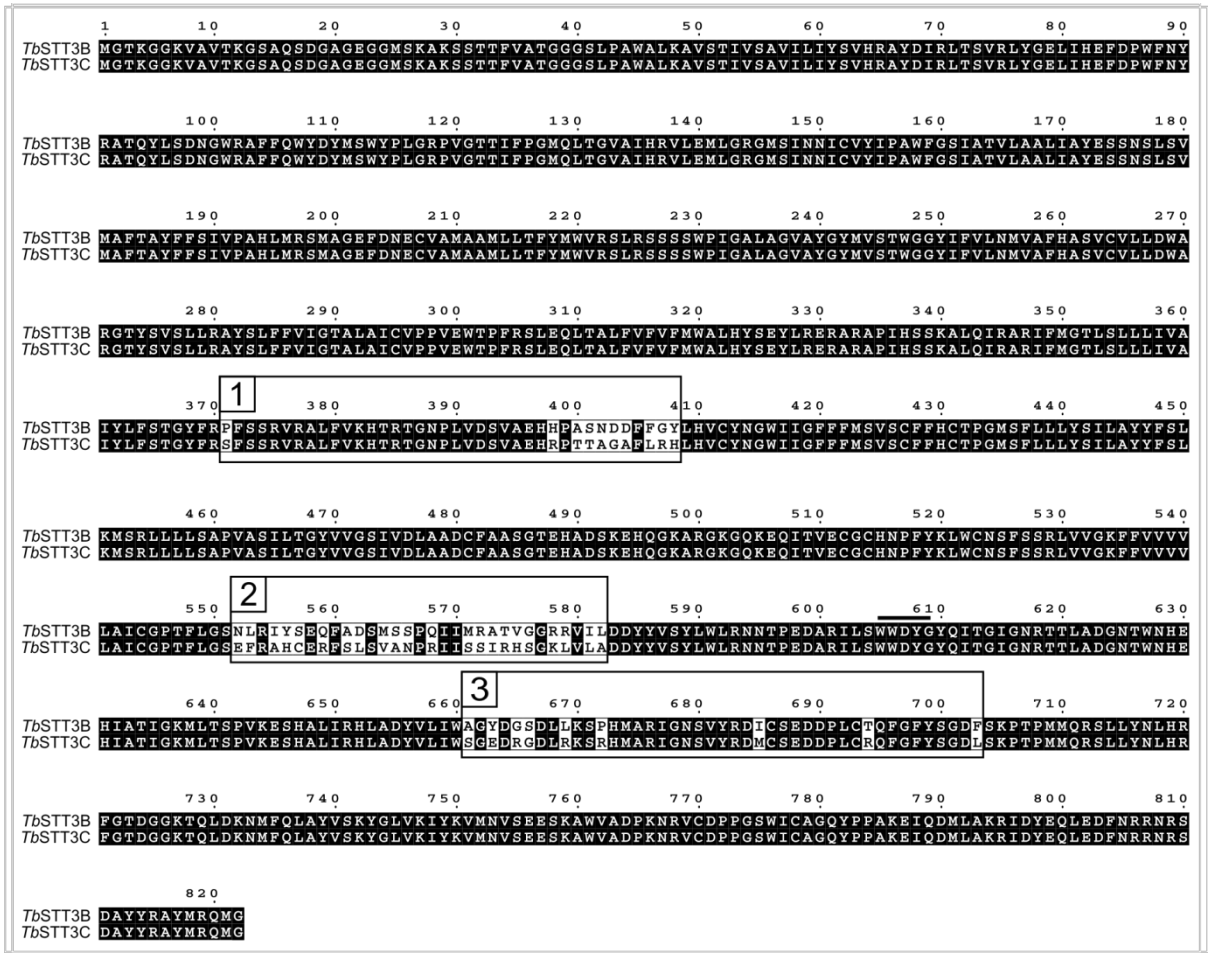

Figure 4. Protein sequence alignment of *Tb*STT3B and *Tb*STT3C.

Protein sequences of *Tb*STT3B and *Tb*STT3C were aligned and identical residues are displayed in black. Residues distinct in *Tb*STT3B and *Tb*STT3C were labelled white. The sequences of *Tb*STT3B and *Tb*STT3C show sequence differences in three discrete regions (1-3) labelled by a rectangle. The conserved WWDXG motif is marked by a horizontal line above the sequence.

The differences in LLO specificity led to the inability of *Tb*STT3B to rescue the growth of the *Δstt3Δalg3* strain, while *Tb*STT3C was able to complement the *STT3* deletion of this strain. *Tb*STT3B-C chimeras were constructed by exchanging single regions of *Tb*STT3B by corresponding regions of *Tb*STT3C (*Tb*STT3B-1C, *Tb*STT3B-2C, *Tb*STT3B-3C) or by combinations of two regions (*Tb*STT3B-1/2C, *Tb*STT3B-2/3C, *Tb*STT3B-1/3C). To test the effect of the region exchange on LLO specificity, *Δstt3Δalg3* cells harbouring the chimeric *Tb*STT3B-C constructs were subjected to 5-FOA induced plasmid shuffling and growth of the cells was assessed (Figure 5A). The exchange of region 1 in *Tb*STT3B strongly reduced growth in the *Δstt3Δalg3* ($Man_5GlcNAc_2$) and as well in the $Glc_3Man_9GlcNAc_2$ accumulating strain. In contrast, the exchange of region 2 (*Tb*STT3B-2C) allowed cell growth in both backgrounds comparable to *Tb*STT3C. Also the exchange of region 3 (*Tb*STT3B-3C) supported growth of *Δstt3Δalg3* cells albeit at a somewhat reduced level. These observations were further substantiated by the *Tb*STT3B-C chimeras with two regions exchanged. Both chimeras containing region 2 (*Tb*STT3B-1/2C, *Tb*STT3B-2/3C) promoted growth similar to *Tb*STT3C, while the chimera with region 1 and 3 (*Tb*STT3B-1/3C) resulted in a severe growth phenotype in *Δstt3Δalg3* cells, but not in cells with normal LLO biosynthesis (Figure 5A and 5B). We concluded that region 2 was required to determine LLO substrate specificity of *Tb*STT3B and *Tb*STT3C describing an oligosaccharide recognition domain of this single subunit OST.

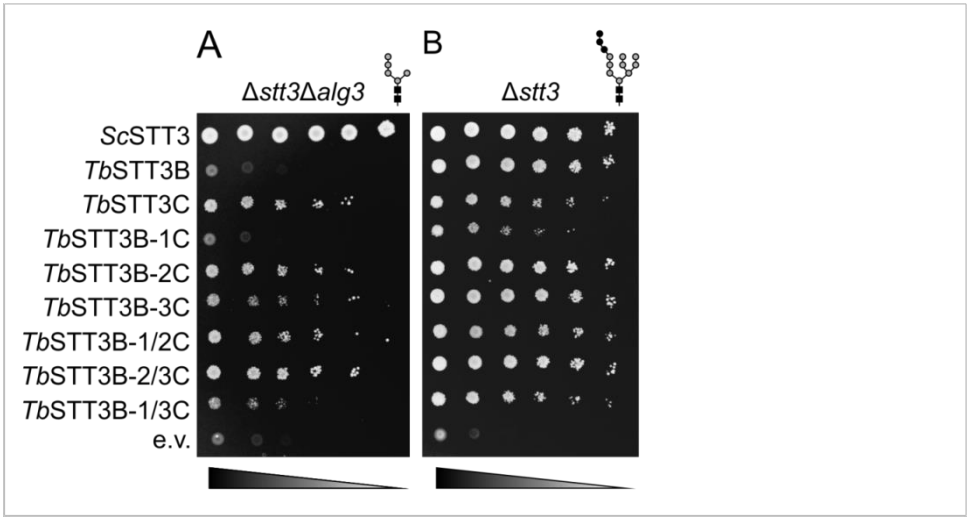

Figure 5. LLO specificity of *Tb*STT3s is provided by distinct regions in the proteins.

Strains deleted for genomic STT3 (*Δstt3*) were complemented by a *URA3*-plasmid encoding yeast *STT3* (*Sc*STT3). The strains harboured a second, *LEU2*-marked plasmid encoding *Tb*STT3B, *Tb*STT3C, *Tb*STT3B-C chimeras (see text for description), *Sc*STT3 or no STT3 gene (e.v.). Serial dilutions of (A) *Δstt3Δalg3* and (B) *Δstt3* were spotted on 5-FOA containing medium and incubated at 23°C for 7 d (*Δstt3*) to 15 d (*Δstt3Δalg3*) to select for *Ura*$^-$ cells. STT3s encoded on the *LEU2*-plasmid complementing the genomic *Δstt3* deletion support growth on 5-FOA containing medium. LLO structures of the respective strains were depicted schematically.

*Tb*STT3A, *Tb*STT3B and *Tb*STT3C display differential preferences for peptide substrates

Having established that region two is responsible for providing specificity towards the LLO donor substrate, we also sought to identify the region(s) of the *Tb*STT3 paralogues that provide(s) specificity towards polypeptide substrates. In the first step, differences in the glycosylation efficiencies of the three *Tb*STT3 paralogues for different glycosylation sites of yeast membrane proteins were addressed. It was previously reported, that *Tb*STT3A and *Tb*STT3C modified glycosylation sites more efficiently that are located in a sequence context with acidic amino acids while *Tb*STT3B did not display a particular preference for specific amino acids in the local environment of the glycosylation site (Izquierdo et al. 2009). A parallel reaction monitoring (PRM) mass spectrometry (MS)-based method was used to determine the occupancy of glycosylation sites from different yeast membrane proteins, which represents the percentage of peptides modified with a glycan at a given glycosylation site compared to same peptide in wild type cells. To monitor all three *T. brucei* OST proteins, we used the *Δstt3Δalg9* yeast strain to compare the glycosylation efficiencies of *Tb*STT3A, *Tb*STT3B and *Tb*STT3C. This strain generates a LLO substrate compatible with all *T. brucei* OSTs and the N-linked glycan is susceptible to EndoH digestion.

The stable isotope labelling with amino acids in cell culture (SILAC) coupled to parallel reaction monitoring (PRM) MS-based technique (Poljak et al.; in preparation) was used to analyse glycosylation occupancy at glycosylation sites on proteins in yeast microsomal membrane preparations. In short, a reference wild type strain was grown in medium containing heavy isotope labelled arginine and lysine while the strains expressing *Tb*STT3s were grown in the corresponding medium using regular amino acids (light). Cells were mixed 1:1, disrupted and samples were enriched for the glycoprotein-rich membrane fraction. N-linked glycans were cleaved by EndoH to maintain the first GlcNAc residue of the glycan on the protein. Proteins were digested enzymatically and the resulting peptides were analysed by liquid chromatography-electro spray-MS/MS. Corresponding light and heavy peptides were paired and site occupancies relative to the reference strain were calculated for *Tb*STT3 expressing cells based on light/heavy (L/H) ratios of the peak area values (Supplementary Table 2). Site occupancy reflected the preference of the OST for a given glycosylation site and its local environment. Glycosylation sites that are favoured by a given OST will be glycosylated more efficiently (i.e. higher site occupancy) as compared to sites not located in a favoured peptide sequence context.

Cluster analysis of the site occupancy data acquired for the *Tb*STT3 paralogues indicated that *Tb*STT3A and *Tb*STT3C glycosylation efficiency of the 55 analysed sites were similar and the efficiency of glycosylation by *Tb*STT3B was distinct from *Tb*STT3A and *Tb*STT3C (Figure 6A). This result confirmed

previously reported differences in the glycosylation efficiency observed for the *Tb*STT3B and *Tb*STT3C (Izquierdo et al. 2009).

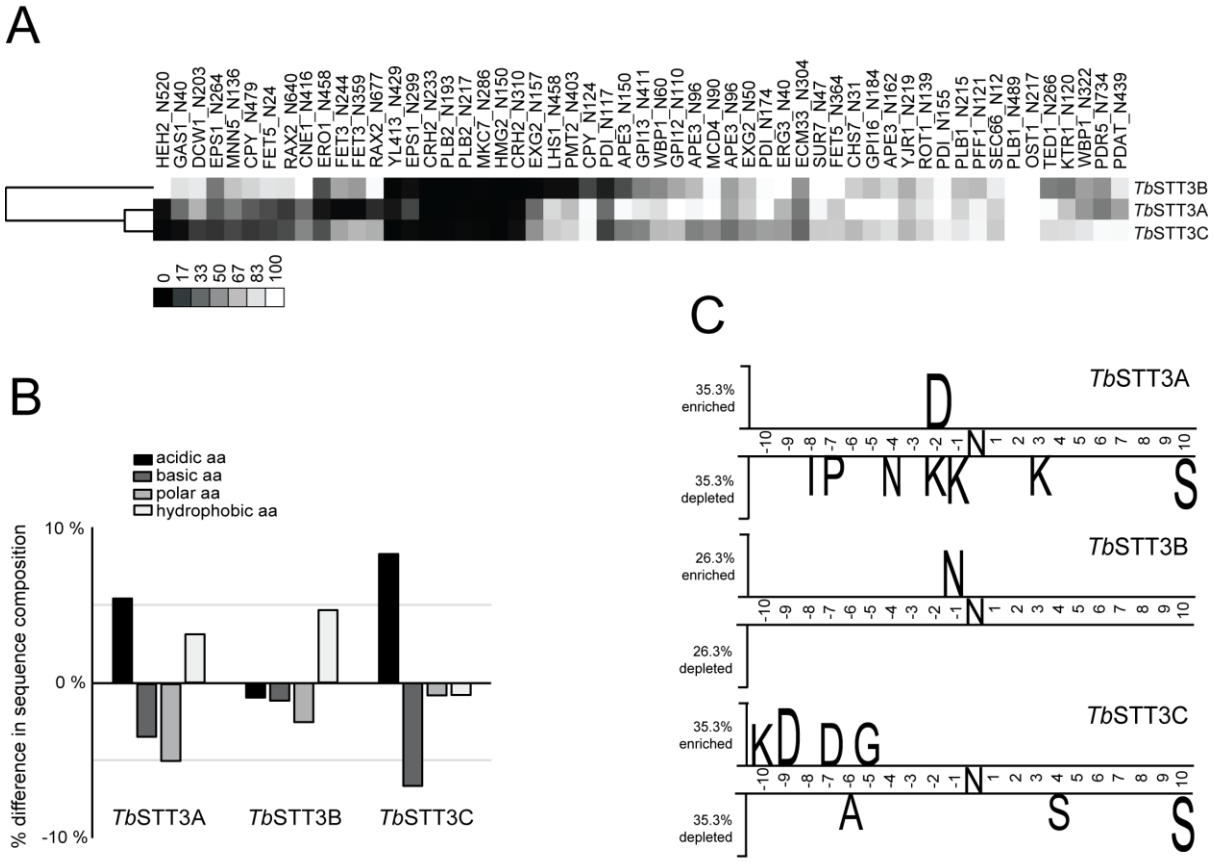

Figure 6. Glycosylation site occupancy and sequence composition analysis for *Tb*STT3s in *Δstt3Δalg9* cells.

Δstt3Δalg9 cells complemented with *Tb*STT3A, *Tb*STT3B and *Tb*STT3C were grown in light medium, mixed 1:1 with the wild type reference strain grown in heavy medium and membrane derived peptides were prepared. Peptide abundance was measured by PRM mass spectrometry. Intensity ratios of glycosylated light to heavy peptides were normalized for expression differences in *Tb*STT3 expressing cells and wild type cells. The resulting ratios represent the site occupancy for the *Tb*STT3 expressing cells relative to the wild type reference strain (reported in %). (A) Site occupancy values for *Tb*STT3A, *Tb*STT3B and *Tb*STT3C were used for cluster analysis. In cluster analysis samples with high similarity are close while samples with low similarity are distant from each other. (B) Sequence composition analysis was preformed where amino acids were grouped based on their polarity. Percentage change in respective ratio of each amino acid group between efficiently and poorly glycosylated sequences upstream of glycosylation sequons was calculated for each *Tb*STT3 expressing strain. (C) Two sample logo analysis (Vacic et al. 2006) was used to visualize differences between efficiently and poorly glycosylated sequences surrounding the glycosylation sites for each TbSTT3 expressing strain.

We then examined the polypeptide substrate specificity of *Tb*STT3 paralogues in the context of sequence polarity. Sequence composition analysis was performed on glycosylation sequons themselves plus ten residues downstream and upstream of the glycosylation sites. Amino acid residues were grouped based on their polarity into acidic (Asp, Glu), basic (Arg, Lys, His), polar (Ser, Thr, Asn, Glu, Cys, Tyr) and hydrophobic (Ala, Val, Ile, Leu, Met, Phe, Trp, Pro, Gly) group. Sequences were divided into 'efficiently' and 'poorly' glycosylated, when the glycosylation occupancy calculated was more than 85% or less than 25% compared to reference strain, respectively. Ratio of each amino acid group was calculated compared to total number. Percentage change in respective ratios of each amino acid group between efficiently and poorly glycosylated sequences downstream and upstream of glycosylation sequon was calculated for each *Tb*STT3 expressing strain. The analysis of sequences downstream of the glycosylation sites showed no apparent difference in sequence specificity between different *Tb*STT3 paralogues (Supplementary Table 3). All three enzymes showed preference for hydrophobic residues while polar residues were not favoured. The analysis of upstream sequences revealed that both *Tb*STT3A and *Tb*STT3C preferred acidic residues (Figure 6B). Additionally, both paralogues showed disfavour towards basic residues. However, *Tb*STT3B showed no specific preference for any amino acid type. These results support previously reported difference in the polypeptide acceptor substrate specificity, where *Tb*STT3A and *Tb*STT3C showed selectivity towards glycosylation sequons flanked by acidic residues while TbSTT3B lacked any obvious preference (Izquierdo et al. 2009). Furthermore, it has been confirmed that upstream amino acids play a dominant role in TbSTT3A acceptor peptide specificity (Jinnelov et al.; personal communication).

Site occupancy data acquired for the *Tb*STT3 paralogues was further exploited to examine if there is a particular preference for specific amino acids in the local environment of the glycosylation sites. To establish if there are consensus sequences or patterns that control site-specific N-glycosylation, two sample logo analysis (Vacic et al. 2006) was used to calculate and visualize statistically significant residues surrounding glycosylation sites (Figure 6C). In agreement with sequence composition analysis, both *Tb*STT3A and *Tb*STT3C showed efficient glycosylation of sites containing aspartic acid. Sequences enriched in aspartic acid at -2 position are more likely to be efficiently glycosylated by *Tb*STT3A, while *Tb*STT3C preferred sequences enriched in aspartic acid at -9 position. Similar to previous data, *Tb*STT3B showed no specific preference. Preference for TbSTT3A for amino acids immediately adjacent to the glycosylation site has been supported (Jinnelov et al.; personal communication).

A distinct protein region influences polypeptide specificity of *Tb*STT3B and *Tb*STT3C

To define the polypeptide substrate specificity more closely, we used *Tb*STT3B-C chimeras to identify regions of the OST proteins that influenced the preference for certain glycosylation sites. Due to the fact that the chimera *Tb*STT3B-1C yielded poor growth of the strains, we took advantage of the stabilising property of the concomitant exchange of the region 3 and compared the *Tb*STT3B-1/3C (= *Tb*STT3C-2B) to the *Tb*STT3B-2/3C (= *Tb*STT3C-1B) chimera that yielded similar growth in *Δstt3Δalg9* cells (Supplementary Figure 2). Glycosylation efficiencies of different chimeras were determined using MS-based method described above and the cluster analysis of the site occupancy data was performed (Figure 7A). *Tb*STT3B-1/3C displayed highest similarity with *Tb*STT3C while the corresponding chimera *Tb*STT3B-2/3C showed only little similarity with *Tb*STT3C. Exchange of region 1 seems to influence glycosylation efficiency of the two TbSTT3 paralogues examined.

We defined this specificity more closely and focused the analysis only on the sites that were differentially glycosylated by *Tb*STT3B and *Tb*STT3C. Sequence composition analysis was performed where the percentage change in respective ratios of acidic and basic amino acid groups between efficiently and poorly glycosylated sequences upstream of glycosylation sequon was calculated for each *Tb*STT3 expressing strain. As expected, *Tb*STT3C showed preference for the acidic residues while, in this analysis, these were disfavoured by *Tb*STT3B enzyme (Figure 7B). Similar to *Tb*STT3C, *Tb*STT3B-1/3C chimera displayed preference for acidic sequences upstream of glycosylation sites. Interestingly, two sample logo analysis revealed that both *Tb*STT3C paralogue and *Tb*STT3B-1/3C chimera showed preference for an aspartic acid at the same position upstream of the glycosylation sequon (Figure 7C). Similar to previous data, *Tb*STT3B showed no specific preference and the same was true for *Tb*STT3B-2/3C chimera. Involvement of region 1 in sequon specificity of *Tb*STT3B and *Tb*STT3C has been demonstrated before where upon genetic rearrangements a chimeric gene was generated containing the first variable region of *Tb*STT3C flanked by *Tb*STT3B sequences. The chimeric *Tb*STT3B/C/B protein described in this publication showed much less efficient recognition of the native substrate of TbSTT3B while it appeared to have attained a peptide acceptor specificity more similar to TbSTT3A than TbSTT3B (Castillo-Acosta et al. 2013).

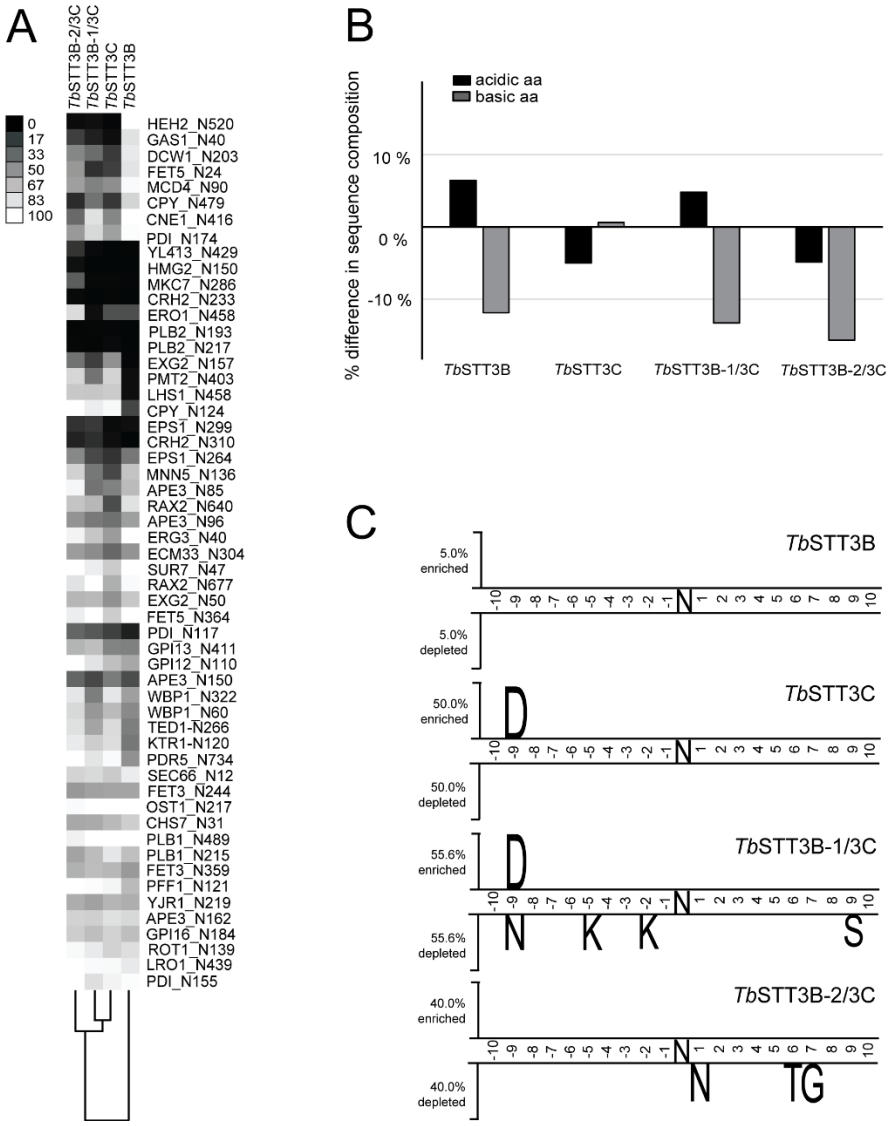

Figure 7. Glycosylation site occupancy and sequence composition analysis for *Tb*STT3B-1/3C and *Tb*STT3B-2/3C chimeras in *Δstt3Δalg9* cells.

Δstt3Δalg9 cells complemented with *Tb*STT3B, *Tb*STT3C, *Tb*STT3B-1/3C and *Tb*STT3B-2/3C were grown in light medium, mixed 1:1 with the wild type reference strain grown in heavy medium and membrane derived peptides were prepared. Intensity ratios of glycosylated light to heavy peptides were normalized for expression differences in *Tb*STT3 expressing cells and wild type cells. The resulting ratios represent the site occupancy for the *Tb*STT3 expressing cells relative to the wild type reference strain (reported in %). (A) Site occupancy values for *Tb*STT3B, *Tb*STT3C, *Tb*STT3B-1/3C and *Tb*STT3B-2/3C were used for cluster analysis. In cluster analysis samples with high similarity are close while samples with low similarity are distant from each other. (B) Sequence composition analysis was preformed where amino acids were grouped based on their polarity. Percentage change in respective ratio of each amino acid group between efficiently and poorly glycosylated sequences upstream of glycosylation sequon was calculated for each *Tb*STT3 expressing strain. (C) Two sample logo analysis (Vacic et al. 2006) was used to visualize differences between efficiently and poorly glycosylated sequences surrounding the glycosylation sites for each TbSTT3 expressing strain.

Discussion

Functional expression of single subunit OSTs from kinetoplastids in *Saccharomyces cerevisiae* has proven to be a useful model system to study the properties of STT3s from *L. major*, *T. cruzi* and *T. brucei* (Castro et al. 2006; Parsaie Nasab et al. 2008; Hese et al. 2009; Izquierdo et al. 2009). Yeast genetics methods allow manipulations of the LLO biosynthesis pathway to generate specific intermediate oligosaccharide structures (Jakob et al. 1998) that can be used to study the influence of altered LLO substrates on OSTs. Consequences of such altered substrates for N-glycosylation can be monitored by analysing N-glycoproteins, the products of the OST catalysed reaction. Both single N-glycoproteins like carboxypeptidase Y (te Heesen et al. 1992; Helenius et al. 2002) and MS-based methods, which allow a broader view on many N-glycoproteins at the same time, were used to study consequences of alterations in the N-glycosylation process (Poljak et al; in preparation). Furthermore, the structures of glycans transferred to proteins can be identified and characterised to gain insights into OST selectivity, *ALG* glycosyltransferase products or processing of protein bound glycans (Jakob et al. 1998; Cipollo and Trimble 2002; Kelleher et al. 2007). The combination of genetics and analytical tools available in *S. cerevisiae* thus represents an excellent system to perform reverse genetics approaches to study particular OST features.

In vivo analysis of the *T. brucei* VSG221 protein showed that *Tb*STT3A transfers $Man_5GlcNAc_2$ glycans to protein, while *Tb*STT3B prefers $Man_9GlcNAc_2$ as substrate for N-glycosylation (Izquierdo et al. 2009). Analysis of VSG221 proteins in *T. brucei Tb*ALG3^{-}/$^{-}$ and *Tb*ALG12^{-}/$^{-}$ mutant strains revealed that also LLO intermediates can serve as substrates for both *Tb*STT3A and *Tb*STT3B, although with reduced efficiency. It was hypothesised that efficient glycosylation of VSG221 by *Tb*STT3A correlates with the absence of the LLO c-branch, while for *Tb*STT3B the presence of the c-branch is an important determinant to improve glycosylation (Manthri et al. 2008; Izquierdo et al. 2012).

Analysis of the LLO specificities of *Tb*STT3A and *Tb*STT3B in *T. brucei* was possible, since the two VSG221 glycosylation sites get selectively modified either by *Tb*STT3A with $Man_5GlcNAc_2$ glycans or by *Tb*STT3B with $Man_9GlcNAc_2$ oligosaccharides . This selectivity for a specific glycosylation sequon is provided by the distinct polypeptide specificities of *Tb*STT3A and *Tb*STT3B (Izquierdo et al. 2009). Since *Tb*STT3C was not expressed in *T. brucei*, its substrate specificity was investigated in the heterologous yeast expression system. *Tb*STT3C shared the preference for acidic sequons with *Tb*STT3A but used $Man_9GlcNAc_2$ as LLO substrate, as observed with *Tb*STT3B (Izquierdo et al. 2009).

Our detailed investigations on LLO specificity in the yeast *in vivo* system confirmed the results obtained from *T. brucei* for *Tb*STT3A and *Tb*STT3B. Furthermore, we could demonstrate that the inability of *Tb*STT3A to complement the *STT3* deletion of yeast cells was independent of LLO glucosylation. Since

terminal Glc residues of the LLO a-branch did not influence *Tb*STT3A, although *T. brucei* synthesises only non-glucosylated LLOs (Samuelson et al. 2005), an interaction of *Tb*STT3A with the terminal Man residue of the LLO a-branch seems unlikely. The inability of *Tb*STT3A to support growth of the *Δstt3* and *Δstt3Δalg6* strains was rather due to the presence of LLO c-branch mannoses which seemed to prevent efficient glycosylation by *Tb*STT3A. *Tb*STT3B was able to support growth of all strains tested with the exception of *Δstt3Δalg3*. In *T. brucei*, *Tb*STT3B modified VSG221 in a *Tb*ALG3$^{-/-}$ strain, although with reduced efficiency (Manthri et al. 2008). The inability of *Tb*STT3B to rescue the growth of *Δstt3Δalg3* yeast cells was therefore likely to result from reduced overall glycosylation levels, which were too low to allow survival of the yeast cells, rather than the inability to use $Man_5GlcNAc_2$ LLOs as substrate in the heterologous host. Opposed to *Tb*STT3A and *Tb*STT3B, which both displayed distinct LLO donor substrate preferences, *Tb*STT3C did not show a specific preference towards the LLO donor substrates tested. It can be speculated that *Tb*STT3C does not recognise or only weakly interact with the Man residues added to the LLO substrate in the ER. Instead *Tb*STT3C may be recognising only a core structure of the LLO that is recognised by all three *Tb*STT3 paralogues. Although *Tb*STT3 paralogues could utilise a range of LLO substrates to glycosylate proteins, no intermediate glycan structures are transferred to protein by *Tb*STT3A and *Tb*STT3B unless *ALG* mutations were introduced (Manthri et al. 2008; Izquierdo et al. 2009; Izquierdo et al. 2012). This indicates, that additional factors like availability or accessibility of LLO biosynthesis intermediate and k_m values of the *ALG* enzymes fine tune the glycosylation machinery leading to the specific transfer of $Man_5GlcNAc_2$ LLOs by *Tb*STT3A and $Man_9GlcNAc_2$ oligosaccharides by *Tb*STT3B (Izquierdo et al. 2009).

We could demonstrate transfer of a $GlcNAc_2$ glycans by all *T. brucei* OSTs to substrate peptides. This had several implications: 1) *Tb*STT3 paralogues recognise the $GlcNAc_2$ core of LLO substrates 2) *T. brucei* OSTs distinguish LLOs by distal Man residues, probably of the c-branch, since the apparent k_m values of all three *Tb*STT3 paralogues for the $GlcNAc_2$ substrate were similar. 3) *Tb*STT3 enzymes are not highly specific for the length of the lipid carrier; although the natural lipid carrier of *T. brucei* has 11-12 isoprene units (Low et al. 1991), both truncated (five isoprene units) and elongated lipid carriers (15-16 isoprene units) (Jung and Tanner 1973; Adair and Cafmeyer 1987) were accepted as LLO substrates *in vitro* and *in vivo*, respectively. Unlike *T. brucei* OSTs, *S. cerevisiae* OST was shown to only efficiently use $GlcNAc_2$ as LLO substrate *in vitro* when dolichol but not truncated lipid carrier moieties were used (Fang et al. 1995; Tai and Imperiali 2001). This may hint towards differences between yeast OST and *Tb*STT3s with regards to the requirements for the lipid-portion of the LLO substrate. One might speculate that the specificity for the lipid moiety of LLOs in yeast may be provided by a non-catalytic OST subunit.

The heterologous expression system allowed us to perform targeted structure-function analyses. Region 2, which was found to be important for LLO specificity, is located in the C-terminal part of the *Tb*STT3 protein after the last predicted transmembrane helix. This C-terminal domain was predicted to be localised in the ER lumen due to the presence of the highly conserved WWDXG motif that is important for the glycosylation reaction of OSTs (Yan and Lennarz 2002; Igura et al. 2008; Lizak et al. 2011). The results presented here identify for the first time regions of the *Tb*STT3 proteins that are important for LLO specificity and provide a basis to further investigate the molecular mechanisms and contribution of single amino acids in OST LLO interaction.

Glycosylation efficiency of a given OST can be determined by analysing site occupancy for different substrate polypeptides (Parsaie Nasab et al. 2008; Izquierdo et al. 2009; Schulz and Aebi 2009; Xu et al. 2015; Zacchi and Schulz 2016; Poljak et al. in preparation). Here we compared the site occupancies for the three *Tb*STT3 paralogues in the *Δstt3Δalg9* strain relative to a wild type reference strain. Our results confirmed previous observations, made in two different expression hosts, that *Tb*STT3A and *Tb*STT3C have similar polypeptide substrate preferences (Izquierdo et al. 2009). We further found, that region 1 influences the glycosylation efficiency of certain polypeptide substrate glycosylation sites. *PglB*, the bacterial homologue of *STT3*, interacts with the threonine/serine residue of the glycosylation sequon of its peptide substrate via residues of the conserved WWDXG motif, which determines the specificity for the sequon sequence. A periplasmic loop connecting transmembrane helices 9 and 10 (i.e. external loop 5; EL5) also showed significant interaction with the peptide substrate. The C-terminal part of EL5 pins the peptide against the periplasmic domain, but it also contains the conserved residue E319 that is part of the catalytic site of PglB (Lizak et al. 2011). In the *Tb*STT3 paralogues, the region surrounding the WWDXG motif is completely conserved. Therefore, it seems unlikely that this region is responsible for the differences observed in site occupancy between *Tb*STT3B and *Tb*STT3C. Sequence alignments between *PglB* from *Campylobacter lari* and *Tb*STT3B and *Tb*STT3C showed that the conserved residue E319 of *PglB* has an equivalent glutamic acid residue in the *Tb*STT3s that is located in region 1 of *Tb*STT3B and *Tb*STT3C (i.e. E396). Hence, it is tempting to speculate that region 1 could be the functional equivalent to the EL5 described in *PglB*. Region 1 might interact with polypeptide substrates and modulate the glycosylation efficiency of *Tb*STT3s. Interestingly, towards the C-terminal end of region one, both *Tb*STT3A and *Tb*STT3C have conserved sequences, while the amino acid residues of *Tb*STT3B at these positions are different. This seemed to coincide with the observed differences in site occupancy and sequence composition for *Tb*STT3A and *Tb*STT3C compared to *Tb*STT3B. We showed that amino acids upstream of glycosylation site play a dominant role in *Tb*STT3s polypeptide specificity. Furthermore, we were able to depict specific amino acid residues in polypeptide substrate sequences that increase the chances of such substrates being

efficiently glycosylated by different *Tb*STT3 paralogues. Sequences enriched in aspartic acid at -2 position are more likely to be efficiently glycosylated by *Tb*STT3A, while *Tb*STT3C preferred sequences enriched for aspartic acid at -9 position. We also showed that sequence preference for a specific amino acid is region 1 dependent. More experimental work and crystal structures of eukaryotic single protein OSTs will provide insights into the molecular basis of polypeptide specificity.

Materials and Methods

Media, Yeast strains and plasmids

Standard yeast media and molecular biology methods were used (Guthrie and Fink 1991). For maintenance of plasmids, cells were grown in appropriate synthetic medium lacking amino acids necessary for selection.

To generate haploid double mutant strains with genomic deletions of *STT3* and *ALG3, ALG9, ALG6* genes to test the complementation by different TbSTT3s, haploid mutant strains with deletions in *ALG3, ALG6* and *ALG9* genes were purchased (Euroscarf): Y13108 (*alg3Δ::KanMX4*), Y01993 (*alg9Δ::KanMX4*) and Y11778 (*alg6Δ::KanMX4*). These strains were individually mated with YBS10 and YBS11 strains, respectively (Parsaie Nasab et al. 2008), sporulation was induced and tetrads were dissected on YPD plates containing 1 M sorbitol. Haploid spores harbouring the *STT3*-plasmid and the two deletions in the *STT3* and *ALG3, ALG6 or ALG9* loci were identified on G418-containing media in nonparental ditype tetrads. The absence of the *ALG3, ALG6* and *ALG9* genes in the double mutant strains was confirmed by PCR. The *Δstt3Δalg12* strain was generated from YG2082 by exchanging LmSTT3D by the plasmid encoding the yeast STT3 locus (Zufferey et al. 1995; Parsaie Nasab et al. 2008).

To test complementation of the *STT3* deletion by *Tb*STT3 paralogues the following strains were used: *Δstt3* (YBS11) (*STT3::kanMX4 MAT*a *his3Δ1 leu2Δ0 met15Δ0 ura3Δ0 lys2Δ0*) (Parsaie Nasab et al. 2008)*; Δstt3Δalg6* (*stt3Δ::kanMX4 alg6Δ::kanMX4 MAT*a *his3Δ1 leu2Δ0 met15Δ0 ura3Δ0 lys2Δ0); Δstt3Δalg12 (stt3Δ::kanMX4 alg12Δ::kanMX4 MATa his3Δ1 leu2Δ0 met15Δ0 ura3Δ0 lys2Δ0); Δstt3Δalg9* (*stt3Δ::kanMX4 alg9Δ::kanMX4 MAT*α *his3Δ1 leu2Δ0 met15Δ0 ura3Δ0 lys2Δ0*)*; Δstt3Δalg3* (*stt3Δ::kanMX4 alg3Δ::kanMX4 MAT*a *his3Δ1 leu2Δ0 ura3Δ0 lys2Δ0*). The *STT3* deletion was complemented by a plasmid encoding the yeast *STT3* locus encoding the yeast STT3 locus in a URA3 marked YEp352 vector (Zufferey et al. 1995). These cells were transformed with *T. brucei* STT3 paralogues encoded by LEU2 marked plasmids under the control of the yeast GPD promoter (Izquierdo et al. 2009). The yeast STT3 locus was cloned as a *Hind III* fragment from the yeast *STT3* locus harbouring plasmid (Zufferey et al. 1995) into the pRS425GPD vector as control for the plasmid shuffling procedure. Cells were grown after plasmid shuffling in appropriate defined medium containing 1 M sorbitol.

*Tb*STT3B-C chimera plasmids were generated by homologous recombination. PCR fragments encoding the different regions (1, 2, 3) were generated with primers 5'-AGCGCAACTACAGAGAAC-3', 5'-ACAGATGGCAAGGACAAC-3', 5'-CGTTCCTGCTGTTGTACTC-3', 5'-GCTATGTGCTCGTGATTCC-3', 5'-CTGAAGATGCCCGTATTCTC-3' and 5'-CGCACGATAATAAGCGTCAC-3' using either *Tb*STT3B or *Tb*STT3C

plasmids as template. PCR fragments were designed to have overlapping sequences with the vector or a PCR fragment containing a neighbouring region. To assemble the different chimeras, *Tb*STT3B vector was gapped with *Nco* I and *Bgl* II and yeast cells were co-transformed with the gapped vector and all possible combinations of PCR fragments encoding for the 3 different regions from either *Tb*STT3B or *Tb*STT3C for homologous recombination. Plasmids were isolated from yeast, amplified in *E. coli* DH5α and correct chimera assembly was confirmed by sequencing the inserted DNA. For overexpression of *ALG12,* previously described constructs were used (Burda et al. 1999). Analysis of glycosylation site occupancy was performed with three biological replicates of the *Δstt3Δalg9* strain harbouring *Tb*STT3A, *Tb*STT3B, *Tb*STT3C or TbSTT3B-C chimera plasmids. KP4 (MATα *his3Δ1 leu2Δ0 lys2Δ0 ura3Δ0 arg4Δ::0*) was used as reference strain.

Specificity for lipid linked oligosaccharides

Lipid-linked oligosaccharide specificity was tested by plasmid shuffling with the respective *Δstt3Δalg*-double mutant strains harbouring both, the *URA3* marked p*ScSTT3* plasmid and the *LEU2* marked *Tb*STT3 or *ScSTT3* encoding plasmids. These cells were subjected as serial dilution to minimal medium containing 1 mg/ml 5-fluoroorotic acid (5-FOA (Boeke et al. 1987)) and 1 M sorbitol. The presence of 5-FOA allowed the selection of cells that lost the Ura^+ p*ScSTT3* plasmid These Ura^- cells only survived when the STT3 genes encoded on the *LEU2*-plasmid could complement the yeast *STT3* deletion. Strains were incubated at 23°C for 7-15 d depending on cell growth.

In vitro glycosylation assay

*ScSTT3, Tb*STT3B and *Tb*STT3C were expressed in *Δstt3* cells and *Tb*STT3A was expressed in *Δstt3Δalg3* cells. Cells were grown to log-phase (OD_{600nm} 2-3), harvested by centrifugation and washed in ice-cold PBS. Cells were resuspended in lysis buffer (PBS (pH7.3); 1 mM DTT; complete protease inhibitor cocktail (PIC; Roche); 10 mM PMSF) and broken with glass beads at 4°C. The lysate was centrifuged (17211 x g, 10 min, 4°C) and the supernatant was subjected to ultracentrifugation (202875 x g, 1 h, 4°C). Pellets were homogenized in resuspension buffer (PBS (pH 7.3); 5% (v/v) glycerol; 5 mM PMSF; PIC) to yield a final concentration of 1 µg pellet material per ml. Resuspended microsomes were used for *in vitro* assays.

The *in vitro* assay method was adapted from (Kohda et al. 2007) and was conducted in reaction buffer (10 mM TrisCl (pH 7.3); 1 mM DTT; 1 mM $MnCl_2$) with 20 µM N-terminally tamra-labeled DANYTK peptide substrate (JPT peptide technologies), varying concentrations of chemically synthesized $GlcNAc_2$ LLO substrate (Robert Woodward) and homogenized microsomes. To show cation

dependency of the glycosylation reaction 1 mM EDTA was added to the reaction mixture. Reactions were incubated at 28°C for 10-12 h. After incubation, samples were mixed with reducing sample buffer 7:3 (v/v) (225 µM TrisCl (pH 6.8); 50% (v/v) glycerol; 5% (w/v) SDS; 0.05% (w/v) bromophenol blue; 25 µM DTT), incubated at 95°C for 5 min and analysed by tricine-SDS-PAGE (Schagger 2006). Fluorescence of the tamra-labeled peptide was detected in gel with a FX Imager Pro Plus (BioRad) scanner. Fluorescence intensities of bands were analysed by ImageJ software and values were used to estimate the degree of conversion from non-glycosylated to glycosylated form of the peptide. These values were used for a determination of the k_{mapp} range.

Analysis of N-linked oligosaccharides

Yeast cells were grown to early logarithmic phase (OD_{600nm} = 0.8-1.2) and 50 OD of cells (5 x 10^8 cells) were harvested by centrifugation, washed with ice-cold water and resuspended in 200 µl of ice-cold water. 25 µl of TCA (100% (w/v)) were added to the cell suspension. After incubation on ice for 3 min, the precipitate was washed twice with ice-cold acetone and dried at 50°C for 10 min. Pellets were resuspended in 200 µl S-buffer (50 mM sodium-phosphate buffer (pH 7.5), 0.4% SDS, 40 mM DTT) and vortexed with maximum speed at 50°C for 1 h with glass beads. The slurry was extracted with 3 x 250 µl S-buffer and cleared by centrifugation. 500 µl supernatant were mixed with 55 µl iodoacetamide (0.5 M) and incubated for 15 min at 37°C. 62 µl NP-40 (10% (v/v)) and 69 µl sodium-phosphate buffer (0.5 M, pH 7.5) were added. Glycans were released by addition of 1 µl of peptide: N-glycosidase F (PNGaseF; New England Biolabs) and incubation at 37°C for 16 h. For the clean-up of released glycans prepacked C 18 Sep Pak columns (Waters) which were connected to columns (extended volume empty reservoirs; Socochim SA) packed with Supelclean ENVI-Carb 120/400 (Sigma-Aldrich) were used. The combined columns were equilibrated with methanol, acetonitrile (ACN), ACN/H_2O (50:50 (v/v)), and ACN/H_2O (2:98 (v/v)). Samples were applied onto the columns after supplementation with ACN/H_2O (2:98 (v/v) final concentration). Columns were washed with ACN/H_2O (2:98 (v/v)), and glycans were eluted from the ENVI-Carb column with ACN/H_2O (25:75 (v/v)). The solvent was evaporated in a speed vacuum. Purified NLOs were fluorescently labelled with 2-aminobenzamide (2-AB) by incubation in 25 µl of labelling solution (70% (v/v) DMSO; 30% (v/v) glacial acetic acid; 0.35 M sodium cyanoborohydride (Fluka); 1 M 2-AB (Sigma)) at 65°C for 2 h. Labelled NLOs were purified with paper columns. 4 filter paper disks were placed in a 1 ml syringe were washed with 2 x 1 ml acetic acid (30% (v/v)) and twice with 1 ml of water. The filter paper was equilibrated with 2 x 1 ml ACN and 2 x 1 ml ACN/H_2O (95:5 (v/v)). Samples were cooled down and ACN was added (final concentration 95% (v/v)). Samples were added to filter paper and washed with 8 x 1 ml ACN/H_2O (95:5 (v/v)). Glycans were eluted with 2 x 50 µl deionized water. Subsequently, ACN was added to samples (final concentration

70% (v/v)) and samples were filtered with 0.45 µm filter spin columns (Millipore). HPLC analysis of the samples was performed using a normal-phase column (Supelcosil LC-NH2, 250 x 4.6 mm; Sigma-Aldrich) and a Supelcosil LC-NH2 Supelguard Cartridge (Sigma-Aldrich). A linear gradient ranging from ACN 70% (v/v) to 55% (v/v) ACN over 75 min (flowrate: 0.8 ml/min) was used to separate NLOs. Fluorescence of 2-AB labelled NLOs was detected using excitation at 330 nm and detection of the emission at 420 nm. NLO peaks were assigned based on retention time of a NLO standard ranging from $Man_5GlcNAc_2$ to $Man_9GlcNAc_2$ isolated from RNAse B (Sigma). Peak areas were calculated with Chromeleon Software (Dionex).

Sample preparation for mass spectrometry

Cells were grown at 25°C in synthetic complete medium (0.67% (w/v) yeast nitrogen base, 2% (w/v) glucose with appropriate amino acid supplements) containing either 20 mg/l light [$^{12}C_6$/$^{14}N_2$] L-lysine and [$^{12}C_6$] L-arginine or heavy [$^{13}C_6$/$^{15}N_2$] L-lysine and [$^{13}C_6$] L-arginine (Cambridge Isotope laboratories). Cells were harvested in early log phase (OD_{600nm} = 0.8-1.2) by centrifugation and mixed 1:1 (w/w) for membrane protein preparation.

Membrane proteins were prepared as described (Mueller et al. 2015). Shortly, cells were lysed and microsomal fractions were collected by high spin centrifugation at 16,000xg, 4°C for 20 min. Proteins were processed using the filter-assisted sample preparation (FASP) protocol (Wisniewski et al., 2009). After reduction and alkylation, proteins were digested with Lys-C (20 µg/ml; Wako Pure Chemical, Richmond, VA) and trypsin (20 µg/ml; Promega) endopeptidases. Protein digestion was directly followed by EndoH (500 U; New England BioLabs) endoglycosidase treatment. Peptides were desalted using C18 ZipTips (Millipore) and dried using speed vacuum. Desalted peptides were resuspended in ACN/H_2O (3:97 (v/v)) with formic acid (FA; 0.1% (v/v)) and analysed by LC-ESI-MS/MS.

Mass Spectrometry analysis

MS analysis was performed by LC-ESI-MS/MS in parallel reaction monitoring (PRM) mode using a Q Exactive HF instrument (Thermo Scientific) coupled to ACQUITY UPLC system (Waters). Peptides were separated on HSS T3 column (78 µm × 150 mm, 1.8 µm) packed with C18 material (Waters). Peptides were eluted using the gradient of 2 - 35% solvent B (99% (v/v) ACN, 0.1% (v/v) FA) over 90 min at a flow rate of 0.3 µl/min. All samples were analysed using two PRM methods at an Orbitrap resolution of 30 000 or 60 000, based on scheduled inclusion lists containing the 175 and 128 target precursor ions, respectively, including retention time iRT standard peptides (Biognosys) (Appendix Table 1). The full scan event was collected using a m/z 50–1400 mass selection, an Orbitrap resolution of 60 000 (at

m/z 400), target automatic gain control (AGC) value of 3 x 10^6 and a maximum injection time of 30 ms. The PRM scan events used an Orbitrap resolution of 30 000 or 60 000, maximum fill time of 30 or 110 ms respectively, an AGC value of 1 x 10^6 and with an isolation width of 2 m/z. Fragmentation was performed with a normalized collision energy of 28 and MS/MS scans were acquired with a starting mass of m/z 150. Scan windows were set to 10 min for each peptide in the final PRM method to ensure the measurement of 6–10 points per LC peak per transition.

Data processing and analysis

Skyline software (v2.6.0) with standard settings was used for data processing (MacLean et al. 2010). Briefly, raw MS data files were imported and the peaks were manually inspected and adjusted to ensure proper peak picking and peak integration. The resulting light to heavy intensity ratio (L/H) for glyco-peptides modified with HexNAc was used to calculate the relative site occupancy for the given peptide/ glycosylation site. The relative site occupancy was normalized for expression differences between heavy labelled reference wild type strain (H) and the *Tb*STT3 expressing light strains (L) by dividing the L/H intensity ratio for the occupied glyco-peptide by the median of L/H intensity ratios reported for all non-glyco (i.e. not containing a NxT/S sequon) peptides from the same protein as the glyco peptide.

Cluster analysis was performed with Cluster 3.0 software (library version 1.50) (Eisen et al. 1998; de Hoon et al. 2004) using the Spearman rank correlation to calculate similarity between site occupancy data for different *Tb*STT3s. Hierarchical clustering with the single linkage method was used to generate a dendrogram visualized with Java TreeView 1.1.6 software.

References

Adair WL, Jr., Cafmeyer N. 1987. Characterization of the Saccharomyces cerevisiae cis-prenyltransferase required for dolichyl phosphate biosynthesis. *Arch Biochem Biophys* **259**: 589-596.

Albright CF, Robbins RW. 1990. The sequence and transcript heterogeneity of the yeast gene ALG1, an essential mannosyltransferase involved in N-glycosylation. *J Biol Chem* **265**: 7042-7049.

Boeke JD, Trueheart J, Natsoulis G, Fink GR. 1987. 5-Fluoroorotic acid as a selective agent in yeast molecular genetics. *Methods Enzymol* **154**: 164-175.

Brachmann CB, Davies A, Cost GJ, Caputo E, Li J, Hieter P, Boeke JD. 1998. Designer deletion strains derived from Saccharomyces cerevisiae S288C: a useful set of strains and plasmids for PCR-mediated gene disruption and other applications. *Yeast* **14**: 115-132.

Burda P, Aebi M. 1999. The dolichol pathway of N-linked glycosylation. *Biochim Biophys Acta* **1426**: 239-257.

Burda P, Jakob CA, Beinhauer J, Hegemann JH, Aebi M. 1999. Ordered assembly of the asymmetrically branched lipid-linked oligosaccharide in the endoplasmic reticulum is ensured by the substrate specificity of the individual glycosyltransferases. *Glycobiology* **9**: 617-625.

Calo D, Kaminski L, Eichler J. 2010. Protein glycosylation in Archaea: sweet and extreme. *Glycobiology* **20**: 1065-1076.

Castillo-Acosta VM, Ruiz-Pérez LM, Etxebarria J, Reichardt NC, Navarro M, Igarashi Y, Liekens S, Balzarini J, González-Pacanowska. 2016. Carbohydrate-Binding Non-Peptidic Pradimicins for the Treatment of Acute Sleeping Sickness in Murine Models. *PLoS Pathog* **12**:e1005851

Castillo-Acosta VM, Vidal AE, Ruiz-Pérez LM, Van Damme EJ, Igarashi Y, Balzarini J, González-Pacanowska D. 2013. Carbohydrate-binding agents act as potent trypanocidals that elicit modifications in VSG glycosylation and reduced virulence in Trypanosoma brucei. *Mol Microbiol* **4**: 665-679

Castro O, Movsichoff F, Parodi AJ. 2006. Preferential transfer of the complete glycan is determined by the oligosaccharyltransferase complex and not by the catalytic subunit. *Proc Natl Acad Sci U S A* **103**: 14756-14760.

Cipollo JF, Trimble RB. 2002. The Saccharomyces cerevisiae alg12delta mutant reveals a role for the middle-arm alpha1,2Man- and upper-arm alpha1,2Manalpha1,6Man- residues of Glc3Man9GlcNAc2-PP-Dol in regulating glycoprotein glycan processing in the endoplasmic reticulum and Golgi apparatus. *Glycobiology* **12**: 749-762.

de Hoon MJ, Imoto S, Nolan J, Miyano S. 2004. Open source clustering software. *Bioinformatics* **20**: 1453-1454.

de la Canal L, Parodi AJ. 1987. Synthesis of dolichol derivatives in trypanosomatids. Characterization of enzymatic patterns. *J Biol Chem* **262**: 11128-11133.

Eisen MB, Spellman PT, Brown PO, Botstein D. 1998. Cluster analysis and display of genome-wide expression patterns. *Proc Natl Acad Sci U S A* **95**: 14863-14868.

Fang X, Gibbs BS, Coward JK. 1995. Synthesis and evaluation of synthetic analogues of dolichyl-P-P-chitobiose as oligosaccharyltransferase substrates. *Bioorganic & Medicinal Chemistry Letters* **5**: 2701-2706.

Gavel Y, von Heijne G. 1990. Sequence differences between glycosylated and non-glycosylated Asn-X-Thr/Ser acceptor sites: implications for protein engineering. *Protein Eng* **3**: 433-442.

Guthrie C, Fink GR. 1991. *Guide to Yeast Genetics and Molecular Biology*. Cold Spring Harbor Laboratory Press, Cold Spring NY.

Helenius A, Aebi M. 2004. Roles of N-linked glycans in the endoplasmic reticulum. *Annu Rev Biochem* **73**: 1019-1049.

Helenius J, Ng DT, Marolda CL, Walter P, Valvano MA, Aebi M. 2002. Translocation of lipid-linked oligosaccharides across the ER membrane requires Rft1 protein. *Nature* **415**: 447-450.

Hese K, Otto C, Routier FH, Lehle L. 2009. The yeast oligosaccharyltransferase complex can be replaced by STT3 from Leishmania major. *Glycobiology* **19**: 160-171.

Igura M, Maita N, Kamishikiryo J, Yamada M, Obita T, Maenaka K, Kohda D. 2008. Structure-guided identification of a new catalytic motif of oligosaccharyltransferase. *The EMBO journal* **27**: 234-243.

Izquierdo L, Mehlert A, Ferguson MA. 2012. The lipid linked oligosaccharide donor specificities of Trypanosoma brucei oligosaccharyltransferases. *Glycobiology*.

Izquierdo L, Schulz BL, Rodrigues JA, Guther ML, Procter JB, Barton GJ, Aebi M, Ferguson MA. 2009. Distinct donor and acceptor specificities of Trypanosoma brucei oligosaccharyltransferases. *The EMBO journal*.

Jakob CA, Burda P, te Heesen S, Aebi M, Roth J. 1998. Genetic tailoring of N-linked oligosaccharides: the role of glucose residues in glycoprotein processing of Saccharomyces cerevisiae in vivo. *Glycobiology* **8**: 155-164.

Jung P, Tanner W. 1973. Identification of the lipid intermediate in yeast mannan biosynthesis. *Eur J Biochem* **37**: 1-6.

Kelleher DJ, Banerjee S, Cura AJ, Samuelson J, Gilmore R. 2007. Dolichol-linked oligosaccharide selection by the oligosaccharyltransferase in protist and fungal organisms. *J Cell Biol* **177**: 29-37.

Kelleher DJ, Gilmore R. 2006. An evolving view of the eukaryotic oligosaccharyltransferase. *Glycobiology* **16**: 47R-62R.

Kelleher DJ, Karaoglu D, Mandon EC, Gilmore R. 2003. Oligosaccharyltransferase isoforms that contain different catalytic STT3 subunits have distinct enzymatic properties. *Mol Cell* **12**: 101-111.

Kohda D, Yamada M, Igura M, Kamishikiryo J, Maenaka K. 2007. New oligosaccharyltransferase assay method. *Glycobiology* **17**: 1175-1182.

Lizak C, Gerber S, Numao S, Aebi M, Locher KP. 2011. X-ray structure of a bacterial oligosaccharyltransferase. *Nature* **474**: 350-355.

Low P, Dallner G, Mayor S, Cohen S, Chait BT, Menon AK. 1991. The mevalonate pathway in the bloodstream form of Trypanosoma brucei. Identification of dolichols containing 11 and 12 isoprene residues. *J Biol Chem* **266**: 19250-19257.

Lowe JB, Marth JD. 2003. A genetic approach to Mammalian glycan function. *Annu Rev Biochem* **72**: 643-691.

MacLean B, Tomazela DM, Shulman N, Chambers M, Finney GL, Frewen B, et al. 2010. Skyline: an open source document editor for creating and analyzing targeted proteomics experiments. *Bioinformatics*. **26**: 966–968.

Manthri S, Guther ML, Izquierdo L, Acosta-Serrano A, Ferguson MA. 2008. Deletion of the TbALG3 gene demonstrates site-specific N-glycosylation and N-glycan processing in Trypanosoma brucei. *Glycobiology* **18**: 367-383.

Mueller S, Wahlander A, Selevsek N, Otto C, Ngwa EM, Poljak K, Frey A, Aebi M and Gauss R. 2015. Protein degradation corrects for imbalanced subunit stoichiometry in OST complex assembly. *Mol Biol Cell* **26**:2596-2608

Munro S. 2001. What can yeast tell us about N-linked glycosylation in the Golgi apparatus? *FEBS Lett* **498**: 223-227.

Nilsson I, Kelleher DJ, Miao Y, Shao Y, Kreibich G, Gilmore R, von Heijne G, Johnson AE. 2003. Photocross-linking of nascent chains to the STT3 subunit of the oligosaccharyltransferase complex. *J Cell Biol* **161**: 715-725.

Ong SE, Blagoev B, Kratchmarova I, Kristensen DB, Steen H, Pandey A, Mann M. 2002. Stable isotope labeling by amino acids in cell culture, SILAC, as a simple and accurate approach to expression proteomics. *Mol Cell Proteomics* **1**: 376-386.

Parodi AJ, Quesada Allue LA, Cazzulo JJ. 1981. Pathway of protein glycosylation in the trypanosomatid Crithidia fasciculata. *Proc Natl Acad Sci U S A* **78**: 6201-6205.

Parsaie Nasab F, Schulz BL, Gamarro F, Parodi AJ, Aebi M. 2008. All in One: Leishmania major STT3 Proteins Substitute for the Whole Oligosaccharyltransferase Complex in Saccharomyces cerevisiae. *Molecular Biology of the Cell* **19**: 3758-3768.

Pathak R, Hendrickson TL, Imperiali B. 1995. Sulfhydryl modification of the yeast Wbp1p inhibits oligosaccharyl transferase activity. *Biochemistry* **34**: 4179-4185.

Reiss G, te Heesen S, Zimmerman J, Robbins PW, Aebi M. 1996. Isolation of the ALG6 locus of Saccharomyces cerevisiae required for glucosylation in the N-linked glycosylation pathway. *Glycobiology* **6**: 493-498.

Roboti P, High S. 2012. The oligosaccharyltransferase subunits OST48, DAD1 and KCP2 function as ubiquitous and selective modulators of mammalian N-glycosylation. *J Cell Sci*.

Samuelson J, Banerjee S, Magnelli P, Cui J, Kelleher DJ, Gilmore R, Robbins PW. 2005. The diversity of dolichol-linked precursors to Asn-linked glycans likely results from secondary loss of sets of glycosyltransferases. *Proc Natl Acad Sci U S A* **102**: 1548-1553.

Schagger H. 2006. Tricine-SDS-PAGE. *Nat Protoc* **1**: 16-22.

Spirig U, Bodmer D, Wacker M, Burda P, Aebi M. 2005. The 3.4-kDa Ost4 protein is required for the assembly of two distinct oligosaccharyltransferase complexes in yeast. *Glycobiology* **15**: 1396-1406.

Tai VW, Imperiali B. 2001. Substrate specificity of the glycosyl donor for oligosaccharyl transferase. *J Org Chem* **66**: 6217-6228.

te Heesen S, Janetzky B, Lehle L, Aebi M. 1992. The yeast WBP1 is essential for oligosaccharyl transferase activity in vivo and in vitro. *The EMBO journal* **11**: 2071-2075.

Trimble RB, Byrd JC, Maley F. 1980. Effect of glucosylation of lipid intermediates on oligosaccharide transfer in solubilized microsomes from Saccharomyces cerevisiae. *J Biol Chem* **255**: 11892-11895.

Vacic V, Iakoucheva LM, and Radivojac P. 2006. Two Sample Logo: A Graphical Representation of the Differences between Two Sets of Sequence Alignments. *Bioinformatics* **22**(12): 1536-1537.

Wacker M, Linton D, Hitchen PG, Nita-Lazar M, Haslam SM, North SJ, Panico M, Morris HR, Dell A, Wren BW et al. 2002. N-linked glycosylation in Campylobacter jejuni and its functional transfer into E. coli. *Science* **298**: 1790-1793.

Wilson CM, Roebuck Q, High S. 2008. Ribophorin I regulates substrate delivery to the oligosaccharyltransferase core. *Proc Natl Acad Sci U S A*.

Wisniewski JR, Zougman A, Mann M. 2009. Combination of FASP and StageTip-based fractionation allows in-depth analysis of the hippocampal membrane proteome. *J Proteome Res* **8**: 5674–5678.

Xu Y, Bailey UM and Schulz B. 2015. Automated measurement of site-specific N-glycosylation occupancy with SWATH MS. *Proteomics* **15**:2177-2186

Yan Q, Lennarz WJ. 2002. Studies on the function of oligosaccharyl transferase subunits. Stt3p is directly involved in the glycosylation process. *J Biol Chem* **277**: 47692-47700.

Zacchi L and Schulz B. 2016. SWATH-MS glycoproteomics reveal consequonces of defects in the glycosylation machinery. *Mol Cell Proteomics* **15**: 2435-2447

Zufferey R, Knauer R, Burda P, Stagljar I, te Heesen S, Lehle L, Aebi M. 1995. STT3, a highly conserved protein required for yeast oligosaccharyl transferase activity in vivo. *The EMBO journal* **14**: 4949-4960.

Chapter 3b

Supplementary Information to Chapter 3

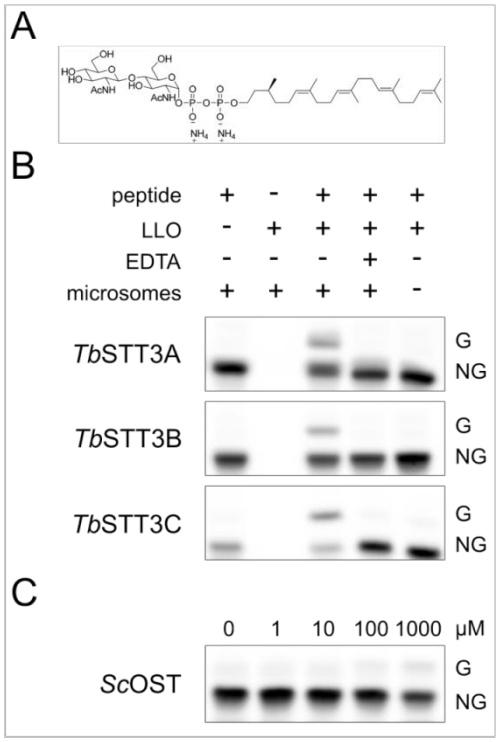

Supplementary Figure 1. Test of *in vitro* activity with *Tb*STT3 paralogues.

(A) Structure of the pentaprenyl-pyrophosphate-$GlcNAc_2$ LLO used for in *vitro assays* (B) Detergent free microsomes were prepared from yeast cells with deletion of endogenous *STT3* and expressing *Tb*STT3A, *Tb*STT3B or *Tb*STT3C. Microsomes, tamra-labelled DANYTK peptide substrate and $GlcNAc_2$ LLO substrate were added to (+) or omitted (-) from the reaction mixture. EDTA was added to test metal ion dependence of the reaction. Glycosylated (G) and non-glycosylated (NG) peptides were separated by tricine SDS PAGE and fluorescence of the tamra label was detected. (C) Microsomes prepared from yeast cells with functional endogenous OST were incubated with tamra-labelled DANYTK peptide and increasing concentrations of $GlcNAc_2$ LLO substrate to test activity of *S. cerevisiae* OST (*Sc*OST) towards the LLO substrate. Glycosylated (G) and non-glycosylated (NG) peptides were separated by tricine SDS PAGE and fluorescence of the tamra label was detected.

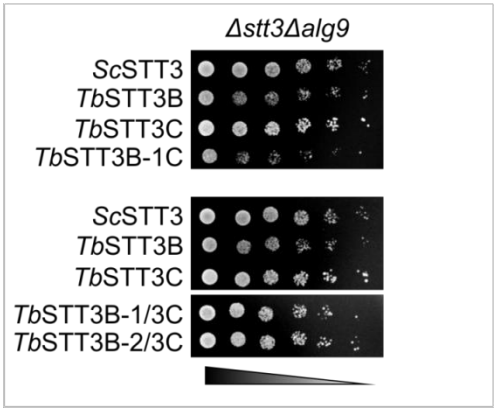

Supplementary Figure 2. Growth phenotypes of *Δstt3Δalg9* cells expressing *Tb*STT3B-C chimeras.
Δstt3Δalg9 complemented by ScSTT3, *Tb*STT3B , *Tb*STT3C, or the *Tb*STT3B-C chimeras (*Tb*STT3B-1C, *Tb*STT3B-1/3C, *Tb*STT3B-2/3C) were grown in medium selecting for the plasmid and containing 1 M sorbitol. Serial dilutions of the cultures were spotted on selective medium containing 1 M sorbitol and cells were incubated for 4 d at 23°C.

Supplementary Table 1. Relative peak areas of protein linked oligosaccharides isolated from *Δstt3Δalg9* cell expressing *Sc*STT3, *Tb*STT3A, *Tb*STT3B or *Tb*STT3C and harbouring additionally e.v. or p*ALG12*.
Values represent percentage of individual peak areas ($Man_6GlcNAc_2$ (Man6)-$Man_{11}GlcNAc_2$ (Man11)) relative to the total peak area of all peaks (Man6-Man11). Values are average values of three individual experiments and standard deviation is indicated by ± values.

	+ e.v.	+ p*ALG12*	+ e.v.	+ p*ALG12*	+ e.v.	+ p*ALG12*	+ e.v.	+ p*ALG12*
Man6	40.1 ± 0.9	23.7 ± 1.0	43.3 ± 1.1	33.4 ± 0.8	35.5 ± 0.8	19.6 ± 3.6	44.5 ± 2.0	29.3 ± 0.7
Man7	16.3 ± 0.2	27.6 ± 0.9	18.0 ± 0.3	22.9 ± 0.5	18.8 ± 0.2	27.3 ± 1.7	21.0 ± 0.6	31.8 ± 1.3
Man8	21.3 ± 0.2	18.6 ± 0.3	18.6 ± 1.0	21.5 ± 0.8	20.2 ± 0.5	20.0 ± 0.2	13.5 ± 0.3	15.1 ± 0.2
Man9	15.9 ± 0.5	17.9 ± 0.5	13.6 ± 0.9	14.0 ± 0.3	16.2 ± 0.3	17.6 ± 0.7	12.6 ± 0.6	12.6 ± 0.7
Man10	5.2 ± 0.3	9.0 ± 0.6	5.1 ± 0.7	6.0 ± 0.1	6.8 ± 0.1	10.8 ± 1.2	6.3 ± 0.6	7.7 ± 0.8
Man11	1.1 ± 0.1	3.1 ± 0.2	1.4 ± 0.3	2.2 ± 0.2	2.3 ± 0.1	4.6 ± 0.7	2.1 ± 0.3	3.6 ± 0.4

Supplementary Table 2. Glycosylation site occupancy values for *Δstt3Δalg9* cells complemented with *Tb*STT3A, *Tb*STT3B, and *Tb*STT3C relative to yeast OST from the wild type reference strain.

Values represent the median of three biological replicates and are expressed as % glycosylation relative to *Sc*OST.

Protein	UniProt accession	Glycosylation site	Peptide sequence	TbSTT3A	TbSTT3B	TbSTT3C
APE3	P37302	APE3_N85	IKVDDLN[+203.1]ATAWDLYR	95.40	73.90	50.05
APE3	P37302	APE3_N96	LAN[+203.1]YSTPDYGHPTR	65.07	62.35	43.77
APE3	P37302	APE3_N150	IISFN[+203.1]LSDAETGK	97.48	29.70	47.86
APE3	P37302	APE3_N162	SFAN[+203.1]TTAFALSPPVDGFVGK	105.21	84.79	87.66
CHS7	P38843	CHS7_N31	THLILSN[+203.1]STIIHDFDPLNLNVGVLPR	101.30	81.38	72.76
CNE1	P27825	CNE1_N416	N[+203.1]VTEAQIIGNK	41.94	100.69	52.64
CPY	P00729	CPY_N124	ILGIDPN[+203.1]VTQYTGYLDVEDEDK	97.24	26.90	96.55
CPY	P00729	CPY_N479	VRN[+203.1]WTASITDEVAGEVK	36.19	83.66	21.88
CRH2	P32623	CRH2_N233/N237	N[+203.1]ETYN[+203.1]ATTQK	0.70	0.38	2.18
CRH2	P32623	CRH2_N310	N[+203.1]GTSAYVYTSSSEFLAK	3.54	0.21	6.54
DCW1	P36091	DCW1_N203	YTGN[+203.1]QTYVDWAEK	69.72	90.95	22.88
ECM33	P38248	ECM33_N304	VQTVGGAIEVTGN[+203.1]FSTLDLSSLK	46.16	57.51	40.42
EPS1	P40557	EPS1_N264	VALVLPN[+203.1]K	35.59	46.64	20.33
EPS1	P40557	EPS1_N299	FPN[+203.1]ITEGELEK	26.91	6.69	4.44
ERG3	P32353	ERG3_N40	LLGLNSGFSN[+203.1]STILQETLNSK	70.93	103.36	60.73
ERO1	Q03103	ERO1_N458	YTIENIN[+203.1]STK	9.82	30.54	31.37
EXG2	P52911	EXG2_N50	FASYYAN[+203.1]DTITVK	81.34	78.58	56.99
EXG2	P52911	EXG2_N157	NLYIDN[+203.1]ITFNDPYVSDGLQLK	41.87	2.73	56.93
FET3	P38993	FET3_N244	N[+203.1]VTDM[+16]LYITVAQR	4.20	64.59	64.58
FET3	P38993	FET3_N359	NGVNYAFFNN[+203.1]ITYTAPK	4.23	60.47	72.12
FET5	P43561	FET5_N24	LN[+203.1]YTASWVTANPDGLHEK	30.13	89.11	24.69
FET5	P43561	FET5_N364	YAFFNN[+203.1]ITYVTPK	79.52	103.32	80.40
GAS1	P22146	GAS1_N40	FFYSNN[+203.1]GSQFYIR	42.56	88.50	6.24
GPI12	P23797	GPI12_N110	VRELN[+203.1]ESAALLLHNER	103.72	65.90	75.29
GPI13	Q07830	GPI13_N411	N[+203.1]ISNTPPTSDPEK	90.80	49.68	50.82
GPI16	P38875	GPI16_N184	SYASDIGAPLFN[+203.1]STEK	101.10	74.93	82.94
HEH2	Q03281	HEH2_N520	SN[+203.1]NTNYIYR	6.14	103.97	1.31
HMG2	P12684	HMG2_N150	IPTELVSEN[+203.1]GTK	0.26	0.01	0.48
KTR1	P27810	KTR1_N120	N[+203.1]VTSALVSGTTK	77.42	46.27	86.64
LHS1	P36016	LHS1_N458	LSN[+203.1]ESELYDVFTR	85.31	6.07	79.97
LRO1	P40345	LRO1_N439	SSSEDALNN[+203.1]NTDTYGNFIR	63.39	90.98	97.14
MCD4	P36051	MCD4_N90	SLVMNN[+203.1]ATYGISHTR	110.09	97.52	55.32
MKC7	P53379	MKC7_N286	STAYSLFAN[+203.1]DSDSK	0.92	1.20	2.99
MNN5	P46982	MNN5_N136	LN[+203.1]FSIPQR	48.98	76.83	27.86
OST1	P41543	OST1_N217	FSSN[+203.1]ETLAIVYSHNAPLNQVVNLR	100.89	105.78	106.60
PDI	P17967	PDI_N117	NSDVN[+203.1]NSIDYEGPR	42.74	12.50	24.94
PDI	P17967	PDI_N155	QSQPAVAVVADLPAYLAN[+203.1]ETFVTPVIVQSGK	105.67	98.10	94.80
PDI	P17967	PDI_N174	IDADFN[+203.1]ATFYSM[+16]ANK	99.54	98.10	62.54
PDR5	P33302	PDR5_N734	GPAYAN[+203.1]ISSTESVC[+57]TVVGAVPGQDYVLGDDFIR	47.76	56.35	97.31
PFF1	P38244	PFF1_N121	SILFQQQDPFN[+203.1]ESSR	94.55	73.51	94.93
PLB1	P39105	PLB1_N215	DAGFN[+203.1]ISLADVWGR	83.48	75.23	89.90
PLB1	P39105	PLB1_N489	N[+203.1]LTDLEYIPPLIVYIPNSR	111.17	116.53	107.01
PLB2	Q03674	PLB2_N193	SIVNPGGSN[+203.1]LTYTIER	0.42	0.24	2.37
PLB2	Q03674	PLB2_N217	SDAGFN[+203.1]ISLSDLWAR	1.33	0.02	4.24
PMT2	P31382	PMT2_N403	GLPSWSEN[+203.1]ETDIEYLKPGTSYR	74.58	6.26	83.43
RAX2	Q12465	RAX2_N640	N[+203.1]SSLYADIYDNK	22.20	88.40	29.81
RAX2	Q12465	RAX2_N677	N[+203.1]QTIQGDVHGITK	17.05	97.33	68.75
ROT1	Q03691	ROT1_N139	YN[+203.1]QTETFK	90.38	87.19	83.04
SEC66	P33754	SEC66_N12	FSNN[+203.1]GTFFETEEPIVETK	82.52	92.36	79.87
SUR7	P54003	SUR7_N47	FYWVQGN[+203.1]TTGIPNAGDETR	95.99	106.67	79.98
TED1	P40533	TED1_N266	DNYWIEYETN[+203.1]TTHPWR	98.16	48.90	86.14
WBP1	P33767	WBP1_N60	LEYLDIN[+203.1]STSTTVDLYDK	86.96	53.61	73.49
WBP1	P33767	WBP1_N332	LTLSPSGN[+203.1]DSETQYYTTGEFILPDR	59.31	62.84	89.81
YJR1	P46992	YJR1_N219	N[+203.1]SSSIGYYDLPAIWLLNDHIAR	78.68	68.28	71.47
YL413	Q06689	YL413_N429	ILNSAVN[+203.1]MTTITPEQLK	9.69	1.14	0.48

Supplementary Table 3. Analysis of sequence preference of different TbSTT3 paralogues, analysed on glycosylation sequons themselves plus ten residues downstream and upstream. Amino acid residues were grouped based on their polarity into acidic (Asp, Glu), basic (Arg, Lys, His), polar (Ser, Thr, Asn, Glu, Cys, Tyr) and hydrophobic (Ala, Val, Ile, Leu, Met, Phe, Trp, Pro, Gly) group. Sequences were divided into 'efficiently' and 'poorly' glycosylated, when the glycosylation occupancy calculated was more than 85% or less than 25% compared to reference strain, respectively. Values represent the number of amino acids present in each group and the percentage compared to the overall number. Percentage difference is calculated by subtracting percentage in efficient to poor sequences.

		TbSTT3A				
		Poor sequences		Efficient sequences		
	AA type	No. of amino acids	% compared to total	No. of amino acids	% compared to total	Difference (%)
Upstream	Acidic AA	18	12.00%	47	17.41%	5.41
	Basic AA	23	15.33%	32	11.85%	-3.48
	Polar AA	47	31.33%	71	26.30%	-5.04
	Hydrophobic A.	62	41.33%	120	44.44%	3.11
	Total	150		270		
Downstream	Acidic AA	10	6.67%	25	9.26%	2.59
	Basic AA	17	11.33%	22	8.15%	-3.19
	Polar AA	48	32.00%	54	20.00%	-12.00
	Hydrophobic A.	75	50.00%	169	62.59%	12.59
		150		270		
Together	Acidic AA	28	9.33%	72	13.33%	4.00
	Basic AA	40	13.33%	54	10.00%	-3.33
	Polar AA	95	31.67%	125	23.15%	-8.52
	Hydrophobic A.	137	45.67%	289	53.52%	7.85
		300		540		
		TbSTT3B				
		Poor sequences		Efficient sequences		
		No. of amino acids	% compared to total	No. of amino acids	% compared to total	Difference (%)
Upstream	Acidic AA	20	12.50%	30	11.54%	-0.96
	Basic AA	24	15.00%	36	13.85%	-1.15
	Polar AA	49	30.63%	73	28.08%	-2.55
	Hydrophobic A.	67	41.88%	121	46.54%	4.66
	Total	160		260		
Downstream	Acidic AA	19	11.88%	28	10.77%	-1.11
	Basic AA	16	10.00%	23	8.85%	-1.15
	Polar AA	44	27.50%	43	16.54%	-10.96
	Hydrophobic A.	81	50.63%	166	63.85%	13.22
		160		260		
Together	Acidic AA	39	12.19%	58	11.15%	-1.03
	Basic AA	40	12.50%	59	11.35%	-1.15
	Polar AA	93	29.06%	116	22.31%	-6.75
	Hydrophobic A.	148	46.25%	287	55.19%	8.94
		320		520		
		TbSTT3C				
		Poor sequences		Efficient sequences		
		No. of amino acids	% compared to total	No. of amino acids	% compared to total	Difference (%)
Upstream	Acidic AA	14	8.24%	33	16.50%	8.26
	Basic AA	30	17.65%	22	11.00%	-6.65
	Polar AA	49	28.82%	56	28.00%	-0.82
	Hydrophobic A.	77	45.29%	89	44.50%	-0.79
	Total	170		200		
Downstream	Acidic AA	17	10.00%	20	10.00%	0.00
	Basic AA	16	9.41%	14	7.00%	-2.41
	Polar AA	54	31.76%	45	22.50%	-9.26
	Hydrophobic A.	86	50.59%	121	60.50%	11.68
		170		200		
Together	Acidic AA	31	9.12%	53	13.25%	4.13
	Basic AA	46	13.53%	36	9.00%	-4.53
	Polar AA	103	30.29%	101	25.25%	-5.04
	Hydrophobic A.	160	47.06%	210	52.50%	5.44
		340		400		

Supplementary Table 4. Glycosylation site occupancy values for *Δstt3Δalg9* cells complemented with *Tb*STT3B, *Tb*STT3C, *Tb*STT3B-1/3C and *Tb*STT3B-2/3C relative to yeast OST from the wild type reference strain.

Values represent the median of three biological replicates and are expressed as % glycosylation relative to *Sc*OST.

Protein	UniProt accession	Glycosylation site	Peptide sequence	TbSTT3B	TbSTT3C	TbSTT3B-1/3C	TbSTT3B-2/3C
APE3	**P37302**	**APE3_N85**	**IKVDDLN[+203.1]ATAWDLYR**	**73.90**	**50.05**	**45.00**	**95.60**
APE3	**P37302**	**APE3_N96**	**LAN[+203.1]YSTPDYGHPTR**	**62.35**	**43.77**	**47.57**	**57.86**
APE3	**P37302**	**APE3_N150**	**IISFN[+203.1]LSDAETGK**	**29.70**	**47.86**	**27.70**	**39.62**
APE3	P37302	APE3_N162	SFAN[+203.1]TTAFALSPPVDGFVGK	84.79	87.66	81.79	82.89
CHS7	P38843	CHS7_N31	THLILSN[+203.1]STIIHDFDPLNLNVGVLPR	81.38	72.76	66.81	66.37
CNE1	**P27825**	**CNE1_N416**	**N[+203.1]VTEAQIIGNK**	**100.69**	**52.64**	**88.05**	**41.43**
CPY	**P00729**	**CPY_N124**	**ILGIDPN[+203.1]VTQYTGYLDVEDEDK**	**26.90**	**96.55**	**92.84**	**100.57**
CPY	**P00729**	**CPY_N479**	**VRN[+203.1]WTASITDEVAGEVK**	**83.66**	**21.88**	**44.88**	**17.14**
CRH2	P32623	CRH2_N233	N[+203.1]ETYN[+203.1]ATTQK	0.38	2.18	0.71	3.40
CRH2	P32623	CRH2_N310	N[+203.1]GTSAYVYTSSSEFLAK	0.21	6.54	18.38	13.80
DCW1	**P36091**	**DCW1_N203**	**YTGN[+203.1]QTYVDWAEK**	**90.95**	**22.88**	**42.14**	**52.48**
ECM33	P38248	ECM33_N304	VQTVGGAIEVTGN[+203.1]FSTLDLSSLK	57.51	40.42	54.98	61.66
EPS1	**P40557**	**EPS1_N264**	**VALVLPN[+203.1]K**	**46.64**	**20.33**	**28.26**	**53.48**
EPS1	P40557	EPS1_N299	FPN[+203.1]ITEGELEK	6.69	4.44	22.08	19.81
ERG3	**P32353**	**ERG3_N40**	**LLGLNSGFSN[+203.1]STILQETLNSK**	**103.36**	**60.73**	**78.18**	**94.64**
ERO1	Q03103	ERO1_N458	YTIENIN[+203.1]STK	30.54	31.37	6.12	85.93
EXG2	**P52911**	**EXG2_N50**	**FASYYAN[+203.1]DTITVK**	**78.58**	**56.99**	**73.20**	**71.82**
EXG2	**P52911**	**EXG2_N157**	**NLYIDN[+203.1]ITFNDPYVSDGLQLK**	**2.73**	**56.93**	**24.19**	**44.67**
FET3	P38993	FET3_N244	N[+203.1]VTDM[+16]LYITVAQR	64.59	64.58	63.61	60.05
FET3	P38993	FET3_N359	NGVNYAFFNN[+203.1]ITYTAPK	60.47	72.12	74.52	69.51
FET5	**P43561**	**FET5_N24**	**LN[+203.1]YTASWVTANPDGLHEK**	**89.11**	**24.69**	**19.12**	**59.68**
FET5	**P43561**	**FET5_N364**	**YAFFNN[+203.1]ITYVTPK**	**103.32**	**80.40**	**104.39**	**92.77**
GAS1	**P22146**	**GAS1_N40**	**FFYSNN[+203.1]GSQFYIR**	**88.50**	**6.24**	**13.02**	**24.73**
GPI12	P23797	GPI12_N110	VRELN[+203.1]ESAALLLHNER	65.90	75.29	89.11	102.85
GPI13	Q07830	GPI13_N411	N[+203.1]ISNTPPTSDPEK	49.68	50.82	74.86	70.56
GPI16	P38875	GPI16_N184	SYASDIGAPLFN[+203.1]STEK	74.93	82.94	74.81	80.72
HMG2	P12684	HMG2_N150	IPTELVSEN[+203.1]GTK	0.01	0.48	0.64	6.81
KTR1	**P27810**	**KTR1_N120**	**N[+203.1]VTSALVSGTTK**	**46.27**	**86.64**	**80.83**	**91.44**
LHS1	**P36016**	**LHS1_N458**	**LSN[+203.1]ESELYDVFTR**	**6.07**	**79.97**	**78.15**	**78.93**
LRO1	P40345	LRO1_N439	SSSEDALNN[+203.1]NTDTYGNFIR	90.98	97.14	97.97	114.16
MCD4	**P36051**	**MCD4_N90**	**SLVMNN[+203.1]ATYGISHTR**	**97.52**	**55.32**	**50.02**	**62.82**
MKC7	P53379	MKC7_N286	STAYSLFAN[+203.1]DSDSK	1.20	2.99	2.97	36.57
MNN5	**P46982**	**MNN5_N136**	**LN[+203.1]FSIPQR**	**76.83**	**27.86**	**46.17**	**82.35**
OST1	P41543	OST1_N217	FSSN[+203.1]ETLAIVYSHNAPLNQVVNLR	105.78	106.60	105.72	97.50
PDI	**P17967**	**PDI_N117**	**NSDVN[+203.1]NSIDYEGPR**	**12.50**	**24.94**	**34.52**	**39.60**
PDI	P17967	PDI_N155	QSQPAVAVVADLPAYLAN[+203.1]ETFVTPVIVQSGK	98.10	94.80	87.36	107.99
PDI	**P17967**	**PDI_N174**	**IDADFN[+203.1]ATFYSM[+16]ANK**	**98.10**	**62.54**	**84.79**	**60.42**
PDR5	**P33302**	**PDR5_N734**	**GPAYAN[+203.1]ISSTESVC[+57]TVVGAVPGQDYVLGDDFIR**	**56.35**	**97.31**	**89.52**	**107.96**
PFF1	**P38244**	**PFF1_N121**	**SILFQQQDPFN[+203.1]ESSR**	**73.51**	**94.93**	**98.73**	**104.94**
PLB1	P39105	PLB1_N215	DAGFN[+203.1]ISLADVWGR	75.23	89.90	74.38	64.48
PLB1	P39105	PLB1_N489	N[+203.1]LTDLEYIPPLIVYIPNSR	116.53	107.01	101.77	93.90
PLB2	Q03674	PLB2_N193	SIVNPGGSN[+203.1]LTYTIER	0.24	2.37	1.59	0.91
PLB2	Q03674	PLB2_N217	SDAGFN[+203.1]ISLSDLWAR	0.02	4.24	0.97	2.16
PMT2	**P31382**	**PMT2_N403**	**GLPSWSEN[+203.1]ETDIEYLKPGTSYR**	**6.26**	**83.43**	**45.15**	**84.38**
RAX2	**Q12465**	**RAX2_N640**	**N[+203.1]SSLYADIYDNK**	**88.40**	**29.81**	**72.42**	**77.27**
RAX2	**Q12465**	**RAX2_N677**	**N[+203.1]QTIQGDVHGITK**	**97.33**	**68.75**	**108.10**	**88.88**
ROT1	Q03691	ROT1_N139	YN[+203.1]QTETFK	87.19	83.04	91.62	96.87
SEC66	P33754	SEC66_N12	FSNN[+203.1]GTFFETEEPIVETK	92.36	79.87	85.12	83.14
SUR7	**P54003**	**SUR7_N47**	**FYWVQGN[+203.1]TTGIPNAGDETR**	**106.67**	**79.98**	**92.89**	**110.82**
TED1	**P40533**	**TED1_N266**	**DNYWIEYETN[+203.1]TTHPWR**	**48.90**	**86.14**	**64.85**	**87.72**
WBP1	P33767	WBP1_N60	LEYLDIN[+203.1]STSTTVDLYDK	53.61	73.49	59.34	84.80
WBP1	**P33767**	**WBP1_N332**	**LTLSPSGN[+203.1]DSETQYYTTGEFILPDR**	**62.84**	**89.81**	**48.78**	**90.15**
YJR1	P46992	YJR1_N219	N[+203.1]SSSIGYYDLPAIWLLNDHIAR	68.28	71.47	63.54	67.89
YL413	Q06689	YL413_N429	ILNSAVN[+203.1]MTTITPEQLK	1.14	0.48	3.96	20.86

Bold: Sites that are differentially glycosylated by TbSTT3B and TbSTT3C that were used for sequence composition and two sample logo analysis.

Chapter 4

Functional Characterization of the Essential Oligosaccharyltransferase Subunit WBP1 in Yeast

Summary

Oligosaccharyltransferase (OST) is an enzyme responsible for N-linked glycosylation, a highly conserved and an essential protein modification that generates a huge diversity of glycoproteins with distinct cellular functions. Yeast OST is a multi-subunit complex composed of nine proteins, where the Wbp1 is an essential glycoprotein whose function within the complex is not known. In order to elucidate the role of Wbp1, we used a reverse genetics strategy to target conserved residues for site directed mutagenesis on the chromosomal level in yeast cells. The effect of the mutations on the OST activity was investigated by examining the OST complex stability and N-glycosylation efficiency *in vivo*. Complex stability analysis was performed by monitoring turnover rates and steady state levels of OST subunits. Glycosylation efficiency was determined by immunoblot analysis. We have identified novel *wbp1* mutants that affect OST activity through complex destabilization, either as a result of Wbp1p destabilization itself or due to impaired interaction with subcomplex partner subunits.

Introduction

N-linked protein glycosylation is an essential and highly conserved process carried out on the ER membrane in eukaryotes. In fungi, plants and mammals the pathway involves the assembly of an oligosaccharide consisting of two N-acetlyglucosamine (GlcNAc), nine mannoses (Man) and three glucoses (Glc) on a lipid carrier dolichol (Dol), which is then transferred *en bloc* by the oligosaccharyltransferase (OST) enzyme. The *ALG* (asparagine-linked glycosylation) genes encode glycosyltransferases involved in sequential addition of sugar residues to the dolichol phosphate (Dol-P). Oligosaccharide assembly starts at the cytoplasmic side of the ER membrane, where the cytoplasmic ALG enzymes involved use nucleotide activated sugar donors (UDP-GlcNAc and GDP-Man). The first GlcNAc residue is added to the Dol-P to form Dol-PP-GlcNAc, followed by the subsequent addition of one GlcNAc and five Man residues resulting in Dol-PP-$GlcNAc_2Man_5$ oligosaccharide. The lipid-linked oligosaccharide (LLO) is then flipped towards the ER lumenal side (Breitling & Aebi 2013). The flipping process is not yet fully understood, although it has been proposed to require Rft1p (Helenius et al. 2002). The ALG enzymes acting in the ER lumen utilize lipid-linked donors (Dol-P-Man and Dol-P-Glc) and are responsible for the addition of four Man and three Glc residues resulting in the mature Dol-PP-$GlcNAc_2Man_9Glc_3$ LLO (Breitling & Aebi 2013). Lower eukaryotes synthesize truncates LLO structures ranging from $GlcNAc_2Man_9$ in *Leishmania major* to the extreme $GlcNAc_2$ in *Giradia lambia* (Samuelson et al. 2005). The bipartite biosynthesis of the LLO and high substrate specificity for the define LLO intermediates makes the process extremely ordered. Therefore, disruption of *ALG* genes acting in the lumenal LLO assembly results in the accumulation of specific LLO intermediates allowing for the analysis of the suboptimal LLO substrate effect on OST glycosylation efficiency.

Fully assembled glycan is transferred by the central enzyme, OST to an asparagine residue located within highly conserved N-X-S/T sequon (X = any amino acid expect proline) of a polypeptide chain. *Saccharomyces cerevisiae* OST is a hetero-oligomeric membrane complex composed of essential subunits encoded by *STT3*, *WBP1*, *OST1*, *OST2* and *SWP1* and the non-essential genes *OST3*, *OST6*, *OST4* and *OST5*, existing in two isoforms containing either Ost3p or Ost6p (Kelleher & Gilmore 2006). Yeast and mammalian OST subunits are homologous: STT3A and STT3B (STT3), OST48 (WBP1), ribophorin I (OST1), ribophorin II (SWP1), N33/Tusc3 and IAP (OST3 and OST6) as well as OST4 (OST4). Mammalian OST was suggested to contain two additional subunits KCP1 and DC2 (Wilson et al. 2011). Some eukaryotes contain only some of the OST subunits found in hetero-oligomeric complex. Hetero-tetrameric OST complexes were described in *Trichomonas vaginalis*, *Entamoeba histolytica* and *Plasmodium falciparum* genomes where homologues of Ost1p, Ost2p, Stt3p and Wbp1p were identified while *Cryptosporidium parvum* contains all the subunits except Swp1p and Ost5p (Kelleher

& Gilmore 2006). One inherent feature to all OST subunits is integration into the complex and interaction with other subunits. Many experiments led to the identification of three subcomplexes formed by Stt3p-Ost4-Ost3/6, Wbp1-Ost2-Swp1p and Ost1-Ost5 (S te Heesen et al. 1993; Silberstein 1995; Fu et al. 1997; Karaoglu et al. 1997; Reiss, te Heesen, Gilmore, Zufferey, Aebi, et al. 1997; Yan et al. 2003). A novel model for OST complex assembly has been proposed where Wbp1p, Ost2 and Swp1p form one subcomplex; Ost1p is first stabilized by Ost5p and then is involved in the formation of the second subcomplex with Stt3p. The two subcomplexes, together with Ost4p, form a bigger subcomplex while Ost4p then anchors Ost3/6p into the final complex (Mueller et al. 2015). Thus, the essential function of the OST subunits in complex stability has to be taken into account when reverse genetic tools are used for functional investigations.

STT3 encodes the catalytic subunit of OST (Yan & Lennarz 2002; Daniel J. Kelleher et al. 2003; Nilsson et al. 2003). Some protozoan, archaeal and bacterial species contain single subunit OSTs, corresponding to eukaryotic STT3 subunit (Wacker 2002; Nasab, Benjamin L Schulz, et al. 2008; Hese et al. 2009; Izquierdo et al. 2009). Some of these (such as *Leishmania major* single subunit OST, *Lm*STT3) are capable of complimenting the loss of yeast STT3 subunit (Nasab, Benjamin L Schulz, et al. 2008; Hese et al. 2009). Thus, cells with a non-functional yeast OST are viable in the presence of *Lm*STT3D protein. Given the fact that a single subunit OST can compensate the function of a hetero-oligomeric complex, one could wonder why such a complex has evolved. Apart from the catalytic Stt3p, two best characterized OST subunits are Ost3p and Ost6p (Schwarz et al. 2005). Ost3p and Ost6p facilitate efficient glycosylation in a site-specific manner (Schulz & Aebi 2009). A model was proposed where different OST isoforms assist the binding of specific polypeptide substrates, via mixed disulphides and noncovalent interactions, increasing the time for the Stt3p to efficiently glycosylate sites that would otherwise be inaccessible (Schulz et al. 2009; Schulz & Aebi 2009; Jamaluddin et al. 2011; Mohd Yusuf et al. 2013; Mohorko et al. 2014). Apart from essential function in contributing to complex stability, little is known about the function of other OST subunits.

WBP1 encodes an essential type I integral membrane glycoprotein with a large luminal domain containing cleavable N-terminal signal sequence and two N-glycans, one transmembrane domain and short cytoplasmic tail with C-terminal dilysine ER retention signal (te Heesen et al. 1991; Gaynor et al. 1994). Wbp1p was the first OST subunit discovered by screening yeast cells for temperature sensitive alleles. Two temperature sensitive alleles were identified, *wbp1-1* and *wbp1-2* respectively, were both led to hypoglycosylation of several glycoproteins *in vivo* and reduced OST activity *in vitro* (S et al. 1992; S te Heesen et al. 1993). The hypoglycosylation phenotype of *wbp1-1* was found to be stronger than of *wbp1-2* (S te Heesen et al. 1993). Both mutations caused a reduction in Wbp1p levels, hence the temperature sensitive phenotype was proposed to result from the general reduction of glycosylation

(te Heesen et al. 1992). OST48, the mammalian homologue of WBP1, was found to be required for glycosylation in mammalian cells (Silberstein et al. 1992; Roboti & High 2012). Knockdown experiments with small interfering RNA (*si*RNA) resulted in reduced levels of glycosylation, similar to *wbp1* mutants (Roboti & High 2012). Currently, the only function of Wbp1p demonstrated is its essential role in OST complex formation. Deletion of *WBP1* results in decreased levels of its subcomplex partners Ost2p and Swp1p, and of Ost3/6p and Stt3p (Mueller et al. 2015). This might be the reason to the hypoglycosylation phenotype. The work of Li and colleagues showed that the lumenal part of the Wbp1p transmembrane domain mediates association with the other subunits (Li et al. 2003).

In this study, we report the identification and characterization of Wbp1p conserved residues and their effect on N-linked glycosylation and the stability of OST complex. We report novel mutants that destabilize OST complex and alter glycosylation by inducing rapid degradation of other OST subunits.

Results

Site-directed mutagenesis of Wbp1p conserved residues

WBP1 is encoded by genomes of all eukaryotes that contain multi-subunit OST complexes, including vertebrates, fungi, nematodes, arthropods, plants and many protists. Wbp1 protein sequences show little variation in the length between different organisms. Polypeptide sequence alignment between 23 Wbp1p homologues was performed, including the homologues from four-subunit OST complex containing *Trichomonas vaginalis*, *Entamoeba histolytica*, *Plasmodium falciparum* and six-subunit OST complex containing *Cryptosporidium parvum* (Supplementary Figure 1). We have identified eight amino acid residues (F102, Q222, R228, N246, W256, Q313, P347 and R376, respectively) that were conserved across all sequences (Figure 1, in red) and five amino acid residues (F355, Y359, F409, S234 and D348, respectively) that were conserved in at least 20 sequences (Figure 1, in black).

```
        10         20         30         40         50         60         70         80         90
MRTDWNFFFC ILLQAIFVVG TQTSRTLVLY DQSTEPLEEY SVYLKDLEQR NYKLEYLDIN STSTTVDLYD KEQRLFDNII VFPTKGGKNL

       100 102               120        130        140        150        160        170        180
ARQIPVKQLI KFFENEGNIL CMSSPGAVPN TIRLFLNELG IYPSPKGHVI RDYFSPSSEE LVVSSNHLLN KYVYNARKSE DFVFGESSAA

       190        200        210            222  228   234         246        256            270
LLENREQIVP ILNAPRTSFT ESKGKCNSWT SGSQGFLVVG FQNLNNARLV WIGSSDFLKN KNQDSNQEFA KELLKWTFNE KSVIKSVHAV

       280   284  290        300            313  320        330        340       347      355 359
HSHADGTSYD EEPYKIKDKV IYSVGFSEWN GEEWLPHIAD DIQFELRQVD PYYRLTLSPS GNDSETQYYT TGEFILPDRH GVFTFLTDYR

       370      376          390        400        409        420        30
KIGLSFTTDK DVKAIRHLAN DEYPRSWEIS NSWVYISAIC GVIVAWIFFV VSFVTTSSVG KKLETFKKTN
```

Figure 1. Conserved residues of *Saccharomyces cerevisiae* Wbp1 protein.

Data from Supplementary Figure 1. N-terminal signal sequence is underlined. Transmembrane domain is highlighted in grey. Strictly conserved residues are in red while other conserved residues are in bold black.

We have developed a strategy for generating point mutations in the chromosomal copy of *WBP1* (Figure 2). In order to complement the deleterious loss of an essential Wbp1p, *Lm*STT3D was introduced on a high-copy number plasmid prior to the knockout of the *WBP1* gene with *Kluyveromyces lactis LEU2* cassette. Simultaneously, a plasmid was constructed carrying the wild type copy of the *WBP1* in frame with the *KanMX* marker cassette using recombination-assisted PCR targeting technique. Site-directed mutagenesis was used to generate point mutations on a plasmid copy of *WBP1* where the conserved residues were replaced by an alanine residue. Mutated version of

wbp1 together with *KanMX* cassette were amplified and reintegrated into the original *WBP1* locus using homologous recombination.

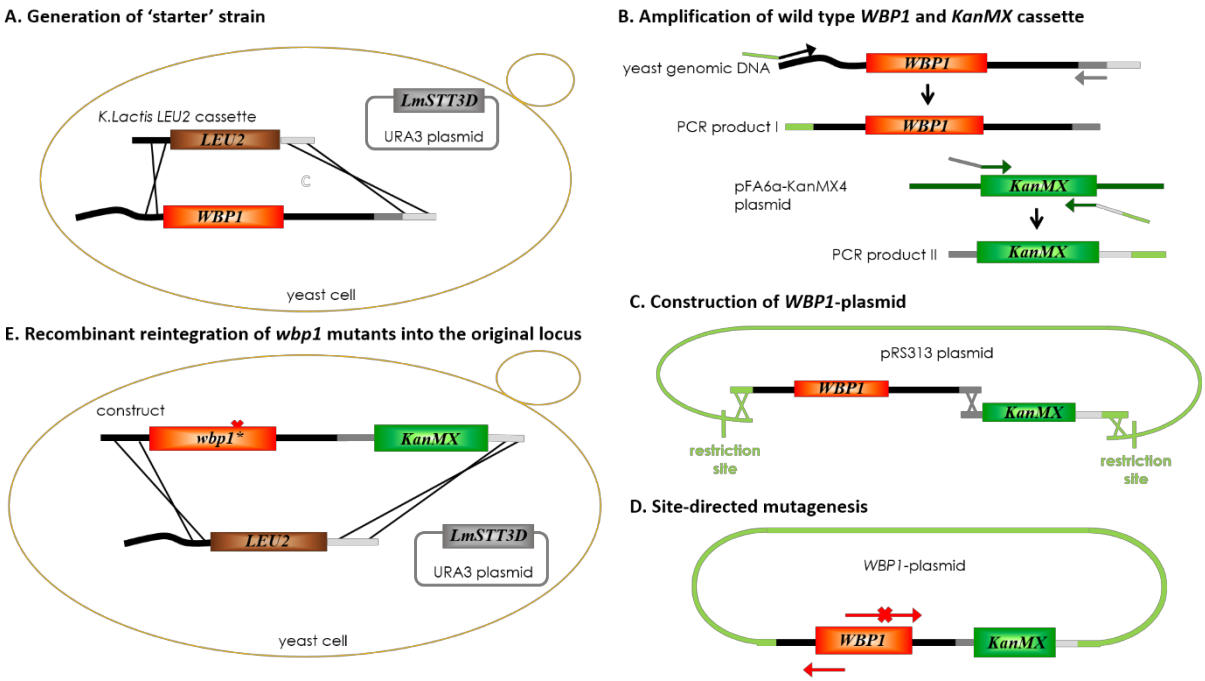

Figure 2. Strategy for the construction of *wbp1* point mutants.

(A) Yeast 'starter strain' was generated in two steps. First, yeast cells were transformed and selected for the *URA3* marker on a plasmid carrying *LmSTT3D* followed by the deletion of endogenous copy of *WBP1* using *K. lactis LEU2* cassette in the . (B) Simultaneously, *WBP1* wild type copy together with sequences 50bp upstream and 200 bp downstream from the ORF were amplified from yeast genomic DNA. *KanMX* cassette was amplified from pFA6a-KanMX4 plasmid using primers carrying sequences homologous to *WBP1* downstream region and to the plasmid region. (C) Separate PCR products were homologously recombined using yeast cells to construct *WBP1*-plasmid. (D) Phusion site-directed mutagenesis was used to generate *wbp1* point mutations on *WBP1*-plasmid. (E) Mutated version of *wbp1-KanMX* cassette was amplified and transformed into yeast 'starter strain'.

All of the conserved Wbp1p residues (Figure 1), three cysteine residues suggested to be involved in binding of Dol-PP-$GlcNAc_2$ (C111, C206 and C400, respectively) and two asparagines that are part of Wbp1 N-linked glycosylation sites (N60 and N322, respectively) were mutated to alanine residues as described above (Pathak et al. 1995).

Evaluation of the experimental system with known *wbp1* mutations

Previously isolated conditional *wbp1-1* and *wbp1-2* alleles were shown to cause temperature-sensitive growth defect and hypoglycosylation of several glycoproteins *in vivo* (te Heesen et al. 1992). We introduced *wbp1-1* (R228Y), and *wbp1-2* (F249S and S294L) mutations in the genomic copy of *WBP1* locus. In the presence of complementing *Lm*STT3D protein we analysed the effect of the two previously described *wbp1* mutants on the OST complex assembly and in its absence, we assayed for growth and glycosylation efficiency using SDS-PAGE and immunoblot analysis. The cells were first subjected to the growth on 5-FOA containing medium where the cells lacking *URA3 LmSTT3D* expression plasmid were selected and their survival was dependent on the ability of the OST to preserve all or some of its activity (Figure 3A). Both *wbp1* mutants reduced the enzyme activity at both permissive (23^{o}) and non-permissive temperature (37^{o}C), resulting in the temperature-sensitive growth phenotype, where *wbp1-1* showed stronger phenotype as in accordance with previously published results (te Heesen et al. 1992). As *wbp1-2* allele contains two point mutations (F249S and S297L, respectively) we introduced these mutations individually and assayed for growth on medium containing 5-FOA (Figure 3A). Individual mutations in the *WBP1* locus had no effect on enzyme activity and cell growth indicating that the temperature-sensitive phenotype of the *wbp1-2* allele is a result of cumulative effect of both mutations.

We examined the effect of *wbp1-1* and *wbp1-2* alleles on the OST activity *in vivo* in the absence of *LmSTT3D* expressing plasmid by analysing the glycosylation efficiency of yeast proteins by SDS-PAGE immunoblot (Figure 3B). Our result demonstrated that both mutants caused hypoglycosylation of all four glycoproteins analysed (i.e. CPY, Pdi1, Ost1 and Wbp1), indicating a systematic hypoglycosylation phenotype where *wbp1-1* mutants showed a more severe effect on the glycosylation efficiency. Furthermore, both mutants resulted in decreased amounts of Wbp1p, as well as Ost3p and Ost6p compared to the cells carrying either endogenous or reintegrated wild type *WBP1* copy (Figure 3B). These results were in agreement with previously published studies (te Heesen et al. 1992).

We next analysed the effect of *wbp1-1* and *wbp1-2* alleles on OST complex stability (Figure 3C). Our results showed reduced steady state levels of Wbp1p, Ost3p and Ost6p in both mutants implying that the OST complex is destabilized (Figure 3B). We used the previously developed SILAC pulse-chase method to analyse protein degradation rates of OST subunit proteins (Mueller et al. 2015). Under the assumption that the OST complex is stable with all subunits present in similar amounts at stoichiometric level in the wild type yeast cells, a perturbation could lead to destabilization of some or all subunits resulting in a faster degradation, with lower amounts of destabilized subunits in the complex. As such, we can analyse the complex stability by calculating the degradation rates of OST

subunits during exponential growth. Yeast microsomal fractions were prepared from Δ*wbp1*, *wbp1-1* and *wbp1-2* cells, proteins were extracted, processed for mass spectrometry and quantified using SRM MS. As previous result had indicated, both mutants resulted in higher turnover of Wbp1p. Degradation of several other proteins, including Ost3p, Ost6p, Ost2p, Swp1p, and to a lesser extent, Ost5p and Stt3p was observed as well (Figure 1C; Supplementary Table 1). This phenotype was similar to the phenotype observed for the *wbp1* deletion strain further indicating that these mutations destabilize Wbp1p resulting in its degradation. The lack of Wbp1p in turn destabilized the rest of the OST complex, thus most of the remaining subunits are affected as well. Our findings are in agreement with previously published results where the lack of Wbp1p was already shown to cause increased degradation rates of the subcomplex partner proteins Ost2 and Swp1, as well as Ost3, Ost6, Ost5 and Stt3 proteins (Mueller et al. 2015).

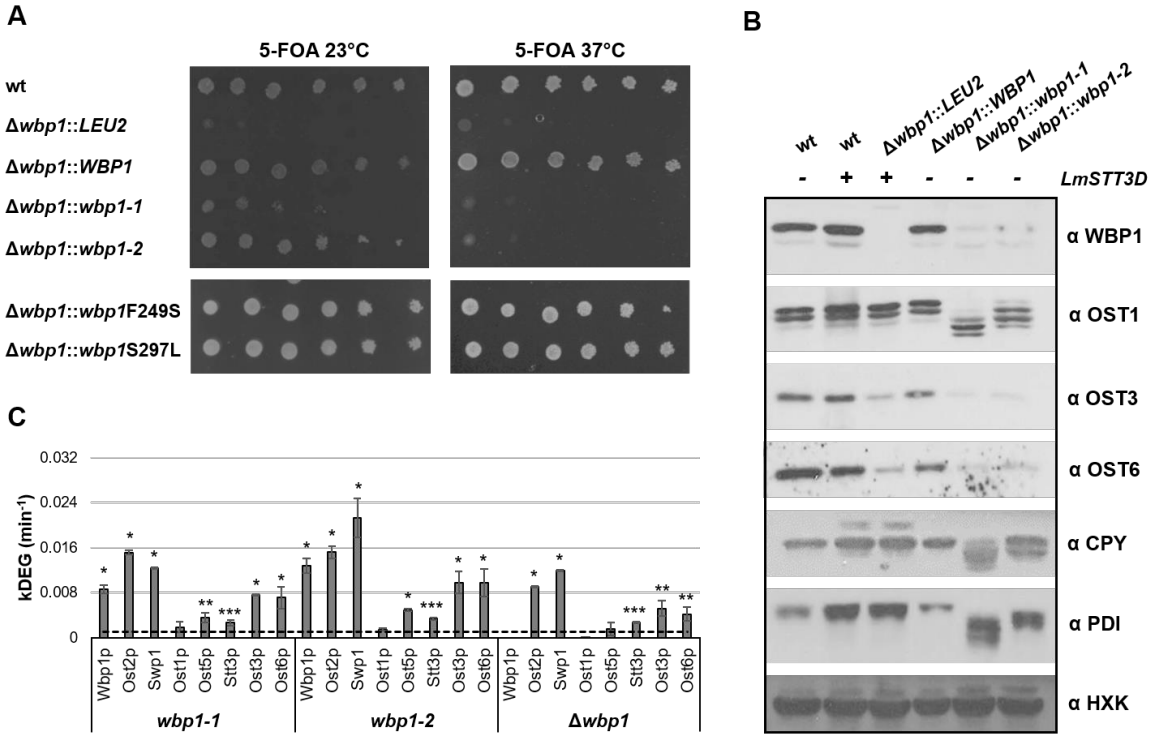

Figure 3. *wbp1-1* and *wbp1-2* alleles result in OST complex destabilization.

(A) 5-FOA spotting assay for the analysis of *wbp1* growth phenotypes. Yeast wild type cells and cells where the endogenous copy of *WBP1* locus was replaced with either the *K.lactis LEU2* cassette, wild type *WBP1* or different *wbp1* alleles were complemented by *URA3 LmSTT3D* expression plasmid. Serial dilutions of wild type and mutant cells were spotted on medium containing 5-FOA and incubated at 23^{o}C or 37^{o}C for five days. Mutations that inactivate the OST enzyme do not support the growth of the cells. (B) Immunoblot analysis of *wbp1* strains. SDS extracts were prepared from wild type cells or mutant cells were the endogenous *WBP1* locus was replaced by either the *K. lactis LEU2* cassette, the wild type *WBP1* or *wbp1-1* and *wbp1-2* loci. Some of the cells were carrying

LmSTT3D expression plasmid as indicated. Equal amounts of protein were separated on a 10% SDS-PAGE gel and transferred to nitrocellulose membrane, followed by detection with specific antibodies. Hexokinase (HXK) was used as a loading control. (C) k_{DEG} values of OST subunits in *wbp1-1*, *wbp1-2* or in cells deleted in *WBP1*, all carrying *LmSTT3D* expression plasmid. After labelling of yeast proteins with heavy arginine and lysine, cells were transferred to light medium and sampled at different time points. Proteins were prepared for mass spectrometry and light-to-heavy (L/H) ratios for peptides detected by SRM. Degradation rates were calculated as described. Error bars represent SD of three biological replicates. *p < 0.001, **p < 0.01, ***p < 0.05. The dashed line indicates a half-life less than 12 hours representing eight cell divisions.

Novel *wbp1* mutations affect OST activity

Polypeptide sequence alignment of Wbp1p homologues revealed residues conserved between 23 species know to contain multi-subunit OST complexes (Figure 1, Supplementary Figure 1). These Wbp1p residues, including two N-linked glycosylation sites and three cysteine residues, were mutated to alanine in the presence of complementing *Lm*STT3D and their effect on cell growth in the presence of 5-FOA was examined (Supplementary Figure 2). Out of 18 mutations analysed, single amino acid changes in three residues (F102A, W256A and Y284A, respectively) resulted in reduced enzyme activity and temperature sensitivity at 37^{o}C while the other mutations had no effect on cell growth on 5-FOA containing medium (Figure 4A; Supplementary Figure 2). Of the three mutants, the replacement of tryptophan at position 256 with an alanine residue had the most severe effect causing the complete loss of OST activity at non-permissive temperature (37^{o}C). The other two mutations were capable of supporting cell growth at non-permissive temperature although they grew slower as compared to the cells with reintegrated wild type *WBP1* copy (Figure 4A).

We then examined the effect of the novel *wbp1* alleles on the OST activity *in vivo* in the absence of *LmSTT3D* expressing plasmid by analysing the glycosylation efficiency of yeast glycoproteins by SDS-PAGE immunoblot (Figure 4B). In line with growth analysis results, W256A mutation resulted in the most severe hypoglycosylation of all four glycoproteins analysed (i.e. Wbp1p, Ost1p, CPYp and Pdi1p) as compared to the other two mutations, indicating a systemic hypoglycosylation phenotype. The other two mutants, *F102A* and *Y284A* respectively, showed less severe hypoglycosylation phenotype as compared to *W256A* mutant, where F102A mutation resulted in a more reduced OST activity as compared to Y284A mutation (Figure 4B).

To investigate OST complex stability, we conducted a pulse chase SILAC SRM experiment and determined degradation rates for all OST subunit proteins as described above (Figure 4C). The two mutations resulting in stronger growth and hypoglycosylation phenotypes, W256A and F102A respectively, induced degradation of Wbp1p where the degree of Wbp1p degradation correlated with

the severity of the two phenotypes. Both mutations resulted in degradation phenotype similar to *wbp1-1* and *wbp1-2* alleles, with two exceptions. Similar to previously described *wbp1* strains, OST subunits Ost2p, Swp1p, Ost3p and Ost6p were severely degraded in *W256A* strain, however Ost5p and Stt3p were more stable in this mutant. Wbp1p F102A mutation resulted in degradation of all of the OST subunits degraded in *wbp1-1* and *wbp1-2* except for Ost2p, which was stable in this mutant. Lastly, all OST subunits were stable in *Y284A* (Figure 4C; Supplementary Table 1).

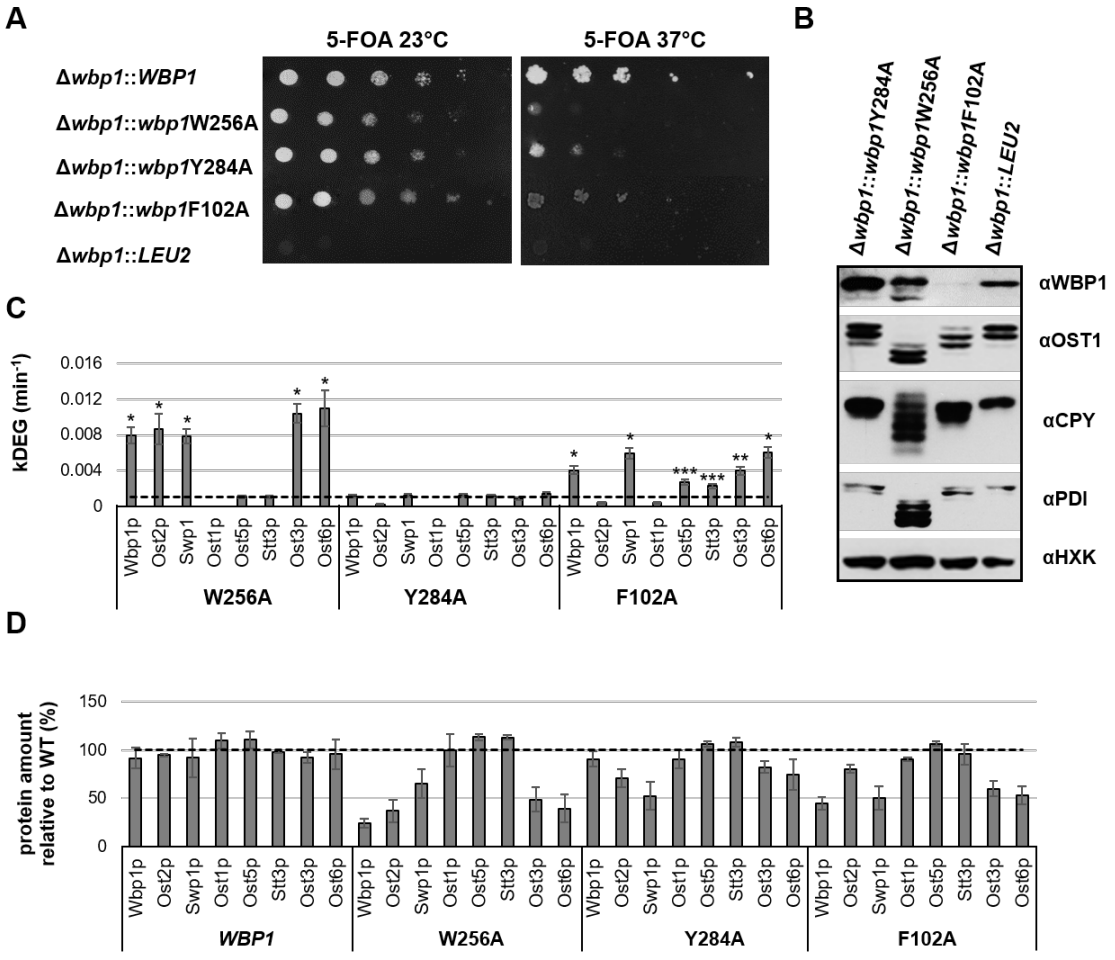

Figure 4. Wbp1p mutations F102A, W256A and F102A reduce OST activity through complex destabilization.
(A) 5-FOA spotting assay for the analysis of *wbp1* growth phenotypes. Yeast cells where the endogenous copy of *WBP1* locus was replaced with either the *K.lactis LEU2* cassette, wild type *WBP1* or different *wbp1* alleles were complemented by *URA3 LmSTT3D* expression plasmid. Serial dilutions of wild type and mutant cells were spotted on medium containing 5-FOA and incubated at 23^{o}C or 37^{o}C for five days. Mutations that inactivate the OST enzyme do not support the growth of the cells. (B) Immunoblot analysis of *wbp1* strains. SDS extracts were prepared from mutant cells were the endogenous *WBP1* locus was replaced by the wild type *WBP1* or the mutated *wbp1* loci. Equal amounts of protein were separated on a 10% SDS-PAGE gel and transferred to nitrocellulose membrane, followed by detection with specific antibodies. Hexokinase (HXK) was used as a loading control. (C) k_{DEG} values of OST subunits in different *wbp1* strains carrying *LmSTT3D* expression plasmid. After

labelling of yeast proteins with heavy arginine and lysine, cells were transferred to light medium and sampled at different time points. Proteins were prepared for mass spectrometry and light-to-heavy (L/H) ratios for peptides detected by SRM. Degradation rates were calculated as described. Error bars represent SD of three biological replicates. *p < 0.001, **p < 0.01, ***p < 0.05. The dashed line indicates a half-life less than 12 hours representing eight cell divisions. (D) Steady state levels of OST subunit proteins in different *wbp1* strains carrying *LmSTT3D* expression plasmid. Yeast wild type cells were grown in heavy arginine and lysine medium, while *wbp1* mutant cells were grown in medium containing light amino acids. Equal amounts of cells were mixed, proteins extracted, and peptides were processed for mass spectrometry. L/H ratios for peptides were detected by SRM. Subunit abundance relative to wild type was calculated as described. Error bars represent the 95% confidence interval of the average of two biological replicates.

As pulse-chase experiments have been shown to lack sensitivity when it comes to detecting small stability differences between different proteins, we examined the effect of *wbp1* alleles on OST complex stability by monitoring steady state levels of OST subunits (Mueller et al. 2015). We performed SILAC experiment where wild type cells grown in medium containing heavy arginine and lysine amino acids were mixed 1:1 with mutant cells grown in medium containing light amino acids. Membranes were isolated, proteins digested and peptides were prepared for SRM MS measurement (Figure 4D). In the control measurement where yeast wild type cells and cells with reintegrated wild type *WBP1* were pooled together, all OST subunit proteins had a normal level (100%) (Figure 4D). Distinct results were observed for different *wbp1* strains. Wbp1p W256A mutation reduced the levels of Wbp1p (to 24%), Ost2p (to 37%), Swp1p (to 65%), Ost3p (to 49%) and Ost6p (to 40%) while the levels of Ost1p, Ost5p and Stt3p were not affected. Together with pulse-chase analysis, these results indicate that W256A mutation severely destabilized Wbp1p resulting in destabilization of OST complex. These results are in accordance with previously published work showing that *WBP1* deletion drastically alters the amounts of Ost2p , Swp1p, Ost3p and Ost6p (Mueller et al. 2015). Similar to pulse-chase evaluation, steady state levels of Wbp1, Swp1, Ost3, and Ost6 proteins in *F102A* mutant were decreased (45%, 50%, 60% and 53%, respectively) while the level of Ost2p was not affected. This result indicates that phenylalanine at position 102 is important for Wbp1p stability as well as for the Wbp1p interaction with Swp1p. Contrary to protein degradation analysis, *Y284A* mutant resulted in the decreased Swp1p (to 50%) and Ost2p (to 70%) levels indicating that this residue is not crucial for Wbp1p stability but for interaction with Swp1 and Ost2 proteins.

The effect of individual point mutations on cell growth and OST activity was examined in the other Wbp1p residues. As mentioned above, these additional mutations had no effect on cell growth on 5-FOA containing medium (Supplementary Figure 2). Using 5-FOA counter-selection *wbp1* mutant cells without *LmSTT3D* expression plasmid were selected and their growth on YPD medium was examined.

Similar to 5-FOA containing medium, no growth phenotypes were detected (data not shown). When we then examined the effect of the these *wbp1* strains on the OST activity *in vivo* in the absence of *LmSTT3D* expressing plasmid by analysing the glycosylation efficiency of yeast glycoproteins by SDS-PAGE immunoblot, no evident hypoglycosylation phenotypes were detected either (Supplementary Figure 3).

Mutations affecting the addition of sugar residues in the lumenal assembly of the LLO do not show any detectable growth defect, but combined accumulation of suboptimal lipid-linked oligosaccharides and reduced oligosaccharyltransferase activity (such as in *stt3-3* mutant) results in synthetic phenotype with growth defects at non-permissive temperature of 37^{o}C (Aebi et al. 1996). It has been demonstrated previously that single mutations of *ALG5*, *ALG6* or *ALG8*, involved in glucosylation of the LLO, in *wbp1-1* cause severe growth defect even at permissive temperature of 30^{o}C (Stagljar et al. 1994). We replaced *ALG3* gene with *NatNT2* cassette in *wbp1* strains. The inactivation of the nonessential *ALG3* gene results in the accumulation of lipid-linked $GlcNAc_2Man_5$. No observable growth arrest resulted in majority of the additional *wbp1* double mutants with two exceptions (Supplementary Figure 4). Double mutants *F355AΔalg3* and *F409A Δalg3* resulted in mild temperature sensitivity at 37^{o}C (Supplementary Figure 4). When we examined the effect of the double mutants on protein glycosylation by SDS-PAGE immunoblot, no synthetic phenotypes were observed (data not shown).

In order to examine if Wbp1p affects glycosylation of specific substrate proteins, SILAC coupled to parallel reaction monitoring (PRM) MS-based technique was used to analyse glycosylation occupancy on yeast microsomal glycoproteins (Poljak et al.; in preparation). Due to time limitations, we only performed a preliminary experiment using one biological replicate for some of the *wbp1* strains. Wild type cells grown in medium containing heavy arginine and lysine amino acids were mixed 1:1 with mutant cells grown in medium containing light amino acids. Membranes were isolated, proteins digested and N-linked glycans were cleaved by EndoH to maintain the first GlcNAc residue of the glycan on the protein. The resulting peptides were analysed by LC-MS/MS and site occupancies relative to the reference strain were calculated for *wbp1* strains (Supplementary Table 2). From the preliminary results of the PRM MS analysis ten out of twelve *WBP1* mutations caused hypoglycosylation of Ero1p (Q222A, S234A, Q313A, P347A, D348A, F355A, Y359A, R376A, F409A and N322A, respectively), where the extent of hypoglycosylation varied in different mutants. Other glycoproteins were affected as well, including Wbp1, CPY, Erg3, Crh2, and Mnn5 proteins. However, the preliminary results need to be confirmed using additional biological replicates. Moreover, although SDS-PAGE immunoblot analysis did not reveal evident decrease of the OST complex subunits, a SILAC SRM experiment needs to be done in order to investigate OST complex stability in those mutants (Supplementary Figure 3).

Discussion

The yeast OST complex is composed of eight subunits where the expression of a majority of the subunits is essential for the cell viability. Except for the catalytic function of Stt3p and the function of isoform-defining Ost3/6p, only little is known about the role of the other subunits. Although several temperature sensitive mutants of Wbp1p were isolated previously, these mutants did not provide information about the role of Wbp1p beyond its importance for the OST complex integrity. Residues conserved between 23 distinct species ranging from single cell eukaryotic organisms to mammals were identified and mutated into alanine using a high throughput strategy for generating point mutations in the chromosomal copy of *WBP1.* In order to further characterize previously isolated conditional *wbp1-1* and *wbp1-2* alleles, we introduced *wbp1-1* (R228Y), and *wbp1-2* (F249S and S294L) mutations in the genomic copy of *WBP1* locus. In accordance with former results, both *wbp1* mutants reduced the enzyme activity at both permissive (23^{o}) and non-permissive temperature (37^{o}C), while the individual *wbp1-2* mutants (F249S and S297L, respectively) had no effect on the cell growth indicating that the temperature-sensitive phenotype of *wbp1-2* mutant is a result of cumulative effect of both mutations. Both, *wbp1-1* and *wbp1-2*, mutants caused systematic hypoglycosylation of glycoproteins. By examining OST subunits protein degradation rates, we have shown that the both mutants destabilize Wbp1p resulting in its degradation. The lack of Wbp1p in turn destabilized the rest of the OST complex, thus most of the remaining subunits (Ost3p, Ost6p, Ost2p, Swp1p, and to a lesser extent, Ost5p and Stt3p) are degraded as well. This phenotype was similar to the phenotype observed for the *wbp1* deletion strain and are in agreement with previously published results (Mueller et al. 2015). When we examined the effect of the alanine replacements of Wbp1p conserved residues, only three mutations (F102A, W256A and Y284A, respectively) resulted in reduced enzyme activity and temperature sensitivity at non-permissive temperature of 37^{o}C. The replacement of tryptophan at position 256 with an alanine residue had the most severe effect, causing the complete loss of OST activity at 37^{o}C and systematic hypoglycosylation at 30^{o}C, similar to *wbp1-1* mutant. Although less severe, F102A mutation had a similar effect. Both, *W256A* and *F102A*, alleles destabilized Wbp1p resulting in destabilization of OST complex. Interestingly, the mutation of phenylalanine at position 102 caused degradation and reduced steady state levels of all of the OST subunits degraded in *wbp1-1* mutant except for Ost2p, which was stable in this mutant. Given the proposal of Mueller and colleagues that one can define interactions between different OST subunits by measuring their turnover rates or steady state levels in different mutants, such a result might indicate that the Ost2p is less important for the assembly of the first subcomplex and that in certain condition could be stable on its own (Mueller et al. 2015). The *Y284A* mutant resulted in the reduced growth at non-permissive temperature of 37^{o}C and hypoglycosylation of some glycoproteins. Steady state protein level

measurements revealed that, although Wbp1p is stable, the amounts of Swp1p and Ost2p are decreased in this mutant. These results indicate that tyrosine residue at position 284 is important for the interaction of Wbp1p with Swp1 and Ost2 proteins. Taken together, these results demonstrate that W256A, F102A and Y284A mutations affect OST activity through complex destabilization, either as a result of Wbp1p destabilization itself or due to impaired interaction with subcomplex subunits. The other mutations, including the mutations affecting the two N-linked glycosylation sites and three cysteine residues, had no effect on the cell growth. Although these mutations did not result in hypoglycosylation of four glycoproteins examined by immunoblot, we identified several mutations that affected glycosylation of six glycoproteins examined by the preliminary MS-based glycosylation occupancy analysis of yeast microsomal fractions. Albeit these results still need to be verified, it is tempting to postulate the role of Wbp1p in influencing the glycosylation of specific substrate proteins. Previous reports have demonstrated that the knockdown of the mammalian OST1 homologue ribophorin I resulted in hypoglycosylation of some membrane proteins while soluble proteins were not affected (Wilson & High 2007; Wilson et al. 2008). Furthermore, deletion of *OST3* and *OST6* in yeast cells have been shown to affect glycosylation of specific proteins (Schulz & Aebi 2009). Another possibility to gain insight into the role of Wbp1p would be to solve the crystal structure of its lumenal domain, similar to Ost6p where the crystal structure of its lumenal domain helped elucidate the function of Ost3/6p subunits (Schulz et al. 2009).

Materials and Methods

Plasmids

Plasmids and primers used in this study are listed in Supplementary Table 3 and 5. Standard cloning and yeast genetic techniques were used (Knop et al. 1999; Gibson 2009). A pRS313 plasmid containing *WBP1* locus and *KanMX* cassette was constructed. *WBP1* locus (starting from 33 bp upstream until 250bp downstream of the ORF) was amplified from wild type genomic DNA using primers P1-wbp1-pRS313_Fw, flanked with pRS313 plasmid homologous region, and P2-wbp1-Rev. *KanMX* cassette was amplified from pFA6a-KanMX4 plasmid using a forward primer containing *WBP1* homologous region (P3-Kan-wbp1-Fw) and a primer containing pRS313 homologous region (P4-Kan-Wbp1-Rev). The pRS313 plasmid was digested with EcoRI restriction enzyme that yielded a linear plasmid DNA with ends homologous to the regions of *WBP1* and *KanMX* PCR products. The two PCR products and digested plasmid were co-transformed into wild type yeast cells resulting in the generation of recombined *WBP1*-plasmid. Transformed cells were grown overnight on rich medium (YPD) and replica plated onto the selective medium containing geneticin (G418) the next day. The plasmid was recovered from yeast cells as described before and amplified in *E.coli*. The plasmid was doubly digested and sequenced to ensure proper gene integration. Phusion site-directed mutagenesis was used to generate point mutations in the *WBP1* ORF on the *WBP1*-plasmid as described before. Shortly, primers were designed to anneal back-to-back to the plasmid where the desired mutation was located in the middle of the forward primer. Primers used for mutagenesis are listed in Supplementary Table 5. The primers were first phosphorylated, *WBP1*-plasmid was PCR amplified and the mutated product was circulated by ligation with T4 ligase. The product was amplified in *E.coli* and the mutations were confirmed by sequencing.

Strains

Strains used in this study are listed in Supplementary Table 4. Standard cloning and yeast genetic techniques were used (Knop et al. 1999). If not mentioned otherwise, all strains were grown at 30^{o}C. The 'wild type' strain (KP4 strain) used in this study was generated by deleting *ARG4* gene in BY4742 (Euroscarf) yeast strain using Cre/loxP system as described before (Güldener et al. 1996). Shortly, the *KanMX* cassette flanked with two direct repeats of *loxP* sites and homologous regions of *ARG4* was amplified from pUG6 plasmid and transformed into BY4742 cells. Transformed cells were grown overnight on YPD medium and replica plated onto the selective medium containing G418 the next day. The proper integration of the cassette and knock out of *ARG4* was confirmed by PCR. The resulting yeast strain was transformed with pSH47 plasmid that carries Cre recombinase under the control of galactose (GAL1) promoter. Shifting cells to galactose medium resulted in the excision of *KanMX*

cassette with a remnant *loxP* site. The complete loss of the cassette was confirmed by PCR. This strain was grown on 5-Fluoroorotic acid (5-FOA) allowing for the selection of the cells that have lost the pSH47 plasmid. The resulting strain, KP4 strain, was termed wild type in this study. In the next step, KP4 strain was transformed with pLmSTT3 plasmid and plasmid-containing cells were selected on -URA plates. Yeast *WBP1* gene was replaced by *K. lactis LEU2* cassette amplified from pUG73 plasmid (using Kl-leu2-Wbp1-Fw and Kl-Leu2-Wbp1-Rev primers) resulting in the deletion of *WBP1* ORF and sequences 133bp upstream and 163bp downstream from the ORF. After transformations, the cells were selected on -URA-LEU plates. The knockout of *WBP1* gene was checked by PCR (using Wbp1-Fw-Check and Wbp1-Rev-Check primers). Resulting strain was termed KP5, or 'starter strain'. Mutant *wbp1* genes and *KanMX* cassette were amplified from mutated *WBP1*-plasmid (using PC-Wbp1-Fw and PC-WBP1-Rev primers) and transformed into KP5 strain. Transformed cells were grown overnight on YPD medium and replica plated onto the selective medium containing G418 the next day. The proper reintegration of mutated *wbp1* locus was confirmed by PCR and sequencing. In most cases, mutant cells were grown on the medium containing 5-FOA allowing for the selection of the cells that have lost the pLmSTT3D plasmid.

Spotting assay for growth

To determine the growth rate of yeast transformants carrying *wbp1* mutants, 15 ODs of cells were collected after the strains were grown to early log phase in either -URA or YPD media at 30 °C. Two microliters of 1:10 serial dilutions of the cells was spotted on either 5-FOA or YPD plates, respectively, and incubated at 25, 30, or 37 °C for 5 or 2 days, respectively.

Immunoblot analysis

Cultures were grown in YPD medium to exponential phase. Cells were lysed with glass beads in sample buffer by vortexing at 4°C for 15 min. The sample buffer contained 2% SDS, 62.5 mM Tris/HCl, pH 6.8, 10% glycerol, 6 M urea, 5% β-mercaptoethanol, 0.02% bromophenol blue, protease inhibitor (Complete, Roche), 5 mM phenylmethylsulfonyl fluoride and 25 mM EDTA. Proteins were dissolved at 37°C for 20 min. Equal amounts of protein were loaded on 10% polyacrylamide gels. Proteins were blotted onto a nitrocellulose membrane. The membrane was hybridized with a primary antibody, washed, and hybridized with appropriate secondary antibodies. Antibodies used are listed in Supplementary Table 5. Proteins were detected with ECL solution (GE Healthcare, Amersham) and light sensitive films (Super RX, Fuji Medical X-Ray Film).

SILAC chase

Yeast cells were grown to exponential phase in SD-URA medium supplemented with 20 mg/L heavy [$^{13}C_6$/$^{15}N_2$] L-lysine and [$^{13}C_6$] L-arginine (Cambridge Isotope laboratories). Cells were collected by filtration, washed with SD medium without arginine and lysine, and resuspended in SD medium containing light isotopes of arginine and lysine to obtain OD_{600} = 0.5. At different time points, 50 OD of cells were collected, frozen in liquid nitrogen, and stored at −80°C followed by the preparation for mass spectrometry.

Steady-state SILAC

Wild type cells were grown in synthetic complete medium containing 20 mg/L heavy [$^{13}C_6$/$^{15}N_2$] L-lysine and [$^{13}C_6$] L-arginine (Cambridge Isotope laboratories). Mutant cells were grown in synthetic complete medium containing 20 mg/L light [$^{12}C_6$/$^{14}N_2$] L-lysine and [$^{12}C_6$] L-arginine. Cells were harvested in early log phase (OD_{600nm} = 0.8-1.2) by centrifugation and mixed 1:1 (w/w) before being processed for mass spectrometry.

Sample preparation for mass spectrometry

Yeast microsomal fractions were prepared as described previously (Mueller et al. 2015). Shortly, cells were lysed and microsomal fractions were collected by high spin centrifugation at 16,000xg, 4°C for 20 min. Proteins were processed using the filter-assisted sample preparation (FASP) protocol (Wiśniewski et al. 2009). After reduction and alkylation, proteins were digested with Lys-C (20 µg/mL; Wako Pure Chemical, Richmond, VA) and trypsin (20 µg/mL; Promega) endopeptidases. When mentioned, protein digestion was directly followed by EndoH (500 U; New England BioLabs) endoglycosidase treatment. Peptides were desalted using C18 ZipTips (Millipore) and dried using speed vacuum. Desalted peptides were resuspended in ACN/H_2O (3:97 (v/v)) with formic acid (FA; 0.1% (v/v)) and analysed by LC-ESI-MS/MS. Retention time iRT peptides (Biognosys) were added to all samples in ratio of 1:40.

SRM mass spectrometry

For each sample, 4 µl was injected onto a nano-frit column (15 cm × 75 µm; OD 375 µm; beads, Magic C18 AQ, 3 µm, 200 Å; Bischoff Chromatography) kept at 50°C and connected to a spray tip (PicoTip emitter, FS360-20-10-N-20-C12; New Objective; MS Wil) coupled to an Eksigent nanoLC-Ultra 1D plus (AB Sciex). Peptides were eluted using a gradient from 3 to 35% solvent B (99% (v/v) acetonitrile, 0.1% (v/v) formic acid) for 57.5 min at a flow rate of 500 nL/min. Targeted SRM analysis was performed on

a QTRAP 5500 (AB Sciex) supplied with a nanospray ion source. Interface temperature was 170°C, ion spray voltage 2000–2500 V, ion source gas pressure 6–10 psi, curtain gas pressure 25 psi, and collision gas was set to high. Declustering potential had a value of 100, collision cell exit potential of 13, and entrance potential of 10. Retention time windows for the transitions were 5-min and a target scan time was 3 s. The scheduled transition list contained 377 transitions (Appendix Table 5). Results from the SRM runs were exported to Skyline software, and peaks were integrated (MacLean et al., 2010). The peaks were manually inspected and adjusted to ensure proper peak picking and peak integration.

PRM mass spectrometry

Peptides were separated on HSS T3 column (78 µm × 150 mm, 1.8 µm) packed with C18 material (Waters) on ACQUITY UPLC system (Waters). Peptides were eluted using the gradient of 2 - 35% solvent B (99% (v/v) ACN, 0.1% (v/v) FA) over 90 min at a flow rate of 0.3 µl/min. MS analysis was performed on Q Exactive HF instrument (Thermo Scientific). Samples were analysed using two PRM methods at an Orbitrap resolution of 30 000 or 60 000, based on scheduled inclusion lists containing the 175 and 128 target precursor ions, respectively, including retention time iRT standard peptides (Biognosys) (Appendix Table 1). The full scan event was collected using a m/z 50–1400 mass selection, an Orbitrap resolution of 60 000 (at m/z 400), target automatic gain control (AGC) value of 3×10^6 and a maximum injection time of 30 ms. The PRM scan events used an Orbitrap resolution of 30 000 or 60 000, maximum fill time of 30 or 110 ms respectively, an AGC value of 1×10^6 and with an isolation width of 2 m/z. Fragmentation was performed with a normalized collision energy of 28 and MS/MS scans were acquired with a starting mass of m/z 150. Scan windows were set to 10 min. Results from the SRM runs were exported to Skyline software, and peaks were integrated (MacLean et al., 2010).

Calculation of protein degradation rates

The degradation rate calculation was done by normalizing the rate of loss of old proteins to the dilution of protein content by cell division. The loss rate of old protein from the cell (k_{LOSS}) was calculated from the time course of isotopic ratios (Larrabee et al. 1980). Values were normalized to the dilution of protein content by cell division. This was done by subtraction of k_{DIL} (= k_{LOSS} of the stable reference protein Rpl5p). Protein half-lives were calculated as $t_{1/2} = \ln(2)/k_{DEG}$. Proteins with $t_{1/2}$ greater than 12 hours, corresponding to 8 cell divisions, were considered stable, otherwise they were considered instable.

Calculation of abundance of OST proteins

Light to heavy intensity ratio (L/H) ratios were calculated for each peptide. The amount of OST subunits relative to wild type was calculated from the average L/H over all peptides of a protein. Values were normalized by dividing by the ribosomal control proteins Rpl5p and Rps1a of each replicate. Results of three biological replicates were expressed as percentage protein level compared to wild type.

Calculation of glycosylation site occupancy

The L/H ratio for glyco-peptides modified with HexNAc was used to calculate the relative site occupancy for the given peptide/ glycosylation site. The relative site occupancy was normalized for expression differences between heavy labelled reference wild type strain (H) and the mutant strains (L) by dividing the L/H intensity ratio for the occupied glyco-peptide by the median of L/H intensity ratios reported for all non-glyco (i.e. not containing a N-X-T/S sequon) peptides from the same protein as the glyco peptide.

References

Beatson, S. & Ponting, C.P., 2004. GIFT domains: linking eukaryotic intraflagellar transport and glycosylation to bacterial gliding. *Trends in biochemical sciences*, 29(8), pp.396–9.

Breitling, J. & Aebi, M., 2013. *N* -Linked Protein Glycosylation in the Endoplasmic Reticulum. *Cold Spring Harbor Perspectives in Biology*.

Fu, J., Ren, M. & Kreibich, G., 1997. Interactions among Subunits of the Oligosaccharyltransferase Complex. *Journal of Biological Chemistry*, 272(47), pp.29687–29692.

Gaynor, E.C. et al., 1994. Signal-mediated retrieval of a membrane protein from the Golgi to the ER in yeast. *The Journal of cell biology*, 127(3), pp.653–65.

Gibson, D.G., 2009. Synthesis of DNA fragments in yeast by one-step assembly of overlapping oligonucleotides. *Nucleic acids research*, 37(20), pp.6984–90.

Gueldener, U. et al., 2002. A second set of loxP marker cassettes for Cre-mediated multiple gene knockouts in budding yeast. *Nucleic acids research*, 30(6), p.e23.

Güldener, U. et al., 1996. A new efficient gene disruption cassette for repeated use in budding yeast. *Nucleic acids research*, 24(13), pp.2519–24.

te Heesen, S. et al., 1991. An essential 45 kDa yeast transmembrane protein reacts with anti-nuclear pore antibodies: purification of the protein, immunolocalization and cloning of the gene. *European journal of cell biology*, 56(1), pp.8–18.

te Heesen, S. et al., 1992. The yeast WBP1 is essential for oligosaccharyl transferase activity in vivo and in vitro. *The EMBO journal*, 11(6), pp.2071–5.

te Heesen, S. et al., 1993. Yeast Wbp1p and Swp1p form a protein complex essential for oligosaccharyl transferase activity. *The EMBO journal*, 12(1), pp.279–84.

Helenius, J. et al., 2002. Translocation of lipid-linked oligosaccharides across the ER membrane requires Rft1 protein. *Nature*, 415(6870), pp.447–50.

Hese, K. et al., 2009. The yeast oligosaccharyltransferase complex can be replaced by STT3 from Leishmania major. *Glycobiology*, 19(2), pp.160–171.

Izquierdo, L. et al., 2009. Distinct donor and acceptor specificities of Trypanosoma brucei oligosaccharyltransferases. *The EMBO journal*, 28(17), pp.2650–61.

Jamaluddin, M.F.B. et al., 2011. Polypeptide binding specificities of saccharomyces cerevisiae oligosaccharyltransferase accessory proteins Ost3p and Ost6p. *Protein Science*, 20(5), pp.849–855.

Karaoglu, D., Kelleher, D.J. & Gilmore, R., 1997. The Highly Conserved Stt3 Protein Is a Subunit of the Yeast Oligosaccharyltransferase and Forms a Subcomplex with Ost3p and Ost4p. *Journal of Biological Chemistry*, 272(51), pp.32513–32520.

Kelleher, D.J. et al., 2003. Oligosaccharyltransferase isoforms that contain different catalytic STT3 subunits have distinct enzymatic properties. *Molecular Cell*, 12(1), pp.101–111.

Kelleher, D.J. & Gilmore, R., 2006. An evolving view of the eukaryotic oligosaccharyltransferase. *Glycobiology*, 16(4), pp.47–62.

Knop, M. et al., 1999. Epitope tagging of yeast genes using a PCR-based strategy: more tags and improved practical routines. *Yeast (Chichester, England)*, 15(10B), pp.963–72.

Larrabee, K.L. et al., 1980. The relative rates of protein synthesis and degradation in a growing culture of Escherichia coli. *The Journal of biological chemistry*, 255(9), pp.4125–30.

Li, G. et al., 2003. A specific segment of the transmembrane domain of Wbp1p is essential for its incorporation into the oligosaccharyl transferase complex. *Biochemistry*, 42(37), pp.11032–11039.

Mohd Yusuf, S.N.H. et al., 2013. Mixed disulfide formation in vitro between a glycoprotein substrate and yeast oligosaccharyltransferase subunits Ost3p and Ost6p. *Biochemical and Biophysical Research Communications*, 432(3), pp.438–443.

Mohorko, E. et al., 2014. Structural basis of substrate specificity of human oligosaccharyl transferase subunit N33/Tusc3 and its role in regulating protein N-glycosylation. *Structure*, 22(4), pp.590–601.

Mueller, S. et al., 2015. Protein degradation corrects for imbalanced subunit stoichiometry in OST complex assembly. *Molecular Biology of the Cell*, 26(14), pp.2596–2608.

Nasab, F.P. et al., 2008. All in one: Leishmania major STT3 proteins substitute for the whole oligosaccharyltransferase complex in Saccharomyces cerevisiae. *Molecular biology of the cell*, 19(9), pp.3758–68.

Nilsson, I. et al., 2003. Photocross-linking of nascent chains to the STT3 subunit of the oligosaccharyltransferase complex. *The Journal of cell biology*, 161(4), pp.715–25.

Reiss, G. et al., 1997. A specific screen for oligosaccharyltransferase mutations identifies the 9 kDa OST5 protein required for optimal activity in vivo and in vitro. *The EMBO journal*, 16(6), pp.1164–72.

Roboti, P. & High, S., 2012. Keratinocyte-associated protein 2 is a bona fide subunit of the mammalian oligosaccharyltransferase. *Journal of Cell Science*, 125(1), pp.220–232.

Samuelson, J. et al., 2005. The diversity of dolichol-linked precursors to Asn-linked glycans likely results from secondary loss of sets of glycosyltransferases. *Proceedings of the National Academy of Sciences of the United States of America*, 102(5), pp.1548–53.

Schulz, B.L. et al., 2009. Oxidoreductase activity of oligosaccharyltransferase subunits Ost3p and Ost6p defines site-specific glycosylation efficiency. *Proceedings of the National Academy of Sciences of the United States of America*, 106(27), pp.11061–6.

Schulz, B.L. & Aebi, M., 2009. Analysis of glycosylation site occupancy reveals a role for Ost3p and Ost6p in site-specific N-glycosylation efficiency. *Molecular & cellular proteomics : MCP*, 8(18), pp.357–364.

Schwarz, M., Knauer, R. & Lehle, L., 2005. Yeast oligosaccharyltransferase consists of two functionally distinct sub-complexes, specified by either the Ost3p or Ost6p subunit. *FEBS Letters*, 579(29), pp.6564–6568.

Sikorski, R.S. & Hieter, P., 1989. A system of shuttle vectors and yeast host strains designed for efficient manipulation of DNA in Saccharomyces cerevisiae. *Genetics*, 122(1), pp.19–27.

Silberstein, S., 1995. The essential OST2 gene encodes the 16-kD subunit of the yeast oligosaccharyltransferase, a highly conserved protein expressed in diverse eukaryotic organisms. *The Journal of Cell Biology*, 131(2), pp.371–383.

Silberstein, S., Kelleher, D.J. & Gilmore, R., 1992. The 48-kDa subunit of the mammalian oligosaccharyltransferase complex is homologous to the essential yeast protein WBP1. *Journal of Biological Chemistry*, 267(33), pp.23658–23663.

te, H.S. et al., 1992. The yeast WBP1 is essential for oligosaccharyl transferase activity in vivo and in vitro. *The EMBO Journal*, 11(6), pp.2071–2075.

Wach, A. et al., 1994. New heterologous modules for classical or PCR-based gene disruptions in Saccharomyces cerevisiae. *Yeast (Chichester, England)*, 10(13), pp.1793–808.

Wacker, M., 2002. N-Linked Glycosylation in Campylobacter jejuni and Its Functional Transfer into E. coli. *Science*, 298(5599), pp.1790–1793.

Wilson, C.M. et al., 2011. DC2 and keratinocyte-associated protein 2 (KCP2), subunits of the oligosaccharyltransferase complex, are regulators of the a-secretase- directed processing of amyloid precursor protein (APP). *Journal of Biological Chemistry*, 286(36), pp.31080–31091.

Wilson, C.M. & High, S., 2007. Ribophorin I acts as a substrate-specific facilitator of N-glycosylation. *Journal of cell science*, 120(Pt 4), pp.648–657.

Wilson, C.M., Roebuck, Q. & High, S., 2008. Ribophorin I regulates substrate delivery to the oligosaccharyltransferase core. *Proceedings of the National Academy of Sciences of the United States of America*, 105(28), pp.9534–9.

Wiśniewski, J.R. et al., 2009. Universal sample preparation method for proteome analysis. *Nature methods*, 6(5), pp.359–62.

Yan, A. et al., 2003. New findings on interactions among the yeast oligosaccharyl transferase subunits using a chemical cross-linker. *The Journal of biological chemistry*, 278(35), pp.33078–87.

Yan, Q. & Lennarz, W.J., 2002. Studies on the function of oligosaccharyl transferase subunits. Stt3p is directly involved in the glycosylation process. *The Journal of biological chemistry*, 277(49), pp.47692–700.

Chapter 4b

Supplementary Information to Chapter 4

Supplementary Figure 1. Polypeptide sequence alignment of Wbp1p homologues from 23 organisms.

Strictly conserved residues are highlighted in red; other conserved residues are in red boxes.

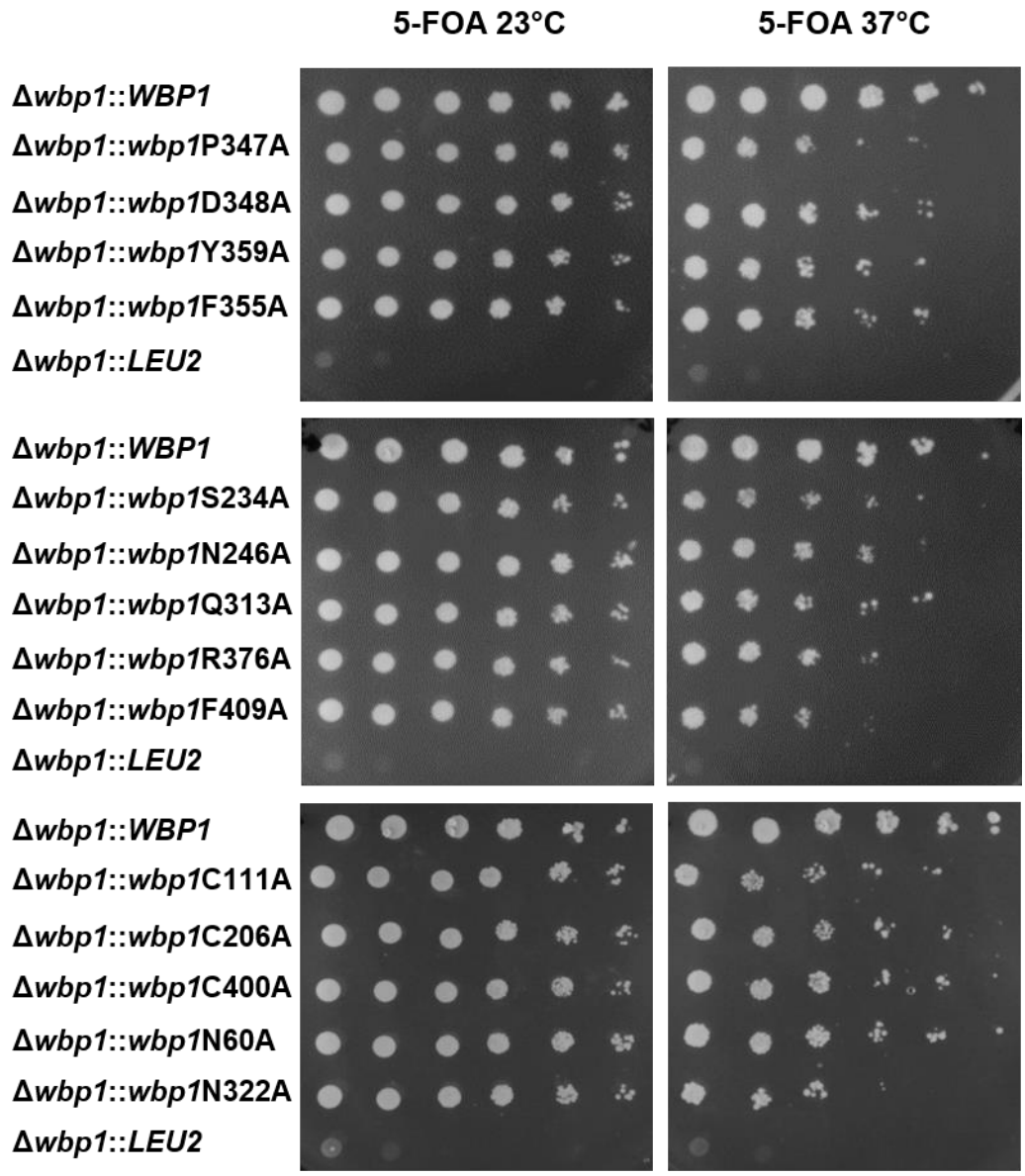

Supplementary Figure 2. 5-FOA spotting assay for the analysis of *wbp1* mutant growth phenotypes.

Yeast cells where the endogenous copy of *WBP1* locus was replaced with either the wild type, mutated *wbp1*, or *K. lactis LEU2* cassette were complemented by *URA3 LmSTT3D* expression plasmid. Serial dilutions of wild type and mutant cells were spotted on medium containing 5-FOA and incubated at 23^{o}C or 37^{o}C for five days. Mutations that inactivate the OST enzyme do not support the growth of the cells.

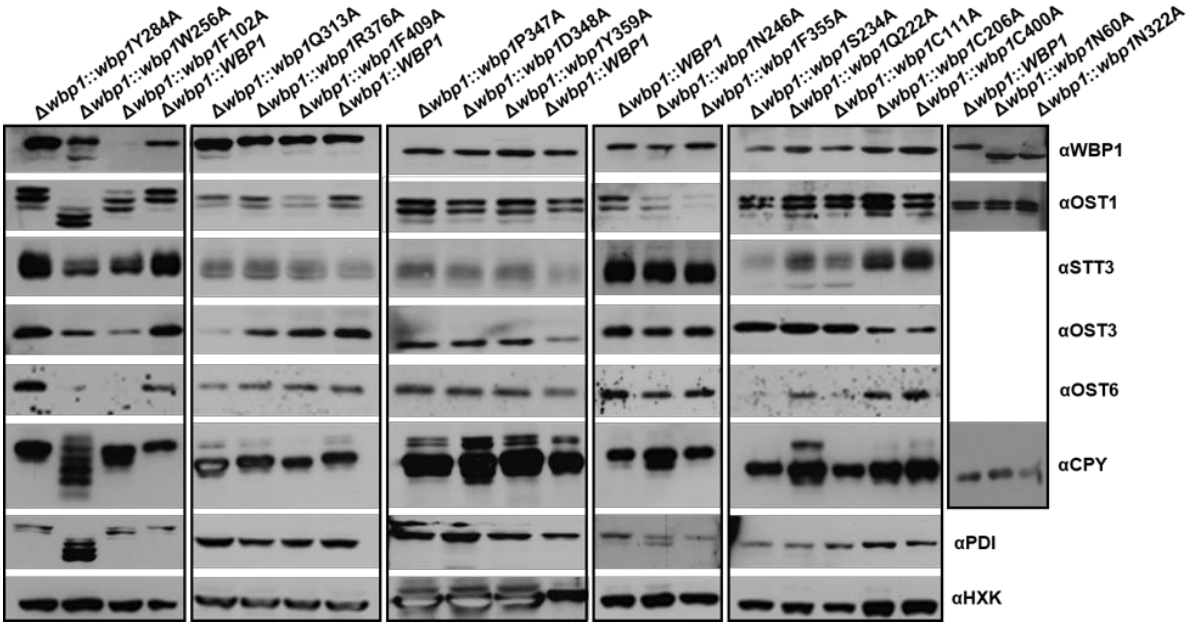

Supplementary Figure 3. Immunoblot analysis of *wbp1* mutants.

SDS extracts were prepared from mutant cells were the endogenous *WBP1* locus was replaced by either the wild type *WBP1* or different *wbp1* mutant loci. Equal amounts of protein were separated on a 10% SDS-PAGE gel and transferred to nitrocellulose membrane, followed by detection with specific antibodies. Hexokinase (HXK) was used as a loading control.

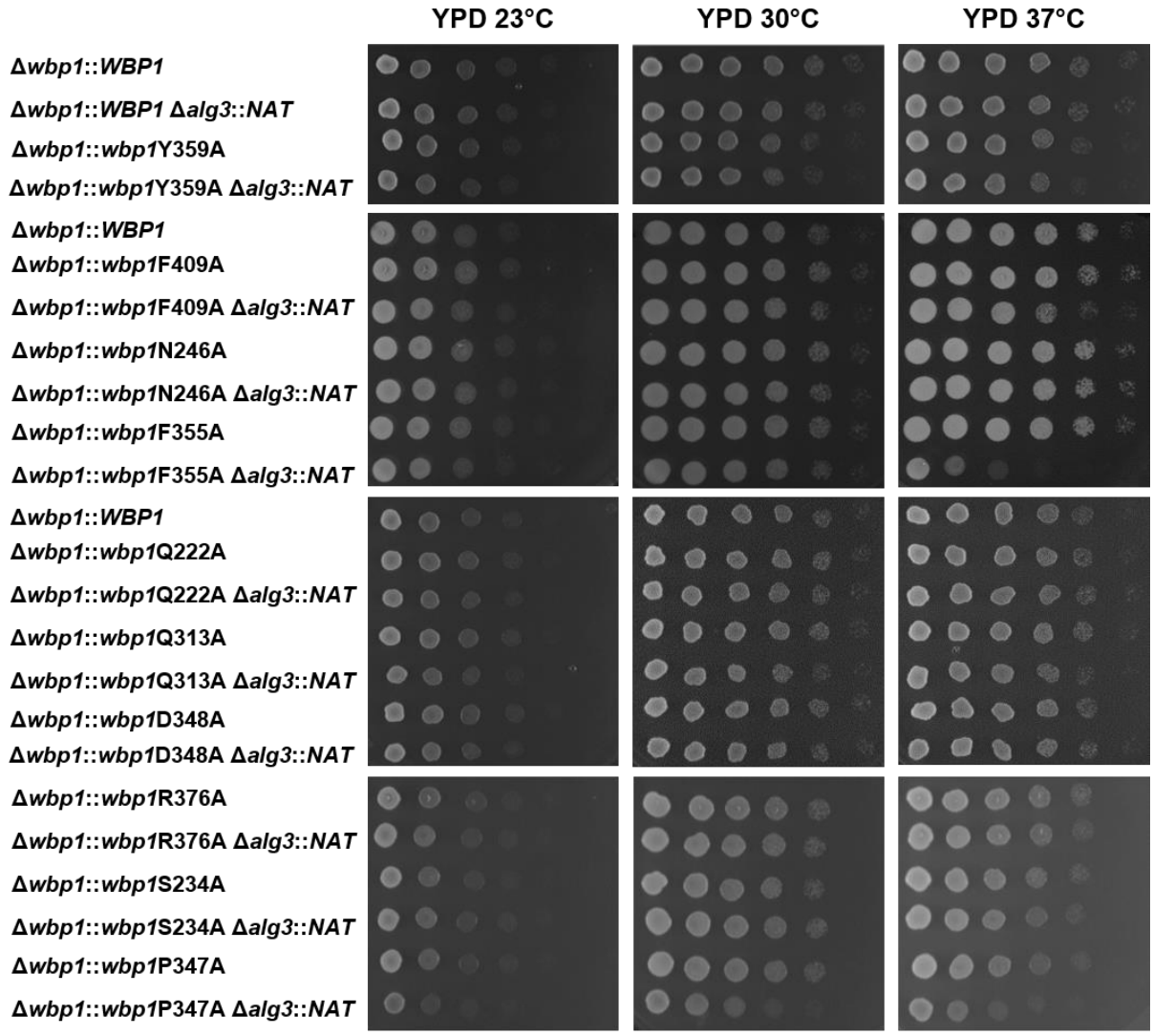

Supplementary Figure 4. YPD spotting assay for the analysis of *wbp1* mutant growth phenotypes.

Yeast wild type cells and cells where the endogenous copy of *WBP1* locus was replaced with different *wbp1* mutants carrying *URA3 LmSTT3D* expression plasmid were grown on medium containing 5-FOA and incubated at 23^{o}C for five days. Mutant cells that do not contain *LmSTT3D* plasmid were selected and *ALG3* loci was deleted using *NatNT2* cassette. Serial dilutions of the *wbp1* mutant cells with and without *ALG3* locus were spotted on YPD medium and incubated at 23^{o}C, 30^{o}C or 37^{o}C for one to two days.

Supplementary Table 1. Protein half-lives of OST subunit proteins in different *wbp1* mutant strains.

	wbp1-1	***wbp1-2***	**Δ*wbp1***	**W256A**	**Y284A**	**F102A**
Wbp1p	1.3 h	0.9 h	/	1.5 h	10.2 h	2.8 h
Ost2p	0.8 h	0.8 h	1.3 h	1.3 h	50 h	30 h
Swp1p	0.9 h	0.5 h	1 h	1.5 h	9.4 h	1.9 h
Ost1p	9 h	10.9 h	28.9 h	31.2 h	45.2 h	28.9 h
Ost5p	3.2 h	2.4 h	7.2 h	10.8 h	9.4 h	4.2 h
Stt3p	4.3 h	3.4 h	4.3 h	10.8 h	9.9 h	5 h
Ost3p	1.5 h	1.2 h	2.2 h	1.1 h	13.3 h	2.9 h
Ost6p	1.6 h	1.2 h	2.8 h	1.1 h	8.1 h	1.9 h

Supplementary Table 2. Relative glycosylation occupancy in different *wbp1* strains.

UniProtID	Protein Name	Glycosylation Site	Q222	S234	Q313	P347	D348	F355	Y359	R376	F409	N60	N322	C206
P00729	**CPY**	**N124**	N/A	**0.50**	1.04	1.01	N/A	N/A	0.96	**0.32**	N/A	0.94	0.84	0.80
P00729	**CPY**	**N479**	N/A	1.01	N/A	N/A	N/A	N/A	0.85	**0.74**	N/A	N/A	N/A	N/A
P12684	HMDH2	N150	N/A	1.04	N/A	0.89	N/A	0.96	0.88	N/A	N/A	0.91	N/A	N/A
P17967	PDI	N174	N/A	1.08	1.02	0.94	0.91	N/A	0.81	0.81	0.87	0.84	0.90	0.84
P17967	PDI	N425	0.96	0.88	0.82	1.01	0.96	0.68	0.99	0.82	0.88	0.99	0.89	0.88
P17967	PDI	N117	1.03	0.97	1.15	1.11	1.00	1.00	1.05	1.14	0.73	1.02	0.81	0.98
P17967	PDI	N155	1.11	0.87	0.85	0.97	0.97	0.78	0.93	1.05	1.06	0.95	0.92	0.91
P22146	GAS1	N40	0.97	0.96	0.97	0.92	1.04	0.89	0.94	0.87	1.15	0.91	0.99	0.90
P23797	GPI12	N110	1.00	0.94	0.95	0.97	0.92	0.84	1.14	0.96	0.86	0.92	0.85	0.83
P27810	KTR1	N120	0.84	0.95	0.85	0.91	1.05	0.91	0.98	0.83	0.99	0.99	1.02	1.04
P27825	CNE1	N416	0.91	0.88	N/A	N/A	0.98	0.04	1.15	0.81	1.02	0.90	0.79	N/A
P31382	PMT2	N403	1.10	0.98	0.87	0.87	1.02	0.77	0.97	1.09	0.99	0.89	0.99	1.00
P32353	**ERG3**	**N40**	0.99	0.95	0.80	0.81	1.02	**0.48**	0.81	0.94	1.10	0.94	1.07	0.83
P32623	**CRH2**	**N310**	0.98	0.93	0.92	0.92	0.78	**0.00**	0.79	0.79	0.91	0.98	0.78	1.05
P33302	PDR5	N734	0.99	0.97	N/A	N/A	0.89	N/A	0.97	1.00	0.78	0.78	0.87	N/A
P33754	SEC66	N12	0.94	0.99	0.83	0.96	0.97	0.76	0.84	0.80	1.04	0.90	0.91	0.88
P33767	**WBP1**	**N60**	1.09	**0.62**	N/A	**0.00**	N/A	N/A	0.81	1.81	0.89	**KO**	1.01	0.00
P33767	**WBP1**	**N322**	**0.05**	0.94	N/A	**0.01**	**0.10**	**0.19**	1.03	1.05	0.93	0.90	**KO**	0.80
P36016	LHS1	N458	0.86	0.79	0.92	1.08	0.86	0.82	0.81	0.81	0.79	1.02	0.81	0.95
P36051	MCD4	N198	N/A	0.73	N/A	0.88	0.69	N/A	N/A	N/A	0.75	0.89	0.84	N/A
P36051	MCD4	N90	N/A	1.03	1.00	1.01	0.96	0.91	1.05	1.04	1.08	0.97	1.05	0.95
P36091	DCW1	N203	0.93	1.05		0.96	0.81	0.83	0.79	0.90	0.97	0.84	0.83	0.75
P37302	APE3	N150	N/A	1.04	1.01	1.01	1.02	0.91	1.10	0.78	0.95	1.04	0.86	1.10
P37302	APE3	N96	N/A	1.07	1.01	1.07	1.11	0.91	1.06	0.85	1.05	1.04	0.93	1.05
P38244	PFF1	N121	0.92	1.03	1.04	1.01	0.89	1.02	1.03	0.97	0.97	1.07	1.07	0.93
P38248	ECM33	N304	1.00	1.00	0.95	0.95	1.04	0.89	0.97	0.92	1.03	0.90	1.00	0.98
P38875	GPI16	N184	0.98	0.82	0.98	0.83	0.99	0.87	0.95	1.14	0.98	0.92	1.07	0.81
P38993	FET3	N244	0.90	1.01	0.84	N/A	1.03	1.00	0.77	N/A	1.03	N/A	0.91	0.95
P38993	FET3	N359	0.82	1.03	0.99	1.06	1.06	N/A	0.91	N/A	1.06	1.02	1.01	0.80
P39007	STT3	N539	0.86	0.97	0.94	0.75	0.98	0.96	0.97	0.88	0.94	0.91	0.86	0.95
P39105	PLB1	N215	0.84	0.89	0.90	N/A	0.91	0.96	0.93	0.92	0.89	0.82	0.84	0.80
P39105	PLB1	N489	1.01	0.94	1.00	N/A	1.01	1.05	0.91	0.93	1.03	0.85	0.97	0.87
P40345	PDAT	N439	N/A	1.02	0.82	0.83	0.97	N/A	0.87	0.96	1.52	0.79	0.96	0.87
P40533	TED1	N266	N/A	0.98	0.90	0.77	1.03	N/A	1.03	1.02	0.74	0.79	0.97	0.89
P40557	EPS1	N299	1.00	0.99	N/A	0.77	0.84	N/A	0.88	1.03	0.85	0.95	1.01	N/A
P40557	EPS1	N264	0.95	1.03	0.80	0.82	0.86	0.80	0.87	0.81	0.99	1.00	1.01	0.83
P41543	OST1	N217	0.96	0.89	1.00	0.97	0.98	0.81	0.89	0.96	0.77	1.03	1.02	0.83
P43561	FET5	N24	0.98	0.94	0.89	1.04	0.83	N/A	0.90	0.93	0.67	0.80	0.89	N/A
P43561	FET5	N364	0.98	1.08	0.94	1.04	0.92	0.71	0.95	0.98	0.71	0.75	1.07	0.84
P46982	**MNN5**	**N136**	0.99	0.88	**0.46**	0.93	0.92	0.86	0.85	1.08	0.96	0.92	0.83	0.86
P46992	YJR1	N219	1.07	1.00	0.88	1.02	1.04	0.82	1.02	1.03	0.95	1.00	0.95	0.94
P52911	EXG2	N50	N/A	0.89	0.80	0.91	0.91	0.77	N/A	N/A	0.90	0.76	0.92	0.84
P52911	EXG2	N157	N/A	1.01	0.84	0.86	1.06	0.89	N/A	N/A	N/A	0.76	0.92	0.93
P53379	MKC7	N286	0.82	1.06	0.82	0.89	0.94	N/A	0.87	1.00	0.93	0.80	1.03	1.02
P54003	SUR7	N47	0.93	0.95	0.98	1.06	0.92	0.84	0.87	1.04	0.93	0.97	0.92	0.91
Q03103	**ERO1**	**N458**	**0.00**	**0.65**	**0.56**	**0.20**	**0.47**	**0.00**	**0.37**	**0.00**	**0.00**	0.82	**0.06**	0.96
Q03281	HEH2	N520	0.73	0.97	N/A	0.83	0.84	0.71	1.00	0.84	0.81	0.84	0.83	1.10
Q03674	PLB2	N217	1.01	0.98	N/A	N/A	1.04	0.82	0.55	0.43	N/A	1.06	0.99	1.00
Q03674	PLB2	N193	0.99	0.92	N/A	N/A	N/A	N/A	0.99	0.96	1.15	0.92	0.98	1.03
Q03691	ROT1	N139	1.04	0.99	0.83	0.94	1.10	0.81	1.00	1.08	0.90	0.94	1.01	0.91
Q06689	YL413	N429	0.82	1.06	1.05	0.98	1.01	1.07	1.00	0.97	0.96	0.98	0.91	0.95
Q07830	GPI13	N411	1.13	1.01	1.01	0.97	1.00	0.83	0.97	0.86	0.95	0.94	0.96	1.09
Q12465	RAX2	N640	N/A	0.88	0.78	0.87	N/A	N/A	1.09	0.86	0.94	0.87	N/A	0.84

N/A, not determined.

Supplementary Table 3. Plasmids used in this study. Related to Materials and Methods.

Name	Gene	Marker	Souce
pLmSTT3D	*LmSTT3D*	URA3	(Nasab, Benjamin L Schulz, et al. 2008)
pUG6	*loxP-KanMX4-loxP*	AmpR	(Güldener et al. 1996)
pSH47	Cre recombinase	URA3	(Güldener et al. 1996)
pUG73	*K.lactis LEU2*	LEU2	(Gueldener et al. 2002)
pFA6-KanMX4	*KanMX4*	AmpR	(Wach et al. 1994)
pRS313		HIS3, AmpR	(Sikorski & Hieter 1989)
pWBP1	*WBP1*	HIS3, KanMX	This study
pWBP1/wbp1-1	*wbp1-1*	HIS3, KanMX	This study
pWBP1/wbp1-2	*wbp1-2*	HIS3, KanMX	This study
pWBP1/wbp1-F102A	*wbp1-F102A*	HIS3, KanMX	This study
pWBP1/wbp1-S234A	*wbp1-S234A*	HIS3, KanMX	This study
pWBP1/wbp1- W256A	*wbp1-F* W256*A*	HIS3, KanMX	This study
pWBP1/wbp1- Q313A	*wbp1*- Q313*A*	HIS3, KanMX	This study
pWBP1/wbp1- P347A	*wbp1*- P347*A*	HIS3, KanMX	This study
pWBP1/wbp1- D348A	*wbp1*- D348*A*	HIS3, KanMX	This study
pWBP1/wbp1- F355A	*wbp1*- F355*A*	HIS3, KanMX	This study
pWBP1/wbp1- Y359A	*wbp1*- Y359*A*	HIS3, KanMX	This study
pWBP1/wbp1- R376A	*wbp1*- R376*A*	HIS3, KanMX	This study
pWBP1/wbp1- F409A	*wbp1*- F409*A*	HIS3, KanMX	This study

Supplementary Table 4. Strains used in this study. Related to Materials and Methods.

Name	Genotype	Source
BY4742	*MATα his3Δ1 leu2Δ0 lys2Δ0 ura3Δ0 arg4Δ0*	Euroscarf
KP4	*MATα his3Δ1 leu2Δ0 lys2Δ0 ura3Δ0 arg4Δ0*	This study
KP5	*MATα his3Δ1 leu2Δ0 lys2Δ0 ura3Δ0 arg4Δ0 pLmSTT3D*	This study
KP8	*MATα his3Δ1 leu2Δ0 lys2Δ0 ura3Δ0 arg4Δ0 Δwbp1::LEU2 pLmSTT3D*	This study
KP8-0	*MATα his3Δ1 leu2Δ0 lys2Δ0 ura3Δ0 arg4Δ0 Δwbp1::wbp1-KanMX pLmSTT3D*	This study
KP8-wbp1-1	*MATα his3Δ1 leu2Δ0 lys2Δ0 ura3Δ0 arg4Δ0 Δwbp1::wbp1-R228Y-KanMX pLmSTT3D*	This study
KP8-wbp1-2	*MATα his3Δ1 leu2Δ0 lys2Δ0 ura3Δ0 arg4Δ0 Δwbp1::wbp1-F249S,S297L-KanMX pLmSTT3D*	This study
KP8/wbp1-F102A	*MATα his3Δ1 leu2Δ0 lys2Δ0 ura3Δ0 arg4Δ0 Δwbp1::wbp1-F102A-KanMX pLmSTT3D*	This study
KP8/wbp1-S234A	*MATα his3Δ1 leu2Δ0 lys2Δ0 ura3Δ0 arg4Δ0 Δwbp1::wbp1-* S234*A-KanMX pLmSTT3D*	This study
KP8/wbp1-N246A	*MATα his3Δ1 leu2Δ0 lys2Δ0 ura3Δ0 arg4Δ0 Δwbp1::wbp1-* N246*A-KanMX pLmSTT3D*	This study
KP8/wbp1-W256A	*MATα his3Δ1 leu2Δ0 lys2Δ0 ura3Δ0 arg4Δ0 Δwbp1::wbp1-* W256*A-KanMX pLmSTT3D*	This study
KP8/wbp1-Q313A	*MATα his3Δ1 leu2Δ0 lys2Δ0 ura3Δ0 arg4Δ0 Δwbp1::wbp1-* Q313*A-KanMX pLmSTT3D*	This study
KP8/wbp1-P347A	*MATα his3Δ1 leu2Δ0 lys2Δ0 ura3Δ0 arg4Δ0 Δwbp1::wbp1-* P347*A-KanMX pLmSTT3D*	This study
KP8/wbp1-D348A	*MATα his3Δ1 leu2Δ0 lys2Δ0 ura3Δ0 arg4Δ0 Δwbp1::wbp1-* D348*A-KanMX pLmSTT3D*	This study
KP8/wbp1-F355A	*MATα his3Δ1 leu2Δ0 lys2Δ0 ura3Δ0 arg4Δ0 Δwbp1::wbp1-* F355*A-KanMX pLmSTT3D*	This study
KP8/wbp1-Y359A	*MATα his3Δ1 leu2Δ0 lys2Δ0 ura3Δ0 arg4Δ0 Δwbp1::wbp1-* Y359*A-KanMX pLmSTT3D*	This study
KP8/wbp1-R376A	*MATα his3Δ1 leu2Δ0 lys2Δ0 ura3Δ0 arg4Δ0 Δwbp1::wbp1-* R376*A-KanMX pLmSTT3D*	This study
KP8/wbp1-F409A	*MATα his3Δ1 leu2Δ0 lys2Δ0 ura3Δ0 arg4Δ0 Δwbp1::wbp1-* F409*A-KanMX pLmSTT3D*	This study
KP4 Δ*alg3*	*MATα his3Δ1 leu2Δ0 lys2Δ0 ura3Δ0 arg4Δ0 Δalg3::NatNT2*	This study
KP8/wbp1-1 Δ*alg3*	*MATα his3Δ1 leu2Δ0 lys2Δ0 ura3Δ0 arg4Δ0 Δwbp1::wbp1-R228Y-KanMX pLmSTT3D Δalg3::NatNT2*	This study
KP8/wbp1-2 Δ*alg3*	*MATα his3Δ1 leu2Δ0 lys2Δ0 ura3Δ0 arg4Δ0 Δwbp1::wbp1-F249S,S297L-KanMX pLmSTT3D Δalg3::NatNT2*	This study
KP8/wbp1-F102A Δ*alg3*	*MATα his3Δ1 leu2Δ0 lys2Δ0 ura3Δ0 arg4Δ0 Δwbp1::wbp1-F102A-KanMX pLmSTT3D Δalg3::NatNT2*	This study
KP8/wbp1-S234A Δ*alg3*	*MATα his3Δ1 leu2Δ0 lys2Δ0 ura3Δ0 arg4Δ0 Δwbp1::wbp1-* S234*A-KanMX pLmSTT3D Δalg3::NatNT2*	This study
KP8/wbp1-W256A Δ*alg3*	*MATα his3Δ1 leu2Δ0 lys2Δ0 ura3Δ0 arg4Δ0 Δwbp1::wbp1-* W256*A-KanMX pLmSTT3D Δalg3::NatNT2*	This study
KP8/wbp1-Q313A Δ*alg3*	*MATα his3Δ1 leu2Δ0 lys2Δ0 ura3Δ0 arg4Δ0 Δwbp1::wbp1-* Q313*A-KanMX pLmSTT3D Δalg3::NatNT2*	This study
KP8/wbp1-P347A Δ*alg3*	*MATα his3Δ1 leu2Δ0 lys2Δ0 ura3Δ0 arg4Δ0 Δwbp1::wbp1-* P347*A-KanMX pLmSTT3D Δalg3::NatNT2*	This study

KP8/wbp1-D348A Δ*alg3*	*MATα his3Δ1 leu2Δ0 lys2Δ0 ura3Δ0 arg4Δ0 Δwbp1::wbp1-* D348*A-KanMX pLmSTT3D Δalg3::NatNT2*	This study
KP8/wbp1-F355A Δ*alg3*	*MATα his3Δ1 leu2Δ0 lys2Δ0 ura3Δ0 arg4Δ0 Δwbp1::wbp1-* F355*A-KanMX pLmSTT3D Δalg3::NatNT2*	This study
KP8/wbp1-Y359A Δ*alg3*	*MATα his3Δ1 leu2Δ0 lys2Δ0 ura3Δ0 arg4Δ0 Δwbp1::wbp1-* Y359*A-KanMX pLmSTT3D Δalg3::NatNT2*	This study
KP8/wbp1-R376A Δ*alg3*	*MATα his3Δ1 leu2Δ0 lys2Δ0 ura3Δ0 arg4Δ0 Δwbp1::wbp1-* R376*A-KanMX pLmSTT3D Δalg3::NatNT2*	This study
KP8/wbp1-F409A Δ*alg3*	*MATα his3Δ1 leu2Δ0 lys2Δ0 ura3Δ0 arg4Δ0 Δwbp1::wbp1-* F409*A-KanMX pLmSTT3D Δalg3::NatNT2*	This study

Supplementary Table 5. Primers used in this study. Related to Materials and Methods.

Name	**Sequence**
A1 primer-arg-Kan	GAA GAG CTC AAA AGC AGG TAA CTA TAT AAC AAG ACT AAG GCA AAC CAG CTG AAG CTT CGT ACG C
A2 primer-arg-Kan	AAG TAC AGA CCT ATG AAA TTC TTG CGC ATA ACG TCG CCA TCT GGC ATA GGC CAC TAG TGG ATC TG
Kl-Leu2-Wbp1-Fw	TGA ATA CTT TAA CAC AAT TGA CGG TGC AAA TTT TGA ATT ATC CTT TTT TGA TGC TCG CTG TGA AGA TCC CAG CAA AG
Kl-Leu2-Wbp1-Rev	ATA TAA AAT CTA TTG CAG TAC TTA GTT TGG CAA AAA ATA TAA ATA GAT CCG CAG GCT AAC CGG AAC
P1-wbp1-pRS313_Fw	GGC CGC TCT AGA ACT AGT GGA TCC CCT TTA ACA CAA TTG ACG GTG C
P2-wbp1_Rev	AAC ACA ATC AGG TAC TCT TAT G
P3-Kan-wbp1-Fw	CTT TAT AAA TGG CTC ACA TAA ATA CAT AAG AGT ACC TGA TTG TGT TCT TCG TAC GCT GCA GGTC
P4-Kan-Wbp1_Rev	CCT CGA GGT CGA CGG TAT CGA TAA GCA TAT AAA ATC TAT TGC AGT ACT TAG TTT GGC AAA AAA TAT AAA TAC ACT GGA TGG CGG CGT TAG TAT CG
Wbp1 Fw Check	TGG CGG AGT AAG ATC TCT GG
Wbp1 Rev Check	GAT AGG TGG CGC ACT TGT TG
Wbp1-PC-Fw	CTT TAA CAC AAT TGA CGG TGC
Wbp1-PC-Rev	ATA TAA AAT CTA TTG CAG TAC TTA GTT TG
Wbp1-S297L-Fw	CTG TAG GCT TTT TGG AAT GGA ATG GAG AAG AAT GGC TAC C
Wbp1-S297L-Rev	AAT AAA TAA CTT TGT CCT TGA TTT TGT AG
Wbp1-F249S-Fw	AAA TCA GGA CTC TAA TCA GGA GTC TGC AAA AGA ATT ACT A
Wbp1-F249S-Rev	TTG TTC TTT AAG AAA TCA CTA CTG CCG ATC C
Wbp1-R228Y-Fw	TCC AGA ACT TAA ACA ATG CTT ATT TAG TAT GGA TCG GCA GTA G
Wbp1-R228Y-Rev	AAC CAA CTA CAA GAA AGC CTT GAG
Wbp1-Q313A-Fw	CGC TGA TGA TAT CGC ATT TGA ACT AAG ACA AG
Wbp1-Q313A-Rev	ATA TGT GGT AGC CAT TCT TCT C
Wbp1-Q222A-Fw	CTT GTA GTT GGT TTC GCG AAC TTA AAC AAT GCT CG
Wbp1-Q222A-Rev	AAA GCC TTG AGA TCC GCT GGT C
Wbp1-N246A-Fw	CAA AAA TCA GGA CTC TGC TCA GGA GTT TGC AAA AG
Wbp1-N246A-Rev	TTC TTT AAG AAA TCA CTA CTG CCG

Wbp1-Y284A-Fw	GTT ATG ACG AAG AGC CCG CCA AAA TCA AGG AC
Wbp1-Y284A-Rev	TAG TAC CAT CCG CAT GTG
Wbp1-P347A-Fw	GTG AAT TCA TCC TTG CAG ACC GCC ATG GAG TG
Wbp1-P347A-Rev	CGG TGG TGT AAT ACT GAG TTT C
Wbp1-D348A-Fw	GTG AAT TCA TCC TTC CAG CCC GCC ATG GAG TGT TTA C
Wbp1-D348A-Rev	CGG TGG TGT AAT ACT GAG
Wbp1-Y359A-Fw	GTT TAC ATT CCT CAC TGA CGC TCG TAA GAT TGG CCT GTC GTT C
Wbp1-Y359A-Rev	ACT CCA TGG CGG TCT GGA AG
Wbp1-F102A-Fw	GCA GTT GAT TAA AGC TTT TGA AAA TGA AG
Wbp1-F102A-Rev	TTA ACT GGG ATT TGT CTC GC
Wbp1-F409A_Fw	GTT GCG TGG ATA TTT GCT GTT GTT TCT TTC GTT ACG ACT TCC TC
Wbp1-F409A-Rev	AAT GAC GCC ACA AAT GGC
Wbp1-S234A_Fw	GTT TAG TAT GGA TCG GCG CTA GTG ATT TCT TAA AGA AC
Wbp1-S234A-Rev	GAG CAT TGT TTA AGT TCT GG
Wbp1-W256A_Fw	CAA AAG AAT TAC TAA AAG CGA CAT TTA ATG AAA AAT C
Wbp1-W256A-Rev	CAA ACT CCT GAT TAG AGT CCT G
Wbp1-F355A_Fw	CAT GGA GTG TTT ACA GCC CTC ACT GAC TAT CGT AAG
Wbp1-F355A-Rev	GCG GTC TGG AAG GAT GAA TTC AC
Wbp1-R376A_Fw	GAC GTT AAA GCT ATC GCT CAC CTT GCT AAT GAT GAA TAC C
Wbp1-R376A-Rev	TTT GTC AGT AGT GAA CGA CAG GCC AAT C
Wbp1-N332A-Fw	GTC GCC AAG CGG AGC CGA TTC TGA AAC TC
Wbp1-N332A-Rev	AAT GTT AGA CGG TAG TAC GGA TCC ACT TG
Wbp1-N60A-Fw	GAA TAT TTA GAT ATT GCC AGT ACT TCC AC
Wbp1-N60A-Rev	AAG TTT GTA ATT CCT TTG TTC
P1-alg3-NAT-Fw	GGA GTG AAA ACA GTA TCA TAG AGT GTG TAT GGG AGA GAG AAA GAG TTA GAT ACT AGT AGT TGC AGC GAC ATG GAG GCC CAG AAT AC
P2-alg3-NAT-Rev	ATA GAT GGT ATA AAG AAA TGA TTT AAA ACA ATA CGA TTA TAT GAT ATT TAT ACA TCT GTT CGG TAT TTC ACA CCG CAC AGG TGT TGT C

Supplementary Table 6. Antibodies used in this study. Related to Materials and Methods.

Name	Production species	Source	Dilution
α-CPY	mouse	Invitrogen	1:1000
α-PDI	rabbit	J. Winther	1:5000
α-Wbp1	rabbit	(te Heesen et al. 1991)	1:1000
α-Ost1	rabbit	R. Gilmore	1:1000
α-Stt3	rabbit	Yoshida	1:1000
α-Ost3	rabbit	own stock	1:1000
α-Ost6	rabbit	R. Knauer and L. Lehle	1:1000
α-Swp1	rabbit	own stock	1:1000
α-HXK	rabbit	Rockland Immunochemicals Inc.	1:3000
α-mouse-IgG-HRP	goat	Santa Cruz Biotechnology	1:10000
α-rabbit-IgG-HRP	goat	Santa Cruz Biotechnology	1:10000

Chapter 5

Concluding Remarks
&
Future Perspectives

Concluding remarks and future perspectives

N-linked glycosylation is an essential, omnipresent modification of proteins that adds an additional level of biological information to polypeptides, not present on the genomic level (Cummings 2009). The glycans attached to proteins have distinct roles; they contribute in protein folding, quality control, stability and solubility, they mediate interaction between cells, and can be involved in modulating immune responses (Helenius 2001; Helenius & Aebi 2004). Although glycans are the most versatile and elaborate protein modification, occurring through the extensive and diverse remodelling by numerous enzymes in the Golgi, the preceding transfer of the glycan onto a protein in the ER is highly consistent and conserved among all three domains of life (Samuelson et al. 2005). The remarkable extent of conservation among eukaryotic organisms allows investigating basic principles of N-linked protein glycosylation in the model organism *Saccharomyces cerevisiae*. The basic mechanism of glycan transfer involves the assembly of the glycan on isoprenoid lipid carrier followed by the *en bloc* transfer of the glycan to an asparagine side chain within signature N-X-S/T sequon on the substrate protein (Breitling & Aebi 2013). Due to the conservancy between yeast and human pathways, discoveries from yeast were used to characterize the cause of congenital disorders of glycosylation (CDGs) associated with the pathway defects in humans (Freeze 2006; Haeuptle & Hennet 2009). On the other hand, high homology of the central enzyme involved in the glycan transfer, the oligosaccharyltransferase (OST), helps in elucidating its function. Fungal, mammalian and plant OSTs are multi-subunit complexes located at the ER membrane, where both attributes restrict their enzymatic and structural characterization. Nonetheless, Stt3p was identified as a catalytic subunit and based on the crystal structure of its bacterial homologue PglB, the mechanism of the glycosylation reaction has been proposed (Lizak et al. 2013). Apart from the assistance in site-specific glycosylation by the non-essential, isoform defining Ost3 and Ost6 subunits, the roles of the remaining complex subunits are still only poorly understood.

The main objective of this thesis was the *in vivo* study of the activity of OSTs from yeast *Saccharomyces cerevisiae* and *Trypanosoma brucei*. The *in vivo* study of the OST activity has largely relied on the immunoblot analysis of a small number of known OST substrates, such as carboxypeptidase CPY. Although a valid approach for the analysis of a systemic impact of the alternations in the N-linked glycosylation of proteins, this method is highly disadvantageous when one wants to examine glycoproteins for which there is no appropriate antiserum available and/or wants to gain qualitative statements about glycosylation at individual sites. Furthermore, as recent studies have demonstrated that Ost3/6p subunits have specifically affected glycosylation on subset of protein substrates, new methods that can follow glycosylation of a wide range of substrates had to be developed (Schulz & Aebi 2009). For this purpose mass spectrometry proved to be a useful tool for measuring N-linked

glycosylation site occupancy in yeast (Schulz et al. 2009; Xu et al. 2015; Yeo et al. 2016; Zacchi & BL. Schulz 2016).

One of the crucial accomplishments described in this thesis is a novel method for the identification and relative quantification of glycosylation site occupancy and the abundance of glycoproteins, described in the second chapter. We have used parallel reaction monitoring (PRM), a novel mass spectrometric technique, in combination with stable isotope labelling (SILAC) to study OST activity *in vivo* on a wide range of polypeptide substrates. As opposed to previous studies, we analysed membrane and lumenal proteins that eliminated the analytical bias present in the complementary approaches that allowed us to monitor all of the OST glycoproteins (Wbp1p, Ost1p and Stt3p) as well as model glycoproteins, CPY and Pdi1. We have successfully used this technique to investigate protein substrate specificities of Ost3 and Ost6 subunits, as well as site-specific polypeptide preference of different OSTs from *S. cerevisiae* and *T. brucei*. As the study of multi-subunit OST complexes is challenging due to their complicated organisation and presence of different isoforms, the discovery of single-subunit OSTs homologous to *STT3* in protozoan organisms that can functionally replace the yeast OST complex, allowed for an easier investigation of basic mechanisms of eukaryotic N-linked glycosylation (Castro et al. 2006; Nasab, Benjamin L Schulz, et al. 2008; Hese et al. 2009; Izquierdo et al. 2009). Yeast as a model organism where yeast genetics can be easily applied to modify endogenous N-linked glycosylation pathway and distinct OSTs expressed, offers an excellent system to address basic questions regarding the pathway in eukaryotes.

Using SILAC strategy combined with PRM, we examined the influence of the suboptimal LLO donor substrate on the glycosylation efficiency of the yeast endogenous OST, described in the second chapter. Previous kinetic studies of single and multi-subunit OSTs have revealed that LLO structure-mediated effect on polypeptide substrate binding affinity is a conserved property of the eukaryotic OSTs that can be assigned to the STT3 active site (Kelleher et al. 2007). We have demonstrated that the polypeptide binding affinity of OST is influenced by the suboptimal LLO donor substrate. These results were in agreement with previous results showing that LLO binding induces conformational changes in the active site where the more complex LLOs promote stronger interaction of the polypeptide substrate with the enzyme (Breuer & Bause 1995; Gibbs & Coward 1999; Karaoglu et al. 2001).

Combining yeast genetics with different analytical methods in the third chapter allowed for detailed analysis of LLO specificity of different single subunit OSTs from *T. brucei* paralogues (*Tb*STT3A, *Tb*STT3B and *Tb*STT3C, respectively). In short, *Tb*STT3B and *Tb*STT3C preferred more complex LLO substrates, while *Tb*STT3A preferred LLOs lacking c-branch mannose residues. Furthermore, structure to function analysis identified regions responsible for the preference of *Tb*STT3s towards specific LLO substrates. This approach was further used in combination with SILAC PRM method to identify polypeptide

preferences of distinct *Tb*STT3 paralogues showing that *Tb*STT3A and *Tb*STT3C have similar preference for acidic polypeptides, as in agreement with previous observations (Izquierdo et al. 2009). A specific region, termed region 1, was identified which influenced the preference of *Tb*STT3s towards the polypeptide substrates. Sequence comparison indicated that this region is homologous to the external loop 5 (EL5), known to interact with the polypeptide substrate in bacterial *STT3* homologue *PglB* (Lizak et al. 2011). Therefore, we speculate that region 1, identified in the eukaryotic STT3s could be a functional equivalent to the EL5 described in PglB. Furthermore, considering the results brought in chapter two and three, it is interesting to postulate that it is the conformational change of region 1 that occurs upon binding of the LLO to the active site of the eukaryotic STT3, and in that way affects the polypeptide preference of eukaryotic OSTs, as EL5 has been proposed to be involved in the glycosylation mechanism of bacteria in the similar way (Lizak et al. 2011). More experimental work and crystal structures of eukaryotic OSTs will provide insights into the molecular basis of polypeptide specificity.

Enzyme kinetic experiments have revealed that higher eukaryotic OST complexes contain one single binding site for the polypeptide substrate while it binds the LLO donor substrate in a cooperative manner. This property is only present in multi-subunit OST complexes that are expressed in organisms that assemble Dol-PP-$GlcNAc_2Man_9Glc_3$ LLOs (Karaoglu et al. 2001; Daniel J Kelleher et al. 2003; Kelleher et al. 2007). A substrate activation model was suggested where the binding of the LLO donor substrate to the regulatory LLO binding site is a prerequisite for the binding of both the polypeptide substrate and second LLO donor substrate to the catalytic site (Karaoglu et al. 2001). Furthermore, as it has been shown that two mammalian isoforms, STT3A and STT3B respectively, have distinct catalytic site kinetics but not the regulatory site kinetic parameters, it has been suggested that the regulatory site is provided by one or more of the non-catalytic subunits (Daniel J Kelleher et al. 2003; Kelleher et al. 2007). Albeit the identity of such subunit(s) has not been described thus far.

The suboptimal LLOs are responsible for the reduced rate of oligosaccharide transfer to nascent polypeptides, resulting in hypoglycosylation of proteins. Furthermore, protein bound oligosaccharide assembly intermediates are less efficiently glucosylated by the UDP-glucose glycoprotein glucosyltransferase (UGGT) enzyme, resulting in the inefficient glycoprotein quality control in the ER (ERQC), protein misfolding and targeting for ER-associated degradation (ERAD) (Trimble et al. 1980; Helenius & Aebi 2004). This is eminently evident in human CDGs (Hennet 2012). Considering the consequences mentioned, it is not surprising that cells have evolved ways to ensure the transfer of the fully assembled donor substrate to the asparagine site chains of nascent polypeptides.

Although there are still many questions to be answered, the findings of this thesis contribute a part towards the understanding of the mechanisms of protein N-linked glycosylation.

References

Breitling, J. & Aebi, M., 2013. *N* -Linked Protein Glycosylation in the Endoplasmic Reticulum. *Cold Spring Harbor Perspectives in Biology*.

Breuer, W. & Bause, E., 1995. Oligosaccharyl transferase is a constitutive component of an oligomeric protein complex from pig liver endoplasmic reticulum. *European journal of biochemistry*, 228(3), pp.689–96.

Castro, O., Movsichoff, F. & Parodi, A.J., 2006. Preferential transfer of the complete glycan is determined by the oligosaccharyltransferase complex and not by the catalytic subunit. *Proceedings of the National Academy of Sciences of the United States of America*, 103(40), pp.14756–60.

Cummings, R.D., 2009. The repertoire of glycan determinants in the human glycome. *Molecular BioSystems*, 5(10), p.1087.

Freeze, H.H., 2006. Genetic defects in the human glycome. *Nature reviews. Genetics*, 7(7), pp.537–51.

Gibbs, B.S. & Coward, J.K., 1999. Dolichylpyrophosphate oligosaccharides: large-scale isolation and evaluation as oligosaccharyltransferase substrates. *Bioorganic & medicinal chemistry*, 7(3), pp.441–7.

Haeuptle, M.A. & Hennet, T., 2009. Congenital disorders of glycosylation: An update on defects affecting the biosynthesis of dolichol-linked oligosaccharides. *Human Mutation*, 30(12), pp.1628–1641.

Helenius, A., 2001. Intracellular Functions of N-Linked Glycans. *Science*, 291(5512), pp.2364–2369.

Helenius, A. & Aebi, M., 2004. Roles of N-linked glycans in the endoplasmic reticulum. *Annual review of biochemistry*, 73, pp.1019–49.

Hennet, T., 2012. Diseases of glycosylation beyond classical congenital disorders of glycosylation. *Biochimica et Biophysica Acta - General Subjects*, 1820(9), pp.1306–1317.

Hese, K. et al., 2009. The yeast oligosaccharyltransferase complex can be replaced by STT3 from Leishmania major. *Glycobiology*, 19(2), pp.160–171.

Izquierdo, L. et al., 2009. Distinct donor and acceptor specificities of Trypanosoma brucei oligosaccharyltransferases. *The EMBO journal*, 28(17), pp.2650–61.

Karaoglu, D., Kelleher, D.J. & Gilmore, R., 2001. Allosteric regulation provides a molecular mechanism for preferential utilization of the fully assembled dolichol-linked oligosaccharide by the yeast oligosaccharyltransferase. *Biochemistry*, 40(40), pp.12193–12206.

Kelleher, D.J. et al., 2007. Dolichol-linked oligosaccharide selection by the oligosaccharyltransferase in protist and fungal organisms. *Journal of Cell Biology*, 177(1), pp.29–37.

Kelleher, D.J. et al., 2003. Oligosaccharyltransferase isoforms that contain different catalytic STT3 subunits have distinct enzymatic properties. *Molecular cell*, 12(1), pp.101–11.

Lizak, C. et al., 2013. Unexpected reactivity and mechanism of carboxamide activation in bacterial N-linked protein glycosylation. *Nature communications*, 4, p.2627.

Lizak, C. et al., 2011. X-ray structure of a bacterial oligosaccharyltransferase. *Nature*, 474(7351), pp.350–355.

Nasab, F.P. et al., 2008. All in one: Leishmania major STT3 proteins substitute for the whole oligosaccharyltransferase complex in Saccharomyces cerevisiae. *Molecular biology of the cell*, 19(9), pp.3758–68.

Samuelson, J. et al., 2005. The diversity of dolichol-linked precursors to Asn-linked glycans likely results from secondary loss of sets of glycosyltransferases. *Proceedings of the National Academy of Sciences of the United States of America*, 102(5), pp.1548–53.

Schulz, B.L. et al., 2009. Oxidoreductase activity of oligosaccharyltransferase subunits Ost3p and Ost6p defines site-specific glycosylation efficiency. *Proceedings of the National Academy of Sciences of the United States of America*, 106(27), pp.11061–6.

Schulz, B.L. & Aebi, M., 2009. Analysis of glycosylation site occupancy reveals a role for Ost3p and Ost6p in site-specific N-glycosylation efficiency. *Molecular & cellular proteomics : MCP*, 8(18), pp.357–364.

Trimble, R.B., Byrd, J.C. & Maley, F., 1980. Effect of glucosylation of lipid intermediates on oligosaccharide transfer in solubilized microsomes from Saccharomyces cerevisiae. *The Journal of biological chemistry*, 255(24), pp.11892–5.

Xu, Y., Bailey, U.M. & Schulz, B.L., 2015. Automated measurement of site-specific N-glycosylation occupancy with SWATH-MS. *Proteomics*, 15(13), pp.2177–2186.

Yeo, K.Y.B. et al., 2016. High-performance targeted mass spectrometry with precision data-independent acquisition reveals site-specific glycosylation macroheterogeneity. *Analytical Biochemistry*, 510, pp.106–113.

Zacchi, L. & Schulz, B.L., 2016. SWATH-MS glycoproteomics reveals consequences of defects in the glycosylation machinery. *Molecular & Cellular Proteomics*, 15, pp.2435–2447.

Appendix

Appendix Table 1. PRM MS assay for quantitative profiling of N-linked glycosylation machinery in yeast.

PRM assay; R=30000

UniProt ID	Protein	Peptide Modified Sequence	Precursor Charge	Isotope Label Type	Precursor Mz	Fragment Ion	Fragment Mz	Normalized Retention Time
P236321	Rpl5	VFLDIGLQR	2	light	530.811116	y8	961.546542	63.23
P236321	Rpl5	VFLDIGLQR	2	light	530.811116	y7	814.478128	63.23
P236321	Rpl5	VFLDIGLQR	2	light	530.811116	y6	701.394064	63.23
P236321	Rpl5	VFLDIGLQR	2	light	530.811116	y5	586.367121	63.23
P236321	Rpl5	VFLDIGLQR	2	light	530.811116	y4	473.283057	63.23
P236321	Rpl5	VFLDIGLQR	2	light	530.811116	b4	475.255111	63.23
P236321	Rpl5	VFLDIGLQR	2	heavy	533.821181	y8	967.566671	63.23
P236321	Rpl5	VFLDIGLQR	2	heavy	533.821181	y7	820.498257	63.23
P236321	Rpl5	VFLDIGLQR	2	heavy	533.821181	y6	707.414193	63.23
P236321	Rpl5	VFLDIGLQR	2	heavy	533.821181	y5	592.38725	63.23
P236321	Rpl5	VFLDIGLQR	2	heavy	533.821181	y4	479.303186	63.23
P236321	Rpl5	VFLDIGLQR	2	heavy	533.821181	b4	475.255111	63.23
P236321	Rpl5	FPGWDFETEEIDPELLR	2	light	1046.99675	y11	1343.6689	115.69
P236321	Rpl5	FPGWDFETEEIDPELLR	2	light	1046.99675	y10	1214.62631	115.69
P236321	Rpl5	FPGWDFETEEIDPELLR	2	light	1046.99675	y5	627.382437	115.69
P236321	Rpl5	FPGWDFETEEIDPELLR	2	light	1046.99675	y3	401.28708	115.69
P236321	Rpl5	FPGWDFETEEIDPELLR	2	light	1046.99675	b3	302.149918	115.69
P236321	Rpl5	FPGWDFETEEIDPELLR	2	light	1046.99675	b5	603.256174	115.69
P236321	Rpl5	FPGWDFETEEIDPELLR	2	heavy	1050.00681	y11	1349.68903	115.69
P236321	Rpl5	FPGWDFETEEIDPELLR	2	heavy	1050.00681	y10	1220.64644	115.69
P236321	Rpl5	FPGWDFETEEIDPELLR	2	heavy	1050.00681	y5	633.402566	115.69
P236321	Rpl5	FPGWDFETEEIDPELLR	2	heavy	1050.00681	y3	407.307209	115.69
P236321	Rpl5	FPGWDFETEEIDPELLR	2	heavy	1050.00681	b3	302.149918	115.69
P236321	Rpl5	FPGWDFETEEIDPELLR	2	heavy	1050.00681	b5	603.256174	115.69
P33442	Rps1a	VISEILTK	2	light	451.781493	y7	803.487296	21.09
P33442	Rps1a	VISEILTK	2	light	451.781493	y6	690.403232	21.09
P33442	Rps1a	VISEILTK	2	light	451.781493	y4	474.32861	21.09
P33442	Rps1a	VISEILTK	2	light	451.781493	y3	361.244546	21.09
P33442	Rps1a	VISEILTK	2	light	451.781493	y2	248.160482	21.09
P33442	Rps1a	VISEILTK	2	light	451.781493	b4	215.120826	21.09
P33442	Rps1a	VISEILTK	2	heavy	455.788592	y7	811.501495	21.09
P33442	Rps1a	VISEILTK	2	heavy	455.788592	y6	698.417431	21.09
P33442	Rps1a	VISEILTK	2	heavy	455.788592	y4	482.342809	21.09
P33442	Rps1a	VISEILTK	2	heavy	455.788592	y3	369.258745	21.09
P33442	Rps1a	VISEILTK	2	heavy	455.788592	y2	256.174681	21.09
P33442	Rps1a	VISEILTK	2	heavy	455.788592	b4	215.120826	21.09
P33442	Rps1a	EVQGSTLAQLTSK	2	light	681.367181	y11	1133.61608	21.82
P33442	Rps1a	EVQGSTLAQLTSK	2	light	681.367181	y10	1005.5575	21.82
P33442	Rps1a	EVQGSTLAQLTSK	2	light	681.367181	y9	948.536037	21.82
P33442	Rps1a	EVQGSTLAQLTSK	2	light	681.367181	y8	861.504009	21.82
P33442	Rps1a	EVQGSTLAQLTSK	2	light	681.367181	y7	760.45633	21.82
P33442	Rps1a	EVQGSTLAQLTSK	2	heavy	685.37428	y11	1141.63028	21.82
P33442	Rps1a	EVQGSTLAQLTSK	2	heavy	685.37428	y10	1013.5717	21.82
P33442	Rps1a	EVQGSTLAQLTSK	2	heavy	685.37428	y9	956.550236	21.82
P33442	Rps1a	EVQGSTLAQLTSK	2	heavy	685.37428	y8	869.518208	21.82
P33442	Rps1a	EVQGSTLAQLTSK	2	heavy	685.37428	y7	768.470529	21.82
P22146	GAS1	FFYSNN[+203.1]GSQFY	2	light	923.425758	y10	1388.64408	59.42
P22146	GAS1	FFYSNN[+203.1]GSQFY	2	light	923.425758	y9	1301.61206	59.42
P22146	GAS1	FFYSNN[+203.1]GSQFY	2	light	923.425758	y7	870.446828	59.42
P22146	GAS1	FFYSNN[+203.1]GSQFY	2	light	923.425758	y6	813.425364	59.42
P22146	GAS1	FFYSNN[+203.1]GSQFY	2	light	923.425758	y5	726.393336	59.42
P22146	GAS1	FFYSNN[+203.1]GSQFY	2	light	923.425758	y4	598.334758	59.42

P22146	GAS1	FFYSNN[+203.1]GSQFY	2	light	923.425758	y3	451.266344	59.42
P22146	GAS1	FFYSNN[+203.1]GSQFY	2	light	923.425758	b5	659.282388	59.42
P22146	GAS1	FFYSNN[+203.1]GSQFY	2	light	923.425758	b6	976.404689	59.42
P22146	GAS1	FFYSNN[+203.1]GSQFY	2	heavy	926.435823	y10	1394.66421	59.42
P22146	GAS1	FFYSNN[+203.1]GSQFY	2	heavy	926.435823	y9	1307.63219	59.42
P22146	GAS1	FFYSNN[+203.1]GSQFY	2	heavy	926.435823	y7	876.466957	59.42
P22146	GAS1	FFYSNN[+203.1]GSQFY	2	heavy	926.435823	y6	819.445493	59.42
P22146	GAS1	FFYSNN[+203.1]GSQFY	2	heavy	926.435823	y5	732.413465	59.42
P22146	GAS1	FFYSNN[+203.1]GSQFY	2	heavy	926.435823	y4	604.354887	59.42
P22146	GAS1	FFYSNN[+203.1]GSQFY	2	heavy	926.435823	y3	457.286473	59.42
P22146	GAS1	FFYSNN[+203.1]GSQFY	2	heavy	926.435823	b5	659.282388	59.42
P22146	GAS1	FFYSNN[+203.1]GSQFY	2	heavy	926.435823	b6	976.404689	59.42
P22146	GAS1	DDPTWTVDLFNSYK	2	light	850.89376	y10	1272.62592	99.55
P22146	GAS1	DDPTWTVDLFNSYK	2	light	850.89376	y9	1086.5466	99.55
P22146	GAS1	DDPTWTVDLFNSYK	2	light	850.89376	y8	985.498923	99.55
P22146	GAS1	DDPTWTVDLFNSYK	2	light	850.89376	y7	886.430509	99.55
P22146	GAS1	DDPTWTVDLFNSYK	2	light	850.89376	y6	771.403566	99.55
P22146	GAS1	DDPTWTVDLFNSYK	2	light	850.89376	y5	658.319502	99.55
P22146	GAS1	DDPTWTVDLFNSYK	2	light	850.89376	y4	511.251088	99.55
P22146	GAS1	DDPTWTVDLFNSYK	2	heavy	854.900859	y10	1280.64011	99.55
P22146	GAS1	DDPTWTVDLFNSYK	2	heavy	854.900859	y9	1094.5608	99.55
P22146	GAS1	DDPTWTVDLFNSYK	2	heavy	854.900859	y8	993.513122	99.55
P22146	GAS1	DDPTWTVDLFNSYK	2	heavy	854.900859	y7	894.444708	99.55
P22146	GAS1	DDPTWTVDLFNSYK	2	heavy	854.900859	y6	779.417765	99.55
P22146	GAS1	DDPTWTVDLFNSYK	2	heavy	854.900859	y5	666.333701	99.55
P22146	GAS1	DDPTWTVDLFNSYK	2	heavy	854.900859	y4	519.265287	99.55
P22146	GAS1	MTDYFAC[+57]GDDDVK	2	light	768.802699	y11	1304.50996	33.57
P22146	GAS1	MTDYFAC[+57]GDDDVK	2	light	768.802699	y10	1189.48302	33.57
P22146	GAS1	MTDYFAC[+57]GDDDVK	2	light	768.802699	y9	1026.41969	33.57
P22146	GAS1	MTDYFAC[+57]GDDDVK	2	light	768.802699	y8	879.351273	33.57
P22146	GAS1	MTDYFAC[+57]GDDDVK	2	light	768.802699	y7	808.314159	33.57
P22146	GAS1	MTDYFAC[+57]GDDDVK	2	light	768.802699	y6	648.283511	33.57
P22146	GAS1	MTDYFAC[+57]GDDDVK	2	light	768.802699	y5	591.262047	33.57
P22146	GAS1	MTDYFAC[+57]GDDDVK	2	light	768.802699	y4	476.235104	33.57
P22146	GAS1	MTDYFAC[+57]GDDDVK	2	heavy	772.809798	y11	1312.52416	33.57
P22146	GAS1	MTDYFAC[+57]GDDDVK	2	heavy	772.809798	y10	1197.49721	33.57
P22146	GAS1	MTDYFAC[+57]GDDDVK	2	heavy	772.809798	y9	1034.43389	33.57
P22146	GAS1	MTDYFAC[+57]GDDDVK	2	heavy	772.809798	y8	887.365472	33.57
P22146	GAS1	MTDYFAC[+57]GDDDVK	2	heavy	772.809798	y7	816.328358	33.57
P22146	GAS1	MTDYFAC[+57]GDDDVK	2	heavy	772.809798	y6	656.29771	33.57
P22146	GAS1	MTDYFAC[+57]GDDDVK	2	heavy	772.809798	y5	599.276246	33.57
P22146	GAS1	MTDYFAC[+57]GDDDVK	2	heavy	772.809798	y4	484.249303	33.57
P27810	KTR1	N[+203.1]VTSALVSGTTK	2	light	690.864471	y9	863.483273	4.33
P27810	KTR1	N[+203.1]VTSALVSGTTK	2	light	690.864471	y8	776.451245	4.33
P27810	KTR1	N[+203.1]VTSALVSGTTK	2	light	690.864471	y7	705.414131	4.33
P27810	KTR1	N[+203.1]VTSALVSGTTK	2	light	690.864471	y6	592.330067	4.33
P27810	KTR1	N[+203.1]VTSALVSGTTK	2	light	690.864471	y5	493.261653	4.33
P27810	KTR1	N[+203.1]VTSALVSGTTK	2	light	690.864471	y4	406.229624	4.33
P27810	KTR1	N[+203.1]VTSALVSGTTK	2	light	690.864471	b3	518.245669	4.33
P27810	KTR1	N[+203.1]VTSALVSGTTK	2	light	690.864471	b4	605.277697	4.33
P27810	KTR1	N[+203.1]VTSALVSGTTK	2	light	690.864471	b5	676.314811	4.33
P27810	KTR1	N[+203.1]VTSALVSGTTK	2	heavy	694.871571	y9	871.497472	4.33
P27810	KTR1	N[+203.1]VTSALVSGTTK	2	heavy	694.871571	y8	784.465444	4.33
P27810	KTR1	N[+203.1]VTSALVSGTTK	2	heavy	694.871571	y7	713.42833	4.33
P27810	KTR1	N[+203.1]VTSALVSGTTK	2	heavy	694.871571	y6	600.344266	4.33
P27810	KTR1	N[+203.1]VTSALVSGTTK	2	heavy	694.871571	y5	501.275852	4.33
P27810	KTR1	N[+203.1]VTSALVSGTTK	2	heavy	694.871571	y4	414.243823	4.33
P27810	KTR1	N[+203.1]VTSALVSGTTK	2	heavy	694.871571	b3	518.245669	4.33
P27810	KTR1	N[+203.1]VTSALVSGTTK	2	heavy	694.871571	b4	605.277697	4.33
P27810	KTR1	N[+203.1]VTSALVSGTTK	2	heavy	694.871571	b5	676.314811	4.33
P27810	KTR1	SPAYSAYFDYLDR	2	light	784.356813	y9	1149.52112	68.81
P27810	KTR1	SPAYSAYFDYLDR	2	light	784.356813	y8	1062.48909	68.81
P27810	KTR1	SPAYSAYFDYLDR	2	light	784.356813	y7	991.451973	68.81

P27810	KTR1	SPAYSAYFDYLDR	2	light	784.356813	y6	828.388644	68.81
P27810	KTR1	SPAYSAYFDYLDR	2	light	784.356813	y5	681.32023	68.81
P27810	KTR1	SPAYSAYFDYLDR	2	light	784.356813	y4	566.293287	68.81
P27810	KTR1	SPAYSAYFDYLDR	2	light	784.356813	y3	403.229959	68.81
P27810	KTR1	SPAYSAYFDYLDR	2	heavy	787.366877	y9	1155.54124	68.81
P27810	KTR1	SPAYSAYFDYLDR	2	heavy	787.366877	y8	1068.50922	68.81
P27810	KTR1	SPAYSAYFDYLDR	2	heavy	787.366877	y7	997.472102	68.81
P27810	KTR1	SPAYSAYFDYLDR	2	heavy	787.366877	y6	834.408773	68.81
P27810	KTR1	SPAYSAYFDYLDR	2	heavy	787.366877	y5	687.340359	68.81
P27810	KTR1	SPAYSAYFDYLDR	2	heavy	787.366877	y4	572.313416	68.81
P27810	KTR1	SPAYSAYFDYLDR	2	heavy	787.366877	y3	409.250088	68.81
P27810	KTR1	EHWSFPEWIDEEK	3	light	577.926493	y8	1045.48367	80.37
P27810	KTR1	EHWSFPEWIDEEK	3	light	577.926493	y7	948.430903	80.37
P27810	KTR1	EHWSFPEWIDEEK	3	light	577.926493	y6	819.38831	80.37
P27810	KTR1	EHWSFPEWIDEEK	3	light	577.926493	y5	633.308997	80.37
P27810	KTR1	EHWSFPEWIDEEK	3	light	577.926493	y4	520.224933	80.37
P27810	KTR1	EHWSFPEWIDEEK	3	light	577.926493	y3	405.19799	80.37
P27810	KTR1	EHWSFPEWIDEEK	3	heavy	580.597893	y8	1053.49787	80.37
P27810	KTR1	EHWSFPEWIDEEK	3	heavy	580.597893	y7	956.445102	80.37
P27810	KTR1	EHWSFPEWIDEEK	3	heavy	580.597893	y6	827.402509	80.37
P27810	KTR1	EHWSFPEWIDEEK	3	heavy	580.597893	y5	641.323196	80.37
P27810	KTR1	EHWSFPEWIDEEK	3	heavy	580.597893	y4	528.239132	80.37
P27810	KTR1	EHWSFPEWIDEEK	3	heavy	580.597893	y3	413.212189	80.37
P46982	MNN5	LN[+203.1]FSIPQR	2	light	589.31422	y6	747.4148	40.87
P46982	MNN5	LN[+203.1]FSIPQR	2	light	589.31422	y5	600.346386	40.87
P46982	MNN5	LN[+203.1]FSIPQR	2	light	589.31422	y4	513.314357	40.87
P46982	MNN5	LN[+203.1]FSIPQR	2	light	589.31422	y3	400.230293	40.87
P46982	MNN5	LN[+203.1]FSIPQR	2	heavy	592.324285	y6	753.434929	40.87
P46982	MNN5	LN[+203.1]FSIPQR	2	heavy	592.324285	y5	606.366515	40.87
P46982	MNN5	LN[+203.1]FSIPQR	2	heavy	592.324285	y4	519.334486	40.87
P46982	MNN5	LN[+203.1]FSIPQR	2	heavy	592.324285	y3	406.250422	40.87
P46982	MNN5	ADPWTLYHENR	2	light	701.330933	y7	932.458455	26.4
P46982	MNN5	ADPWTLYHENR	2	light	701.330933	y6	831.410777	26.4
P46982	MNN5	ADPWTLYHENR	2	light	701.330933	y5	718.326713	26.4
P46982	MNN5	ADPWTLYHENR	2	light	701.330933	y4	555.263384	26.4
P46982	MNN5	ADPWTLYHENR	2	light	701.330933	y9	608.298904	26.4
P46982	MNN5	ADPWTLYHENR	2	light	701.330933	b3	284.124097	26.4
P46982	MNN5	ADPWTLYHENR	2	light	701.330933	b8	492.732334	26.4
P46982	MNN5	ADPWTLYHENR	2	heavy	704.340997	y7	938.478584	26.4
P46982	MNN5	ADPWTLYHENR	2	heavy	704.340997	y6	837.430906	26.4
P46982	MNN5	ADPWTLYHENR	2	heavy	704.340997	y5	724.346842	26.4
P46982	MNN5	ADPWTLYHENR	2	heavy	704.340997	y4	561.283513	26.4
P46982	MNN5	ADPWTLYHENR	2	heavy	704.340997	y9	611.308969	26.4
P46982	MNN5	ADPWTLYHENR	2	heavy	704.340997	b3	284.124097	26.4
P46982	MNN5	ADPWTLYHENR	2	heavy	704.340997	b8	492.732334	26.4
P46982	MNN5	EALFSGSEGIVTIGGGK	2	light	811.425227	y13	1161.61099	69.23
P46982	MNN5	EALFSGSEGIVTIGGGK	2	light	811.425227	y12	1074.57896	69.23
P46982	MNN5	EALFSGSEGIVTIGGGK	2	light	811.425227	y10	930.525472	69.23
P46982	MNN5	EALFSGSEGIVTIGGGK	2	light	811.425227	y9	801.482879	69.23
P46982	MNN5	EALFSGSEGIVTIGGGK	2	light	811.425227	y7	631.377351	69.23
P46982	MNN5	EALFSGSEGIVTIGGGK	2	light	811.425227	y6	532.308937	69.23
P46982	MNN5	EALFSGSEGIVTIGGGK	2	light	811.425227	y5	431.261259	69.23
P46982	MNN5	EALFSGSEGIVTIGGGK	2	heavy	815.432326	y13	1169.62519	69.23
P46982	MNN5	EALFSGSEGIVTIGGGK	2	heavy	815.432326	y12	1082.59316	69.23
P46982	MNN5	EALFSGSEGIVTIGGGK	2	heavy	815.432326	y10	938.539671	69.23
P46982	MNN5	EALFSGSEGIVTIGGGK	2	heavy	815.432326	y9	809.497078	69.23
P46982	MNN5	EALFSGSEGIVTIGGGK	2	heavy	815.432326	y7	639.39155	69.23
P46982	MNN5	EALFSGSEGIVTIGGGK	2	heavy	815.432326	y6	540.323136	69.23
P46982	MNN5	EALFSGSEGIVTIGGGK	2	heavy	815.432326	y5	439.275458	69.23
P37302	APE3	IISFN[+203.1]LSDAETGK	2	light	799.401418	y8	820.404688	54.38
P37302	APE3	IISFN[+203.1]LSDAETGK	2	light	799.401418	y7	707.320624	54.38
P37302	APE3	IISFN[+203.1]LSDAETGK	2	light	799.401418	y5	505.261653	54.38
P37302	APE3	IISFN[+203.1]LSDAETGK	2	light	799.401418	y3	305.181946	54.38

P37302	APE3	IISFN[+203.1]LSDAETGH	2	heavy	803.408517	y8	828.418887	54.38
P37302	APE3	IISFN[+203.1]LSDAETGH	2	heavy	803.408517	y7	715.334823	54.38
P37302	APE3	IISFN[+203.1]LSDAETGH	2	heavy	803.408517	y5	513.275852	54.38
P37302	APE3	IISFN[+203.1]LSDAETGH	2	heavy	803.408517	y3	313.196145	54.38
P37302	APE3	LAN[+203.1]YSTPDYGH[	3	light	598.947957	y10	1130.52251	8.12
P37302	APE3	LAN[+203.1]YSTPDYGH[	3	light	598.947957	y7	845.390041	8.12
P37302	APE3	LAN[+203.1]YSTPDYGH[	3	light	598.947957	y6	730.363098	8.12
P37302	APE3	LAN[+203.1]YSTPDYGH[	3	light	598.947957	y5	567.29977	8.12
P37302	APE3	LAN[+203.1]YSTPDYGH[	3	light	598.947957	y3	373.219394	8.12
P37302	APE3	LAN[+203.1]YSTPDYGH[	3	light	598.947957	y8	471.725041	8.12
P37302	APE3	LAN[+203.1]YSTPDYGH[	3	light	598.947957	b2	185.128454	8.12
P37302	APE3	LAN[+203.1]YSTPDYGH[	3	heavy	600.954667	y10	1136.54264	8.12
P37302	APE3	LAN[+203.1]YSTPDYGH[	3	heavy	600.954667	y7	851.41017	8.12
P37302	APE3	LAN[+203.1]YSTPDYGH[	3	heavy	600.954667	y6	736.383227	8.12
P37302	APE3	LAN[+203.1]YSTPDYGH[	3	heavy	600.954667	y5	573.319899	8.12
P37302	APE3	LAN[+203.1]YSTPDYGH[	3	heavy	600.954667	y3	379.239523	8.12
P37302	APE3	LAN[+203.1]YSTPDYGH[	3	heavy	600.954667	y8	474.735105	8.12
P37302	APE3	LAN[+203.1]YSTPDYGH[	3	heavy	600.954667	b2	185.128454	8.12
P37302	APE3	AHHLN[+203.1]YTLVPF[	2	light	921.9603	y9	1067.55202	36.72
P37302	APE3	AHHLN[+203.1]YTLVPF[	2	light	921.9603	y8	904.488693	36.72
P37302	APE3	AHHLN[+203.1]YTLVPF[	2	light	921.9603	y7	803.441014	36.72
P37302	APE3	AHHLN[+203.1]YTLVPF[	2	light	921.9603	y6	690.35695	36.72
P37302	APE3	AHHLN[+203.1]YTLVPF[	2	light	921.9603	y5	591.288536	36.72
P37302	APE3	AHHLN[+203.1]YTLVPF[	2	light	921.9603	y4	494.235772	36.72
P37302	APE3	AHHLN[+203.1]YTLVPF[	2	light	921.9603	b2	209.103302	36.72
P37302	APE3	AHHLN[+203.1]YTLVPF[	2	heavy	924.970364	y9	1073.57215	36.72
P37302	APE3	AHHLN[+203.1]YTLVPF[	2	heavy	924.970364	y8	910.508822	36.72
P37302	APE3	AHHLN[+203.1]YTLVPF[	2	heavy	924.970364	y7	809.461143	36.72
P37302	APE3	AHHLN[+203.1]YTLVPF[	2	heavy	924.970364	y6	696.377079	36.72
P37302	APE3	AHHLN[+203.1]YTLVPF[	2	heavy	924.970364	y5	597.308665	36.72
P37302	APE3	AHHLN[+203.1]YTLVPF[	2	heavy	924.970364	y4	500.255901	36.72
P37302	APE3	AHHLN[+203.1]YTLVPF[	2	heavy	924.970364	b2	209.103302	36.72
P37302	APE3	AHHLN[+203.1]YTLVPF[	4	light	461.483788	y5	591.288536	36.72
P37302	APE3	AHHLN[+203.1]YTLVPF[	4	light	461.483788	y4	494.235772	36.72
P37302	APE3	AHHLN[+203.1]YTLVPF[	4	light	461.483788	y3	347.167359	36.72
P37302	APE3	AHHLN[+203.1]YTLVPF[	4	heavy	462.98882	y5	597.308665	36.72
P37302	APE3	AHHLN[+203.1]YTLVPF[	4	heavy	462.98882	y4	500.255901	36.72
P37302	APE3	AHHLN[+203.1]YTLVPF[	4	heavy	462.98882	y3	353.187488	36.72
P37302	APE3	IKVDDLN[+203.1]ATAW[	3	light	666.005583	y9	1312.61681	66.86
P37302	APE3	IKVDDLN[+203.1]ATAW[	3	light	666.005583	y8	995.494506	66.86
P37302	APE3	IKVDDLN[+203.1]ATAW[	3	light	666.005583	y7	924.457393	66.86
P37302	APE3	IKVDDLN[+203.1]ATAW[	3	light	666.005583	y6	823.409714	66.86
P37302	APE3	IKVDDLN[+203.1]ATAW[	3	light	666.005583	y5	752.3726	66.86
P37302	APE3	IKVDDLN[+203.1]ATAW[	3	light	666.005583	y4	566.293287	66.86
P37302	APE3	IKVDDLN[+203.1]ATAW[	3	light	666.005583	y3	451.266344	66.86
P37302	APE3	IKVDDLN[+203.1]ATAW[	3	heavy	670.683693	y9	1318.63694	66.86
P37302	APE3	IKVDDLN[+203.1]ATAW[	3	heavy	670.683693	y8	1001.51464	66.86
P37302	APE3	IKVDDLN[+203.1]ATAW[	3	heavy	670.683693	y7	930.477522	66.86
P37302	APE3	IKVDDLN[+203.1]ATAW[	3	heavy	670.683693	y6	829.429843	66.86
P37302	APE3	IKVDDLN[+203.1]ATAW[	3	heavy	670.683693	y5	758.392729	66.86
P37302	APE3	IKVDDLN[+203.1]ATAW[	3	heavy	670.683693	y4	572.313416	66.86
P37302	APE3	IKVDDLN[+203.1]ATAW[	3	heavy	670.683693	y3	457.286473	66.86
P37302	APE3	SFAN[+203.1]TTAFALSF	2	light	1115.05733	y12	1186.64665	88.86
P37302	APE3	SFAN[+203.1]TTAFALSF	2	light	1115.05733	y10	1002.52547	88.86
P37302	APE3	SFAN[+203.1]TTAFALSF	2	light	1115.05733	y9	915.493444	88.86
P37302	APE3	SFAN[+203.1]TTAFALSF	2	light	1115.05733	y5	507.292559	88.86
P37302	APE3	SFAN[+203.1]TTAFALSF	2	light	1115.05733	y3	152.104979	88.86
P37302	APE3	SFAN[+203.1]TTAFALSF	2	light	1115.05733	b2	235.107718	88.86
P37302	APE3	SFAN[+203.1]TTAFALSF	2	heavy	1119.06443	y12	1194.66085	88.86
P37302	APE3	SFAN[+203.1]TTAFALSF	2	heavy	1119.06443	y10	1010.53967	88.86
P37302	APE3	SFAN[+203.1]TTAFALSF	2	heavy	1119.06443	y9	923.507643	88.86
P37302	APE3	SFAN[+203.1]TTAFALSF	2	heavy	1119.06443	y5	515.306758	88.86
P37302	APE3	SFAN[+203.1]TTAFALSF	2	heavy	1119.06443	y3	156.112078	88.86

P37302	APE3	SFAN[+203.1]TTAFALSF	2	heavy	1119.06443	b2	235.107718	88.86
P37302	APE3	HTVATVGVPYK	2	light	586.32713	y10	1034.58807	2.98
P37302	APE3	HTVATVGVPYK	2	light	586.32713	y9	933.540394	2.98
P37302	APE3	HTVATVGVPYK	2	light	586.32713	y8	834.47198	2.98
P37302	APE3	HTVATVGVPYK	2	light	586.32713	y5	563.318774	2.98
P37302	APE3	HTVATVGVPYK	2	light	586.32713	y3	407.228896	2.98
P37302	APE3	HTVATVGVPYK	2	heavy	590.33423	y10	1042.60227	2.98
P37302	APE3	HTVATVGVPYK	2	heavy	590.33423	y9	941.554593	2.98
P37302	APE3	HTVATVGVPYK	2	heavy	590.33423	y8	842.486179	2.98
P37302	APE3	HTVATVGVPYK	2	heavy	590.33423	y5	571.332973	2.98
P37302	APE3	HTVATVGVPYK	2	heavy	590.33423	y3	415.243095	2.98
P37302	APE3	LIAHSVATYADSFEGFPI	3	light	651.663269	y9	997.462538	69.16
P37302	APE3	LIAHSVATYADSFEGFPI	3	light	651.663269	y8	926.425424	69.16
P37302	APE3	LIAHSVATYADSFEGFPI	3	light	651.663269	y7	811.398481	69.16
P37302	APE3	LIAHSVATYADSFEGFPI	3	light	651.663269	y6	724.366452	69.16
P37302	APE3	LIAHSVATYADSFEGFPI	3	light	651.663269	y5	577.298038	69.16
P37302	APE3	LIAHSVATYADSFEGFPI	3	light	651.663269	y4	448.255445	69.16
P37302	APE3	LIAHSVATYADSFEGFPI	3	heavy	654.334669	y9	1005.47674	69.16
P37302	APE3	LIAHSVATYADSFEGFPI	3	heavy	654.334669	y8	934.439623	69.16
P37302	APE3	LIAHSVATYADSFEGFPI	3	heavy	654.334669	y7	819.41268	69.16
P37302	APE3	LIAHSVATYADSFEGFPI	3	heavy	654.334669	y6	732.380651	69.16
P37302	APE3	LIAHSVATYADSFEGFPI	3	heavy	654.334669	y5	585.312237	69.16
P37302	APE3	LIAHSVATYADSFEGFPI	3	heavy	654.334669	y4	456.269644	69.16
P00729	CBPY	VRN[+203.1]WTASITDE\	3	light	693.351531	y9	947.468017	56.41
P00729	CBPY	VRN[+203.1]WTASITDE\	3	light	693.351531	y8	846.420339	56.41
P00729	CBPY	VRN[+203.1]WTASITDE\	3	light	693.351531	y7	731.393395	56.41
P00729	CBPY	VRN[+203.1]WTASITDE\	3	light	693.351531	y6	602.350802	56.41
P00729	CBPY	VRN[+203.1]WTASITDE\	3	light	693.351531	y5	503.282388	56.41
P00729	CBPY	VRN[+203.1]WTASITDE\	3	light	693.351531	b6	931.463207	56.41
P00729	CBPY	VRN[+203.1]WTASITDE\	3	light	693.351531	b7	1018.49524	56.41
P00729	CBPY	VRN[+203.1]WTASITDE\	3	heavy	698.02964	y9	955.482216	56.41
P00729	CBPY	VRN[+203.1]WTASITDE\	3	heavy	698.02964	y8	854.434538	56.41
P00729	CBPY	VRN[+203.1]WTASITDE\	3	heavy	698.02964	y7	739.407594	56.41
P00729	CBPY	VRN[+203.1]WTASITDE\	3	heavy	698.02964	y6	610.365001	56.41
P00729	CBPY	VRN[+203.1]WTASITDE\	3	heavy	698.02964	y5	511.296587	56.41
P00729	CBPY	VRN[+203.1]WTASITDE\	3	heavy	698.02964	b6	937.483336	56.41
P00729	CBPY	VRN[+203.1]WTASITDE\	3	heavy	698.02964	b7	1024.51536	56.41
P00729	CBPY	ILGIDPN[+203.1]VTQYT(	2	light	1350.64235	y11	1283.56377	90.52
P00729	CBPY	ILGIDPN[+203.1]VTQYT(	2	light	1350.64235	y10	1182.51609	90.52
P00729	CBPY	ILGIDPN[+203.1]VTQYT(	2	light	1350.64235	y7	849.347233	90.52
P00729	CBPY	ILGIDPN[+203.1]VTQYT(	2	light	1350.64235	y6	734.32029	90.52
P00729	CBPY	ILGIDPN[+203.1]VTQYT(	2	light	1350.64235	y4	506.209283	90.52
P00729	CBPY	ILGIDPN[+203.1]VTQYT(	2	light	1350.64235	b2	227.175404	90.52
P00729	CBPY	ILGIDPN[+203.1]VTQYT(	2	light	1350.64235	b3	284.196868	90.52
P00729	CBPY	ILGIDPN[+203.1]VTQYT(	2	heavy	1354.64945	y11	1291.57797	90.52
P00729	CBPY	ILGIDPN[+203.1]VTQYT(	2	heavy	1354.64945	y10	1190.53029	90.52
P00729	CBPY	ILGIDPN[+203.1]VTQYT(	2	heavy	1354.64945	y7	857.361432	90.52
P00729	CBPY	ILGIDPN[+203.1]VTQYT(	2	heavy	1354.64945	y6	742.334489	90.52
P00729	CBPY	ILGIDPN[+203.1]VTQYT(	2	heavy	1354.64945	y4	514.223482	90.52
P00729	CBPY	ILGIDPN[+203.1]VTQYT(	2	heavy	1354.64945	b2	227.175404	90.52
P00729	CBPY	ILGIDPN[+203.1]VTQYT(	2	heavy	1354.64945	b3	284.196868	90.52
P00729	CBPY	AWTDVLPWK	2	light	558.297841	y7	858.47198	87.3
P00729	CBPY	AWTDVLPWK	2	light	558.297841	y6	757.424302	87.3
P00729	CBPY	AWTDVLPWK	2	light	558.297841	y5	642.397359	87.3
P00729	CBPY	AWTDVLPWK	2	light	558.297841	y4	543.328945	87.3
P00729	CBPY	AWTDVLPWK	2	light	558.297841	y3	430.244881	87.3
P00729	CBPY	AWTDVLPWK	2	heavy	562.304941	y7	866.486179	87.3
P00729	CBPY	AWTDVLPWK	2	heavy	562.304941	y6	765.438501	87.3
P00729	CBPY	AWTDVLPWK	2	heavy	562.304941	y5	650.411558	87.3
P00729	CBPY	AWTDVLPWK	2	heavy	562.304941	y4	551.343144	87.3
P00729	CBPY	AWTDVLPWK	2	heavy	562.304941	y3	438.25908	87.3
P00729	CBPY	DFIC[+57]NWLGNK	2	light	633.800422	y8	1004.49821	74.17
P00729	CBPY	DFIC[+57]NWLGNK	2	light	633.800422	y7	891.414148	74.17

P00729	CBPY	DFIC[+57]NWLGNK	2	light	633.800422	y6	731.383499	74.17
P00729	CBPY	DFIC[+57]NWLGNK	2	light	633.800422	y5	617.340572	74.17
P00729	CBPY	DFIC[+57]NWLGNK	2	light	633.800422	y4	431.261259	74.17
P00729	CBPY	DFIC[+57]NWLGNK	2	light	633.800422	y3	318.177195	74.17
P00729	CBPY	DFIC[+57]NWLGNK	2	heavy	637.807522	y8	1012.51241	74.17
P00729	CBPY	DFIC[+57]NWLGNK	2	heavy	637.807522	y7	899.428347	74.17
P00729	CBPY	DFIC[+57]NWLGNK	2	heavy	637.807522	y6	739.397698	74.17
P00729	CBPY	DFIC[+57]NWLGNK	2	heavy	637.807522	y5	625.354771	74.17
P00729	CBPY	DFIC[+57]NWLGNK	2	heavy	637.807522	y4	439.275458	74.17
P00729	CBPY	DFIC[+57]NWLGNK	2	heavy	637.807522	y3	326.191394	74.17
P41543	OST1	FSSN[+203.1]ETLAIVYS	3	light	963.829555	y12	1374.76006	90.49
P41543	OST1	FSSN[+203.1]ETLAIVYS	3	light	963.829555	y11	1237.70115	90.49
P41543	OST1	FSSN[+203.1]ETLAIVYS	3	light	963.829555	y10	1123.65822	90.49
P41543	OST1	FSSN[+203.1]ETLAIVYS	3	light	963.829555	y9	1052.6211	90.49
P41543	OST1	FSSN[+203.1]ETLAIVYS	3	light	963.829555	y7	842.484276	90.49
P41543	OST1	FSSN[+203.1]ETLAIVYS	3	light	963.829555	y5	600.382771	90.49
P41543	OST1	FSSN[+203.1]ETLAIVYS	3	light	963.829555	y3	402.245943	90.49
P41543	OST1	FSSN[+203.1]ETLAIVYS	3	light	963.829555	b2	235.107718	90.49
P41543	OST1	FSSN[+203.1]ETLAIVYS	3	heavy	965.836265	y12	1380.78019	90.49
P41543	OST1	FSSN[+203.1]ETLAIVYS	3	heavy	965.836265	y11	1243.72127	90.49
P41543	OST1	FSSN[+203.1]ETLAIVYS	3	heavy	965.836265	y10	1129.67835	90.49
P41543	OST1	FSSN[+203.1]ETLAIVYS	3	heavy	965.836265	y9	1058.64123	90.49
P41543	OST1	FSSN[+203.1]ETLAIVYS	3	heavy	965.836265	y7	848.504405	90.49
P41543	OST1	FSSN[+203.1]ETLAIVYS	3	heavy	965.836265	y5	606.4029	90.49
P41543	OST1	FSSN[+203.1]ETLAIVYS	3	heavy	965.836265	y3	408.266072	90.49
P41543	OST1	FSSN[+203.1]ETLAIVYS	3	heavy	965.836265	b2	235.107718	90.49
P41543	OST1	LSDFLHVSSGSDEK	3	light	507.579093	y9	945.427215	26.3
P41543	OST1	LSDFLHVSSGSDEK	3	light	507.579093	y8	808.368303	26.3
P41543	OST1	LSDFLHVSSGSDEK	3	light	507.579093	y7	709.299889	26.3
P41543	OST1	LSDFLHVSSGSDEK	3	light	507.579093	y6	622.267861	26.3
P41543	OST1	LSDFLHVSSGSDEK	3	light	507.579093	y2	276.155397	26.3
P41543	OST1	LSDFLHVSSGSDEK	3	heavy	510.250493	y9	953.441414	26.3
P41543	OST1	LSDFLHVSSGSDEK	3	heavy	510.250493	y8	816.382502	26.3
P41543	OST1	LSDFLHVSSGSDEK	3	heavy	510.250493	y7	717.314088	26.3
P41543	OST1	LSDFLHVSSGSDEK	3	heavy	510.250493	y6	630.28206	26.3
P41543	OST1	LSDFLHVSSGSDEK	3	heavy	510.250493	y2	284.169596	26.3
P41543	OST1	ANGNSFEFGPWEDIPR	2	light	918.421007	y9	1116.54727	91.42
P41543	OST1	ANGNSFEFGPWEDIPR	2	light	918.421007	y8	969.478856	91.42
P41543	OST1	ANGNSFEFGPWEDIPR	2	light	918.421007	y7	912.457393	91.42
P41543	OST1	ANGNSFEFGPWEDIPR	2	light	918.421007	y3	385.25578	91.42
P41543	OST1	ANGNSFEFGPWEDIPR	2	light	918.421007	y2	272.171716	91.42
P41543	OST1	ANGNSFEFGPWEDIPR	2	heavy	921.431072	y9	1122.5674	91.42
P41543	OST1	ANGNSFEFGPWEDIPR	2	heavy	921.431072	y8	975.498985	91.42
P41543	OST1	ANGNSFEFGPWEDIPR	2	heavy	921.431072	y7	918.477522	91.42
P41543	OST1	ANGNSFEFGPWEDIPR	2	heavy	921.431072	y3	391.275909	91.42
P41543	OST1	ANGNSFEFGPWEDIPR	2	heavy	921.431072	y2	278.191845	91.42
P33767	WBP1	LEYLDIN[+203.1]STSTT\	2	light	1147.05211	y11	1229.58959	65.81
P33767	WBP1	LEYLDIN[+203.1]STSTT\	2	light	1147.05211	y10	1142.55756	65.81
P33767	WBP1	LEYLDIN[+203.1]STSTT\	2	light	1147.05211	y9	1041.50988	65.81
P33767	WBP1	LEYLDIN[+203.1]STSTT\	2	light	1147.05211	y8	954.477853	65.81
P33767	WBP1	LEYLDIN[+203.1]STSTT\	2	light	1147.05211	y7	853.430175	65.81
P33767	WBP1	LEYLDIN[+203.1]STSTT\	2	light	1147.05211	y6	752.382496	65.81
P33767	WBP1	LEYLDIN[+203.1]STSTT\	2	light	1147.05211	y5	653.314082	65.81
P33767	WBP1	LEYLDIN[+203.1]STSTT\	2	light	1147.05211	y4	538.287139	65.81
P33767	WBP1	LEYLDIN[+203.1]STSTT\	2	light	1147.05211	y3	425.203075	65.81
P33767	WBP1	LEYLDIN[+203.1]STSTT\	2	light	1147.05211	b3	406.197262	65.81
P33767	WBP1	LEYLDIN[+203.1]STSTT\	2	light	1147.05211	b5	634.308269	65.81
P33767	WBP1	LEYLDIN[+203.1]STSTT\	2	heavy	1151.05921	y11	1237.60379	65.81
P33767	WBP1	LEYLDIN[+203.1]STSTT\	2	heavy	1151.05921	y10	1150.57176	65.81
P33767	WBP1	LEYLDIN[+203.1]STSTT\	2	heavy	1151.05921	y9	1049.52408	65.81
P33767	WBP1	LEYLDIN[+203.1]STSTT\	2	heavy	1151.05921	y8	962.492052	65.81
P33767	WBP1	LEYLDIN[+203.1]STSTT\	2	heavy	1151.05921	y7	861.444374	65.81
P33767	WBP1	LEYLDIN[+203.1]STSTT\	2	heavy	1151.05921	y6	760.396695	65.81

P33767	WBP1	LEYLDIN[+203.1]STSTT\	2	heavy	1151.05921	y5	661.328281	65.81
P33767	WBP1	LEYLDIN[+203.1]STSTT\	2	heavy	1151.05921	y4	546.301338	65.81
P33767	WBP1	LEYLDIN[+203.1]STSTT\	2	heavy	1151.05921	y3	433.217274	65.81
P33767	WBP1	LEYLDIN[+203.1]STSTT\	2	heavy	1151.05921	b3	406.197262	65.81
P33767	WBP1	LEYLDIN[+203.1]STSTT\	2	heavy	1151.05921	b5	634.308269	65.81
P33767	WBP1	LTLSPSGN[+203.1]DSE]	3	light	1003.14001	y11	1311.65794	78.46
P33767	WBP1	LTLSPSGN[+203.1]DSE]	3	light	1003.14001	y10	1148.59462	78.46
P33767	WBP1	LTLSPSGN[+203.1]DSE]	3	light	1003.14001	y9	1047.54694	78.46
P33767	WBP1	LTLSPSGN[+203.1]DSE]	3	light	1003.14001	y8	946.499258	78.46
P33767	WBP1	LTLSPSGN[+203.1]DSE]	3	light	1003.14001	y6	760.435201	78.46
P33767	WBP1	LTLSPSGN[+203.1]DSE]	3	light	1003.14001	y4	500.282723	78.46
P33767	WBP1	LTLSPSGN[+203.1]DSE]	3	light	1003.14001	y3	387.198659	78.46
P33767	WBP1	LTLSPSGN[+203.1]DSE]	3	heavy	1005.14672	y11	1317.67807	78.46
P33767	WBP1	LTLSPSGN[+203.1]DSE]	3	heavy	1005.14672	y10	1154.61474	78.46
P33767	WBP1	LTLSPSGN[+203.1]DSE]	3	heavy	1005.14672	y9	1053.56707	78.46
P33767	WBP1	LTLSPSGN[+203.1]DSE]	3	heavy	1005.14672	y8	952.519387	78.46
P33767	WBP1	LTLSPSGN[+203.1]DSE]	3	heavy	1005.14672	y6	766.45533	78.46
P33767	WBP1	LTLSPSGN[+203.1]DSE]	3	heavy	1005.14672	y4	506.302852	78.46
P33767	WBP1	LTLSPSGN[+203.1]DSE]	3	heavy	1005.14672	y3	393.218788	78.46
P33767	WBP1	LVWIGSSDFLK	2	light	632.850438	y9	1052.54112	91.21
P33767	WBP1	LVWIGSSDFLK	2	light	632.850438	y8	866.461809	91.21
P33767	WBP1	LVWIGSSDFLK	2	light	632.850438	y7	753.377745	91.21
P33767	WBP1	LVWIGSSDFLK	2	light	632.850438	y6	696.356282	91.21
P33767	WBP1	LVWIGSSDFLK	2	light	632.850438	y5	609.324253	91.21
P33767	WBP1	LVWIGSSDFLK	2	light	632.850438	y4	522.292225	91.21
P33767	WBP1	LVWIGSSDFLK	2	light	632.850438	y3	407.265282	91.21
P33767	WBP1	LVWIGSSDFLK	2	heavy	636.857538	y9	1060.55532	91.21
P33767	WBP1	LVWIGSSDFLK	2	heavy	636.857538	y8	874.476008	91.21
P33767	WBP1	LVWIGSSDFLK	2	heavy	636.857538	y7	761.391944	91.21
P33767	WBP1	LVWIGSSDFLK	2	heavy	636.857538	y6	704.370481	91.21
P33767	WBP1	LVWIGSSDFLK	2	heavy	636.857538	y5	617.338452	91.21
P33767	WBP1	LVWIGSSDFLK	2	heavy	636.857538	y4	530.306424	91.21
P33767	WBP1	LVWIGSSDFLK	2	heavy	636.857538	y3	415.279481	91.21
P33767	WBP1	IGLSFTTDK	2	light	491.266207	y8	868.441074	38.14
P33767	WBP1	IGLSFTTDK	2	light	491.266207	y7	811.41961	38.14
P33767	WBP1	IGLSFTTDK	2	light	491.266207	y6	698.335546	38.14
P33767	WBP1	IGLSFTTDK	2	light	491.266207	y5	611.303518	38.14
P33767	WBP1	IGLSFTTDK	2	light	491.266207	y4	464.235104	38.14
P33767	WBP1	IGLSFTTDK	2	light	491.266207	y3	363.187425	38.14
P33767	WBP1	IGLSFTTDK	2	heavy	495.273306	y8	876.455273	38.14
P33767	WBP1	IGLSFTTDK	2	heavy	495.273306	y7	819.433809	38.14
P33767	WBP1	IGLSFTTDK	2	heavy	495.273306	y6	706.349745	38.14
P33767	WBP1	IGLSFTTDK	2	heavy	495.273306	y5	619.317717	38.14
P33767	WBP1	IGLSFTTDK	2	heavy	495.273306	y4	472.249303	38.14
P33767	WBP1	IGLSFTTDK	2	heavy	495.273306	y3	371.201624	38.14
P39007	STT3	TTLVDNNTWN[+203.1]N	3	light	772.060639	y10	1269.67974	51.32
P39007	STT3	TTLVDNNTWN[+203.1]N	3	light	772.060639	y9	952.557441	51.32
P39007	STT3	TTLVDNNTWN[+203.1]N	3	light	772.060639	y8	838.514514	51.32
P39007	STT3	TTLVDNNTWN[+203.1]N	3	light	772.060639	y7	737.466835	51.32
P39007	STT3	TTLVDNNTWN[+203.1]N	3	light	772.060639	y6	600.407923	51.32
P39007	STT3	TTLVDNNTWN[+203.1]N	3	light	772.060639	y5	487.323859	51.32
P39007	STT3	TTLVDNNTWN[+203.1]N	3	light	772.060639	y4	416.286745	51.32
P39007	STT3	TTLVDNNTWN[+203.1]N	3	light	772.060639	b4	415.255111	51.32
P39007	STT3	TTLVDNNTWN[+203.1]N	3	light	772.060639	b8	859.415587	51.32
P39007	STT3	TTLVDNNTWN[+203.1]N	3	light	772.060639	b9	1045.4949	51.32
P39007	STT3	TTLVDNNTWN[+203.1]N	3	light	772.060639	b10	1362.6172	51.32
P39007	STT3	TTLVDNNTWN[+203.1]N	3	heavy	774.732039	y10	1277.69394	51.32
P39007	STT3	TTLVDNNTWN[+203.1]N	3	heavy	774.732039	y9	960.57164	51.32
P39007	STT3	TTLVDNNTWN[+203.1]N	3	heavy	774.732039	y8	846.528713	51.32
P39007	STT3	TTLVDNNTWN[+203.1]N	3	heavy	774.732039	y7	745.481034	51.32
P39007	STT3	TTLVDNNTWN[+203.1]N	3	heavy	774.732039	y6	608.422122	51.32
P39007	STT3	TTLVDNNTWN[+203.1]N	3	heavy	774.732039	y5	495.338058	51.32
P39007	STT3	TTLVDNNTWN[+203.1]N	3	heavy	774.732039	y4	424.300944	51.32

P39007	STT3	TTLVDNNTWN[+203.1]N	3	heavy	774.732039	b4	415.255111	51.32
P39007	STT3	TTLVDNNTWN[+203.1]N	3	heavy	774.732039	b8	859.415587	51.32
P39007	STT3	TTLVDNNTWN[+203.1]N	3	heavy	774.732039	b9	1045.4949	51.32
P39007	STT3	TTLVDNNTWN[+203.1]N	3	heavy	774.732039	b10	1362.6172	51.32
P39007	STT3	TAYSSPSVVLPSQTPDG	2	light	917.46508	y10	1041.5575	37.62
P39007	STT3	TAYSSPSVVLPSQTPDG	2	light	917.46508	y9	942.489087	37.62
P39007	STT3	TAYSSPSVVLPSQTPDG	2	light	917.46508	y8	829.405023	37.62
P39007	STT3	TAYSSPSVVLPSQTPDG	2	light	917.46508	y5	517.261653	37.62
P39007	STT3	TAYSSPSVVLPSQTPDG	2	light	917.46508	y4	416.213974	37.62
P39007	STT3	TAYSSPSVVLPSQTPDG	2	light	917.46508	y3	319.161211	37.62
P39007	STT3	TAYSSPSVVLPSQTPDG	2	light	917.46508	y16	831.422684	37.62
P39007	STT3	TAYSSPSVVLPSQTPDG	2	heavy	921.47218	y10	1049.5717	37.62
P39007	STT3	TAYSSPSVVLPSQTPDG	2	heavy	921.47218	y9	950.503286	37.62
P39007	STT3	TAYSSPSVVLPSQTPDG	2	heavy	921.47218	y8	837.419222	37.62
P39007	STT3	TAYSSPSVVLPSQTPDG	2	heavy	921.47218	y5	525.275852	37.62
P39007	STT3	TAYSSPSVVLPSQTPDG	2	heavy	921.47218	y4	424.228173	37.62
P39007	STT3	TAYSSPSVVLPSQTPDG	2	heavy	921.47218	y3	327.17541	37.62
P39007	STT3	TAYSSPSVVLPSQTPDG	2	heavy	921.47218	y16	835.429784	37.62
P39007	STT3	ISEGIWPEEIK	2	light	650.84281	y10	1187.59428	54.67
P39007	STT3	ISEGIWPEEIK	2	light	650.84281	y9	1100.56225	54.67
P39007	STT3	ISEGIWPEEIK	2	light	650.84281	y8	971.519659	54.67
P39007	STT3	ISEGIWPEEIK	2	light	650.84281	y6	801.414131	54.67
P39007	STT3	ISEGIWPEEIK	2	light	650.84281	y5	615.334818	54.67
P39007	STT3	ISEGIWPEEIK	2	heavy	654.84991	y10	1195.60848	54.67
P39007	STT3	ISEGIWPEEIK	2	heavy	654.84991	y9	1108.57645	54.67
P39007	STT3	ISEGIWPEEIK	2	heavy	654.84991	y8	979.533858	54.67
P39007	STT3	ISEGIWPEEIK	2	heavy	654.84991	y6	809.42833	54.67
P39007	STT3	ISEGIWPEEIK	2	heavy	654.84991	y5	623.349017	54.67
Q03103	ERO1	YTIENIN[+203.1]STK	2	light	693.343371	y9	1222.61614	5.59
Q03103	ERO1	YTIENIN[+203.1]STK	2	light	693.343371	y8	1121.56846	5.59
Q03103	ERO1	YTIENIN[+203.1]STK	2	light	693.343371	y7	1008.4844	5.59
Q03103	ERO1	YTIENIN[+203.1]STK	2	light	693.343371	y6	879.441803	5.59
Q03103	ERO1	YTIENIN[+203.1]STK	2	light	693.343371	y5	765.398875	5.59
Q03103	ERO1	YTIENIN[+203.1]STK	2	light	693.343371	y4	652.314811	5.59
Q03103	ERO1	YTIENIN[+203.1]STK	2	light	693.343371	y3	335.192511	5.59
Q03103	ERO1	YTIENIN[+203.1]STK	2	heavy	697.350471	y9	1230.63034	5.59
Q03103	ERO1	YTIENIN[+203.1]STK	2	heavy	697.350471	y8	1129.58266	5.59
Q03103	ERO1	YTIENIN[+203.1]STK	2	heavy	697.350471	y7	1016.4986	5.59
Q03103	ERO1	YTIENIN[+203.1]STK	2	heavy	697.350471	y6	887.456002	5.59
Q03103	ERO1	YTIENIN[+203.1]STK	2	heavy	697.350471	y5	773.413074	5.59
Q03103	ERO1	YTIENIN[+203.1]STK	2	heavy	697.350471	y4	660.32901	5.59
Q03103	ERO1	YTIENIN[+203.1]STK	2	heavy	697.350471	y3	343.20671	5.59
Q03103	ERO1	WEPNLDLFMAR	2	light	696.342454	y9	1076.55573	99.25
Q03103	ERO1	WEPNLDLFMAR	2	light	696.342454	y8	979.502963	99.25
Q03103	ERO1	WEPNLDLFMAR	2	light	696.342454	y7	865.460035	99.25
Q03103	ERO1	WEPNLDLFMAR	2	light	696.342454	y6	752.375971	99.25
Q03103	ERO1	WEPNLDLFMAR	2	light	696.342454	y5	637.349028	99.25
Q03103	ERO1	WEPNLDLFMAR	2	light	696.342454	y4	524.264964	99.25
Q03103	ERO1	WEPNLDLFMAR	2	heavy	699.352519	y9	1082.57586	99.25
Q03103	ERO1	WEPNLDLFMAR	2	heavy	699.352519	y8	985.523092	99.25
Q03103	ERO1	WEPNLDLFMAR	2	heavy	699.352519	y7	871.480164	99.25
Q03103	ERO1	WEPNLDLFMAR	2	heavy	699.352519	y6	758.3961	99.25
Q03103	ERO1	WEPNLDLFMAR	2	heavy	699.352519	y5	643.369157	99.25
Q03103	ERO1	WEPNLDLFMAR	2	heavy	699.352519	y4	530.285093	99.25
Q03103	ERO1	NAVLIDLTANPER	2	light	713.388447	y11	1240.68958	55.39
Q03103	ERO1	NAVLIDLTANPER	2	light	713.388447	y10	1141.62116	55.39
Q03103	ERO1	NAVLIDLTANPER	2	light	713.388447	y9	1028.5371	55.39
Q03103	ERO1	NAVLIDLTANPER	2	light	713.388447	y8	915.453036	55.39
Q03103	ERO1	NAVLIDLTANPER	2	light	713.388447	y7	800.426093	55.39
Q03103	ERO1	NAVLIDLTANPER	2	light	713.388447	y6	687.342029	55.39
Q03103	ERO1	NAVLIDLTANPER	2	light	713.388447	y5	586.29435	55.39
Q03103	ERO1	NAVLIDLTANPER	2	light	713.388447	y4	515.257236	55.39
Q03103	ERO1	NAVLIDLTANPER	2	heavy	716.398512	y11	1246.70971	55.39

Q03103	ERO1	NAVLIDLTANPER	2	heavy	716.398512	y10	1147.64129	55.39
Q03103	ERO1	NAVLIDLTANPER	2	heavy	716.398512	y9	1034.55723	55.39
Q03103	ERO1	NAVLIDLTANPER	2	heavy	716.398512	y8	921.473165	55.39
Q03103	ERO1	NAVLIDLTANPER	2	heavy	716.398512	y7	806.446222	55.39
Q03103	ERO1	NAVLIDLTANPER	2	heavy	716.398512	y6	693.362158	55.39
Q03103	ERO1	NAVLIDLTANPER	2	heavy	716.398512	y5	592.314479	55.39
Q03103	ERO1	NAVLIDLTANPER	2	heavy	716.398512	y4	521.277365	55.39
P38875	GPI16	SYASDIGAPLFN[+203.1]	2	light	951.952003	y11	1379.70529	50.7
P38875	GPI16	SYASDIGAPLFN[+203.1]	2	light	951.952003	y10	1266.62122	50.7
P38875	GPI16	SYASDIGAPLFN[+203.1]	2	light	951.952003	y9	1209.59976	50.7
P38875	GPI16	SYASDIGAPLFN[+203.1]	2	light	951.952003	y8	1138.56265	50.7
P38875	GPI16	SYASDIGAPLFN[+203.1]	2	light	951.952003	y7	1041.50988	50.7
P38875	GPI16	SYASDIGAPLFN[+203.1]	2	light	951.952003	y6	928.425818	50.7
P38875	GPI16	SYASDIGAPLFN[+203.1]	2	light	951.952003	y5	781.357404	50.7
P38875	GPI16	SYASDIGAPLFN[+203.1]	2	light	951.952003	y4	464.235104	50.7
P38875	GPI16	SYASDIGAPLFN[+203.1]	2	light	951.952003	b2	251.102633	50.7
P38875	GPI16	SYASDIGAPLFN[+203.1]	2	light	951.952003	b3	322.139747	50.7
P38875	GPI16	SYASDIGAPLFN[+203.1]	2	heavy	955.959102	y11	1387.71949	50.7
P38875	GPI16	SYASDIGAPLFN[+203.1]	2	heavy	955.959102	y10	1274.63542	50.7
P38875	GPI16	SYASDIGAPLFN[+203.1]	2	heavy	955.959102	y9	1217.61396	50.7
P38875	GPI16	SYASDIGAPLFN[+203.1]	2	heavy	955.959102	y8	1146.57685	50.7
P38875	GPI16	SYASDIGAPLFN[+203.1]	2	heavy	955.959102	y7	1049.52408	50.7
P38875	GPI16	SYASDIGAPLFN[+203.1]	2	heavy	955.959102	y6	936.440017	50.7
P38875	GPI16	SYASDIGAPLFN[+203.1]	2	heavy	955.959102	y5	789.371603	50.7
P38875	GPI16	SYASDIGAPLFN[+203.1]	2	heavy	955.959102	y4	472.249303	50.7
P38875	GPI16	SYASDIGAPLFN[+203.1]	2	heavy	955.959102	b2	251.102633	50.7
P38875	GPI16	SYASDIGAPLFN[+203.1]	2	heavy	955.959102	b3	322.139747	50.7
P38875	GPI16	AIPPLLESTATR	2	light	634.864077	y10	1084.5997	45.38
P38875	GPI16	AIPPLLESTATR	2	light	634.864077	y9	987.546936	45.38
P38875	GPI16	AIPPLLESTATR	2	light	634.864077	y8	890.494172	45.38
P38875	GPI16	AIPPLLESTATR	2	light	634.864077	y7	777.410108	45.38
P38875	GPI16	AIPPLLESTATR	2	light	634.864077	y6	664.326044	45.38
P38875	GPI16	AIPPLLESTATR	2	light	634.864077	y5	535.283451	45.38
P38875	GPI16	AIPPLLESTATR	2	heavy	637.874141	y10	1090.61983	45.38
P38875	GPI16	AIPPLLESTATR	2	heavy	637.874141	y9	993.567065	45.38
P38875	GPI16	AIPPLLESTATR	2	heavy	637.874141	y8	896.514301	45.38
P38875	GPI16	AIPPLLESTATR	2	heavy	637.874141	y7	783.430237	45.38
P38875	GPI16	AIPPLLESTATR	2	heavy	637.874141	y6	670.346173	45.38
P38875	GPI16	AIPPLLESTATR	2	heavy	637.874141	y5	541.30358	45.38
P38875	GPI16	VTPIVPVPIHVSR	3	light	471.957399	y9	1003.60473	60.33
P38875	GPI16	VTPIVPVPIHVSR	3	light	471.957399	y8	904.536312	60.33
P38875	GPI16	VTPIVPVPIHVSR	3	light	471.957399	y7	807.483548	60.33
P38875	GPI16	VTPIVPVPIHVSR	3	light	471.957399	y6	708.415134	60.33
P38875	GPI16	VTPIVPVPIHVSR	3	light	471.957399	y5	611.36237	60.33
P38875	GPI16	VTPIVPVPIHVSR	3	light	471.957399	y4	498.278306	60.33
P38875	GPI16	VTPIVPVPIHVSR	3	light	471.957399	y3	361.219394	60.33
P38875	GPI16	VTPIVPVPIHVSR	3	heavy	473.964109	y9	1009.62486	60.33
P38875	GPI16	VTPIVPVPIHVSR	3	heavy	473.964109	y8	910.556441	60.33
P38875	GPI16	VTPIVPVPIHVSR	3	heavy	473.964109	y7	813.503677	60.33
P38875	GPI16	VTPIVPVPIHVSR	3	heavy	473.964109	y6	714.435263	60.33
P38875	GPI16	VTPIVPVPIHVSR	3	heavy	473.964109	y5	617.382499	60.33
P38875	GPI16	VTPIVPVPIHVSR	3	heavy	473.964109	y4	504.298435	60.33
P38875	GPI16	VTPIVPVPIHVSR	3	heavy	473.964109	y3	367.239523	60.33
Q07830	GPI13	N[+203.1]ISNTPPTSDPE	2	light	801.878307	y12	1285.62704	-9.49
Q07830	GPI13	N[+203.1]ISNTPPTSDPE	2	light	801.878307	y11	1172.54297	-9.49
Q07830	GPI13	N[+203.1]ISNTPPTSDPE	2	light	801.878307	y10	1085.51094	-9.49
Q07830	GPI13	N[+203.1]ISNTPPTSDPE	2	light	801.878307	y9	971.468017	-9.49
Q07830	GPI13	N[+203.1]ISNTPPTSDPE	2	light	801.878307	y8	870.420339	-9.49
Q07830	GPI13	N[+203.1]ISNTPPTSDPE	2	light	801.878307	y7	773.367575	-9.49
Q07830	GPI13	N[+203.1]ISNTPPTSDPE	2	light	801.878307	y3	373.208161	-9.49
Q07830	GPI13	N[+203.1]ISNTPPTSDPE	2	light	801.878307	y8	435.713807	-9.49
Q07830	GPI13	N[+203.1]ISNTPPTSDPE	2	light	801.878307	y7	387.187425	-9.49
Q07830	GPI13	N[+203.1]ISNTPPTSDPE	2	heavy	805.885406	y12	1293.64124	-9.49

Q07830	GPI13	N[+203.1]ISNTPPTSDPE	2	heavy	805.885406	y11	1180.55717	-9.49
Q07830	GPI13	N[+203.1]ISNTPPTSDPE	2	heavy	805.885406	y10	1093.52514	-9.49
Q07830	GPI13	N[+203.1]ISNTPPTSDPE	2	heavy	805.885406	y9	979.482216	-9.49
Q07830	GPI13	N[+203.1]ISNTPPTSDPE	2	heavy	805.885406	y8	878.434538	-9.49
Q07830	GPI13	N[+203.1]ISNTPPTSDPE	2	heavy	805.885406	y7	781.381774	-9.49
Q07830	GPI13	N[+203.1]ISNTPPTSDPE	2	heavy	805.885406	y3	381.22236	-9.49
Q07830	GPI13	N[+203.1]ISNTPPTSDPE	2	heavy	805.885406	y8	439.720907	-9.49
Q07830	GPI13	N[+203.1]ISNTPPTSDPE	2	heavy	805.885406	y7	391.194525	-9.49
Q07830	GPI13	ETSNYNIDNLGHDYR	2	light	905.903179	y10	1216.57053	25.6
Q07830	GPI13	ETSNYNIDNLGHDYR	2	light	905.903179	y9	1102.5276	25.6
Q07830	GPI13	ETSNYNIDNLGHDYR	2	light	905.903179	y8	989.443534	25.6
Q07830	GPI13	ETSNYNIDNLGHDYR	2	light	905.903179	y7	874.41659	25.6
Q07830	GPI13	ETSNYNIDNLGHDYR	2	light	905.903179	y6	760.373663	25.6
Q07830	GPI13	ETSNYNIDNLGHDYR	2	light	905.903179	y5	647.289599	25.6
Q07830	GPI13	ETSNYNIDNLGHDYR	2	light	905.903179	y2	338.18228	25.6
Q07830	GPI13	ETSNYNIDNLGHDYR	2	heavy	908.913243	y10	1222.59065	25.6
Q07830	GPI13	ETSNYNIDNLGHDYR	2	heavy	908.913243	y9	1108.54773	25.6
Q07830	GPI13	ETSNYNIDNLGHDYR	2	heavy	908.913243	y8	995.463663	25.6
Q07830	GPI13	ETSNYNIDNLGHDYR	2	heavy	908.913243	y7	880.436719	25.6
Q07830	GPI13	ETSNYNIDNLGHDYR	2	heavy	908.913243	y6	766.393792	25.6
Q07830	GPI13	ETSNYNIDNLGHDYR	2	heavy	908.913243	y5	653.309728	25.6
Q07830	GPI13	ETSNYNIDNLGHDYR	2	heavy	908.913243	y2	344.202409	25.6
P36016	LHS1	LSN[+203.1]ESELYDVFT	2	light	888.420339	y10	1258.59501	64.41
P36016	LHS1	LSN[+203.1]ESELYDVFT	2	light	888.420339	y9	1129.55242	64.41
P36016	LHS1	LSN[+203.1]ESELYDVFT	2	light	888.420339	y8	1042.52039	64.41
P36016	LHS1	LSN[+203.1]ESELYDVFT	2	light	888.420339	y7	913.477794	64.41
P36016	LHS1	LSN[+203.1]ESELYDVFT	2	light	888.420339	y6	800.39373	64.41
P36016	LHS1	LSN[+203.1]ESELYDVFT	2	light	888.420339	y5	637.330401	64.41
P36016	LHS1	LSN[+203.1]ESELYDVFT	2	light	888.420339	y4	522.303458	64.41
P36016	LHS1	LSN[+203.1]ESELYDVFT	2	light	888.420339	y3	423.235044	64.41
P36016	LHS1	LSN[+203.1]ESELYDVFT	2	heavy	891.430403	y10	1264.61514	64.41
P36016	LHS1	LSN[+203.1]ESELYDVFT	2	heavy	891.430403	y9	1135.57254	64.41
P36016	LHS1	LSN[+203.1]ESELYDVFT	2	heavy	891.430403	y8	1048.54052	64.41
P36016	LHS1	LSN[+203.1]ESELYDVFT	2	heavy	891.430403	y7	919.497923	64.41
P36016	LHS1	LSN[+203.1]ESELYDVFT	2	heavy	891.430403	y6	806.413859	64.41
P36016	LHS1	LSN[+203.1]ESELYDVFT	2	heavy	891.430403	y5	643.35053	64.41
P36016	LHS1	LSN[+203.1]ESELYDVFT	2	heavy	891.430403	y4	528.323587	64.41
P36016	LHS1	LSN[+203.1]ESELYDVFT	2	heavy	891.430403	y3	429.255173	64.41
P36016	LHS1	AIVVSPQAPLELVLTPEA	3	light	659.053986	y11	1209.70892	110.06
P36016	LHS1	AIVVSPQAPLELVLTPEA	3	light	659.053986	y8	870.529495	110.06
P36016	LHS1	AIVVSPQAPLELVLTPEA	3	light	659.053986	y7	757.445431	110.06
P36016	LHS1	AIVVSPQAPLELVLTPEA	3	light	659.053986	y6	658.377017	110.06
P36016	LHS1	AIVVSPQAPLELVLTPEA	3	light	659.053986	y5	545.292953	110.06
P36016	LHS1	AIVVSPQAPLELVLTPEA	3	light	659.053986	y4	444.245275	110.06
P36016	LHS1	AIVVSPQAPLELVLTPEA	3	heavy	661.725385	y11	1217.72312	110.06
P36016	LHS1	AIVVSPQAPLELVLTPEA	3	heavy	661.725385	y8	878.543694	110.06
P36016	LHS1	AIVVSPQAPLELVLTPEA	3	heavy	661.725385	y7	765.45963	110.06
P36016	LHS1	AIVVSPQAPLELVLTPEA	3	heavy	661.725385	y6	666.391216	110.06
P36016	LHS1	AIVVSPQAPLELVLTPEA	3	heavy	661.725385	y5	553.307152	110.06
P36016	LHS1	AIVVSPQAPLELVLTPEA	3	heavy	661.725385	y4	452.259474	110.06
P36016	LHS1	ALSTWEETLTSFK	2	light	756.882664	y9	1140.55717	86.05
P36016	LHS1	ALSTWEETLTSFK	2	light	756.882664	y8	954.477853	86.05
P36016	LHS1	ALSTWEETLTSFK	2	light	756.882664	y7	825.43526	86.05
P36016	LHS1	ALSTWEETLTSFK	2	light	756.882664	y6	696.392667	86.05
P36016	LHS1	ALSTWEETLTSFK	2	light	756.882664	y5	595.344989	86.05
P36016	LHS1	ALSTWEETLTSFK	2	light	756.882664	y4	482.260925	86.05
P36016	LHS1	ALSTWEETLTSFK	2	light	756.882664	y3	381.213246	86.05
P36016	LHS1	ALSTWEETLTSFK	2	heavy	760.889763	y9	1148.57137	86.05
P36016	LHS1	ALSTWEETLTSFK	2	heavy	760.889763	y8	962.492052	86.05
P36016	LHS1	ALSTWEETLTSFK	2	heavy	760.889763	y7	833.449459	86.05
P36016	LHS1	ALSTWEETLTSFK	2	heavy	760.889763	y6	704.406866	86.05
P36016	LHS1	ALSTWEETLTSFK	2	heavy	760.889763	y5	603.359188	86.05
P36016	LHS1	ALSTWEETLTSFK	2	heavy	760.889763	y4	490.275124	86.05

P36016	LHS1	ALSTWEETLTSFK	2	heavy	760.889763	y3	389.227445	86.05
P39105	PLB1	DAGFN[+203.1]ISLADVV	2	light	862.417933	y9	1016.55236	97.47
P39105	PLB1	DAGFN[+203.1]ISLADVV	2	light	862.417933	y8	903.468292	97.47
P39105	PLB1	DAGFN[+203.1]ISLADVV	2	light	862.417933	y7	816.436263	97.47
P39105	PLB1	DAGFN[+203.1]ISLADVV	2	light	862.417933	y6	703.352199	97.47
P39105	PLB1	DAGFN[+203.1]ISLADVV	2	light	862.417933	y4	517.288142	97.47
P39105	PLB1	DAGFN[+203.1]ISLADVV	2	light	862.417933	y3	418.219728	97.47
P39105	PLB1	DAGFN[+203.1]ISLADVV	2	light	862.417933	b2	187.071333	97.47
P39105	PLB1	DAGFN[+203.1]ISLADVV	2	heavy	865.427998	y9	1022.57249	97.47
P39105	PLB1	DAGFN[+203.1]ISLADVV	2	heavy	865.427998	y8	909.488421	97.47
P39105	PLB1	DAGFN[+203.1]ISLADVV	2	heavy	865.427998	y7	822.456392	97.47
P39105	PLB1	DAGFN[+203.1]ISLADVV	2	heavy	865.427998	y6	709.372328	97.47
P39105	PLB1	DAGFN[+203.1]ISLADVV	2	heavy	865.427998	y4	523.308271	97.47
P39105	PLB1	DAGFN[+203.1]ISLADVV	2	heavy	865.427998	y3	424.239857	97.47
P39105	PLB1	DAGFN[+203.1]ISLADVV	2	heavy	865.427998	b2	187.071333	97.47
P39105	PLB1	N[+203.1]LTDLEYIPPLIV	2	light	1217.14922	y12	1381.8202	121.93
P39105	PLB1	N[+203.1]LTDLEYIPPLIV	2	light	1217.14922	y11	1268.73613	121.93
P39105	PLB1	N[+203.1]LTDLEYIPPLIV	2	light	1217.14922	y10	1171.68337	121.93
P39105	PLB1	N[+203.1]LTDLEYIPPLIV	2	light	1217.14922	y9	1074.63061	121.93
P39105	PLB1	N[+203.1]LTDLEYIPPLIV	2	light	1217.14922	y8	961.546542	121.93
P39105	PLB1	N[+203.1]LTDLEYIPPLIV	2	light	1217.14922	y7	848.462478	121.93
P39105	PLB1	N[+203.1]LTDLEYIPPLIV	2	light	1217.14922	y6	749.394064	121.93
P39105	PLB1	N[+203.1]LTDLEYIPPLIV	2	light	1217.14922	y5	586.330736	121.93
P39105	PLB1	N[+203.1]LTDLEYIPPLIV	2	light	1217.14922	y4	473.246672	121.93
P39105	PLB1	N[+203.1]LTDLEYIPPLIV	2	light	1217.14922	b3	532.261319	121.93
P39105	PLB1	N[+203.1]LTDLEYIPPLIV	2	light	1217.14922	b4	647.288262	121.93
P39105	PLB1	N[+203.1]LTDLEYIPPLIV	2	heavy	1220.15929	y12	1387.84033	121.93
P39105	PLB1	N[+203.1]LTDLEYIPPLIV	2	heavy	1220.15929	y11	1274.75626	121.93
P39105	PLB1	N[+203.1]LTDLEYIPPLIV	2	heavy	1220.15929	y10	1177.7035	121.93
P39105	PLB1	N[+203.1]LTDLEYIPPLIV	2	heavy	1220.15929	y9	1080.65074	121.93
P39105	PLB1	N[+203.1]LTDLEYIPPLIV	2	heavy	1220.15929	y8	967.566671	121.93
P39105	PLB1	N[+203.1]LTDLEYIPPLIV	2	heavy	1220.15929	y7	854.482607	121.93
P39105	PLB1	N[+203.1]LTDLEYIPPLIV	2	heavy	1220.15929	y6	755.414193	121.93
P39105	PLB1	N[+203.1]LTDLEYIPPLIV	2	heavy	1220.15929	y5	592.350865	121.93
P39105	PLB1	N[+203.1]LTDLEYIPPLIV	2	heavy	1220.15929	y4	479.266801	121.93
P39105	PLB1	N[+203.1]LTDLEYIPPLIV	2	heavy	1220.15929	b3	532.261319	121.93
P39105	PLB1	N[+203.1]LTDLEYIPPLIV	2	heavy	1220.15929	b4	647.288262	121.93
P39105	PLB1	IPLVPLLQK	2	light	510.844428	y7	810.544751	75.23
P39105	PLB1	IPLVPLLQK	2	light	510.844428	y6	697.460687	75.23
P39105	PLB1	IPLVPLLQK	2	light	510.844428	y5	598.392273	75.23
P39105	PLB1	IPLVPLLQK	2	light	510.844428	y7	405.776014	75.23
P39105	PLB1	IPLVPLLQK	2	light	510.844428	b3	324.228168	75.23
P39105	PLB1	IPLVPLLQK	2	light	510.844428	b4	423.296582	75.23
P39105	PLB1	IPLVPLLQK	2	heavy	514.851527	y7	818.55895	75.23
P39105	PLB1	IPLVPLLQK	2	heavy	514.851527	y6	705.474886	75.23
P39105	PLB1	IPLVPLLQK	2	heavy	514.851527	y5	606.406472	75.23
P39105	PLB1	IPLVPLLQK	2	heavy	514.851527	y7	409.783113	75.23
P39105	PLB1	IPLVPLLQK	2	heavy	514.851527	b3	324.228168	75.23
P39105	PLB1	IPLVPLLQK	2	heavy	514.851527	b4	423.296582	75.23
P39105	PLB1	IAVAC[+57]SGGGYR	2	light	555.771665	y10	997.45199	-5.55
P39105	PLB1	IAVAC[+57]SGGGYR	2	light	555.771665	y9	926.414876	-5.55
P39105	PLB1	IAVAC[+57]SGGGYR	2	light	555.771665	y8	827.346462	-5.55
P39105	PLB1	IAVAC[+57]SGGGYR	2	light	555.771665	y7	756.309348	-5.55
P39105	PLB1	IAVAC[+57]SGGGYR	2	light	555.771665	y6	596.2787	-5.55
P39105	PLB1	IAVAC[+57]SGGGYR	2	light	555.771665	y5	509.246672	-5.55
P39105	PLB1	IAVAC[+57]SGGGYR	2	light	555.771665	b2	185.128454	-5.55
P39105	PLB1	IAVAC[+57]SGGGYR	2	light	555.771665	b3	284.196868	-5.55
P39105	PLB1	IAVAC[+57]SGGGYR	2	heavy	558.78173	y10	1003.47212	-5.55
P39105	PLB1	IAVAC[+57]SGGGYR	2	heavy	558.78173	y9	932.435005	-5.55
P39105	PLB1	IAVAC[+57]SGGGYR	2	heavy	558.78173	y8	833.366591	-5.55
P39105	PLB1	IAVAC[+57]SGGGYR	2	heavy	558.78173	y7	762.329477	-5.55
P39105	PLB1	IAVAC[+57]SGGGYR	2	heavy	558.78173	y6	602.298829	-5.55
P39105	PLB1	IAVAC[+57]SGGGYR	2	heavy	558.78173	y5	515.266801	-5.55

P39105	PLB1	IAVAC[+57]SGGGYR	2	heavy	558.78173	b2	185.128454	-5.55
P39105	PLB1	IAVAC[+57]SGGGYR	2	heavy	558.78173	b3	284.196868	-5.55
Q03674	PLB2	SIVNPGGSN[+203.1]LTY	2	light	962.486544	y10	1356.66415	46.6
Q03674	PLB2	SIVNPGGSN[+203.1]LTY	2	light	962.486544	y9	1299.64269	46.6
Q03674	PLB2	SIVNPGGSN[+203.1]LTY	2	light	962.486544	y8	1212.61066	46.6
Q03674	PLB2	SIVNPGGSN[+203.1]LTY	2	light	962.486544	y7	895.488358	46.6
Q03674	PLB2	SIVNPGGSN[+203.1]LTY	2	light	962.486544	y6	782.404294	46.6
Q03674	PLB2	SIVNPGGSN[+203.1]LTY	2	light	962.486544	y5	681.356616	46.6
Q03674	PLB2	SIVNPGGSN[+203.1]LTY	2	light	962.486544	y4	518.293287	46.6
Q03674	PLB2	SIVNPGGSN[+203.1]LTY	2	light	962.486544	y3	417.245609	46.6
Q03674	PLB2	SIVNPGGSN[+203.1]LTY	2	light	962.486544	b3	300.191782	46.6
Q03674	PLB2	SIVNPGGSN[+203.1]LTY	2	heavy	965.496609	y10	1362.68428	46.6
Q03674	PLB2	SIVNPGGSN[+203.1]LTY	2	heavy	965.496609	y9	1305.66282	46.6
Q03674	PLB2	SIVNPGGSN[+203.1]LTY	2	heavy	965.496609	y8	1218.63079	46.6
Q03674	PLB2	SIVNPGGSN[+203.1]LTY	2	heavy	965.496609	y7	901.508488	46.6
Q03674	PLB2	SIVNPGGSN[+203.1]LTY	2	heavy	965.496609	y6	788.424423	46.6
Q03674	PLB2	SIVNPGGSN[+203.1]LTY	2	heavy	965.496609	y5	687.376745	46.6
Q03674	PLB2	SIVNPGGSN[+203.1]LTY	2	heavy	965.496609	y4	524.313416	46.6
Q03674	PLB2	SIVNPGGSN[+203.1]LTY	2	heavy	965.496609	y3	423.265738	46.6
Q03674	PLB2	SIVNPGGSN[+203.1]LTY	2	heavy	965.496609	b3	300.191782	46.6
Q03674	PLB2	SDAGFN[+203.1]ISLSDL	2	light	927.947055	y10	1377.70087	98.73
Q03674	PLB2	SDAGFN[+203.1]ISLSDL	2	light	927.947055	y9	1060.57857	98.73
Q03674	PLB2	SDAGFN[+203.1]ISLSDL	2	light	927.947055	y8	947.494506	98.73
Q03674	PLB2	SDAGFN[+203.1]ISLSDL	2	light	927.947055	y7	860.462478	98.73
Q03674	PLB2	SDAGFN[+203.1]ISLSDL	2	light	927.947055	y6	747.378414	98.73
Q03674	PLB2	SDAGFN[+203.1]ISLSDL	2	light	927.947055	y5	660.346386	98.73
Q03674	PLB2	SDAGFN[+203.1]ISLSDL	2	light	927.947055	y4	545.319443	98.73
Q03674	PLB2	SDAGFN[+203.1]ISLSDL	2	light	927.947055	b3	137.555319	98.73
Q03674	PLB2	SDAGFN[+203.1]ISLSDL	2	heavy	930.957119	y10	1383.721	98.73
Q03674	PLB2	SDAGFN[+203.1]ISLSDL	2	heavy	930.957119	y9	1066.5987	98.73
Q03674	PLB2	SDAGFN[+203.1]ISLSDL	2	heavy	930.957119	y8	953.514635	98.73
Q03674	PLB2	SDAGFN[+203.1]ISLSDL	2	heavy	930.957119	y7	866.482607	98.73
Q03674	PLB2	SDAGFN[+203.1]ISLSDL	2	heavy	930.957119	y6	753.398543	98.73
Q03674	PLB2	SDAGFN[+203.1]ISLSDL	2	heavy	930.957119	y5	666.366515	98.73
Q03674	PLB2	SDAGFN[+203.1]ISLSDL	2	heavy	930.957119	y4	551.339572	98.73
Q03674	PLB2	SDAGFN[+203.1]ISLSDL	2	heavy	930.957119	b3	137.555319	98.73
Q03674	PLB2	IGIAC[+57]SGGGYR	2	light	555.771665	y10	997.45199	1.06
Q03674	PLB2	IGIAC[+57]SGGGYR	2	light	555.771665	y8	827.346462	1.06
Q03674	PLB2	IGIAC[+57]SGGGYR	2	light	555.771665	y7	756.309348	1.06
Q03674	PLB2	IGIAC[+57]SGGGYR	2	light	555.771665	y6	596.2787	1.06
Q03674	PLB2	IGIAC[+57]SGGGYR	2	light	555.771665	y5	509.246672	1.06
Q03674	PLB2	IGIAC[+57]SGGGYR	2	light	555.771665	b2	171.112804	1.06
Q03674	PLB2	IGIAC[+57]SGGGYR	2	light	555.771665	b3	284.196868	1.06
Q03674	PLB2	IGIAC[+57]SGGGYR	2	heavy	558.78173	y10	1003.47212	1.06
Q03674	PLB2	IGIAC[+57]SGGGYR	2	heavy	558.78173	y8	833.366591	1.06
Q03674	PLB2	IGIAC[+57]SGGGYR	2	heavy	558.78173	y7	762.329477	1.06
Q03674	PLB2	IGIAC[+57]SGGGYR	2	heavy	558.78173	y6	602.298829	1.06
Q03674	PLB2	IGIAC[+57]SGGGYR	2	heavy	558.78173	y5	515.266801	1.06
Q03674	PLB2	IGIAC[+57]SGGGYR	2	heavy	558.78173	b2	171.112804	1.06
Q03674	PLB2	IGIAC[+57]SGGGYR	2	heavy	558.78173	b3	284.196868	1.06
Q03674	PLB2	EALHSFLSR	2	light	530.282723	y7	859.478462	15.56
Q03674	PLB2	EALHSFLSR	2	light	530.282723	y6	746.394398	15.56
Q03674	PLB2	EALHSFLSR	2	light	530.282723	y5	609.335487	15.56
Q03674	PLB2	EALHSFLSR	2	light	530.282723	y4	522.303458	15.56
Q03674	PLB2	EALHSFLSR	2	light	530.282723	y3	375.235044	15.56
Q03674	PLB2	EALHSFLSR	2	light	530.282723	y6	373.700837	15.56
Q03674	PLB2	EALHSFLSR	2	heavy	533.292787	y7	865.498591	15.56
Q03674	PLB2	EALHSFLSR	2	heavy	533.292787	y6	752.414527	15.56
Q03674	PLB2	EALHSFLSR	2	heavy	533.292787	y5	615.355616	15.56
Q03674	PLB2	EALHSFLSR	2	heavy	533.292787	y4	528.323587	15.56
Q03674	PLB2	EALHSFLSR	2	heavy	533.292787	y3	381.255173	15.56
Q03674	PLB2	EALHSFLSR	2	heavy	533.292787	y6	376.710902	15.56
P32623	CRH2	N[+203.1]ETYN[+203.1]A	2	light	788.354665	y9	1258.57975	-33.32

P32623	CRH2	N[+203.1]ETYN[+203.1]A	2	light	788.354665	y8	1129.53716	-33.32
P32623	CRH2	N[+203.1]ETYN[+203.1]A	2	light	788.354665	y7	1028.48948	-33.32
P32623	CRH2	N[+203.1]ETYN[+203.1]A	2	light	788.354665	y6	865.426153	-33.32
P32623	CRH2	N[+203.1]ETYN[+203.1]A	2	light	788.354665	y5	548.303852	-33.32
P32623	CRH2	N[+203.1]ETYN[+203.1]A	2	light	788.354665	y4	477.266738	-33.32
P32623	CRH2	N[+203.1]ETYN[+203.1]A	2	light	788.354665	y3	376.21906	-33.32
P32623	CRH2	N[+203.1]ETYN[+203.1]A	2	light	788.354665	y2	138.089329	-33.32
P32623	CRH2	N[+203.1]ETYN[+203.1]A	2	heavy	792.361764	y9	1266.59395	-33.32
P32623	CRH2	N[+203.1]ETYN[+203.1]A	2	heavy	792.361764	y8	1137.55136	-33.32
P32623	CRH2	N[+203.1]ETYN[+203.1]A	2	heavy	792.361764	y7	1036.50368	-33.32
P32623	CRH2	N[+203.1]ETYN[+203.1]A	2	heavy	792.361764	y6	873.440352	-33.32
P32623	CRH2	N[+203.1]ETYN[+203.1]A	2	heavy	792.361764	y5	556.318051	-33.32
P32623	CRH2	N[+203.1]ETYN[+203.1]A	2	heavy	792.361764	y4	485.280937	-33.32
P32623	CRH2	N[+203.1]ETYN[+203.1]A	2	heavy	792.361764	y3	384.233259	-33.32
P32623	CRH2	N[+203.1]ETYN[+203.1]A	2	heavy	792.361764	y2	142.096428	-33.32
P32623	CRH2	N[+203.1]GTSAYVYTSS	2	light	1014.47584	y11	1231.6205	48.5
P32623	CRH2	N[+203.1]GTSAYVYTSS	2	light	1014.47584	y10	1132.55208	48.5
P32623	CRH2	N[+203.1]GTSAYVYTSS	2	light	1014.47584	y9	969.488752	48.5
P32623	CRH2	N[+203.1]GTSAYVYTSS	2	light	1014.47584	y7	781.409046	48.5
P32623	CRH2	N[+203.1]GTSAYVYTSS	2	light	1014.47584	y4	478.302396	48.5
P32623	CRH2	N[+203.1]GTSAYVYTSS	2	light	1014.47584	y3	331.233982	48.5
P32623	CRH2	N[+203.1]GTSAYVYTSS	2	heavy	1018.48294	y11	1239.63469	48.5
P32623	CRH2	N[+203.1]GTSAYVYTSS	2	heavy	1018.48294	y10	1140.56628	48.5
P32623	CRH2	N[+203.1]GTSAYVYTSS	2	heavy	1018.48294	y9	977.502951	48.5
P32623	CRH2	N[+203.1]GTSAYVYTSS	2	heavy	1018.48294	y7	789.423245	48.5
P32623	CRH2	N[+203.1]GTSAYVYTSS	2	heavy	1018.48294	y4	486.316595	48.5
P32623	CRH2	N[+203.1]GTSAYVYTSS	2	heavy	1018.48294	y3	339.248181	48.5
P32623	CRH2	NSGGTVLSSTR	2	light	539.778001	y10	964.505799	-19.1
P32623	CRH2	NSGGTVLSSTR	2	light	539.778001	y9	877.473771	-19.1
P32623	CRH2	NSGGTVLSSTR	2	light	539.778001	y8	820.452307	-19.1
P32623	CRH2	NSGGTVLSSTR	2	light	539.778001	y7	763.430844	-19.1
P32623	CRH2	NSGGTVLSSTR	2	light	539.778001	y6	662.383165	-19.1
P32623	CRH2	NSGGTVLSSTR	2	light	539.778001	y5	563.314751	-19.1
P32623	CRH2	NSGGTVLSSTR	2	light	539.778001	y4	450.230687	-19.1
P32623	CRH2	NSGGTVLSSTR	2	heavy	542.788066	y10	970.525928	-19.1
P32623	CRH2	NSGGTVLSSTR	2	heavy	542.788066	y9	883.4939	-19.1
P32623	CRH2	NSGGTVLSSTR	2	heavy	542.788066	y8	826.472436	-19.1
P32623	CRH2	NSGGTVLSSTR	2	heavy	542.788066	y7	769.450973	-19.1
P32623	CRH2	NSGGTVLSSTR	2	heavy	542.788066	y6	668.403294	-19.1
P32623	CRH2	NSGGTVLSSTR	2	heavy	542.788066	y5	569.33488	-19.1
P32623	CRH2	NSGGTVLSSTR	2	heavy	542.788066	y4	456.250816	-19.1
P32623	CRH2	YQYPQTPSK	2	light	556.274563	y7	820.419945	-5.31
P32623	CRH2	YQYPQTPSK	2	light	556.274563	y6	657.356616	-5.31
P32623	CRH2	YQYPQTPSK	2	light	556.274563	y5	560.303852	-5.31
P32623	CRH2	YQYPQTPSK	2	light	556.274563	y4	432.245275	-5.31
P32623	CRH2	YQYPQTPSK	2	light	556.274563	y3	331.197596	-5.31
P32623	CRH2	YQYPQTPSK	2	light	556.274563	y2	234.144832	-5.31
P32623	CRH2	YQYPQTPSK	2	heavy	560.281663	y7	828.434144	-5.31
P32623	CRH2	YQYPQTPSK	2	heavy	560.281663	y6	665.370815	-5.31
P32623	CRH2	YQYPQTPSK	2	heavy	560.281663	y5	568.318051	-5.31
P32623	CRH2	YQYPQTPSK	2	heavy	560.281663	y4	440.259474	-5.31
P32623	CRH2	YQYPQTPSK	2	heavy	560.281663	y3	339.211795	-5.31
P32623	CRH2	YQYPQTPSK	2	heavy	560.281663	y2	242.159031	-5.31
P54003	SUR7	FYWVQGN[+203.1]TTGI	2	light	1165.0402	y11	1130.54364	53.25
P54003	SUR7	FYWVQGN[+203.1]TTGI	2	light	1165.0402	y10	1029.49596	53.25
P54003	SUR7	FYWVQGN[+203.1]TTGI	2	light	1165.0402	y9	972.474499	53.25
P54003	SUR7	FYWVQGN[+203.1]TTGI	2	light	1165.0402	y8	859.390435	53.25
P54003	SUR7	FYWVQGN[+203.1]TTGI	2	light	1165.0402	y5	577.25763	53.25
P54003	SUR7	FYWVQGN[+203.1]TTGI	2	light	1165.0402	y4	520.236166	53.25
P54003	SUR7	FYWVQGN[+203.1]TTGI	2	light	1165.0402	y3	405.209223	53.25
P54003	SUR7	FYWVQGN[+203.1]TTGI	2	light	1165.0402	y2	276.16663	53.25
P54003	SUR7	FYWVQGN[+203.1]TTGI	2	light	1165.0402	b2	311.139019	53.25
P54003	SUR7	FYWVQGN[+203.1]TTGI	2	light	1165.0402	b3	497.218332	53.25

P54003	SUR7	FYWVQGN[+203.1]TTGI	2	heavy	1168.05027	y11	1136.56377	53.25
P54003	SUR7	FYWVQGN[+203.1]TTGI	2	heavy	1168.05027	y10	1035.51609	53.25
P54003	SUR7	FYWVQGN[+203.1]TTGI	2	heavy	1168.05027	y9	978.494628	53.25
P54003	SUR7	FYWVQGN[+203.1]TTGI	2	heavy	1168.05027	y8	865.410564	53.25
P54003	SUR7	FYWVQGN[+203.1]TTGI	2	heavy	1168.05027	y5	583.277759	53.25
P54003	SUR7	FYWVQGN[+203.1]TTGI	2	heavy	1168.05027	y4	526.256295	53.25
P54003	SUR7	FYWVQGN[+203.1]TTGI	2	heavy	1168.05027	y3	411.229352	53.25
P54003	SUR7	FYWVQGN[+203.1]TTGI	2	heavy	1168.05027	y2	282.186759	53.25
P54003	SUR7	FYWVQGN[+203.1]TTGI	2	heavy	1168.05027	b2	311.139019	53.25
P54003	SUR7	FYWVQGN[+203.1]TTGI	2	heavy	1168.05027	b3	497.218332	53.25
P54003	SUR7	LASTYSIDNSR	2	light	613.804216	y10	1113.51709	3.28
P54003	SUR7	LASTYSIDNSR	2	light	613.804216	y9	1042.47998	3.28
P54003	SUR7	LASTYSIDNSR	2	light	613.804216	y8	955.44795	3.28
P54003	SUR7	LASTYSIDNSR	2	light	613.804216	y7	854.400272	3.28
P54003	SUR7	LASTYSIDNSR	2	light	613.804216	y6	691.336943	3.28
P54003	SUR7	LASTYSIDNSR	2	light	613.804216	y5	604.304915	3.28
P54003	SUR7	LASTYSIDNSR	2	light	613.804216	y4	491.220851	3.28
P54003	SUR7	LASTYSIDNSR	2	light	613.804216	y3	376.193908	3.28
P54003	SUR7	LASTYSIDNSR	2	heavy	616.814281	y10	1119.53722	3.28
P54003	SUR7	LASTYSIDNSR	2	heavy	616.814281	y9	1048.50011	3.28
P54003	SUR7	LASTYSIDNSR	2	heavy	616.814281	y8	961.468079	3.28
P54003	SUR7	LASTYSIDNSR	2	heavy	616.814281	y7	860.420401	3.28
P54003	SUR7	LASTYSIDNSR	2	heavy	616.814281	y6	697.357072	3.28
P54003	SUR7	LASTYSIDNSR	2	heavy	616.814281	y5	610.325044	3.28
P54003	SUR7	LASTYSIDNSR	2	heavy	616.814281	y4	497.24098	3.28
P54003	SUR7	LASTYSIDNSR	2	heavy	616.814281	y3	382.214037	3.28
P54003	SUR7	WTFWGAC[+57]LQDK	2	light	706.326804	y9	1124.51934	79.41
P54003	SUR7	WTFWGAC[+57]LQDK	2	light	706.326804	y8	977.450927	79.41
P54003	SUR7	WTFWGAC[+57]LQDK	2	light	706.326804	y7	791.371614	79.41
P54003	SUR7	WTFWGAC[+57]LQDK	2	light	706.326804	y6	734.350151	79.41
P54003	SUR7	WTFWGAC[+57]LQDK	2	light	706.326804	y5	663.313037	79.41
P54003	SUR7	WTFWGAC[+57]LQDK	2	light	706.326804	y3	390.198324	79.41
P54003	SUR7	WTFWGAC[+57]LQDK	2	light	706.326804	y2	262.139747	79.41
P54003	SUR7	WTFWGAC[+57]LQDK	2	light	706.326804	b2	288.134267	79.41
P54003	SUR7	WTFWGAC[+57]LQDK	2	heavy	710.333904	y9	1132.53354	79.41
P54003	SUR7	WTFWGAC[+57]LQDK	2	heavy	710.333904	y8	985.465126	79.41
P54003	SUR7	WTFWGAC[+57]LQDK	2	heavy	710.333904	y7	799.385813	79.41
P54003	SUR7	WTFWGAC[+57]LQDK	2	heavy	710.333904	y6	742.36435	79.41
P54003	SUR7	WTFWGAC[+57]LQDK	2	heavy	710.333904	y5	671.327236	79.41
P54003	SUR7	WTFWGAC[+57]LQDK	2	heavy	710.333904	y3	398.212523	79.41
P54003	SUR7	WTFWGAC[+57]LQDK	2	heavy	710.333904	y2	270.153946	79.41
P54003	SUR7	WTFWGAC[+57]LQDK	2	heavy	710.333904	b2	288.134267	79.41
P33754	SEC66	FSNN[+203.1]GTFFETEI	2	light	1146.53135	y11	1321.65219	59.3
P33754	SEC66	FSNN[+203.1]GTFFETEI	2	light	1146.53135	y10	1174.58378	59.3
P33754	SEC66	FSNN[+203.1]GTFFETEI	2	light	1146.53135	y9	1045.54118	59.3
P33754	SEC66	FSNN[+203.1]GTFFETEI	2	light	1146.53135	y8	944.493503	59.3
P33754	SEC66	FSNN[+203.1]GTFFETEI	2	light	1146.53135	y6	686.408317	59.3
P33754	SEC66	FSNN[+203.1]GTFFETEI	2	light	1146.53135	y4	476.271489	59.3
P33754	SEC66	FSNN[+203.1]GTFFETEI	2	light	1146.53135	y2	248.160482	59.3
P33754	SEC66	FSNN[+203.1]GTFFETEI	2	heavy	1150.53845	y11	1329.66639	59.3
P33754	SEC66	FSNN[+203.1]GTFFETEI	2	heavy	1150.53845	y10	1182.59797	59.3
P33754	SEC66	FSNN[+203.1]GTFFETEI	2	heavy	1150.53845	y9	1053.55538	59.3
P33754	SEC66	FSNN[+203.1]GTFFETEI	2	heavy	1150.53845	y8	952.507702	59.3
P33754	SEC66	FSNN[+203.1]GTFFETEI	2	heavy	1150.53845	y6	694.422516	59.3
P33754	SEC66	FSNN[+203.1]GTFFETEI	2	heavy	1150.53845	y4	484.285688	59.3
P33754	SEC66	FSNN[+203.1]GTFFETEI	2	heavy	1150.53845	y2	256.174681	59.3
P33754	SEC66	EIC[+57]FNQALSR	2	light	619.303329	y8	995.472725	32.79
P33754	SEC66	EIC[+57]FNQALSR	2	light	619.303329	y7	835.442077	32.79
P33754	SEC66	EIC[+57]FNQALSR	2	light	619.303329	y6	688.373663	32.79
P33754	SEC66	EIC[+57]FNQALSR	2	light	619.303329	y5	574.330736	32.79
P33754	SEC66	EIC[+57]FNQALSR	2	light	619.303329	y4	446.272158	32.79
P33754	SEC66	EIC[+57]FNQALSR	2	light	619.303329	y3	375.235044	32.79
P33754	SEC66	EIC[+57]FNQALSR	2	heavy	622.313394	y8	1001.49285	32.79

P33754	SEC66	EIC[+57]FNQALSR	2	heavy	622.313394	y7	841.462206	32.79
P33754	SEC66	EIC[+57]FNQALSR	2	heavy	622.313394	y6	694.393792	32.79
P33754	SEC66	EIC[+57]FNQALSR	2	heavy	622.313394	y5	580.350865	32.79
P33754	SEC66	EIC[+57]FNQALSR	2	heavy	622.313394	y4	452.292287	32.79
P33754	SEC66	EIC[+57]FNQALSR	2	heavy	622.313394	y3	381.255173	32.79
P33754	SEC66	LIELEFK	2	light	446.262936	y6	778.434532	49.94
P33754	SEC66	LIELEFK	2	light	446.262936	y5	665.350468	49.94
P33754	SEC66	LIELEFK	2	light	446.262936	y4	536.307875	49.94
P33754	SEC66	LIELEFK	2	light	446.262936	y3	423.223811	49.94
P33754	SEC66	LIELEFK	2	light	446.262936	y2	294.181218	49.94
P33754	SEC66	LIELEFK	2	light	446.262936	y6	389.720904	49.94
P33754	SEC66	LIELEFK	2	heavy	450.270036	y6	786.448731	49.94
P33754	SEC66	LIELEFK	2	heavy	450.270036	y5	673.364667	49.94
P33754	SEC66	LIELEFK	2	heavy	450.270036	y4	544.322074	49.94
P33754	SEC66	LIELEFK	2	heavy	450.270036	y3	431.23801	49.94
P33754	SEC66	LIELEFK	2	heavy	450.270036	y2	302.195417	49.94
P33754	SEC66	LIELEFK	2	heavy	450.270036	y6	393.728003	49.94
P32353	ERG3	LLGLNSGFSN[+203.1]ST	2	light	1220.1343	y10	1146.63648	88.76
P32353	ERG3	LLGLNSGFSN[+203.1]ST	2	light	1220.1343	y9	1045.5888	88.76
P32353	ERG3	LLGLNSGFSN[+203.1]ST	2	light	1220.1343	y8	932.504737	88.76
P32353	ERG3	LLGLNSGFSN[+203.1]ST	2	light	1220.1343	y7	819.420673	88.76
P32353	ERG3	LLGLNSGFSN[+203.1]ST	2	light	1220.1343	y6	691.362095	88.76
P32353	ERG3	LLGLNSGFSN[+203.1]ST	2	light	1220.1343	y5	562.319502	88.76
P32353	ERG3	LLGLNSGFSN[+203.1]ST	2	light	1220.1343	y4	461.271824	88.76
P32353	ERG3	LLGLNSGFSN[+203.1]ST	2	light	1220.1343	y3	348.18776	88.76
P32353	ERG3	LLGLNSGFSN[+203.1]ST	2	heavy	1224.1414	y10	1154.65068	88.76
P32353	ERG3	LLGLNSGFSN[+203.1]ST	2	heavy	1224.1414	y9	1053.603	88.76
P32353	ERG3	LLGLNSGFSN[+203.1]ST	2	heavy	1224.1414	y8	940.518936	88.76
P32353	ERG3	LLGLNSGFSN[+203.1]ST	2	heavy	1224.1414	y7	827.434872	88.76
P32353	ERG3	LLGLNSGFSN[+203.1]ST	2	heavy	1224.1414	y6	699.376294	88.76
P32353	ERG3	LLGLNSGFSN[+203.1]ST	2	heavy	1224.1414	y5	570.333701	88.76
P32353	ERG3	LLGLNSGFSN[+203.1]ST	2	heavy	1224.1414	y4	469.286023	88.76
P32353	ERG3	LLGLNSGFSN[+203.1]ST	2	heavy	1224.1414	y3	356.201959	88.76
P32353	ERG3	VLPASLAANIPVK	2	light	646.900462	y11	1080.64117	64.86
P32353	ERG3	VLPASLAANIPVK	2	light	646.900462	y10	983.588407	64.86
P32353	ERG3	VLPASLAANIPVK	2	light	646.900462	y9	912.551293	64.86
P32353	ERG3	VLPASLAANIPVK	2	light	646.900462	y7	712.435201	64.86
P32353	ERG3	VLPASLAANIPVK	2	light	646.900462	y6	641.398087	64.86
P32353	ERG3	VLPASLAANIPVK	2	light	646.900462	y3	343.233982	64.86
P32353	ERG3	VLPASLAANIPVK	2	light	646.900462	y11	540.824223	64.86
P32353	ERG3	VLPASLAANIPVK	2	heavy	650.907562	y11	1088.65537	64.86
P32353	ERG3	VLPASLAANIPVK	2	heavy	650.907562	y10	991.602606	64.86
P32353	ERG3	VLPASLAANIPVK	2	heavy	650.907562	y9	920.565492	64.86
P32353	ERG3	VLPASLAANIPVK	2	heavy	650.907562	y7	720.4494	64.86
P32353	ERG3	VLPASLAANIPVK	2	heavy	650.907562	y6	649.412286	64.86
P32353	ERG3	VLPASLAANIPVK	2	heavy	650.907562	y3	351.248181	64.86
P32353	ERG3	VLPASLAANIPVK	2	heavy	650.907562	y11	544.831323	64.86
P38248	ECM33	VQTVGGAIEVTGN[+203	2	light	1270.16052	y9	963.535703	88.21
P38248	ECM33	VQTVGGAIEVTGN[+203	2	light	1270.16052	y7	775.455996	88.21
P38248	ECM33	VQTVGGAIEVTGN[+203	2	light	1270.16052	y6	662.371932	88.21
P38248	ECM33	VQTVGGAIEVTGN[+203	2	light	1270.16052	y5	547.344989	88.21
P38248	ECM33	VQTVGGAIEVTGN[+203	2	light	1270.16052	y4	434.260925	88.21
P38248	ECM33	VQTVGGAIEVTGN[+203	2	light	1270.16052	y3	347.228896	88.21
P38248	ECM33	VQTVGGAIEVTGN[+203	2	light	1270.16052	b2	228.134267	88.21
P38248	ECM33	VQTVGGAIEVTGN[+203	2	light	1270.16052	b3	329.181946	88.21
P38248	ECM33	VQTVGGAIEVTGN[+203	2	heavy	1274.16762	y9	971.549902	88.21
P38248	ECM33	VQTVGGAIEVTGN[+203	2	heavy	1274.16762	y7	783.470195	88.21
P38248	ECM33	VQTVGGAIEVTGN[+203	2	heavy	1274.16762	y6	670.386131	88.21
P38248	ECM33	VQTVGGAIEVTGN[+203	2	heavy	1274.16762	y5	555.359188	88.21
P38248	ECM33	VQTVGGAIEVTGN[+203	2	heavy	1274.16762	y4	442.275124	88.21
P38248	ECM33	VQTVGGAIEVTGN[+203	2	heavy	1274.16762	y3	355.243095	88.21
P38248	ECM33	VQTVGGAIEVTGN[+203	2	heavy	1274.16762	b2	228.134267	88.21
P38248	ECM33	VQTVGGAIEVTGN[+203	2	heavy	1274.16762	b3	329.181946	88.21

P38248	ECM33	VNVFNINNNR	2	light	602.315085	y8	990.511554	29.44
P38248	ECM33	VNVFNINNNR	2	light	602.315085	y7	891.44314	29.44
P38248	ECM33	VNVFNINNNR	2	light	602.315085	y6	744.374726	29.44
P38248	ECM33	VNVFNINNNR	2	light	602.315085	y5	630.331798	29.44
P38248	ECM33	VNVFNINNNR	2	light	602.315085	y4	517.247734	29.44
P38248	ECM33	VNVFNINNNR	2	light	602.315085	b2	214.118617	29.44
P38248	ECM33	VNVFNINNNR	2	light	602.315085	b3	313.187031	29.44
P38248	ECM33	VNVFNINNNR	2	heavy	605.32515	y8	996.531683	29.44
P38248	ECM33	VNVFNINNNR	2	heavy	605.32515	y7	897.463269	29.44
P38248	ECM33	VNVFNINNNR	2	heavy	605.32515	y6	750.394855	29.44
P38248	ECM33	VNVFNINNNR	2	heavy	605.32515	y5	636.351927	29.44
P38248	ECM33	VNVFNINNNR	2	heavy	605.32515	y4	523.267863	29.44
P38248	ECM33	VNVFNINNNR	2	heavy	605.32515	b2	214.118617	29.44
P38248	ECM33	VNVFNINNNR	2	heavy	605.32515	b3	313.187031	29.44
P38248	ECM33	VGQSLSIVSNDELSK	2	light	788.414859	y10	1091.5579	39.46
P38248	ECM33	VGQSLSIVSNDELSK	2	light	788.414859	y8	891.441802	39.46
P38248	ECM33	VGQSLSIVSNDELSK	2	light	788.414859	y7	792.373388	39.46
P38248	ECM33	VGQSLSIVSNDELSK	2	light	788.414859	y5	591.298432	39.46
P38248	ECM33	VGQSLSIVSNDELSK	2	light	788.414859	y4	476.271489	39.46
P38248	ECM33	VGQSLSIVSNDELSK	2	light	788.414859	y8	446.224539	39.46
P38248	ECM33	VGQSLSIVSNDELSK	2	light	788.414859	b3	285.155731	39.46
P38248	ECM33	VGQSLSIVSNDELSK	2	heavy	792.421959	y10	1099.57209	39.46
P38248	ECM33	VGQSLSIVSNDELSK	2	heavy	792.421959	y8	899.456001	39.46
P38248	ECM33	VGQSLSIVSNDELSK	2	heavy	792.421959	y7	800.387587	39.46
P38248	ECM33	VGQSLSIVSNDELSK	2	heavy	792.421959	y5	599.312631	39.46
P38248	ECM33	VGQSLSIVSNDELSK	2	heavy	792.421959	y4	484.285688	39.46
P38248	ECM33	VGQSLSIVSNDELSK	2	heavy	792.421959	y8	450.231639	39.46
P38248	ECM33	VGQSLSIVSNDELSK	2	heavy	792.421959	b3	285.155731	39.46
P33302	PDR5	GPAYAN[+203.1]ISSTES	3	light	1220.91732	y9	1097.56259	97.31
P33302	PDR5	GPAYAN[+203.1]ISSTES	3	light	1220.91732	y8	934.499258	97.31
P33302	PDR5	GPAYAN[+203.1]ISSTES	3	light	1220.91732	y7	835.430844	97.31
P33302	PDR5	GPAYAN[+203.1]ISSTES	3	light	1220.91732	y6	722.34678	97.31
P33302	PDR5	GPAYAN[+203.1]ISSTES	3	light	1220.91732	y5	665.325316	97.31
P33302	PDR5	GPAYAN[+203.1]ISSTES	3	light	1220.91732	y4	550.298373	97.31
P33302	PDR5	GPAYAN[+203.1]ISSTES	3	light	1220.91732	y3	435.27143	97.31
P33302	PDR5	GPAYAN[+203.1]ISSTES	3	light	1220.91732	b2	155.081504	97.31
P33302	PDR5	GPAYAN[+203.1]ISSTES	3	heavy	1222.92403	y9	1103.58272	97.31
P33302	PDR5	GPAYAN[+203.1]ISSTES	3	heavy	1222.92403	y8	940.519387	97.31
P33302	PDR5	GPAYAN[+203.1]ISSTES	3	heavy	1222.92403	y7	841.450973	97.31
P33302	PDR5	GPAYAN[+203.1]ISSTES	3	heavy	1222.92403	y6	728.366909	97.31
P33302	PDR5	GPAYAN[+203.1]ISSTES	3	heavy	1222.92403	y5	671.345445	97.31
P33302	PDR5	GPAYAN[+203.1]ISSTES	3	heavy	1222.92403	y4	556.318502	97.31
P33302	PDR5	GPAYAN[+203.1]ISSTES	3	heavy	1222.92403	y3	441.291559	97.31
P33302	PDR5	GPAYAN[+203.1]ISSTES	3	heavy	1222.92403	b2	155.081504	97.31
P33302	PDR5	AVQSELDWMER	2	light	682.319176	y9	1193.52555	52.41
P33302	PDR5	AVQSELDWMER	2	light	682.319176	y8	1065.46697	52.41
P33302	PDR5	AVQSELDWMER	2	light	682.319176	y7	978.434943	52.41
P33302	PDR5	AVQSELDWMER	2	light	682.319176	y6	849.39235	52.41
P33302	PDR5	AVQSELDWMER	2	light	682.319176	y5	736.308286	52.41
P33302	PDR5	AVQSELDWMER	2	light	682.319176	y4	621.281343	52.41
P33302	PDR5	AVQSELDWMER	2	heavy	685.329241	y9	1199.54568	52.41
P33302	PDR5	AVQSELDWMER	2	heavy	685.329241	y8	1071.4871	52.41
P33302	PDR5	AVQSELDWMER	2	heavy	685.329241	y7	984.455072	52.41
P33302	PDR5	AVQSELDWMER	2	heavy	685.329241	y6	855.412479	52.41
P33302	PDR5	AVQSELDWMER	2	heavy	685.329241	y5	742.328415	52.41
P33302	PDR5	AVQSELDWMER	2	heavy	685.329241	y4	627.301472	52.41
P33302	PDR5	QTTADFLTSVTSPSER	2	light	870.425955	y10	1076.55823	57.98
P33302	PDR5	QTTADFLTSVTSPSER	2	light	870.425955	y9	963.474165	57.98
P33302	PDR5	QTTADFLTSVTSPSER	2	light	870.425955	y8	862.426487	57.98
P33302	PDR5	QTTADFLTSVTSPSER	2	light	870.425955	y6	676.326044	57.98
P33302	PDR5	QTTADFLTSVTSPSER	2	light	870.425955	y4	488.246337	57.98
P33302	PDR5	QTTADFLTSVTSPSER	2	light	870.425955	b9	965.457452	57.98
P33302	PDR5	QTTADFLTSVTSPSER	2	heavy	873.43602	y10	1082.57836	57.98

P33302	PDR5	QTTADFLTSVTSPSER	2	heavy	873.43602	y9	969.494294	57.98
P33302	PDR5	QTTADFLTSVTSPSER	2	heavy	873.43602	y8	868.446616	57.98
P33302	PDR5	QTTADFLTSVTSPSER	2	heavy	873.43602	y6	682.346173	57.98
P33302	PDR5	QTTADFLTSVTSPSER	2	heavy	873.43602	y4	494.266466	57.98
P33302	PDR5	QTTADFLTSVTSPSER	2	heavy	873.43602	b9	965.457452	57.98
P31382	PMT2	GLPSWSEN[+203.1]ETD	3	light	915.76785	y11	1326.70523	65.76
P31382	PMT2	GLPSWSEN[+203.1]ETD	3	light	915.76785	y10	1213.62116	65.76
P31382	PMT2	GLPSWSEN[+203.1]ETD	3	light	915.76785	y9	1084.57857	65.76
P31382	PMT2	GLPSWSEN[+203.1]ETD	3	light	915.76785	y8	921.515242	65.76
P31382	PMT2	GLPSWSEN[+203.1]ETD	3	light	915.76785	y7	808.431178	65.76
P31382	PMT2	GLPSWSEN[+203.1]ETD	3	light	915.76785	y6	680.336215	65.76
P31382	PMT2	GLPSWSEN[+203.1]ETD	3	light	915.76785	y3	425.214309	65.76
P31382	PMT2	GLPSWSEN[+203.1]ETD	3	heavy	920.445959	y11	1340.73956	65.76
P31382	PMT2	GLPSWSEN[+203.1]ETD	3	heavy	920.445959	y10	1227.65549	65.76
P31382	PMT2	GLPSWSEN[+203.1]ETD	3	heavy	920.445959	y9	1098.6129	65.76
P31382	PMT2	GLPSWSEN[+203.1]ETD	3	heavy	920.445959	y8	935.54957	65.76
P31382	PMT2	GLPSWSEN[+203.1]ETD	3	heavy	920.445959	y7	822.465506	65.76
P31382	PMT2	GLPSWSEN[+203.1]ETD	3	heavy	920.445959	y6	686.356344	65.76
P31382	PMT2	GLPSWSEN[+203.1]ETD	3	heavy	920.445959	y3	431.234438	65.76
P31382	PMT2	EKPAAQSSLLR	2	light	600.340769	y9	942.536706	-9.99
P31382	PMT2	EKPAAQSSLLR	2	light	600.340769	y8	845.483942	-9.99
P31382	PMT2	EKPAAQSSLLR	2	light	600.340769	y7	774.446828	-9.99
P31382	PMT2	EKPAAQSSLLR	2	light	600.340769	y6	703.409714	-9.99
P31382	PMT2	EKPAAQSSLLR	2	light	600.340769	y5	575.351137	-9.99
P31382	PMT2	EKPAAQSSLLR	2	heavy	607.357933	y9	948.556835	-9.99
P31382	PMT2	EKPAAQSSLLR	2	heavy	607.357933	y8	851.504071	-9.99
P31382	PMT2	EKPAAQSSLLR	2	heavy	607.357933	y7	780.466957	-9.99
P31382	PMT2	EKPAAQSSLLR	2	heavy	607.357933	y6	709.429843	-9.99
P31382	PMT2	EKPAAQSSLLR	2	heavy	607.357933	y5	581.371266	-9.99
P31382	PMT2	NLHTHPVAAPVSK	2	light	685.880593	y9	905.520327	-17.87
P31382	PMT2	NLHTHPVAAPVSK	2	light	685.880593	y8	768.461415	-17.87
P31382	PMT2	NLHTHPVAAPVSK	2	light	685.880593	y4	430.26601	-17.87
P31382	PMT2	NLHTHPVAAPVSK	2	light	685.880593	y2	234.144832	-17.87
P31382	PMT2	NLHTHPVAAPVSK	2	light	685.880593	y4	215.636643	-17.87
P31382	PMT2	NLHTHPVAAPVSK	2	light	685.880593	b3	365.193179	-17.87
P31382	PMT2	NLHTHPVAAPVSK	2	light	685.880593	b5	603.29977	-17.87
P31382	PMT2	NLHTHPVAAPVSK	2	light	685.880593	b9	941.495175	-17.87
P31382	PMT2	NLHTHPVAAPVSK	2	heavy	689.887692	y9	913.534526	-17.87
P31382	PMT2	NLHTHPVAAPVSK	2	heavy	689.887692	y8	776.475614	-17.87
P31382	PMT2	NLHTHPVAAPVSK	2	heavy	689.887692	y4	438.280209	-17.87
P31382	PMT2	NLHTHPVAAPVSK	2	heavy	689.887692	y2	242.159031	-17.87
P31382	PMT2	NLHTHPVAAPVSK	2	heavy	689.887692	y4	219.643743	-17.87
P31382	PMT2	NLHTHPVAAPVSK	2	heavy	689.887692	b3	365.193179	-17.87
P31382	PMT2	NLHTHPVAAPVSK	2	heavy	689.887692	b5	603.29977	-17.87
P31382	PMT2	NLHTHPVAAPVSK	2	heavy	689.887692	b9	941.495175	-17.87
P36091	DCW1	YTGN[+203.1]QTYVDW/	2	light	889.399406	y8	1011.47819	28.88
P36091	DCW1	YTGN[+203.1]QTYVDW/	2	light	889.399406	y6	747.367181	28.88
P36091	DCW1	YTGN[+203.1]QTYVDW/	2	light	889.399406	y5	648.298767	28.88
P36091	DCW1	YTGN[+203.1]QTYVDW/	2	light	889.399406	y4	533.271824	28.88
P36091	DCW1	YTGN[+203.1]QTYVDW/	2	light	889.399406	y3	347.192511	28.88
P36091	DCW1	YTGN[+203.1]QTYVDW/	2	light	889.399406	b2	265.118283	28.88
P36091	DCW1	YTGN[+203.1]QTYVDW/	2	heavy	893.406506	y8	1019.49239	28.88
P36091	DCW1	YTGN[+203.1]QTYVDW/	2	heavy	893.406506	y6	755.38138	28.88
P36091	DCW1	YTGN[+203.1]QTYVDW/	2	heavy	893.406506	y5	656.312966	28.88
P36091	DCW1	YTGN[+203.1]QTYVDW/	2	heavy	893.406506	y4	541.286023	28.88
P36091	DCW1	YTGN[+203.1]QTYVDW/	2	heavy	893.406506	y3	355.20671	28.88
P36091	DCW1	YTGN[+203.1]QTYVDW/	2	heavy	893.406506	b2	265.118283	28.88
P36091	DCW1	NTVSNGALFHIAAR	3	light	490.931913	y6	714.404569	38.37
P36091	DCW1	NTVSNGALFHIAAR	3	light	490.931913	y5	567.336155	38.37
P36091	DCW1	NTVSNGALFHIAAR	3	light	490.931913	y4	430.277243	38.37
P36091	DCW1	NTVSNGALFHIAAR	3	light	490.931913	y3	317.193179	38.37
P36091	DCW1	NTVSNGALFHIAAR	3	light	490.931913	y12	628.348928	38.37
P36091	DCW1	NTVSNGALFHIAAR	3	light	490.931913	y11	578.814721	38.37

P36091	DCW1	NTVSNGALFHIAAR	3	light	490.931913	y10	535.298707	38.37
P36091	DCW1	NTVSNGALFHIAAR	3	light	490.931913	y4	215.64226	38.37
P36091	DCW1	NTVSNGALFHIAAR	3	heavy	492.938623	y6	720.424698	38.37
P36091	DCW1	NTVSNGALFHIAAR	3	heavy	492.938623	y5	573.356284	38.37
P36091	DCW1	NTVSNGALFHIAAR	3	heavy	492.938623	y4	436.297372	38.37
P36091	DCW1	NTVSNGALFHIAAR	3	heavy	492.938623	y3	323.213308	38.37
P36091	DCW1	NTVSNGALFHIAAR	3	heavy	492.938623	y12	631.358993	38.37
P36091	DCW1	NTVSNGALFHIAAR	3	heavy	492.938623	y11	581.824786	38.37
P36091	DCW1	NTVSNGALFHIAAR	3	heavy	492.938623	y10	538.308772	38.37
P36091	DCW1	NTVSNGALFHIAAR	3	heavy	492.938623	y4	218.652324	38.37
Q06689	YL413	ILNSAVN[+203.1]MTTITF	2	light	1038.54829	y9	1030.5779	63.4
Q06689	YL413	ILNSAVN[+203.1]MTTITF	2	light	1038.54829	y8	929.530223	63.4
Q06689	YL413	ILNSAVN[+203.1]MTTITF	2	light	1038.54829	y7	828.482545	63.4
Q06689	YL413	ILNSAVN[+203.1]MTTITF	2	light	1038.54829	y6	715.398481	63.4
Q06689	YL413	ILNSAVN[+203.1]MTTITF	2	light	1038.54829	y5	614.350802	63.4
Q06689	YL413	ILNSAVN[+203.1]MTTITF	2	light	1038.54829	b3	341.218332	63.4
Q06689	YL413	ILNSAVN[+203.1]MTTITF	2	light	1038.54829	b5	499.287474	63.4
Q06689	YL413	ILNSAVN[+203.1]MTTITF	2	light	1038.54829	b6	598.355888	63.4
Q06689	YL413	ILNSAVN[+203.1]MTTITF	2	light	1038.54829	b7	915.478188	63.4
Q06689	YL413	ILNSAVN[+203.1]MTTITF	2	heavy	1042.55539	y9	1038.5921	63.4
Q06689	YL413	ILNSAVN[+203.1]MTTITF	2	heavy	1042.55539	y8	937.544422	63.4
Q06689	YL413	ILNSAVN[+203.1]MTTITF	2	heavy	1042.55539	y7	836.496744	63.4
Q06689	YL413	ILNSAVN[+203.1]MTTITF	2	heavy	1042.55539	y6	723.41268	63.4
Q06689	YL413	ILNSAVN[+203.1]MTTITF	2	heavy	1042.55539	y5	622.365001	63.4
Q06689	YL413	ILNSAVN[+203.1]MTTITF	2	heavy	1042.55539	b3	341.218332	63.4
Q06689	YL413	ILNSAVN[+203.1]MTTITF	2	heavy	1042.55539	b5	499.287474	63.4
Q06689	YL413	ILNSAVN[+203.1]MTTITF	2	heavy	1042.55539	b6	598.355888	63.4
Q06689	YL413	ILNSAVN[+203.1]MTTITF	2	heavy	1042.55539	b7	915.478188	63.4
Q06689	YL413	IN[+203.1]VTK	2	light	389.221268	y4	664.351197	-40.31
Q06689	YL413	IN[+203.1]VTK	2	light	389.221268	y3	347.228896	-40.31
Q06689	YL413	IN[+203.1]VTK	2	light	389.221268	y2	248.160482	-40.31
Q06689	YL413	IN[+203.1]VTK	2	light	389.221268	b2	431.21364	-40.31
Q06689	YL413	IN[+203.1]VTK	2	light	389.221268	b3	530.282054	-40.31
Q06689	YL413	IN[+203.1]VTK	2	light	389.221268	b4	631.329733	-40.31
Q06689	YL413	IN[+203.1]VTK	2	heavy	393.228368	y4	672.365396	-40.31
Q06689	YL413	IN[+203.1]VTK	2	heavy	393.228368	y3	355.243095	-40.31
Q06689	YL413	IN[+203.1]VTK	2	heavy	393.228368	y2	256.174681	-40.31
Q06689	YL413	IN[+203.1]VTK	2	heavy	393.228368	b2	431.21364	-40.31
Q06689	YL413	IN[+203.1]VTK	2	heavy	393.228368	b3	530.282054	-40.31
Q06689	YL413	IN[+203.1]VTK	2	heavy	393.228368	b4	631.329733	-40.31
Q06689	YL413	SHAVQNMDFR	2	light	602.780021	y8	980.461826	-5.33
Q06689	YL413	SHAVQNMDFR	2	light	602.780021	y7	909.424712	-5.33
Q06689	YL413	SHAVQNMDFR	2	light	602.780021	y6	810.356298	-5.33
Q06689	YL413	SHAVQNMDFR	2	light	602.780021	y2	322.187366	-5.33
Q06689	YL413	SHAVQNMDFR	2	light	602.780021	b2	225.098216	-5.33
Q06689	YL413	SHAVQNMDFR	2	light	602.780021	b3	296.13533	-5.33
Q06689	YL413	SHAVQNMDFR	2	light	602.780021	b4	395.203744	-5.33
Q06689	YL413	SHAVQNMDFR	2	heavy	605.790086	y8	986.481955	-5.33
Q06689	YL413	SHAVQNMDFR	2	heavy	605.790086	y7	915.444841	-5.33
Q06689	YL413	SHAVQNMDFR	2	heavy	605.790086	y6	816.376427	-5.33
Q06689	YL413	SHAVQNMDFR	2	heavy	605.790086	y2	328.207495	-5.33
Q06689	YL413	SHAVQNMDFR	2	heavy	605.790086	b2	225.098216	-5.33
Q06689	YL413	SHAVQNMDFR	2	heavy	605.790086	b3	296.13533	-5.33
Q06689	YL413	SHAVQNMDFR	2	heavy	605.790086	b4	395.203744	-5.33
P46992	YJR1	N[+203.1]SSSIGYYDLPA	3	light	907.788808	y10	1250.70042	116.46
P46992	YJR1	N[+203.1]SSSIGYYDLPA	3	light	907.788808	y9	1137.61635	116.46
P46992	YJR1	N[+203.1]SSSIGYYDLPA	3	light	907.788808	y8	951.53704	116.46
P46992	YJR1	N[+203.1]SSSIGYYDLPA	3	light	907.788808	y7	838.452976	116.46
P46992	YJR1	N[+203.1]SSSIGYYDLPA	3	light	907.788808	y6	725.368912	116.46
P46992	YJR1	N[+203.1]SSSIGYYDLPA	3	light	907.788808	y5	611.325985	116.46
P46992	YJR1	N[+203.1]SSSIGYYDLPA	3	light	907.788808	y4	496.299041	116.46
P46992	YJR1	N[+203.1]SSSIGYYDLPA	3	light	907.788808	b3	492.193633	116.46
P46992	YJR1	N[+203.1]SSSIGYYDLPA	3	light	907.788808	b4	579.225662	116.46

P46992	YJR1	N[+203.1]SSSIGYYDLPA	3	heavy	909.795518	y10	1256.72055	116.46
P46992	YJR1	N[+203.1]SSSIGYYDLPA	3	heavy	909.795518	y9	1143.63648	116.46
P46992	YJR1	N[+203.1]SSSIGYYDLPA	3	heavy	909.795518	y8	957.557169	116.46
P46992	YJR1	N[+203.1]SSSIGYYDLPA	3	heavy	909.795518	y7	844.473105	116.46
P46992	YJR1	N[+203.1]SSSIGYYDLPA	3	heavy	909.795518	y6	731.389041	116.46
P46992	YJR1	N[+203.1]SSSIGYYDLPA	3	heavy	909.795518	y5	617.346114	116.46
P46992	YJR1	N[+203.1]SSSIGYYDLPA	3	heavy	909.795518	y4	502.31917	116.46
P46992	YJR1	N[+203.1]SSSIGYYDLPA	3	heavy	909.795518	b3	492.193633	116.46
P46992	YJR1	N[+203.1]SSSIGYYDLPA	3	heavy	909.795518	b4	579.225662	116.46
P46992	YJR1	PLADYLSVHFR	2	light	659.351137	y10	1220.64223	18.41
P46992	YJR1	PLADYLSVHFR	2	light	659.351137	y9	1107.55817	18.41
P46992	YJR1	PLADYLSVHFR	2	light	659.351137	y8	1036.52106	18.41
P46992	YJR1	PLADYLSVHFR	2	light	659.351137	y5	645.34672	18.41
P46992	YJR1	PLADYLSVHFR	2	light	659.351137	y3	459.246278	18.41
P46992	YJR1	PLADYLSVHFR	2	light	659.351137	b2	211.144104	18.41
P46992	YJR1	PLADYLSVHFR	2	light	659.351137	b4	397.208161	18.41
P46992	YJR1	PLADYLSVHFR	2	heavy	662.361201	y10	1226.66236	18.41
P46992	YJR1	PLADYLSVHFR	2	heavy	662.361201	y9	1113.5783	18.41
P46992	YJR1	PLADYLSVHFR	2	heavy	662.361201	y8	1042.54119	18.41
P46992	YJR1	PLADYLSVHFR	2	heavy	662.361201	y5	651.366849	18.41
P46992	YJR1	PLADYLSVHFR	2	heavy	662.361201	y3	465.266407	18.41
P46992	YJR1	PLADYLSVHFR	2	heavy	662.361201	b2	211.144104	18.41
P46992	YJR1	PLADYLSVHFR	2	heavy	662.361201	b4	397.208161	18.41
P46992	YJR1	SGIPAYYGYGGTTK	2	light	717.848624	y11	1177.55242	26.28
P46992	YJR1	SGIPAYYGYGGTTK	2	light	717.848624	y10	1080.49965	26.28
P46992	YJR1	SGIPAYYGYGGTTK	2	light	717.848624	y9	1009.46254	26.28
P46992	YJR1	SGIPAYYGYGGTTK	2	light	717.848624	y8	846.399209	26.28
P46992	YJR1	SGIPAYYGYGGTTK	2	light	717.848624	y7	683.335881	26.28
P46992	YJR1	SGIPAYYGYGGTTK	2	light	717.848624	y5	463.251088	26.28
P46992	YJR1	SGIPAYYGYGGTTK	2	light	717.848624	y11	589.279846	26.28
P46992	YJR1	SGIPAYYGYGGTTK	2	light	717.848624	b6	589.298038	26.28
P46992	YJR1	SGIPAYYGYGGTTK	2	heavy	721.855723	y11	1185.56661	26.28
P46992	YJR1	SGIPAYYGYGGTTK	2	heavy	721.855723	y10	1088.51385	26.28
P46992	YJR1	SGIPAYYGYGGTTK	2	heavy	721.855723	y9	1017.47674	26.28
P46992	YJR1	SGIPAYYGYGGTTK	2	heavy	721.855723	y8	854.413408	26.28
P46992	YJR1	SGIPAYYGYGGTTK	2	heavy	721.855723	y7	691.35008	26.28
P46992	YJR1	SGIPAYYGYGGTTK	2	heavy	721.855723	y5	471.265287	26.28
P46992	YJR1	SGIPAYYGYGGTTK	2	heavy	721.855723	y11	593.286945	26.28
P46992	YJR1	SGIPAYYGYGGTTK	2	heavy	721.855723	b6	589.298038	26.28

PRM assay; R=60000

UniProt ID	Protein	Peptide Modified Sequence	Precursor Charge	Isotope Label Type	Precursor Mz	Fragment Ion	Fragment Mz	Normalized Retention Time
P12684	HMDH2	IPTELVSEN[+203.1]GTK	2	light	745.882861	y10	1280.62162	12.04
P12684	HMDH2	IPTELVSEN[+203.1]GTK	2	light	745.882861	y9	1179.57394	12.04
P12684	HMDH2	IPTELVSEN[+203.1]GTK	2	light	745.882861	y8	1050.53135	12.04
P12684	HMDH2	IPTELVSEN[+203.1]GTK	2	light	745.882861	y7	937.447282	12.04
P12684	HMDH2	IPTELVSEN[+203.1]GTK	2	light	745.882861	y6	838.378868	12.04
P12684	HMDH2	IPTELVSEN[+203.1]GTK	2	light	745.882861	y5	751.34684	12.04
P12684	HMDH2	IPTELVSEN[+203.1]GTK	2	light	745.882861	y3	305.181946	12.04
P12684	HMDH2	IPTELVSEN[+203.1]GTK	2	light	745.882861	b4	441.234376	12.04
P12684	HMDH2	IPTELVSEN[+203.1]GTK	2	heavy	749.88996	y10	1288.63582	12.04
P12684	HMDH2	IPTELVSEN[+203.1]GTK	2	heavy	749.88996	y9	1187.58814	12.04
P12684	HMDH2	IPTELVSEN[+203.1]GTK	2	heavy	749.88996	y8	1058.54555	12.04
P12684	HMDH2	IPTELVSEN[+203.1]GTK	2	heavy	749.88996	y7	945.461481	12.04
P12684	HMDH2	IPTELVSEN[+203.1]GTK	2	heavy	749.88996	y6	846.393067	12.04
P12684	HMDH2	IPTELVSEN[+203.1]GTK	2	heavy	749.88996	y5	759.361039	12.04
P12684	HMDH2	IPTELVSEN[+203.1]GTK	2	heavy	749.88996	y3	313.196145	12.04
P12684	HMDH2	IPTELVSEN[+203.1]GTK	2	heavy	749.88996	b4	441.234376	12.04
P12684	HMDH2	ALSTLAESPILVSEK	2	light	779.440346	y11	1185.67253	62.06

P12684	HMDH2	ALSTLAESPILVSEK	2	light	779.440346	y10	1072.58847	62.06
P12684	HMDH2	ALSTLAESPILVSEK	2	light	779.440346	y9	1001.55135	62.06
P12684	HMDH2	ALSTLAESPILVSEK	2	light	779.440346	y8	872.50876	62.06
P12684	HMDH2	ALSTLAESPILVSEK	2	light	779.440346	y7	785.476731	62.06
P12684	HMDH2	ALSTLAESPILVSEK	2	light	779.440346	y5	575.339903	62.06
P12684	HMDH2	ALSTLAESPILVSEK	2	light	779.440346	y4	462.255839	62.06
P12684	HMDH2	ALSTLAESPILVSEK	2	light	779.440346	y3	363.187425	62.06
P12684	HMDH2	ALSTLAESPILVSEK	2	heavy	783.447445	y11	1193.68673	62.06
P12684	HMDH2	ALSTLAESPILVSEK	2	heavy	783.447445	y10	1080.60267	62.06
P12684	HMDH2	ALSTLAESPILVSEK	2	heavy	783.447445	y9	1009.56555	62.06
P12684	HMDH2	ALSTLAESPILVSEK	2	heavy	783.447445	y8	880.522959	62.06
P12684	HMDH2	ALSTLAESPILVSEK	2	heavy	783.447445	y7	793.49093	62.06
P12684	HMDH2	ALSTLAESPILVSEK	2	heavy	783.447445	y5	583.354102	62.06
P12684	HMDH2	ALSTLAESPILVSEK	2	heavy	783.447445	y4	470.270038	62.06
P12684	HMDH2	ALSTLAESPILVSEK	2	heavy	783.447445	y3	371.201624	62.06
P53379	MKC7	STAYSLFAN[+203.1]DSI	2	light	854.881046	y9	1199.54264	28.88
P53379	MKC7	STAYSLFAN[+203.1]DSI	2	light	854.881046	y8	1086.45858	28.88
P53379	MKC7	STAYSLFAN[+203.1]DSI	2	light	854.881046	y7	939.390161	28.88
P53379	MKC7	STAYSLFAN[+203.1]DSI	2	light	854.881046	y6	868.353047	28.88
P53379	MKC7	STAYSLFAN[+203.1]DSI	2	light	854.881046	y5	551.230747	28.88
P53379	MKC7	STAYSLFAN[+203.1]DSI	2	light	854.881046	y4	436.203804	28.88
P53379	MKC7	STAYSLFAN[+203.1]DSI	2	light	854.881046	b3	260.124097	28.88
P53379	MKC7	STAYSLFAN[+203.1]DSI	2	heavy	858.888146	y9	1207.55684	28.88
P53379	MKC7	STAYSLFAN[+203.1]DSI	2	heavy	858.888146	y8	1094.47277	28.88
P53379	MKC7	STAYSLFAN[+203.1]DSI	2	heavy	858.888146	y7	947.40436	28.88
P53379	MKC7	STAYSLFAN[+203.1]DSI	2	heavy	858.888146	y6	876.367246	28.88
P53379	MKC7	STAYSLFAN[+203.1]DSI	2	heavy	858.888146	y5	559.244946	28.88
P53379	MKC7	STAYSLFAN[+203.1]DSI	2	heavy	858.888146	y4	444.218003	28.88
P53379	MKC7	STAYSLFAN[+203.1]DSI	2	heavy	858.888146	b3	260.124097	28.88
P53379	MKC7	HGTILFGAVDHGK	3	light	451.242087	y7	683.347114	12.33
P53379	MKC7	HGTILFGAVDHGK	3	light	451.242087	y5	555.288536	12.33
P53379	MKC7	HGTILFGAVDHGK	3	light	451.242087	y4	456.220122	12.33
P53379	MKC7	HGTILFGAVDHGK	3	light	451.242087	y3	341.193179	12.33
P53379	MKC7	HGTILFGAVDHGK	3	light	451.242087	b3	296.13533	12.33
P53379	MKC7	HGTILFGAVDHGK	3	light	451.242087	b4	409.219394	12.33
P53379	MKC7	HGTILFGAVDHGK	3	light	451.242087	b5	522.303458	12.33
P53379	MKC7	HGTILFGAVDHGK	3	heavy	453.913487	y7	691.361313	12.33
P53379	MKC7	HGTILFGAVDHGK	3	heavy	453.913487	y5	563.302735	12.33
P53379	MKC7	HGTILFGAVDHGK	3	heavy	453.913487	y4	464.234321	12.33
P53379	MKC7	HGTILFGAVDHGK	3	heavy	453.913487	y3	349.207378	12.33
P53379	MKC7	HGTILFGAVDHGK	3	heavy	453.913487	b3	296.13533	12.33
P53379	MKC7	HGTILFGAVDHGK	3	heavy	453.913487	b4	409.219394	12.33
P53379	MKC7	HGTILFGAVDHGK	3	heavy	453.913487	b5	522.303458	12.33
P53379	MKC7	YAGDLYTIPIINTLQHR	2	light	994.533632	y11	1305.76375	96.93
P53379	MKC7	YAGDLYTIPIINTLQHR	2	light	994.533632	y10	1204.71607	96.93
P53379	MKC7	YAGDLYTIPIINTLQHR	2	light	994.533632	y9	1091.632	96.93
P53379	MKC7	YAGDLYTIPIINTLQHR	2	light	994.533632	y8	994.579239	96.93
P53379	MKC7	YAGDLYTIPIINTLQHR	2	light	994.533632	y10	602.861672	96.93
P53379	MKC7	YAGDLYTIPIINTLQHR	2	light	994.533632	b4	407.156125	96.93
P53379	MKC7	YAGDLYTIPIINTLQHR	2	light	994.533632	b9	994.488024	96.93
P53379	MKC7	YAGDLYTIPIINTLQHR	2	heavy	997.543696	y11	1311.78388	96.93
P53379	MKC7	YAGDLYTIPIINTLQHR	2	heavy	997.543696	y10	1210.7362	96.93
P53379	MKC7	YAGDLYTIPIINTLQHR	2	heavy	997.543696	y9	1097.65213	96.93
P53379	MKC7	YAGDLYTIPIINTLQHR	2	heavy	997.543696	y8	1000.59937	96.93
P53379	MKC7	YAGDLYTIPIINTLQHR	2	heavy	997.543696	y10	605.871736	96.93
P53379	MKC7	YAGDLYTIPIINTLQHR	2	heavy	997.543696	b4	407.156125	96.93
P53379	MKC7	YAGDLYTIPIINTLQHR	2	heavy	997.543696	b9	994.488024	96.93
Q12465	RAX2	EIGPETSSHGLVYYSN[+	3	light	1193.20781	y11	1262.5859	58.14
Q12465	RAX2	EIGPETSSHGLVYYSN[+	3	light	1193.20781	y10	1149.50184	58.14
Q12465	RAX2	EIGPETSSHGLVYYSN[+	3	light	1193.20781	y9	1021.44326	58.14
Q12465	RAX2	EIGPETSSHGLVYYSN[+	3	light	1193.20781	y8	908.359195	58.14
Q12465	RAX2	EIGPETSSHGLVYYSN[+	3	light	1193.20781	y7	779.316602	58.14
Q12465	RAX2	EIGPETSSHGLVYYSN[+	3	light	1193.20781	y6	664.289659	58.14

Q12465	RAX2	EIGPETSSHGLVYYSN[+	3	light	1193.20781	y5	593.252545	58.14
Q12465	RAX2	EIGPETSSHGLVYYSN[+	3	light	1193.20781	y4	506.220516	58.14
Q12465	RAX2	EIGPETSSHGLVYYSN[+	3	heavy	1195.21452	y11	1268.60603	58.14
Q12465	RAX2	EIGPETSSHGLVYYSN[+	3	heavy	1195.21452	y10	1155.52197	58.14
Q12465	RAX2	EIGPETSSHGLVYYSN[+	3	heavy	1195.21452	y9	1027.46339	58.14
Q12465	RAX2	EIGPETSSHGLVYYSN[+	3	heavy	1195.21452	y8	914.379324	58.14
Q12465	RAX2	EIGPETSSHGLVYYSN[+	3	heavy	1195.21452	y7	785.336731	58.14
Q12465	RAX2	EIGPETSSHGLVYYSN[+	3	heavy	1195.21452	y6	670.309788	58.14
Q12465	RAX2	EIGPETSSHGLVYYSN[+	3	heavy	1195.21452	y5	599.272674	58.14
Q12465	RAX2	EIGPETSSHGLVYYSN[+	3	heavy	1195.21452	y4	512.240645	58.14
Q12465	RAX2	N[+203.1]SSLYADIYDNK	2	light	803.367575	y8	1001.45745	30.57
Q12465	RAX2	N[+203.1]SSLYADIYDNK	2	light	803.367575	y7	838.394124	30.57
Q12465	RAX2	N[+203.1]SSLYADIYDNK	2	light	803.367575	y6	767.35701	30.57
Q12465	RAX2	N[+203.1]SSLYADIYDNK	2	light	803.367575	y5	652.330067	30.57
Q12465	RAX2	N[+203.1]SSLYADIYDNK	2	light	803.367575	y4	539.246003	30.57
Q12465	RAX2	N[+203.1]SSLYADIYDNK	2	light	803.367575	b4	605.277697	30.57
Q12465	RAX2	N[+203.1]SSLYADIYDNK	2	light	803.367575	b5	768.341026	30.57
Q12465	RAX2	N[+203.1]SSLYADIYDNK	2	heavy	807.374674	y8	1009.47165	30.57
Q12465	RAX2	N[+203.1]SSLYADIYDNK	2	heavy	807.374674	y7	846.408323	30.57
Q12465	RAX2	N[+203.1]SSLYADIYDNK	2	heavy	807.374674	y6	775.371209	30.57
Q12465	RAX2	N[+203.1]SSLYADIYDNK	2	heavy	807.374674	y5	660.344266	30.57
Q12465	RAX2	N[+203.1]SSLYADIYDNK	2	heavy	807.374674	y4	547.260202	30.57
Q12465	RAX2	N[+203.1]SSLYADIYDNK	2	heavy	807.374674	b4	605.277697	30.57
Q12465	RAX2	N[+203.1]SSLYADIYDNK	2	heavy	807.374674	b5	768.341026	30.57
Q12465	RAX2	N[+203.1]QTIQGDVHGIT	2	light	807.410108	y11	1168.63206	-0.35
Q12465	RAX2	N[+203.1]QTIQGDVHGIT	2	light	807.410108	y10	1067.58438	-0.35
Q12465	RAX2	N[+203.1]QTIQGDVHGIT	2	light	807.410108	y9	954.50032	-0.35
Q12465	RAX2	N[+203.1]QTIQGDVHGIT	2	light	807.410108	y8	826.441743	-0.35
Q12465	RAX2	N[+203.1]QTIQGDVHGIT	2	light	807.410108	y6	654.393336	-0.35
Q12465	RAX2	N[+203.1]QTIQGDVHGIT	2	light	807.410108	y5	555.324922	-0.35
Q12465	RAX2	N[+203.1]QTIQGDVHGIT	2	light	807.410108	y4	418.26601	-0.35
Q12465	RAX2	N[+203.1]QTIQGDVHGIT	2	light	807.410108	b2	446.188154	-0.35
Q12465	RAX2	N[+203.1]QTIQGDVHGIT	2	light	807.410108	b3	547.235833	-0.35
Q12465	RAX2	N[+203.1]QTIQGDVHGIT	2	light	807.410108	b4	660.319897	-0.35
Q12465	RAX2	N[+203.1]QTIQGDVHGIT	2	heavy	811.417208	y11	1176.64626	-0.35
Q12465	RAX2	N[+203.1]QTIQGDVHGIT	2	heavy	811.417208	y10	1075.59858	-0.35
Q12465	RAX2	N[+203.1]QTIQGDVHGIT	2	heavy	811.417208	y9	962.514519	-0.35
Q12465	RAX2	N[+203.1]QTIQGDVHGIT	2	heavy	811.417208	y8	834.455942	-0.35
Q12465	RAX2	N[+203.1]QTIQGDVHGIT	2	heavy	811.417208	y6	662.407535	-0.35
Q12465	RAX2	N[+203.1]QTIQGDVHGIT	2	heavy	811.417208	y5	563.339121	-0.35
Q12465	RAX2	N[+203.1]QTIQGDVHGIT	2	heavy	811.417208	y4	426.280209	-0.35
Q12465	RAX2	N[+203.1]QTIQGDVHGIT	2	heavy	811.417208	b2	446.188154	-0.35
Q12465	RAX2	N[+203.1]QTIQGDVHGIT	2	heavy	811.417208	b3	547.235833	-0.35
Q12465	RAX2	N[+203.1]QTIQGDVHGIT	2	heavy	811.417208	b4	660.319897	-0.35
Q12465	RAX2	IPVLLDSGTTISYMPTEL'	2	light	1089.09233	y9	1067.54416	112.33
Q12465	RAX2	IPVLLDSGTTISYMPTEL'	2	light	1089.09233	y8	980.51213	112.33
Q12465	RAX2	IPVLLDSGTTISYMPTEL'	2	light	1089.09233	y7	817.448802	112.33
Q12465	RAX2	IPVLLDSGTTISYMPTEL'	2	light	1089.09233	y6	686.408317	112.33
Q12465	RAX2	IPVLLDSGTTISYMPTEL'	2	light	1089.09233	y5	589.355553	112.33
Q12465	RAX2	IPVLLDSGTTISYMPTEL'	2	light	1089.09233	y3	359.265282	112.33
Q12465	RAX2	IPVLLDSGTTISYMPTEL'	2	heavy	1093.09943	y9	1075.55836	112.33
Q12465	RAX2	IPVLLDSGTTISYMPTEL'	2	heavy	1093.09943	y8	988.526329	112.33
Q12465	RAX2	IPVLLDSGTTISYMPTEL'	2	heavy	1093.09943	y7	825.463001	112.33
Q12465	RAX2	IPVLLDSGTTISYMPTEL'	2	heavy	1093.09943	y6	694.422516	112.33
Q12465	RAX2	IPVLLDSGTTISYMPTEL'	2	heavy	1093.09943	y5	597.369752	112.33
Q12465	RAX2	IPVLLDSGTTISYMPTEL'	2	heavy	1093.09943	y3	367.279481	112.33
Q12465	RAX2	YVPDQNEPIPR	2	light	664.335684	y9	1065.53235	13.01
Q12465	RAX2	YVPDQNEPIPR	2	light	664.335684	y8	968.479585	13.01
Q12465	RAX2	YVPDQNEPIPR	2	light	664.335684	y7	853.452642	13.01
Q12465	RAX2	YVPDQNEPIPR	2	light	664.335684	y6	725.394064	13.01
Q12465	RAX2	YVPDQNEPIPR	2	light	664.335684	y5	611.351137	13.01
Q12465	RAX2	YVPDQNEPIPR	2	light	664.335684	y4	482.308544	13.01
Q12465	RAX2	YVPDQNEPIPR	2	heavy	667.345748	y9	1071.55248	13.01

Q12465	RAX2	YVPDQNEPIPR	2	heavy	667.345748	y8	974.499714	13.01
Q12465	RAX2	YVPDQNEPIPR	2	heavy	667.345748	y7	859.472771	13.01
Q12465	RAX2	YVPDQNEPIPR	2	heavy	667.345748	y6	731.414193	13.01
Q12465	RAX2	YVPDQNEPIPR	2	heavy	667.345748	y5	617.371266	13.01
Q12465	RAX2	YVPDQNEPIPR	2	heavy	667.345748	y4	488.328673	13.01
P27825	CALXorCN	N[+203.1]VTEAQIIGN[+2	2	light	796.904325	y10	1275.67907	6.09
P27825	CALXorCN	N[+203.1]VTEAQIIGN[+2	2	light	796.904325	y9	1176.61066	6.09
P27825	CALXorCN	N[+203.1]VTEAQIIGN[+2	2	light	796.904325	y8	1075.56298	6.09
P27825	CALXorCN	N[+203.1]VTEAQIIGN[+2	2	light	796.904325	y7	946.520387	6.09
P27825	CALXorCN	N[+203.1]VTEAQIIGN[+2	2	light	796.904325	y6	875.483274	6.09
P27825	CALXorCN	N[+203.1]VTEAQIIGN[+2	2	light	796.904325	y5	747.424696	6.09
P27825	CALXorCN	N[+203.1]VTEAQIIGN[+2	2	light	796.904325	y4	634.340632	6.09
P27825	CALXorCN	N[+203.1]VTEAQIIGN[+2	2	light	796.904325	y3	521.256568	6.09
P27825	CALXorCN	N[+203.1]VTEAQIIGN[+2	2	light	796.904325	b5	718.325376	6.09
P27825	CALXorCN	N[+203.1]VTEAQIIGN[+2	2	light	796.904325	b6	846.383953	6.09
P27825	CALXorCN	N[+203.1]VTEAQIIGN[+2	2	light	796.904325	b7	959.468017	6.09
P27825	CALXorCN	N[+203.1]VTEAQIIGN[+2	2	light	796.904325	b9	1129.57355	6.09
P27825	CALXorCN	N[+203.1]VTEAQIIGN[+2	2	heavy	800.911424	y10	1283.69327	6.09
P27825	CALXorCN	N[+203.1]VTEAQIIGN[+2	2	heavy	800.911424	y9	1184.62486	6.09
P27825	CALXorCN	N[+203.1]VTEAQIIGN[+2	2	heavy	800.911424	y8	1083.57718	6.09
P27825	CALXorCN	N[+203.1]VTEAQIIGN[+2	2	heavy	800.911424	y7	954.534586	6.09
P27825	CALXorCN	N[+203.1]VTEAQIIGN[+2	2	heavy	800.911424	y6	883.497473	6.09
P27825	CALXorCN	N[+203.1]VTEAQIIGN[+2	2	heavy	800.911424	y5	755.438895	6.09
P27825	CALXorCN	N[+203.1]VTEAQIIGN[+2	2	heavy	800.911424	y4	642.354831	6.09
P27825	CALXorCN	N[+203.1]VTEAQIIGN[+2	2	heavy	800.911424	y3	529.270767	6.09
P27825	CALXorCN	N[+203.1]VTEAQIIGN[+2	2	heavy	800.911424	b5	718.325376	6.09
P27825	CALXorCN	N[+203.1]VTEAQIIGN[+2	2	heavy	800.911424	b6	846.383953	6.09
P27825	CALXorCN	N[+203.1]VTEAQIIGN[+2	2	heavy	800.911424	b7	959.468017	6.09
P27825	CALXorCN	N[+203.1]VTEAQIIGN[+2	2	heavy	800.911424	b9	1129.57355	6.09
P27825	CALXorCN	LDNSLTC[+57]GGAFIK	2	light	698.350476	y10	1053.53974	40.75
P27825	CALXorCN	LDNSLTC[+57]GGAFIK	2	light	698.350476	y9	966.507714	40.75
P27825	CALXorCN	LDNSLTC[+57]GGAFIK	2	light	698.350476	y8	853.42365	40.75
P27825	CALXorCN	LDNSLTC[+57]GGAFIK	2	light	698.350476	y7	752.375971	40.75
P27825	CALXorCN	LDNSLTC[+57]GGAFIK	2	light	698.350476	y6	592.345323	40.75
P27825	CALXorCN	LDNSLTC[+57]GGAFIK	2	light	698.350476	y5	535.323859	40.75
P27825	CALXorCN	LDNSLTC[+57]GGAFIK	2	light	698.350476	y3	407.265282	40.75
P27825	CALXorCN	LDNSLTC[+57]GGAFIK	2	heavy	702.357576	y10	1061.55394	40.75
P27825	CALXorCN	LDNSLTC[+57]GGAFIK	2	heavy	702.357576	y9	974.521913	40.75
P27825	CALXorCN	LDNSLTC[+57]GGAFIK	2	heavy	702.357576	y8	861.437849	40.75
P27825	CALXorCN	LDNSLTC[+57]GGAFIK	2	heavy	702.357576	y7	760.39017	40.75
P27825	CALXorCN	LDNSLTC[+57]GGAFIK	2	heavy	702.357576	y6	600.359522	40.75
P27825	CALXorCN	LDNSLTC[+57]GGAFIK	2	heavy	702.357576	y5	543.338058	40.75
P27825	CALXorCN	LDNSLTC[+57]GGAFIK	2	heavy	702.357576	y3	415.279481	40.75
P40557	EPS1	VALVLPN[+203.1]K	2	light	528.818607	y7	957.561524	26.67
P40557	EPS1	VALVLPN[+203.1]K	2	light	528.818607	y6	886.52441	26.67
P40557	EPS1	VALVLPN[+203.1]K	2	light	528.818607	y5	773.440346	26.67
P40557	EPS1	VALVLPN[+203.1]K	2	light	528.818607	y4	674.371932	26.67
P40557	EPS1	VALVLPN[+203.1]K	2	light	528.818607	b3	284.196868	26.67
P40557	EPS1	VALVLPN[+203.1]K	2	heavy	532.825706	y7	965.575723	26.67
P40557	EPS1	VALVLPN[+203.1]K	2	heavy	532.825706	y6	894.538609	26.67
P40557	EPS1	VALVLPN[+203.1]K	2	heavy	532.825706	y5	781.454545	26.67
P40557	EPS1	VALVLPN[+203.1]K	2	heavy	532.825706	y4	682.386131	26.67
P40557	EPS1	VALVLPN[+203.1]K	2	heavy	532.825706	b3	284.196868	26.67
P40557	EPS1	FPN[+203.1]ITEGELEK	2	light	740.364304	y10	1332.65292	38.09
P40557	EPS1	FPN[+203.1]ITEGELEK	2	light	740.364304	y9	1235.60015	38.09
P40557	EPS1	FPN[+203.1]ITEGELEK	2	light	740.364304	y8	918.477853	38.09
P40557	EPS1	FPN[+203.1]ITEGELEK	2	light	740.364304	y7	805.393789	38.09
P40557	EPS1	FPN[+203.1]ITEGELEK	2	light	740.364304	y6	704.346111	38.09
P40557	EPS1	FPN[+203.1]ITEGELEK	2	light	740.364304	y5	575.303518	38.09
P40557	EPS1	FPN[+203.1]ITEGELEK	2	light	740.364304	y4	518.282054	38.09
P40557	EPS1	FPN[+203.1]ITEGELEK	2	light	740.364304	y3	389.239461	38.09
P40557	EPS1	FPN[+203.1]ITEGELEK	2	heavy	744.371403	y10	1340.66712	38.09
P40557	EPS1	FPN[+203.1]ITEGELEK	2	heavy	744.371403	y9	1243.61435	38.09

P40557	EPS1	FPN[+203.1]ITEGELEK	2	heavy	744.371403	y8	926.492052	38.09
P40557	EPS1	FPN[+203.1]ITEGELEK	2	heavy	744.371403	y7	813.407988	38.09
P40557	EPS1	FPN[+203.1]ITEGELEK	2	heavy	744.371403	y6	712.36031	38.09
P40557	EPS1	FPN[+203.1]ITEGELEK	2	heavy	744.371403	y5	583.317717	38.09
P40557	EPS1	FPN[+203.1]ITEGELEK	2	heavy	744.371403	y4	526.296253	38.09
P40557	EPS1	FPN[+203.1]ITEGELEK	2	heavy	744.371403	y3	397.25366	38.09
P40557	EPS1	EAFVSLNIPSK	2	light	602.832245	y9	1004.57751	53.17
P40557	EPS1	EAFVSLNIPSK	2	light	602.832245	y8	857.509094	53.17
P40557	EPS1	EAFVSLNIPSK	2	light	602.832245	y7	758.44068	53.17
P40557	EPS1	EAFVSLNIPSK	2	light	602.832245	y6	671.408652	53.17
P40557	EPS1	EAFVSLNIPSK	2	light	602.832245	y5	558.324588	53.17
P40557	EPS1	EAFVSLNIPSK	2	light	602.832245	y4	444.28166	53.17
P40557	EPS1	EAFVSLNIPSK	2	light	602.832245	y3	331.197596	53.17
P40557	EPS1	EAFVSLNIPSK	2	heavy	606.839345	y9	1012.59171	53.17
P40557	EPS1	EAFVSLNIPSK	2	heavy	606.839345	y8	865.523293	53.17
P40557	EPS1	EAFVSLNIPSK	2	heavy	606.839345	y7	766.454879	53.17
P40557	EPS1	EAFVSLNIPSK	2	heavy	606.839345	y6	679.422851	53.17
P40557	EPS1	EAFVSLNIPSK	2	heavy	606.839345	y5	566.338787	53.17
P40557	EPS1	EAFVSLNIPSK	2	heavy	606.839345	y4	452.295859	53.17
P40557	EPS1	EAFVSLNIPSK	2	heavy	606.839345	y3	339.211795	53.17
P40557	EPS1	NIDAIMDWVK	2	light	602.805173	y8	977.476079	13.47
P40557	EPS1	NIDAIMDWVK	2	light	602.805173	y7	862.449136	13.47
P40557	EPS1	NIDAIMDWVK	2	light	602.805173	y6	791.412022	13.47
P40557	EPS1	NIDAIMDWVK	2	light	602.805173	y5	678.327958	13.47
P40557	EPS1	NIDAIMDWVK	2	light	602.805173	y4	547.287474	13.47
P40557	EPS1	NIDAIMDWVK	2	light	602.805173	y3	432.260531	13.47
P40557	EPS1	NIDAIMDWVK	2	heavy	606.812273	y8	985.490278	13.47
P40557	EPS1	NIDAIMDWVK	2	heavy	606.812273	y7	870.463335	13.47
P40557	EPS1	NIDAIMDWVK	2	heavy	606.812273	y6	799.426221	13.47
P40557	EPS1	NIDAIMDWVK	2	heavy	606.812273	y5	686.342157	13.47
P40557	EPS1	NIDAIMDWVK	2	heavy	606.812273	y4	555.301673	13.47
P40557	EPS1	NIDAIMDWVK	2	heavy	606.812273	y3	440.27473	13.47
P52911	EXG2	FASYYAN[+203.1]DTITV	2	light	848.409243	y10	1390.67365	36.42
P52911	EXG2	FASYYAN[+203.1]DTITV	2	light	848.409243	y9	1227.61033	36.42
P52911	EXG2	FASYYAN[+203.1]DTITV	2	light	848.409243	y8	1064.547	36.42
P52911	EXG2	FASYYAN[+203.1]DTITV	2	light	848.409243	y7	993.509882	36.42
P52911	EXG2	FASYYAN[+203.1]DTITV	2	light	848.409243	y5	561.360639	36.42
P52911	EXG2	FASYYAN[+203.1]DTITV	2	light	848.409243	b3	306.144832	36.42
P52911	EXG2	FASYYAN[+203.1]DTITV	2	heavy	852.416342	y10	1398.68785	36.42
P52911	EXG2	FASYYAN[+203.1]DTITV	2	heavy	852.416342	y9	1235.62452	36.42
P52911	EXG2	FASYYAN[+203.1]DTITV	2	heavy	852.416342	y8	1072.5612	36.42
P52911	EXG2	FASYYAN[+203.1]DTITV	2	heavy	852.416342	y7	1001.52408	36.42
P52911	EXG2	FASYYAN[+203.1]DTITV	2	heavy	852.416342	y5	569.374838	36.42
P52911	EXG2	FASYYAN[+203.1]DTITV	2	heavy	852.416342	b3	306.144832	36.42
P52911	EXG2	NLYIDN[+203.1]ITFNDP\	2	light	1323.15269	y11	1234.63139	95.86
P52911	EXG2	NLYIDN[+203.1]ITFNDP\	2	light	1323.15269	y10	1119.60445	95.86
P52911	EXG2	NLYIDN[+203.1]ITFNDP\	2	light	1323.15269	y9	1022.55169	95.86
P52911	EXG2	NLYIDN[+203.1]ITFNDP\	2	light	1323.15269	y8	859.488358	95.86
P52911	EXG2	NLYIDN[+203.1]ITFNDP\	2	light	1323.15269	y7	760.419945	95.86
P52911	EXG2	NLYIDN[+203.1]ITFNDP\	2	light	1323.15269	y6	673.387916	95.86
P52911	EXG2	NLYIDN[+203.1]ITFNDP\	2	light	1323.15269	y5	558.360973	95.86
P52911	EXG2	NLYIDN[+203.1]ITFNDP\	2	light	1323.15269	b3	391.197596	95.86
P52911	EXG2	NLYIDN[+203.1]ITFNDP\	2	heavy	1327.15979	y11	1242.64559	95.86
P52911	EXG2	NLYIDN[+203.1]ITFNDP\	2	heavy	1327.15979	y10	1127.61865	95.86
P52911	EXG2	NLYIDN[+203.1]ITFNDP\	2	heavy	1327.15979	y9	1030.56589	95.86
P52911	EXG2	NLYIDN[+203.1]ITFNDP\	2	heavy	1327.15979	y8	867.502558	95.86
P52911	EXG2	NLYIDN[+203.1]ITFNDP\	2	heavy	1327.15979	y7	768.434144	95.86
P52911	EXG2	NLYIDN[+203.1]ITFNDP\	2	heavy	1327.15979	y6	681.402115	95.86
P52911	EXG2	NLYIDN[+203.1]ITFNDP\	2	heavy	1327.15979	y5	566.375172	95.86
P52911	EXG2	NLYIDN[+203.1]ITFNDP\	2	heavy	1327.15979	b3	391.197596	95.86
P52911	EXG2	IPIGYWAWK	2	light	567.310752	y8	1020.53016	79.7
P52911	EXG2	IPIGYWAWK	2	light	567.310752	y7	923.4774	79.7
P52911	EXG2	IPIGYWAWK	2	light	567.310752	y6	810.393336	79.7

P52911	EXG2	IPIGYWAWK	2	light	567.310752	y5	753.371872	79.7
P52911	EXG2	IPIGYWAWK	2	light	567.310752	y4	590.308544	79.7
P52911	EXG2	IPIGYWAWK	2	light	567.310752	y3	404.229231	79.7
P52911	EXG2	IPIGYWAWK	2	light	567.310752	y2	333.192117	79.7
P52911	EXG2	IPIGYWAWK	2	light	567.310752	y8	510.76872	79.7
P52911	EXG2	IPIGYWAWK	2	heavy	571.317851	y8	1028.54436	79.7
P52911	EXG2	IPIGYWAWK	2	heavy	571.317851	y7	931.491599	79.7
P52911	EXG2	IPIGYWAWK	2	heavy	571.317851	y6	818.407535	79.7
P52911	EXG2	IPIGYWAWK	2	heavy	571.317851	y5	761.386071	79.7
P52911	EXG2	IPIGYWAWK	2	heavy	571.317851	y4	598.322743	79.7
P52911	EXG2	IPIGYWAWK	2	heavy	571.317851	y3	412.24343	79.7
P52911	EXG2	IPIGYWAWK	2	heavy	571.317851	y2	341.206316	79.7
P52911	EXG2	IPIGYWAWK	2	heavy	571.317851	y8	514.775819	79.7
P52911	EXG2	ILYGDLGWLR	2	light	603.337498	y9	1092.58366	88.87
P52911	EXG2	ILYGDLGWLR	2	light	603.337498	y8	979.499592	88.87
P52911	EXG2	ILYGDLGWLR	2	light	603.337498	y7	816.436263	88.87
P52911	EXG2	ILYGDLGWLR	2	light	603.337498	y6	759.4148	88.87
P52911	EXG2	ILYGDLGWLR	2	light	603.337498	y5	644.387856	88.87
P52911	EXG2	ILYGDLGWLR	2	light	603.337498	y4	531.303792	88.87
P52911	EXG2	ILYGDLGWLR	2	heavy	606.347562	y9	1098.60379	88.87
P52911	EXG2	ILYGDLGWLR	2	heavy	606.347562	y8	985.519721	88.87
P52911	EXG2	ILYGDLGWLR	2	heavy	606.347562	y7	822.456392	88.87
P52911	EXG2	ILYGDLGWLR	2	heavy	606.347562	y6	765.434929	88.87
P52911	EXG2	ILYGDLGWLR	2	heavy	606.347562	y5	650.407985	88.87
P52911	EXG2	ILYGDLGWLR	2	heavy	606.347562	y4	537.323921	88.87
P23797	GPI12	VRELN[+203.1]ESAALLL	3	light	689.699153	y10	1123.62183	26.38
P23797	GPI12	VRELN[+203.1]ESAALLL	3	light	689.699153	y9	1036.5898	26.38
P23797	GPI12	VRELN[+203.1]ESAALLL	3	light	689.699153	y8	965.55269	26.38
P23797	GPI12	VRELN[+203.1]ESAALLL	3	light	689.699153	y7	894.515576	26.38
P23797	GPI12	VRELN[+203.1]ESAALLL	3	light	689.699153	y6	781.431512	26.38
P23797	GPI12	VRELN[+203.1]ESAALLL	3	light	689.699153	y5	668.347448	26.38
P23797	GPI12	VRELN[+203.1]ESAALLL	3	light	689.699153	y4	555.263384	26.38
P23797	GPI12	VRELN[+203.1]ESAALLL	3	light	689.699153	b4	498.303458	26.38
P23797	GPI12	VRELN[+203.1]ESAALLL	3	light	689.699153	b5	815.425759	26.38
P23797	GPI12	VRELN[+203.1]ESAALLL	3	light	689.699153	b6	944.468352	26.38
P23797	GPI12	VRELN[+203.1]ESAALLL	3	heavy	693.712573	y10	1129.64196	26.38
P23797	GPI12	VRELN[+203.1]ESAALLL	3	heavy	693.712573	y9	1042.60993	26.38
P23797	GPI12	VRELN[+203.1]ESAALLL	3	heavy	693.712573	y8	971.572819	26.38
P23797	GPI12	VRELN[+203.1]ESAALLL	3	heavy	693.712573	y7	900.535705	26.38
P23797	GPI12	VRELN[+203.1]ESAALLL	3	heavy	693.712573	y6	787.451641	26.38
P23797	GPI12	VRELN[+203.1]ESAALLL	3	heavy	693.712573	y5	674.367577	26.38
P23797	GPI12	VRELN[+203.1]ESAALLL	3	heavy	693.712573	y4	561.283513	26.38
P23797	GPI12	VRELN[+203.1]ESAALLL	3	heavy	693.712573	b4	504.323587	26.38
P23797	GPI12	VRELN[+203.1]ESAALLL	3	heavy	693.712573	b5	821.445888	26.38
P23797	GPI12	VRELN[+203.1]ESAALLL	3	heavy	693.712573	b6	950.488481	26.38
P23797	GPI12	TVPFNIIC[+57]LSK	2	light	646.357573	y9	1091.59178	81.7
P23797	GPI12	TVPFNIIC[+57]LSK	2	light	646.357573	y8	994.539014	81.7
P23797	GPI12	TVPFNIIC[+57]LSK	2	light	646.357573	y7	847.4706	81.7
P23797	GPI12	TVPFNIIC[+57]LSK	2	light	646.357573	y6	733.427673	81.7
P23797	GPI12	TVPFNIIC[+57]LSK	2	light	646.357573	y5	620.343609	81.7
P23797	GPI12	TVPFNIIC[+57]LSK	2	light	646.357573	y4	507.259545	81.7
P23797	GPI12	TVPFNIIC[+57]LSK	2	light	646.357573	y3	347.228896	81.7
P23797	GPI12	TVPFNIIC[+57]LSK	2	heavy	650.364673	y9	1099.60598	81.7
P23797	GPI12	TVPFNIIC[+57]LSK	2	heavy	650.364673	y8	1002.55321	81.7
P23797	GPI12	TVPFNIIC[+57]LSK	2	heavy	650.364673	y7	855.484799	81.7
P23797	GPI12	TVPFNIIC[+57]LSK	2	heavy	650.364673	y6	741.441872	81.7
P23797	GPI12	TVPFNIIC[+57]LSK	2	heavy	650.364673	y5	628.357808	81.7
P23797	GPI12	TVPFNIIC[+57]LSK	2	heavy	650.364673	y4	515.273744	81.7
P23797	GPI12	TVPFNIIC[+57]LSK	2	heavy	650.364673	y3	355.243095	81.7
P23797	GPI12	GNAEGLGETR	2	light	502.243795	y8	832.415922	-22.82
P23797	GPI12	GNAEGLGETR	2	light	502.243795	y7	761.378808	-22.82
P23797	GPI12	GNAEGLGETR	2	light	502.243795	y6	632.336215	-22.82
P23797	GPI12	GNAEGLGETR	2	light	502.243795	y5	575.314751	-22.82

P23797	GPI12	GNAEGLGETR	2	light	502.243795	y4	462.230687	-22.82
P23797	GPI12	GNAEGLGETR	2	light	502.243795	y3	405.209223	-22.82
P23797	GPI12	GNAEGLGETR	2	heavy	505.253859	y8	838.436051	-22.82
P23797	GPI12	GNAEGLGETR	2	heavy	505.253859	y7	767.398937	-22.82
P23797	GPI12	GNAEGLGETR	2	heavy	505.253859	y6	638.356344	-22.82
P23797	GPI12	GNAEGLGETR	2	heavy	505.253859	y5	581.33488	-22.82
P23797	GPI12	GNAEGLGETR	2	heavy	505.253859	y4	468.250816	-22.82
P23797	GPI12	GNAEGLGETR	2	heavy	505.253859	y3	411.229352	-22.82
P40345	PDAT	SSSEDALNN[+203.1]NTI	2	light	1161.01184	y10	1200.56438	40.17
P40345	PDAT	SSSEDALNN[+203.1]NTI	2	light	1161.01184	y9	1086.52145	40.17
P40345	PDAT	SSSEDALNN[+203.1]NTI	2	light	1161.01184	y8	985.473771	40.17
P40345	PDAT	SSSEDALNN[+203.1]NTI	2	light	1161.01184	y7	870.446828	40.17
P40345	PDAT	SSSEDALNN[+203.1]NTI	2	light	1161.01184	y6	769.399149	40.17
P40345	PDAT	SSSEDALNN[+203.1]NTI	2	light	1161.01184	y5	606.335821	40.17
P40345	PDAT	SSSEDALNN[+203.1]NTI	2	heavy	1164.02191	y10	1206.58451	40.17
P40345	PDAT	SSSEDALNN[+203.1]NTI	2	heavy	1164.02191	y9	1092.54158	40.17
P40345	PDAT	SSSEDALNN[+203.1]NTI	2	heavy	1164.02191	y8	991.4939	40.17
P40345	PDAT	SSSEDALNN[+203.1]NTI	2	heavy	1164.02191	y7	876.466957	40.17
P40345	PDAT	SSSEDALNN[+203.1]NTI	2	heavy	1164.02191	y6	775.419278	40.17
P40345	PDAT	SSSEDALNN[+203.1]NTI	2	heavy	1164.02191	y5	612.35595	40.17
P40345	PDAT	MLQTWGGIPSMLPK	2	light	779.909647	y11	1186.62889	91.84
P40345	PDAT	MLQTWGGIPSMLPK	2	light	779.909647	y10	1085.58121	91.84
P40345	PDAT	MLQTWGGIPSMLPK	2	light	779.909647	y9	899.5019	91.84
P40345	PDAT	MLQTWGGIPSMLPK	2	light	779.909647	y8	842.480436	91.84
P40345	PDAT	MLQTWGGIPSMLPK	2	light	779.909647	y6	672.374909	91.84
P40345	PDAT	MLQTWGGIPSMLPK	2	light	779.909647	y2	244.165568	91.84
P40345	PDAT	MLQTWGGIPSMLPK	2	heavy	783.916746	y11	1194.64309	91.84
P40345	PDAT	MLQTWGGIPSMLPK	2	heavy	783.916746	y10	1093.59541	91.84
P40345	PDAT	MLQTWGGIPSMLPK	2	heavy	783.916746	y9	907.516099	91.84
P40345	PDAT	MLQTWGGIPSMLPK	2	heavy	783.916746	y8	850.494635	91.84
P40345	PDAT	MLQTWGGIPSMLPK	2	heavy	783.916746	y6	680.389108	91.84
P40345	PDAT	MLQTWGGIPSMLPK	2	heavy	783.916746	y2	252.179767	91.84
P40345	PDAT	IASGNGDLVEPR	2	light	614.320033	y11	1114.54873	3.67
P40345	PDAT	IASGNGDLVEPR	2	light	614.320033	y10	1043.51161	3.67
P40345	PDAT	IASGNGDLVEPR	2	light	614.320033	y9	956.479585	3.67
P40345	PDAT	IASGNGDLVEPR	2	light	614.320033	y8	899.458121	3.67
P40345	PDAT	IASGNGDLVEPR	2	light	614.320033	y7	785.415194	3.67
P40345	PDAT	IASGNGDLVEPR	2	light	614.320033	y6	728.39373	3.67
P40345	PDAT	IASGNGDLVEPR	2	light	614.320033	y5	613.366787	3.67
P40345	PDAT	IASGNGDLVEPR	2	light	614.320033	y4	500.282723	3.67
P40345	PDAT	IASGNGDLVEPR	2	heavy	617.330098	y11	1120.56886	3.67
P40345	PDAT	IASGNGDLVEPR	2	heavy	617.330098	y10	1049.53174	3.67
P40345	PDAT	IASGNGDLVEPR	2	heavy	617.330098	y9	962.499714	3.67
P40345	PDAT	IASGNGDLVEPR	2	heavy	617.330098	y8	905.47825	3.67
P40345	PDAT	IASGNGDLVEPR	2	heavy	617.330098	y7	791.435323	3.67
P40345	PDAT	IASGNGDLVEPR	2	heavy	617.330098	y6	734.413859	3.67
P40345	PDAT	IASGNGDLVEPR	2	heavy	617.330098	y5	619.386916	3.67
P40345	PDAT	IASGNGDLVEPR	2	heavy	617.330098	y4	506.302852	3.67
P38244	M28P1orF	SILFQQQDPFN[+203.1]E	2	light	999.973801	y9	1282.5546	55.8
P38244	M28P1orF	SILFQQQDPFN[+203.1]E	2	light	999.973801	y8	1154.49602	55.8
P38244	M28P1orF	SILFQQQDPFN[+203.1]E	2	light	999.973801	y7	1039.46908	55.8
P38244	M28P1orF	SILFQQQDPFN[+203.1]E	2	light	999.973801	y3	349.183009	55.8
P38244	M28P1orF	SILFQQQDPFN[+203.1]E	2	light	999.973801	b3	314.207432	55.8
P38244	M28P1orF	SILFQQQDPFN[+203.1]E	2	heavy	1002.98387	y9	1288.57473	55.8
P38244	M28P1orF	SILFQQQDPFN[+203.1]E	2	heavy	1002.98387	y8	1160.51615	55.8
P38244	M28P1orF	SILFQQQDPFN[+203.1]E	2	heavy	1002.98387	y7	1045.48921	55.8
P38244	M28P1orF	SILFQQQDPFN[+203.1]E	2	heavy	1002.98387	y3	355.203138	55.8
P38244	M28P1orF	SILFQQQDPFN[+203.1]E	2	heavy	1002.98387	b3	314.207432	55.8
P38244	M28P1orF	GSNSMEEGLSTR	2	light	634.282791	y9	1009.46189	-2.49
P38244	M28P1orF	GSNSMEEGLSTR	2	light	634.282791	y8	922.429857	-2.49
P38244	M28P1orF	GSNSMEEGLSTR	2	light	634.282791	y7	791.389373	-2.49
P38244	M28P1orF	GSNSMEEGLSTR	2	light	634.282791	y6	662.34678	-2.49
P38244	M28P1orF	GSNSMEEGLSTR	2	light	634.282791	y5	533.304186	-2.49

P38244	M28P1orF	GSNSMEEGLSTR	2	heavy	637.292855	y9	1015.48202	-2.49
P38244	M28P1orF	GSNSMEEGLSTR	2	heavy	637.292855	y8	928.449986	-2.49
P38244	M28P1orF	GSNSMEEGLSTR	2	heavy	637.292855	y7	797.409502	-2.49
P38244	M28P1orF	GSNSMEEGLSTR	2	heavy	637.292855	y6	668.366909	-2.49
P38244	M28P1orF	GSNSMEEGLSTR	2	heavy	637.292855	y5	539.324315	-2.49
P38244	M28P1orF	FSQNIDLSQGNAASVHV	2	light	1057.04288	y11	1080.59087	50.29
P38244	M28P1orF	FSQNIDLSQGNAASVHV	2	light	1057.04288	y10	1023.5694	50.29
P38244	M28P1orF	FSQNIDLSQGNAASVHV	2	light	1057.04288	y9	909.526475	50.29
P38244	M28P1orF	FSQNIDLSQGNAASVHV	2	light	1057.04288	y8	838.489362	50.29
P38244	M28P1orF	FSQNIDLSQGNAASVHV	2	light	1057.04288	y7	767.452248	50.29
P38244	M28P1orF	FSQNIDLSQGNAASVHV	2	light	1057.04288	y6	680.420219	50.29
P38244	M28P1orF	FSQNIDLSQGNAASVHV	2	light	1057.04288	y5	581.351805	50.29
P38244	M28P1orF	FSQNIDLSQGNAASVHV	2	light	1057.04288	y4	444.292893	50.29
P38244	M28P1orF	FSQNIDLSQGNAASVHV	2	heavy	1060.05295	y11	1086.611	50.29
P38244	M28P1orF	FSQNIDLSQGNAASVHV	2	heavy	1060.05295	y10	1029.58953	50.29
P38244	M28P1orF	FSQNIDLSQGNAASVHV	2	heavy	1060.05295	y9	915.546604	50.29
P38244	M28P1orF	FSQNIDLSQGNAASVHV	2	heavy	1060.05295	y8	844.509491	50.29
P38244	M28P1orF	FSQNIDLSQGNAASVHV	2	heavy	1060.05295	y7	773.472377	50.29
P38244	M28P1orF	FSQNIDLSQGNAASVHV	2	heavy	1060.05295	y6	686.440348	50.29
P38244	M28P1orF	FSQNIDLSQGNAASVHV	2	heavy	1060.05295	y5	587.371934	50.29
P38244	M28P1orF	FSQNIDLSQGNAASVHV	2	heavy	1060.05295	y4	450.313022	50.29
P17967	PDI	LAPTYQELADTYAN[+20	3	light	891.116479	y11	1305.68964	91.36
P17967	PDI	LAPTYQELADTYAN[+20	3	light	891.116479	y10	1234.65252	91.36
P17967	PDI	LAPTYQELADTYAN[+20	3	light	891.116479	y9	917.530223	91.36
P17967	PDI	LAPTYQELADTYAN[+20	3	light	891.116479	y8	846.49311	91.36
P17967	PDI	LAPTYQELADTYAN[+20	3	light	891.116479	y7	745.445431	91.36
P17967	PDI	LAPTYQELADTYAN[+20	3	light	891.116479	y4	444.318046	91.36
P17967	PDI	LAPTYQELADTYAN[+20	3	light	891.116479	y3	331.233982	91.36
P17967	PDI	LAPTYQELADTYAN[+20	3	light	891.116479	y2	218.149918	91.36
P17967	PDI	LAPTYQELADTYAN[+20	3	light	891.116479	b7	803.393395	91.36
P17967	PDI	LAPTYQELADTYAN[+20	3	heavy	893.787879	y11	1313.70384	91.36
P17967	PDI	LAPTYQELADTYAN[+20	3	heavy	893.787879	y10	1242.66672	91.36
P17967	PDI	LAPTYQELADTYAN[+20	3	heavy	893.787879	y8	854.507309	91.36
P17967	PDI	LAPTYQELADTYAN[+20	3	heavy	893.787879	y7	753.45963	91.36
P17967	PDI	LAPTYQELADTYAN[+20	3	heavy	893.787879	y4	452.332245	91.36
P17967	PDI	LAPTYQELADTYAN[+20	3	heavy	893.787879	y3	339.248181	91.36
P17967	PDI	LAPTYQELADTYAN[+20	3	heavy	893.787879	y2	226.164117	91.36
P17967	PDI	LAPTYQELADTYAN[+20	3	heavy	893.787879	b7	803.393395	91.36
P17967	PDI	NSDVN[+203.1]NSIDYEC	2	light	891.892477	y9	1050.48506	12.59
P17967	PDI	NSDVN[+203.1]NSIDYEC	2	light	891.892477	y8	936.442137	12.59
P17967	PDI	NSDVN[+203.1]NSIDYEC	2	light	891.892477	y7	849.410108	12.59
P17967	PDI	NSDVN[+203.1]NSIDYEC	2	light	891.892477	y6	736.326044	12.59
P17967	PDI	NSDVN[+203.1]NSIDYEC	2	light	891.892477	y5	621.299101	12.59
P17967	PDI	NSDVN[+203.1]NSIDYEC	2	light	891.892477	y4	458.235772	12.59
P17967	PDI	NSDVN[+203.1]NSIDYEC	2	light	891.892477	y3	329.193179	12.59
P17967	PDI	NSDVN[+203.1]NSIDYEC	2	heavy	894.902541	y9	1056.50519	12.59
P17967	PDI	NSDVN[+203.1]NSIDYEC	2	heavy	894.902541	y8	942.462266	12.59
P17967	PDI	NSDVN[+203.1]NSIDYEC	2	heavy	894.902541	y7	855.430237	12.59
P17967	PDI	NSDVN[+203.1]NSIDYEC	2	heavy	894.902541	y6	742.346173	12.59
P17967	PDI	NSDVN[+203.1]NSIDYEC	2	heavy	894.902541	y5	627.31923	12.59
P17967	PDI	NSDVN[+203.1]NSIDYEC	2	heavy	894.902541	y4	464.255901	12.59
P17967	PDI	NSDVN[+203.1]NSIDYEC	2	heavy	894.902541	y3	335.213308	12.59
P17967	PDI	IDADFN[+203.1]ATFYSM	2	light	963.924931	y9	1048.47681	43.62
P17967	PDI	IDADFN[+203.1]ATFYSM	2	light	963.924931	y8	977.439694	43.62
P17967	PDI	IDADFN[+203.1]ATFYSM	2	light	963.924931	y7	876.392016	43.62
P17967	PDI	IDADFN[+203.1]ATFYSM	2	light	963.924931	y6	729.323602	43.62
P17967	PDI	IDADFN[+203.1]ATFYSM	2	light	963.924931	y5	566.260273	43.62
P17967	PDI	IDADFN[+203.1]ATFYSM	2	light	963.924931	y3	332.192845	43.62
P17967	PDI	IDADFN[+203.1]ATFYSM	2	light	963.924931	b4	415.18234	43.62
P17967	PDI	IDADFN[+203.1]ATFYSM	2	light	963.924931	b6	879.373054	43.62
P17967	PDI	IDADFN[+203.1]ATFYSM	2	light	963.924931	b7	950.410168	43.62
P17967	PDI	IDADFN[+203.1]ATFYSM	2	light	963.924931	b8	1051.45785	43.62
P17967	PDI	IDADFN[+203.1]ATFYSM	2	light	963.924931	b9	1198.52626	43.62

P17967	PDI	IDADFN[+203.1]ATFYSM	2	heavy	967.932031	y9	1056.49101	43.62
P17967	PDI	IDADFN[+203.1]ATFYSM	2	heavy	967.932031	y8	985.453893	43.62
P17967	PDI	IDADFN[+203.1]ATFYSM	2	heavy	967.932031	y7	884.406215	43.62
P17967	PDI	IDADFN[+203.1]ATFYSM	2	heavy	967.932031	y6	737.337801	43.62
P17967	PDI	IDADFN[+203.1]ATFYSM	2	heavy	967.932031	y5	574.274472	43.62
P17967	PDI	IDADFN[+203.1]ATFYSM	2	heavy	967.932031	y3	340.207044	43.62
P17967	PDI	IDADFN[+203.1]ATFYSM	2	heavy	967.932031	b4	415.18234	43.62
P17967	PDI	IDADFN[+203.1]ATFYSM	2	heavy	967.932031	b6	879.373054	43.62
P17967	PDI	IDADFN[+203.1]ATFYSM	2	heavy	967.932031	b7	950.410168	43.62
P17967	PDI	IDADFN[+203.1]ATFYSM	2	heavy	967.932031	b8	1051.45785	43.62
P17967	PDI	IDADFN[+203.1]ATFYSM	2	heavy	967.932031	b9	1198.52626	43.62
P17967	PDI	QSQPAVAVVADLPAYLA	3	light	1139.27136	y12	1275.73071	150.03
P17967	PDI	QSQPAVAVVADLPAYLA	3	light	1139.27136	y11	1174.68304	150.03
P17967	PDI	QSQPAVAVVADLPAYLA	3	light	1139.27136	y10	1027.61462	150.03
P17967	PDI	QSQPAVAVVADLPAYLA	3	light	1139.27136	y9	928.546208	150.03
P17967	PDI	QSQPAVAVVADLPAYLA	3	light	1139.27136	y8	827.498529	150.03
P17967	PDI	QSQPAVAVVADLPAYLA	3	light	1139.27136	y5	518.293287	150.03
P17967	PDI	QSQPAVAVVADLPAYLA	3	light	1139.27136	y4	419.224873	150.03
P17967	PDI	QSQPAVAVVADLPAYLA	3	heavy	1141.94276	y12	1283.74491	150.03
P17967	PDI	QSQPAVAVVADLPAYLA	3	heavy	1141.94276	y11	1182.69724	150.03
P17967	PDI	QSQPAVAVVADLPAYLA	3	heavy	1141.94276	y10	1035.62882	150.03
P17967	PDI	QSQPAVAVVADLPAYLA	3	heavy	1141.94276	y9	936.560407	150.03
P17967	PDI	QSQPAVAVVADLPAYLA	3	heavy	1141.94276	y8	835.512728	150.03
P17967	PDI	QSQPAVAVVADLPAYLA	3	heavy	1141.94276	y5	526.307486	150.03
P17967	PDI	QSQPAVAVVADLPAYLA	3	heavy	1141.94276	y4	427.239072	150.03
P17967	PDI	N[+203.1]ITLAQIDC[+57]	3	light	1159.87055	y11	1238.6528	98.13
P17967	PDI	N[+203.1]ITLAQIDC[+57]	3	light	1159.87055	y10	1109.61021	98.13
P17967	PDI	N[+203.1]ITLAQIDC[+57]	3	light	1159.87055	y9	972.551293	98.13
P17967	PDI	N[+203.1]ITLAQIDC[+57]	3	light	1159.87055	y8	858.508366	98.13
P17967	PDI	N[+203.1]ITLAQIDC[+57]	3	light	1159.87055	y7	745.424302	98.13
P17967	PDI	N[+203.1]ITLAQIDC[+57]	3	light	1159.87055	y4	444.28166	98.13
P17967	PDI	N[+203.1]ITLAQIDC[+57]	3	light	1159.87055	b2	431.21364	98.13
P17967	PDI	N[+203.1]ITLAQIDC[+57]	3	light	1159.87055	b3	532.261319	98.13
P17967	PDI	N[+203.1]ITLAQIDC[+57]	3	light	1159.87055	b4	645.345383	98.13
P17967	PDI	N[+203.1]ITLAQIDC[+57]	3	light	1159.87055	b5	716.382497	98.13
P17967	PDI	N[+203.1]ITLAQIDC[+57]	3	heavy	1162.54195	y11	1246.667	98.13
P17967	PDI	N[+203.1]ITLAQIDC[+57]	3	heavy	1162.54195	y10	1117.6244	98.13
P17967	PDI	N[+203.1]ITLAQIDC[+57]	3	heavy	1162.54195	y9	980.565492	98.13
P17967	PDI	N[+203.1]ITLAQIDC[+57]	3	heavy	1162.54195	y8	866.522565	98.13
P17967	PDI	N[+203.1]ITLAQIDC[+57]	3	heavy	1162.54195	y7	753.438501	98.13
P17967	PDI	N[+203.1]ITLAQIDC[+57]	3	heavy	1162.54195	y4	452.295859	98.13
P17967	PDI	N[+203.1]ITLAQIDC[+57]	3	heavy	1162.54195	b2	431.21364	98.13
P17967	PDI	N[+203.1]ITLAQIDC[+57]	3	heavy	1162.54195	b3	532.261319	98.13
P17967	PDI	N[+203.1]ITLAQIDC[+57]	3	heavy	1162.54195	b4	645.345383	98.13
P17967	PDI	N[+203.1]ITLAQIDC[+57]	3	heavy	1162.54195	b5	716.382497	98.13
P17967	PDI	TAEAIVQFMIK	2	light	625.844299	y9	1078.59653	82.79
P17967	PDI	TAEAIVQFMIK	2	light	625.844299	y8	949.553936	82.79
P17967	PDI	TAEAIVQFMIK	2	light	625.844299	y7	878.516822	82.79
P17967	PDI	TAEAIVQFMIK	2	light	625.844299	y6	765.432758	82.79
P17967	PDI	TAEAIVQFMIK	2	light	625.844299	y4	538.305766	82.79
P17967	PDI	TAEAIVQFMIK	2	heavy	629.851398	y9	1086.61073	82.79
P17967	PDI	TAEAIVQFMIK	2	heavy	629.851398	y8	957.568135	82.79
P17967	PDI	TAEAIVQFMIK	2	heavy	629.851398	y7	886.531021	82.79
P17967	PDI	TAEAIVQFMIK	2	heavy	629.851398	y6	773.446957	82.79
P17967	PDI	TAEAIVQFMIK	2	heavy	629.851398	y4	546.319965	82.79
P17967	PDI	GLMNFVSIDAR	2	light	611.816072	y9	1052.51934	72.95
P17967	PDI	GLMNFVSIDAR	2	light	611.816072	y7	807.435929	72.95
P17967	PDI	GLMNFVSIDAR	2	light	611.816072	y6	660.367515	72.95
P17967	PDI	GLMNFVSIDAR	2	light	611.816072	y5	561.299101	72.95
P17967	PDI	GLMNFVSIDAR	2	light	611.816072	y3	361.183009	72.95
P17967	PDI	GLMNFVSIDAR	2	light	611.816072	y2	246.156066	72.95
P17967	PDI	GLMNFVSIDAR	2	heavy	614.826137	y9	1058.53947	72.95
P17967	PDI	GLMNFVSIDAR	2	heavy	614.826137	y7	813.456058	72.95

P17967	PDI	GLMNFVSIDAR	2	heavy	614.826137	y6	666.387644	72.95
P17967	PDI	GLMNFVSIDAR	2	heavy	614.826137	y5	567.31923	72.95
P17967	PDI	GLMNFVSIDAR	2	heavy	614.826137	y3	367.203138	72.95
P17967	PDI	GLMNFVSIDAR	2	heavy	614.826137	y2	252.176195	72.95
Q03691	ROT1	YN[+203.1]QTETFK	2	light	617.285325	y7	1070.50005	-12.58
Q03691	ROT1	YN[+203.1]QTETFK	2	light	617.285325	y6	753.377745	-12.58
Q03691	ROT1	YN[+203.1]QTETFK	2	light	617.285325	y5	625.319168	-12.58
Q03691	ROT1	YN[+203.1]QTETFK	2	light	617.285325	y4	524.271489	-12.58
Q03691	ROT1	YN[+203.1]QTETFK	2	light	617.285325	y3	395.228896	-12.58
Q03691	ROT1	YN[+203.1]QTETFK	2	light	617.285325	y2	294.181218	-12.58
Q03691	ROT1	YN[+203.1]QTETFK	2	light	617.285325	b2	481.192905	-12.58
Q03691	ROT1	YN[+203.1]QTETFK	2	light	617.285325	b3	609.251483	-12.58
Q03691	ROT1	YN[+203.1]QTETFK	2	light	617.285325	b4	710.299161	-12.58
Q03691	ROT1	YN[+203.1]QTETFK	2	heavy	621.292425	y7	1078.51425	-12.58
Q03691	ROT1	YN[+203.1]QTETFK	2	heavy	621.292425	y6	761.391944	-12.58
Q03691	ROT1	YN[+203.1]QTETFK	2	heavy	621.292425	y5	633.333367	-12.58
Q03691	ROT1	YN[+203.1]QTETFK	2	heavy	621.292425	y4	532.285688	-12.58
Q03691	ROT1	YN[+203.1]QTETFK	2	heavy	621.292425	y3	403.243095	-12.58
Q03691	ROT1	YN[+203.1]QTETFK	2	heavy	621.292425	y2	302.195417	-12.58
Q03691	ROT1	YN[+203.1]QTETFK	2	heavy	621.292425	b2	481.192905	-12.58
Q03691	ROT1	YN[+203.1]QTETFK	2	heavy	621.292425	b3	609.251483	-12.58
Q03691	ROT1	YN[+203.1]QTETFK	2	heavy	621.292425	b4	710.299161	-12.58
Q03691	ROT1	EDESNSIYGTWSSK	2	light	801.849549	y11	1229.57969	32.31
Q03691	ROT1	EDESNSIYGTWSSK	2	light	801.849549	y9	1028.50474	32.31
Q03691	ROT1	EDESNSIYGTWSSK	2	light	801.849549	y8	941.472708	32.31
Q03691	ROT1	EDESNSIYGTWSSK	2	light	801.849549	y7	828.388644	32.31
Q03691	ROT1	EDESNSIYGTWSSK	2	light	801.849549	y6	665.325316	32.31
Q03691	ROT1	EDESNSIYGTWSSK	2	light	801.849549	y4	507.256174	32.31
Q03691	ROT1	EDESNSIYGTWSSK	2	light	801.849549	y3	321.176861	32.31
Q03691	ROT1	EDESNSIYGTWSSK	2	heavy	805.856649	y11	1237.59389	32.31
Q03691	ROT1	EDESNSIYGTWSSK	2	heavy	805.856649	y9	1036.51894	32.31
Q03691	ROT1	EDESNSIYGTWSSK	2	heavy	805.856649	y8	949.486907	32.31
Q03691	ROT1	EDESNSIYGTWSSK	2	heavy	805.856649	y7	836.402843	32.31
Q03691	ROT1	EDESNSIYGTWSSK	2	heavy	805.856649	y6	673.339515	32.31
Q03691	ROT1	EDESNSIYGTWSSK	2	heavy	805.856649	y4	515.270373	32.31
Q03691	ROT1	EDESNSIYGTWSSK	2	heavy	805.856649	y3	329.19106	32.31
Q03691	ROT1	QLFSDPC[+57]NDDGVS	2	light	980.920711	y10	1113.48071	40.28
Q03691	ROT1	QLFSDPC[+57]NDDGVS	2	light	980.920711	y9	999.43778	40.28
Q03691	ROT1	QLFSDPC[+57]NDDGVS	2	light	980.920711	y8	884.410836	40.28
Q03691	ROT1	QLFSDPC[+57]NDDGVS	2	light	980.920711	y7	769.383893	40.28
Q03691	ROT1	QLFSDPC[+57]NDDGVS	2	light	980.920711	y5	613.294016	40.28
Q03691	ROT1	QLFSDPC[+57]NDDGVS	2	light	980.920711	y3	425.214309	40.28
Q03691	ROT1	QLFSDPC[+57]NDDGVS	2	heavy	983.930776	y10	1119.50084	40.28
Q03691	ROT1	QLFSDPC[+57]NDDGVS	2	heavy	983.930776	y9	1005.45791	40.28
Q03691	ROT1	QLFSDPC[+57]NDDGVS	2	heavy	983.930776	y8	890.430965	40.28
Q03691	ROT1	QLFSDPC[+57]NDDGVS	2	heavy	983.930776	y7	775.404022	40.28
Q03691	ROT1	QLFSDPC[+57]NDDGVS	2	heavy	983.930776	y5	619.314145	40.28
Q03691	ROT1	QLFSDPC[+57]NDDGVS	2	heavy	983.930776	y3	431.234438	40.28
P40533	TED1	DNYWIEYETN[+203.1]T	3	light	776.678306	y8	1215.57528	57.47
P40533	TED1	DNYWIEYETN[+203.1]T	3	light	776.678306	y7	1114.5276	57.47
P40533	TED1	DNYWIEYETN[+203.1]T	3	light	776.678306	y6	797.405297	57.47
P40533	TED1	DNYWIEYETN[+203.1]T	3	light	776.678306	y5	696.357619	57.47
P40533	TED1	DNYWIEYETN[+203.1]T	3	light	776.678306	y4	595.30994	57.47
P40533	TED1	DNYWIEYETN[+203.1]T	3	light	776.678306	y3	458.251029	57.47
P40533	TED1	DNYWIEYETN[+203.1]T	3	light	776.678306	b2	230.077147	57.47
P40533	TED1	DNYWIEYETN[+203.1]T	3	light	776.678306	b3	393.140475	57.47
P40533	TED1	DNYWIEYETN[+203.1]T	3	heavy	778.685016	y8	1221.59541	57.47
P40533	TED1	DNYWIEYETN[+203.1]T	3	heavy	778.685016	y7	1120.54773	57.47
P40533	TED1	DNYWIEYETN[+203.1]T	3	heavy	778.685016	y6	803.425426	57.47
P40533	TED1	DNYWIEYETN[+203.1]T	3	heavy	778.685016	y5	702.377748	57.47
P40533	TED1	DNYWIEYETN[+203.1]T	3	heavy	778.685016	y4	601.330069	57.47
P40533	TED1	DNYWIEYETN[+203.1]T	3	heavy	778.685016	y3	464.271158	57.47
P40533	TED1	DNYWIEYETN[+203.1]T	3	heavy	778.685016	b2	230.077147	57.47

P40533	TED1	DNYWIEYETN[+203.1]T	3	heavy	778.685016	b3	393.140475	57.47
P40533	TED1	NIESDVFVK	2	light	525.776939	y7	823.41961	30.03
P40533	TED1	NIESDVFVK	2	light	525.776939	y6	694.377017	30.03
P40533	TED1	NIESDVFVK	2	light	525.776939	y5	607.344989	30.03
P40533	TED1	NIESDVFVK	2	light	525.776939	y4	492.318046	30.03
P40533	TED1	NIESDVFVK	2	light	525.776939	y3	393.249632	30.03
P40533	TED1	NIESDVFVK	2	light	525.776939	y2	246.181218	30.03
P40533	TED1	NIESDVFVK	2	light	525.776939	y5	304.176132	30.03
P40533	TED1	NIESDVFVK	2	heavy	529.784038	y7	831.433809	30.03
P40533	TED1	NIESDVFVK	2	heavy	529.784038	y6	702.391216	30.03
P40533	TED1	NIESDVFVK	2	heavy	529.784038	y5	615.359188	30.03
P40533	TED1	NIESDVFVK	2	heavy	529.784038	y4	500.332245	30.03
P40533	TED1	NIESDVFVK	2	heavy	529.784038	y3	401.263831	30.03
P40533	TED1	NIESDVFVK	2	heavy	529.784038	y2	254.195417	30.03
P40533	TED1	NIESDVFVK	2	heavy	529.784038	y5	308.183232	30.03
P40533	TED1	EGLC[+57]VDGPDTR	2	light	609.774602	y8	919.393806	5.72
P40533	TED1	EGLC[+57]VDGPDTR	2	light	609.774602	y7	759.363158	5.72
P40533	TED1	EGLC[+57]VDGPDTR	2	light	609.774602	y6	660.294744	5.72
P40533	TED1	EGLC[+57]VDGPDTR	2	light	609.774602	y5	545.267801	5.72
P40533	TED1	EGLC[+57]VDGPDTR	2	light	609.774602	y4	488.246337	5.72
P40533	TED1	EGLC[+57]VDGPDTR	2	light	609.774602	y3	391.193573	5.72
P40533	TED1	EGLC[+57]VDGPDTR	2	heavy	612.784666	y8	925.413935	5.72
P40533	TED1	EGLC[+57]VDGPDTR	2	heavy	612.784666	y7	765.383287	5.72
P40533	TED1	EGLC[+57]VDGPDTR	2	heavy	612.784666	y6	666.314873	5.72
P40533	TED1	EGLC[+57]VDGPDTR	2	heavy	612.784666	y5	551.28793	5.72
P40533	TED1	EGLC[+57]VDGPDTR	2	heavy	612.784666	y4	494.266466	5.72
P40533	TED1	EGLC[+57]VDGPDTR	2	heavy	612.784666	y3	397.213702	5.72
P43611	OSW7	NLDDLN[+203.1]TTVNE(	2	light	1191.08956	y10	1192.62083	84.34
P43611	OSW7	NLDDLN[+203.1]TTVNE(	2	light	1191.08956	y9	1078.5779	84.34
P43611	OSW7	NLDDLN[+203.1]TTVNE(	2	light	1191.08956	y8	949.535309	84.34
P43611	OSW7	NLDDLN[+203.1]TTVNE(	2	light	1191.08956	y7	821.476731	84.34
P43611	OSW7	NLDDLN[+203.1]TTVNE(	2	light	1191.08956	y6	708.392667	84.34
P43611	OSW7	NLDDLN[+203.1]TTVNE(	2	light	1191.08956	y5	609.324253	84.34
P43611	OSW7	NLDDLN[+203.1]TTVNE(	2	light	1191.08956	y4	462.255839	84.34
P43611	OSW7	NLDDLN[+203.1]TTVNE(	2	light	1191.08956	y3	349.171775	84.34
P43611	OSW7	NLDDLN[+203.1]TTVNE(	2	light	1191.08956	y2	234.144832	84.34
P43611	OSW7	NLDDLN[+203.1]TTVNE(	2	light	1191.08956	b6	444.700897	84.34
P43611	OSW7	NLDDLN[+203.1]TTVNE(	2	light	1191.08956	b7	495.224736	84.34
P43611	OSW7	NLDDLN[+203.1]TTVNE(	2	heavy	1195.09666	y10	1200.63503	84.34
P43611	OSW7	NLDDLN[+203.1]TTVNE(	2	heavy	1195.09666	y9	1086.5921	84.34
P43611	OSW7	NLDDLN[+203.1]TTVNE(	2	heavy	1195.09666	y8	957.549508	84.34
P43611	OSW7	NLDDLN[+203.1]TTVNE(	2	heavy	1195.09666	y7	829.49093	84.34
P43611	OSW7	NLDDLN[+203.1]TTVNE(	2	heavy	1195.09666	y6	716.406866	84.34
P43611	OSW7	NLDDLN[+203.1]TTVNE(	2	heavy	1195.09666	y5	617.338452	84.34
P43611	OSW7	NLDDLN[+203.1]TTVNE(	2	heavy	1195.09666	y4	470.270038	84.34
P43611	OSW7	NLDDLN[+203.1]TTVNE(	2	heavy	1195.09666	y3	357.185974	84.34
P43611	OSW7	NLDDLN[+203.1]TTVNE(	2	heavy	1195.09666	y2	242.159031	84.34
P43611	OSW7	NLDDLN[+203.1]TTVNE(	2	heavy	1195.09666	b6	444.700897	84.34
P43611	OSW7	NLDDLN[+203.1]TTVNE(	2	heavy	1195.09666	b7	495.224736	84.34
P43611	OSW7	SSITSILK	2	light	424.758018	y7	761.476731	24.96
P43611	OSW7	SSITSILK	2	light	424.758018	y6	674.444703	24.96
P43611	OSW7	SSITSILK	2	light	424.758018	y5	561.360639	24.96
P43611	OSW7	SSITSILK	2	light	424.758018	y4	460.31296	24.96
P43611	OSW7	SSITSILK	2	light	424.758018	y3	373.280932	24.96
P43611	OSW7	SSITSILK	2	light	424.758018	b2	175.071333	24.96
P43611	OSW7	SSITSILK	2	heavy	428.765117	y7	769.49093	24.96
P43611	OSW7	SSITSILK	2	heavy	428.765117	y6	682.458902	24.96
P43611	OSW7	SSITSILK	2	heavy	428.765117	y5	569.374838	24.96
P43611	OSW7	SSITSILK	2	heavy	428.765117	y4	468.327159	24.96
P43611	OSW7	SSITSILK	2	heavy	428.765117	y3	381.295131	24.96
P43611	OSW7	SSITSILK	2	heavy	428.765117	b2	175.071333	24.96
P36051	MCD4	HLDQLFHN[+203.1]STLN	4	light	706.342434	y9	1313.62195	52.41
P36051	MCD4	HLDQLFHN[+203.1]STLN	4	light	706.342434	y8	996.499651	52.41

P36051	MCD4	HLDQLFHN[+203.1]STLN	4	light	706.342434	y7	909.467623	52.41
P36051	MCD4	HLDQLFHN[+203.1]STLN	4	light	706.342434	y6	808.419945	52.41
P36051	MCD4	HLDQLFHN[+203.1]STLN	4	light	706.342434	y5	695.335881	52.41
P36051	MCD4	HLDQLFHN[+203.1]STLN	4	light	706.342434	y4	580.308937	52.41
P36051	MCD4	HLDQLFHN[+203.1]STLN	4	light	706.342434	y2	288.203016	52.41
P36051	MCD4	HLDQLFHN[+203.1]STLN	4	light	706.342434	y13	966.45765	52.41
P36051	MCD4	HLDQLFHN[+203.1]STLN	4	light	706.342434	y12	807.896499	52.41
P36051	MCD4	HLDQLFHN[+203.1]STLN	4	light	706.342434	y5	348.171578	52.41
P36051	MCD4	HLDQLFHN[+203.1]STLN	4	light	706.342434	b2	251.150252	52.41
P36051	MCD4	HLDQLFHN[+203.1]STLN	4	heavy	707.847467	y9	1319.64208	52.41
P36051	MCD4	HLDQLFHN[+203.1]STLN	4	heavy	707.847467	y8	1002.51978	52.41
P36051	MCD4	HLDQLFHN[+203.1]STLN	4	heavy	707.847467	y7	915.487752	52.41
P36051	MCD4	HLDQLFHN[+203.1]STLN	4	heavy	707.847467	y6	814.440074	52.41
P36051	MCD4	HLDQLFHN[+203.1]STLN	4	heavy	707.847467	y5	701.35601	52.41
P36051	MCD4	HLDQLFHN[+203.1]STLN	4	heavy	707.847467	y4	586.329066	52.41
P36051	MCD4	HLDQLFHN[+203.1]STLN	4	heavy	707.847467	y2	294.223145	52.41
P36051	MCD4	HLDQLFHN[+203.1]STLN	4	heavy	707.847467	y13	969.467714	52.41
P36051	MCD4	HLDQLFHN[+203.1]STLN	4	heavy	707.847467	y12	810.906564	52.41
P36051	MCD4	HLDQLFHN[+203.1]STLN	4	heavy	707.847467	y5	351.181643	52.41
P36051	MCD4	HLDQLFHN[+203.1]STLN	4	heavy	707.847467	b2	251.150252	52.41
P36051	MCD4	SLVMNN[+203.1]ATYGIS	3	light	622.971997	y10	1322.63352	5.72
P36051	MCD4	SLVMNN[+203.1]ATYGIS	3	light	622.971997	y9	1005.51122	5.72
P36051	MCD4	SLVMNN[+203.1]ATYGIS	3	light	622.971997	y8	934.474105	5.72
P36051	MCD4	SLVMNN[+203.1]ATYGIS	3	light	622.971997	y7	833.426427	5.72
P36051	MCD4	SLVMNN[+203.1]ATYGIS	3	light	622.971997	y6	670.363098	5.72
P36051	MCD4	SLVMNN[+203.1]ATYGIS	3	light	622.971997	y5	613.341635	5.72
P36051	MCD4	SLVMNN[+203.1]ATYGIS	3	light	622.971997	y4	500.257571	5.72
P36051	MCD4	SLVMNN[+203.1]ATYGIS	3	heavy	624.978706	y10	1328.65365	5.72
P36051	MCD4	SLVMNN[+203.1]ATYGIS	3	heavy	624.978706	y9	1011.53135	5.72
P36051	MCD4	SLVMNN[+203.1]ATYGIS	3	heavy	624.978706	y8	940.494234	5.72
P36051	MCD4	SLVMNN[+203.1]ATYGIS	3	heavy	624.978706	y7	839.446556	5.72
P36051	MCD4	SLVMNN[+203.1]ATYGIS	3	heavy	624.978706	y6	676.383227	5.72
P36051	MCD4	SLVMNN[+203.1]ATYGIS	3	heavy	624.978706	y5	619.361764	5.72
P36051	MCD4	SLVMNN[+203.1]ATYGIS	3	heavy	624.978706	y4	506.2777	5.72
P36051	MCD4	TEFLAPFIR	2	light	547.305666	y7	863.513785	81.57
P36051	MCD4	TEFLAPFIR	2	light	547.305666	y6	716.445371	81.57
P36051	MCD4	TEFLAPFIR	2	light	547.305666	y5	603.361307	81.57
P36051	MCD4	TEFLAPFIR	2	light	547.305666	y4	532.324194	81.57
P36051	MCD4	TEFLAPFIR	2	light	547.305666	b2	231.097548	81.57
P36051	MCD4	TEFLAPFIR	2	light	547.305666	b3	378.165962	81.57
P36051	MCD4	TEFLAPFIR	2	heavy	550.315731	y7	869.533914	81.57
P36051	MCD4	TEFLAPFIR	2	heavy	550.315731	y6	722.4655	81.57
P36051	MCD4	TEFLAPFIR	2	heavy	550.315731	y5	609.381436	81.57
P36051	MCD4	TEFLAPFIR	2	heavy	550.315731	y4	538.344323	81.57
P36051	MCD4	TEFLAPFIR	2	heavy	550.315731	b2	231.097548	81.57
P36051	MCD4	TEFLAPFIR	2	heavy	550.315731	b3	378.165962	81.57
P36051	MCD4	YIDDQIPILIDK	2	light	723.39795	y10	1169.64123	80.17
P36051	MCD4	YIDDQIPILIDK	2	light	723.39795	y7	811.528767	80.17
P36051	MCD4	YIDDQIPILIDK	2	light	723.39795	y6	698.444703	80.17
P36051	MCD4	YIDDQIPILIDK	2	light	723.39795	y4	488.307875	80.17
P36051	MCD4	YIDDQIPILIDK	2	light	723.39795	y3	375.223811	80.17
P36051	MCD4	YIDDQIPILIDK	2	light	723.39795	y2	262.139747	80.17
P36051	MCD4	YIDDQIPILIDK	2	light	723.39795	b2	277.154669	80.17
P36051	MCD4	YIDDQIPILIDK	2	heavy	727.405049	y10	1177.65543	80.17
P36051	MCD4	YIDDQIPILIDK	2	heavy	727.405049	y7	819.542966	80.17
P36051	MCD4	YIDDQIPILIDK	2	heavy	727.405049	y6	706.458902	80.17
P36051	MCD4	YIDDQIPILIDK	2	heavy	727.405049	y4	496.322074	80.17
P36051	MCD4	YIDDQIPILIDK	2	heavy	727.405049	y3	383.23801	80.17
P36051	MCD4	YIDDQIPILIDK	2	heavy	727.405049	y2	270.153946	80.17
P36051	MCD4	YIDDQIPILIDK	2	heavy	727.405049	b2	277.154669	80.17
Q03281	HEH2	SN[+203.1]NTNYIYR	2	light	674.312406	y8	1260.58551	-4.39
Q03281	HEH2	SN[+203.1]NTNYIYR	2	light	674.312406	y7	943.463206	-4.39
Q03281	HEH2	SN[+203.1]NTNYIYR	2	light	674.312406	y6	829.420279	-4.39

Q03281	HEH2	SN[+203.1]NTNYIYR	2	light	674.312406	y5	728.3726	-4.39
Q03281	HEH2	SN[+203.1]NTNYIYR	2	light	674.312406	y4	614.329673	-4.39
Q03281	HEH2	SN[+203.1]NTNYIYR	2	light	674.312406	y3	451.266344	-4.39
Q03281	HEH2	SN[+203.1]NTNYIYR	2	light	674.312406	y2	338.18228	-4.39
Q03281	HEH2	SN[+203.1]NTNYIYR	2	light	674.312406	b3	260.105904	-4.39
Q03281	HEH2	SN[+203.1]NTNYIYR	2	light	674.312406	b4	310.629743	-4.39
Q03281	HEH2	SN[+203.1]NTNYIYR	2	heavy	677.32247	y8	1266.60564	-4.39
Q03281	HEH2	SN[+203.1]NTNYIYR	2	heavy	677.32247	y7	949.483335	-4.39
Q03281	HEH2	SN[+203.1]NTNYIYR	2	heavy	677.32247	y6	835.440408	-4.39
Q03281	HEH2	SN[+203.1]NTNYIYR	2	heavy	677.32247	y5	734.392729	-4.39
Q03281	HEH2	SN[+203.1]NTNYIYR	2	heavy	677.32247	y4	620.349802	-4.39
Q03281	HEH2	SN[+203.1]NTNYIYR	2	heavy	677.32247	y3	457.286473	-4.39
Q03281	HEH2	SN[+203.1]NTNYIYR	2	heavy	677.32247	y2	344.202409	-4.39
Q03281	HEH2	SN[+203.1]NTNYIYR	2	heavy	677.32247	b3	260.105904	-4.39
Q03281	HEH2	SN[+203.1]NTNYIYR	2	heavy	677.32247	b4	310.629743	-4.39
Q03281	HEH2	ATLLSDIPNIK	2	light	592.847895	y9	1012.60372	68.31
Q03281	HEH2	ATLLSDIPNIK	2	light	592.847895	y8	899.519659	68.31
Q03281	HEH2	ATLLSDIPNIK	2	light	592.847895	y7	786.435595	68.31
Q03281	HEH2	ATLLSDIPNIK	2	light	592.847895	y6	699.403566	68.31
Q03281	HEH2	ATLLSDIPNIK	2	light	592.847895	y5	584.376623	68.31
Q03281	HEH2	ATLLSDIPNIK	2	light	592.847895	y4	471.292559	68.31
Q03281	HEH2	ATLLSDIPNIK	2	light	592.847895	y3	374.239795	68.31
Q03281	HEH2	ATLLSDIPNIK	2	light	592.847895	b3	286.176132	68.31
Q03281	HEH2	ATLLSDIPNIK	2	heavy	596.854995	y9	1020.61792	68.31
Q03281	HEH2	ATLLSDIPNIK	2	heavy	596.854995	y8	907.533858	68.31
Q03281	HEH2	ATLLSDIPNIK	2	heavy	596.854995	y7	794.449794	68.31
Q03281	HEH2	ATLLSDIPNIK	2	heavy	596.854995	y6	707.417765	68.31
Q03281	HEH2	ATLLSDIPNIK	2	heavy	596.854995	y5	592.390822	68.31
Q03281	HEH2	ATLLSDIPNIK	2	heavy	596.854995	y4	479.306758	68.31
Q03281	HEH2	ATLLSDIPNIK	2	heavy	596.854995	y3	382.253994	68.31
Q03281	HEH2	ATLLSDIPNIK	2	heavy	596.854995	b3	286.176132	68.31
Q03281	HEH2	SSILETYGIIPFPK	2	light	782.934699	y11	1277.714	107.41
Q03281	HEH2	SSILETYGIIPFPK	2	light	782.934699	y10	1164.62994	107.41
Q03281	HEH2	SSILETYGIIPFPK	2	light	782.934699	y9	1035.58734	107.41
Q03281	HEH2	SSILETYGIIPFPK	2	light	782.934699	y8	934.539666	107.41
Q03281	HEH2	SSILETYGIIPFPK	2	light	782.934699	y7	771.476337	107.41
Q03281	HEH2	SSILETYGIIPFPK	2	light	782.934699	y5	601.370809	107.41
Q03281	HEH2	SSILETYGIIPFPK	2	light	782.934699	y4	488.286745	107.41
Q03281	HEH2	SSILETYGIIPFPK	2	light	782.934699	y3	391.233982	107.41
Q03281	HEH2	SSILETYGIIPFPK	2	heavy	786.941799	y11	1285.7282	107.41
Q03281	HEH2	SSILETYGIIPFPK	2	heavy	786.941799	y10	1172.64414	107.41
Q03281	HEH2	SSILETYGIIPFPK	2	heavy	786.941799	y9	1043.60154	107.41
Q03281	HEH2	SSILETYGIIPFPK	2	heavy	786.941799	y8	942.553865	107.41
Q03281	HEH2	SSILETYGIIPFPK	2	heavy	786.941799	y7	779.490536	107.41
Q03281	HEH2	SSILETYGIIPFPK	2	heavy	786.941799	y5	609.385008	107.41
Q03281	HEH2	SSILETYGIIPFPK	2	heavy	786.941799	y4	496.300944	107.41
Q03281	HEH2	SSILETYGIIPFPK	2	heavy	786.941799	y3	399.248181	107.41
P38993	FET3	NGVNYAFFNN[+203.1]I1	2	light	1069.01547	y10	1371.67907	77.55
P38993	FET3	NGVNYAFFNN[+203.1]I1	2	light	1069.01547	y9	1224.61066	77.55
P38993	FET3	NGVNYAFFNN[+203.1]I1	2	light	1069.01547	y8	1110.56773	77.55
P38993	FET3	NGVNYAFFNN[+203.1]I1	2	light	1069.01547	y7	793.445431	77.55
P38993	FET3	NGVNYAFFNN[+203.1]I1	2	light	1069.01547	y6	680.361367	77.55
P38993	FET3	NGVNYAFFNN[+203.1]I1	2	light	1069.01547	y4	416.25036	77.55
P38993	FET3	NGVNYAFFNN[+203.1]I1	2	light	1069.01547	y2	244.165568	77.55
P38993	FET3	NGVNYAFFNN[+203.1]I1	2	heavy	1073.02257	y10	1379.69327	77.55
P38993	FET3	NGVNYAFFNN[+203.1]I1	2	heavy	1073.02257	y9	1232.62486	77.55
P38993	FET3	NGVNYAFFNN[+203.1]I1	2	heavy	1073.02257	y8	1118.58193	77.55
P38993	FET3	NGVNYAFFNN[+203.1]I1	2	heavy	1073.02257	y7	801.45963	77.55
P38993	FET3	NGVNYAFFNN[+203.1]I1	2	heavy	1073.02257	y6	688.375566	77.55
P38993	FET3	NGVNYAFFNN[+203.1]I1	2	heavy	1073.02257	y4	424.264559	77.55
P38993	FET3	NGVNYAFFNN[+203.1]I1	2	heavy	1073.02257	y2	252.179767	77.55
P38993	FET3	N[+203.1]VTDM[+16]LYI	2	light	871.935102	y10	1225.62454	49.73
P38993	FET3	N[+203.1]VTDM[+16]LYI	2	light	871.935102	y9	1110.59759	49.73

P38993	FET3	N[+203.1]VTDM[+16]LYI	2	light	871.935102	y8	963.562192	49.73
P38993	FET3	N[+203.1]VTDM[+16]LYI	2	light	871.935102	y7	850.478128	49.73
P38993	FET3	N[+203.1]VTDM[+16]LYI	2	light	871.935102	y6	687.4148	49.73
P38993	FET3	N[+203.1]VTDM[+16]LYI	2	light	871.935102	y5	574.330736	49.73
P38993	FET3	N[+203.1]VTDM[+16]LYI	2	light	871.935102	y3	374.214643	49.73
P38993	FET3	N[+203.1]VTDM[+16]LYI	2	heavy	874.945166	y10	1231.64466	49.73
P38993	FET3	N[+203.1]VTDM[+16]LYI	2	heavy	874.945166	y9	1116.61772	49.73
P38993	FET3	N[+203.1]VTDM[+16]LYI	2	heavy	874.945166	y8	969.582321	49.73
P38993	FET3	N[+203.1]VTDM[+16]LYI	2	heavy	874.945166	y7	856.498257	49.73
P38993	FET3	N[+203.1]VTDM[+16]LYI	2	heavy	874.945166	y6	693.434929	49.73
P38993	FET3	N[+203.1]VTDM[+16]LYI	2	heavy	874.945166	y5	580.350865	49.73
P38993	FET3	N[+203.1]VTDM[+16]LYI	2	heavy	874.945166	y3	380.234772	49.73
P38993	FET3	DLHVDPEVLLNEVDENE	2	light	1132.53749	y9	1133.47054	96.12
P38993	FET3	DLHVDPEVLLNEVDENE	2	light	1132.53749	y5	676.289659	96.12
P38993	FET3	DLHVDPEVLLNEVDENE	2	light	1132.53749	y2	304.161545	96.12
P38993	FET3	DLHVDPEVLLNEVDENE	2	light	1132.53749	b3	366.177195	96.12
P38993	FET3	DLHVDPEVLLNEVDENE	2	light	1132.53749	b4	465.245609	96.12
P38993	FET3	DLHVDPEVLLNEVDENE	2	light	1132.53749	b5	580.272552	96.12
P38993	FET3	DLHVDPEVLLNEVDENE	2	heavy	1135.54756	y9	1139.49067	96.12
P38993	FET3	DLHVDPEVLLNEVDENE	2	heavy	1135.54756	y5	682.309788	96.12
P38993	FET3	DLHVDPEVLLNEVDENE	2	heavy	1135.54756	y2	310.181674	96.12
P38993	FET3	DLHVDPEVLLNEVDENE	2	heavy	1135.54756	b3	366.177195	96.12
P38993	FET3	DLHVDPEVLLNEVDENE	2	heavy	1135.54756	b4	465.245609	96.12
P38993	FET3	DLHVDPEVLLNEVDENE	2	heavy	1135.54756	b5	580.272552	96.12
P43561	FET5	YAFFNN[+203.1]ITYVTP	2	light	890.943253	y9	1252.64196	67.95
P43561	FET5	YAFFNN[+203.1]ITYVTP	2	light	890.943253	y8	1138.59903	67.95
P43561	FET5	YAFFNN[+203.1]ITYVTP	2	light	890.943253	y7	821.476731	67.95
P43561	FET5	YAFFNN[+203.1]ITYVTP	2	light	890.943253	y6	708.392667	67.95
P43561	FET5	YAFFNN[+203.1]ITYVTP	2	light	890.943253	y5	607.344989	67.95
P43561	FET5	YAFFNN[+203.1]ITYVTP	2	light	890.943253	y4	444.28166	67.95
P43561	FET5	YAFFNN[+203.1]ITYVTP	2	light	890.943253	y3	345.213246	67.95
P43561	FET5	YAFFNN[+203.1]ITYVTP	2	heavy	894.950352	y9	1260.65616	67.95
P43561	FET5	YAFFNN[+203.1]ITYVTP	2	heavy	894.950352	y8	1146.61323	67.95
P43561	FET5	YAFFNN[+203.1]ITYVTP	2	heavy	894.950352	y7	829.49093	67.95
P43561	FET5	YAFFNN[+203.1]ITYVTP	2	heavy	894.950352	y6	716.406866	67.95
P43561	FET5	YAFFNN[+203.1]ITYVTP	2	heavy	894.950352	y5	615.359188	67.95
P43561	FET5	YAFFNN[+203.1]ITYVTP	2	heavy	894.950352	y4	452.295859	67.95
P43561	FET5	YAFFNN[+203.1]ITYVTP	2	heavy	894.950352	y3	353.227445	67.95
P43561	FET5	LN[+203.1]YTASWVTAN	3	light	740.358685	y11	1180.59568	45.99
P43561	FET5	LN[+203.1]YTASWVTAN	3	light	740.358685	y10	1081.52726	45.99
P43561	FET5	LN[+203.1]YTASWVTAN	3	light	740.358685	y9	980.479585	45.99
P43561	FET5	LN[+203.1]YTASWVTAN	3	light	740.358685	y8	909.442471	45.99
P43561	FET5	LN[+203.1]YTASWVTAN	3	light	740.358685	y7	795.399543	45.99
P43561	FET5	LN[+203.1]YTASWVTAN	3	light	740.358685	y6	698.34678	45.99
P43561	FET5	LN[+203.1]YTASWVTAN	3	light	740.358685	y5	583.319837	45.99
P43561	FET5	LN[+203.1]YTASWVTAN	3	light	740.358685	y3	413.214309	45.99
P43561	FET5	LN[+203.1]YTASWVTAN	3	light	740.358685	b3	594.276969	45.99
P43561	FET5	LN[+203.1]YTASWVTAN	3	light	740.358685	b4	695.324648	45.99
P43561	FET5	LN[+203.1]YTASWVTAN	3	heavy	743.030085	y11	1188.60988	45.99
P43561	FET5	LN[+203.1]YTASWVTAN	3	heavy	743.030085	y10	1089.54146	45.99
P43561	FET5	LN[+203.1]YTASWVTAN	3	heavy	743.030085	y9	988.493784	45.99
P43561	FET5	LN[+203.1]YTASWVTAN	3	heavy	743.030085	y8	917.45667	45.99
P43561	FET5	LN[+203.1]YTASWVTAN	3	heavy	743.030085	y7	803.413742	45.99
P43561	FET5	LN[+203.1]YTASWVTAN	3	heavy	743.030085	y6	706.360979	45.99
P43561	FET5	LN[+203.1]YTASWVTAN	3	heavy	743.030085	y5	591.334036	45.99
P43561	FET5	LN[+203.1]YTASWVTAN	3	heavy	743.030085	y3	421.228508	45.99
P43561	FET5	LN[+203.1]YTASWVTAN	3	heavy	743.030085	b3	594.276969	45.99
P43561	FET5	LN[+203.1]YTASWVTAN	3	heavy	743.030085	b4	695.324648	45.99
P43561	FET5	VPTLTTLLTSGK	2	light	615.868828	y10	1034.6092	75.1
P43561	FET5	VPTLTTLLTSGK	2	light	615.868828	y9	933.561523	75.1
P43561	FET5	VPTLTTLLTSGK	2	light	615.868828	y8	820.477459	75.1
P43561	FET5	VPTLTTLLTSGK	2	light	615.868828	y7	719.429781	75.1
P43561	FET5	VPTLTTLLTSGK	2	light	615.868828	y5	505.298038	75.1

P43561	FET5	VPTLTTLLTSGK	2	light	615.868828	y4	392.213974	75.1
P43561	FET5	VPTLTTLLTSGK	2	heavy	619.875927	y10	1042.6234	75.1
P43561	FET5	VPTLTTLLTSGK	2	heavy	619.875927	y9	941.575722	75.1
P43561	FET5	VPTLTTLLTSGK	2	heavy	619.875927	y8	828.491658	75.1
P43561	FET5	VPTLTTLLTSGK	2	heavy	619.875927	y7	727.44398	75.1
P43561	FET5	VPTLTTLLTSGK	2	heavy	619.875927	y5	513.312237	75.1
P43561	FET5	VPTLTTLLTSGK	2	heavy	619.875927	y4	400.228173	75.1
P38843	CHS7	THLILSN[+203.1]STIIHDI	3	light	1034.55918	y11	1191.72082	101.65
P38843	CHS7	THLILSN[+203.1]STIIHDI	3	light	1034.55918	y10	1094.66805	101.65
P38843	CHS7	THLILSN[+203.1]STIIHDI	3	light	1034.55918	y9	981.58399	101.65
P38843	CHS7	THLILSN[+203.1]STIIHDI	3	light	1034.55918	y8	867.541063	101.65
P38843	CHS7	THLILSN[+203.1]STIIHDI	3	light	1034.55918	y7	754.456999	101.65
P38843	CHS7	THLILSN[+203.1]STIIHDI	3	light	1034.55918	y6	640.414071	101.65
P38843	CHS7	THLILSN[+203.1]STIIHDI	3	light	1034.55918	y5	541.345657	101.65
P38843	CHS7	THLILSN[+203.1]STIIHDI	3	light	1034.55918	b3	352.19793	101.65
P38843	CHS7	THLILSN[+203.1]STIIHDI	3	light	1034.55918	b4	465.281994	101.65
P38843	CHS7	THLILSN[+203.1]STIIHDI	3	heavy	1036.56589	y11	1197.74095	101.65
P38843	CHS7	THLILSN[+203.1]STIIHDI	3	heavy	1036.56589	y10	1100.68818	101.65
P38843	CHS7	THLILSN[+203.1]STIIHDI	3	heavy	1036.56589	y9	987.604119	101.65
P38843	CHS7	THLILSN[+203.1]STIIHDI	3	heavy	1036.56589	y8	873.561192	101.65
P38843	CHS7	THLILSN[+203.1]STIIHDI	3	heavy	1036.56589	y7	760.477128	101.65
P38843	CHS7	THLILSN[+203.1]STIIHDI	3	heavy	1036.56589	y6	646.4342	101.65
P38843	CHS7	THLILSN[+203.1]STIIHDI	3	heavy	1036.56589	y5	547.365786	101.65
P38843	CHS7	THLILSN[+203.1]STIIHDI	3	heavy	1036.56589	b3	352.19793	101.65
P38843	CHS7	THLILSN[+203.1]STIIHDI	3	heavy	1036.56589	b4	465.281994	101.65
P38843	CHS7	TPLPLC[+57]SVIK	2	light	564.328284	y8	929.548851	58.01
P38843	CHS7	TPLPLC[+57]SVIK	2	light	564.328284	y7	816.464787	58.01
P38843	CHS7	TPLPLC[+57]SVIK	2	light	564.328284	y5	606.327959	58.01
P38843	CHS7	TPLPLC[+57]SVIK	2	light	564.328284	y4	446.29731	58.01
P38843	CHS7	TPLPLC[+57]SVIK	2	light	564.328284	b3	312.191782	58.01
P38843	CHS7	TPLPLC[+57]SVIK	2	heavy	568.335384	y8	937.56305	58.01
P38843	CHS7	TPLPLC[+57]SVIK	2	heavy	568.335384	y7	824.478986	58.01
P38843	CHS7	TPLPLC[+57]SVIK	2	heavy	568.335384	y5	614.342158	58.01
P38843	CHS7	TPLPLC[+57]SVIK	2	heavy	568.335384	y4	454.311509	58.01
P38843	CHS7	TPLPLC[+57]SVIK	2	heavy	568.335384	b3	312.191782	58.01

Appendix Table 2. PRM MS assay for quantitive profiling of mevalonate, ergosterol and dolichol pathways.

PRM assay; R=30000								
UniProt ID	**Protein**	**Peptide Modified Sequence**	**Precursor Charge**	**Isotope Label Type**	**Precursor Mz**	**Fragment Ion**	**Fragment Mz**	**Normalized Retention Time**
P236321	Rpl5	VFLDIGLQR	2	light	530.811116	y8	961.546542	63.23
P236321	Rpl5	VFLDIGLQR	2	light	530.811116	y7	814.478128	63.23
P236321	Rpl5	VFLDIGLQR	2	light	530.811116	y6	701.394064	63.23
P236321	Rpl5	VFLDIGLQR	2	light	530.811116	y5	586.367121	63.23
P236321	Rpl5	VFLDIGLQR	2	heavy	533.821181	y8	967.566671	63.23
P236321	Rpl5	VFLDIGLQR	2	heavy	533.821181	y7	820.498257	63.23
P236321	Rpl5	VFLDIGLQR	2	heavy	533.821181	y6	707.414193	63.23
P236321	Rpl5	VFLDIGLQR	2	heavy	533.821181	y5	592.38725	63.23
P236321	Rpl5	FPGWDFETEEIDPELLI	2	light	1046.996745	y11	1343.6689	115.69
P236321	Rpl5	FPGWDFETEEIDPELLI	2	light	1046.996745	y10	1214.62631	115.69
P236321	Rpl5	FPGWDFETEEIDPELLI	2	light	1046.996745	y5	627.382437	115.69
P236321	Rpl5	FPGWDFETEEIDPELLI	2	light	1046.996745	y3	401.28708	115.69
P236321	Rpl5	FPGWDFETEEIDPELLI	2	light	1046.996745	b2	245.128454	115.69
P236321	Rpl5	FPGWDFETEEIDPELLI	2	light	1046.996745	b3	302.149918	115.69
P236321	Rpl5	FPGWDFETEEIDPELLI	2	light	1046.996745	b5	603.256174	115.69
P236321	Rpl5	FPGWDFETEEIDPELLI	2	heavy	1050.006809	y11	1349.68903	115.69
P236321	Rpl5	FPGWDFETEEIDPELLI	2	heavy	1050.006809	y10	1220.64644	115.69
P236321	Rpl5	FPGWDFETEEIDPELLI	2	heavy	1050.006809	y5	633.402566	115.69
P236321	Rpl5	FPGWDFETEEIDPELLI	2	heavy	1050.006809	y3	407.307209	115.69
P236321	Rpl5	FPGWDFETEEIDPELLI	2	heavy	1050.006809	y1	181.139081	115.69
P236321	Rpl5	FPGWDFETEEIDPELLI	2	heavy	1050.006809	b2	245.128454	115.69
P236321	Rpl5	FPGWDFETEEIDPELLI	2	heavy	1050.006809	b3	302.149918	115.69
P236321	Rpl5	FPGWDFETEEIDPELLI	2	heavy	1050.006809	b5	603.256174	115.69
P33442	Rps1a	VISEILTK	2	light	451.781493	y7	803.487296	21.09
P33442	Rps1a	VISEILTK	2	light	451.781493	y6	690.403232	21.09
P33442	Rps1a	VISEILTK	2	light	451.781493	y4	474.32861	21.09
P33442	Rps1a	VISEILTK	2	light	451.781493	y3	361.244546	21.09
P33442	Rps1a	VISEILTK	2	light	451.781493	y2	248.160482	21.09
P33442	Rps1a	VISEILTK	2	heavy	455.788592	y7	811.501495	21.09
P33442	Rps1a	VISEILTK	2	heavy	455.788592	y6	698.417431	21.09
P33442	Rps1a	VISEILTK	2	heavy	455.788592	y4	482.342809	21.09
P33442	Rps1a	VISEILTK	2	heavy	455.788592	y3	369.258745	21.09
P33442	Rps1a	VISEILTK	2	heavy	455.788592	y2	256.174681	21.09
P33442	Rps1a	EVQGSTLAQLTSK	2	light	681.367181	y11	1133.61608	21.82
P33442	Rps1a	EVQGSTLAQLTSK	2	light	681.367181	y10	1005.5575	21.82
P33442	Rps1a	EVQGSTLAQLTSK	2	light	681.367181	y9	948.536037	21.82
P33442	Rps1a	EVQGSTLAQLTSK	2	light	681.367181	y8	861.504009	21.82
P33442	Rps1a	EVQGSTLAQLTSK	2	light	681.367181	y7	760.45633	21.82
P33442	Rps1a	EVQGSTLAQLTSK	2	heavy	685.37428	y11	1141.63028	21.82
P33442	Rps1a	EVQGSTLAQLTSK	2	heavy	685.37428	y10	1013.5717	21.82
P33442	Rps1a	EVQGSTLAQLTSK	2	heavy	685.37428	y9	956.550236	21.82
P33442	Rps1a	EVQGSTLAQLTSK	2	heavy	685.37428	y8	869.518208	21.82
P33442	Rps1a	EVQGSTLAQLTSK	2	heavy	685.37428	y7	768.470529	21.82
P32353	ERG3	VLPASLAANIPVK	2	light	646.900462	y11	1080.64117	64.86
P32353	ERG3	VLPASLAANIPVK	2	light	646.900462	y10	983.588407	64.86
P32353	ERG3	VLPASLAANIPVK	2	light	646.900462	y9	912.551293	64.86
P32353	ERG3	VLPASLAANIPVK	2	light	646.900462	y7	712.435201	64.86
P32353	ERG3	VLPASLAANIPVK	2	light	646.900462	y6	641.398087	64.86
P32353	ERG3	VLPASLAANIPVK	2	light	646.900462	y11	540.824223	64.86
P32353	ERG3	VLPASLAANIPVK	2	light	646.900462	b2	213.159754	64.86
P32353	ERG3	VLPASLAANIPVK	2	heavy	650.907562	y11	1088.65537	64.86
P32353	ERG3	VLPASLAANIPVK	2	heavy	650.907562	y10	991.602606	64.86
P32353	ERG3	VLPASLAANIPVK	2	heavy	650.907562	y9	920.565492	64.86

P32353	ERG3	VLPASLAANIPVK	2	heavy	650.907562	y7	720.4494	64.86
P32353	ERG3	VLPASLAANIPVK	2	heavy	650.907562	y6	649.412286	64.86
P32353	ERG3	VLPASLAANIPVK	2	heavy	650.907562	y11	544.831323	64.86
P32353	ERG3	VLPASLAANIPVK	2	heavy	650.907562	b2	213.159754	64.86
P25087	ERG6	MFHVDVAR	2	light	487.747461	y6	696.378748	9.49
P25087	ERG6	MFHVDVAR	2	light	487.747461	y5	559.319837	9.49
P25087	ERG6	MFHVDVAR	2	light	487.747461	y4	460.251423	9.49
P25087	ERG6	MFHVDVAR	2	light	487.747461	y3	345.22448	9.49
P25087	ERG6	MFHVDVAR	2	light	487.747461	y2	246.156066	9.49
P25087	ERG6	MFHVDVAR	2	light	487.747461	y6	348.693012	9.49
P25087	ERG6	MFHVDVAR	2	light	487.747461	b3	416.175086	9.49
P25087	ERG6	MFHVDVAR	2	heavy	490.757526	y6	702.398877	9.49
P25087	ERG6	MFHVDVAR	2	heavy	490.757526	y5	565.339966	9.49
P25087	ERG6	MFHVDVAR	2	heavy	490.757526	y4	466.271552	9.49
P25087	ERG6	MFHVDVAR	2	heavy	490.757526	y3	351.244608	9.49
P25087	ERG6	MFHVDVAR	2	heavy	490.757526	y2	252.176195	9.49
P25087	ERG6	MFHVDVAR	2	heavy	490.757526	y6	351.703077	9.49
P25087	ERG6	MFHVDVAR	2	heavy	490.757526	b3	416.175086	9.49
P25087	ERG6	AGIQRGDLVLDVGC[+5	3	light	689.696978	y10	929.462161	54.27
P25087	ERG6	AGIQRGDLVLDVGC[+5	3	light	689.696978	y9	830.393747	54.27
P25087	ERG6	AGIQRGDLVLDVGC[+5	3	light	689.696978	y7	613.341635	54.27
P25087	ERG6	AGIQRGDLVLDVGC[+5	3	light	689.696978	y5	457.251757	54.27
P25087	ERG6	AGIQRGDLVLDVGC[+5	3	light	689.696978	b8	811.442077	54.27
P25087	ERG6	AGIQRGDLVLDVGC[+5	3	light	689.696978	b9	910.510491	54.27
P25087	ERG6	AGIQRGDLVLDVGC[+5	3	light	689.696978	b11	1138.6215	54.27
P25087	ERG6	AGIQRGDLVLDVGC[+5	3	heavy	693.710398	y10	935.48229	54.27
P25087	ERG6	AGIQRGDLVLDVGC[+5	3	heavy	693.710398	y9	836.413876	54.27
P25087	ERG6	AGIQRGDLVLDVGC[+5	3	heavy	693.710398	y7	619.361764	54.27
P25087	ERG6	AGIQRGDLVLDVGC[+5	3	heavy	693.710398	y5	463.271886	54.27
P25087	ERG6	AGIQRGDLVLDVGC[+5	3	heavy	693.710398	b8	817.462206	54.27
P25087	ERG6	AGIQRGDLVLDVGC[+5	3	heavy	693.710398	b9	916.53062	54.27
P25087	ERG6	AGIQRGDLVLDVGC[+5	3	heavy	693.710398	b11	1144.64163	54.27
P25087	ERG6	EVTAALENAAVGLVAG	2	light	835.459601	y12	1085.59495	83.72
P25087	ERG6	EVTAALENAAVGLVAG	2	light	835.459601	y11	956.552356	83.72
P25087	ERG6	EVTAALENAAVGLVAG	2	light	835.459601	y9	771.472314	83.72
P25087	ERG6	EVTAALENAAVGLVAG	2	light	835.459601	y7	601.366787	83.72
P25087	ERG6	EVTAALENAAVGLVAG	2	light	835.459601	y5	431.261259	83.72
P25087	ERG6	EVTAALENAAVGLVAG	2	light	835.459601	y4	332.192845	83.72
P25087	ERG6	EVTAALENAAVGLVAG	2	light	835.459601	y3	261.155731	83.72
P25087	ERG6	EVTAALENAAVGLVAG	2	heavy	839.466701	y12	1093.60915	83.72
P25087	ERG6	EVTAALENAAVGLVAG	2	heavy	839.466701	y11	964.566555	83.72
P25087	ERG6	EVTAALENAAVGLVAG	2	heavy	839.466701	y9	779.486513	83.72
P25087	ERG6	EVTAALENAAVGLVAG	2	heavy	839.466701	y7	609.380986	83.72
P25087	ERG6	EVTAALENAAVGLVAG	2	heavy	839.466701	y5	439.275458	83.72
P25087	ERG6	EVTAALENAAVGLVAG	2	heavy	839.466701	y4	340.207044	83.72
P25087	ERG6	EVTAALENAAVGLVAG	2	heavy	839.466701	y3	269.16993	83.72
P32352	ERG2	DALASHYGDEYINR	2	light	812.373526	y10	1253.55454	17.95
P32352	ERG2	DALASHYGDEYINR	2	light	812.373526	y9	1166.52251	17.95
P32352	ERG2	DALASHYGDEYINR	2	light	812.373526	y8	1029.4636	17.95
P32352	ERG2	DALASHYGDEYINR	2	light	812.373526	y7	866.400272	17.95
P32352	ERG2	DALASHYGDEYINR	2	light	812.373526	y5	694.351865	17.95
P32352	ERG2	DALASHYGDEYINR	2	light	812.373526	y4	565.309272	17.95
P32352	ERG2	DALASHYGDEYINR	2	light	812.373526	b2	187.071333	17.95
P32352	ERG2	DALASHYGDEYINR	2	light	812.373526	b3	300.155397	17.95
P32352	ERG2	DALASHYGDEYINR	2	heavy	815.38359	y10	1259.57467	17.95
P32352	ERG2	DALASHYGDEYINR	2	heavy	815.38359	y9	1172.54264	17.95
P32352	ERG2	DALASHYGDEYINR	2	heavy	815.38359	y8	1035.48373	17.95
P32352	ERG2	DALASHYGDEYINR	2	heavy	815.38359	y7	872.420401	17.95
P32352	ERG2	DALASHYGDEYINR	2	heavy	815.38359	y5	700.371994	17.95
P32352	ERG2	DALASHYGDEYINR	2	heavy	815.38359	y4	571.329401	17.95
P32352	ERG2	DALASHYGDEYINR	2	heavy	815.38359	b2	187.071333	17.95
P32352	ERG2	DALASHYGDEYINR	2	heavy	815.38359	b3	300.155397	17.95
P32352	ERG2	DALASHYGDEYINR	3	light	541.918109	y8	1029.4636	17.95

P32352	ERG2	DALASHYGDEYINR	3	light	541.918109	y7	866.400272	17.95
P32352	ERG2	DALASHYGDEYINR	3	light	541.918109	y3	402.245943	17.95
P32352	ERG2	DALASHYGDEYINR	3	light	541.918109	y12	719.341497	17.95
P32352	ERG2	DALASHYGDEYINR	3	light	541.918109	y11	662.799465	17.95
P32352	ERG2	DALASHYGDEYINR	3	light	541.918109	y10	627.280908	17.95
P32352	ERG2	DALASHYGDEYINR	3	heavy	543.924819	y8	1035.48373	17.95
P32352	ERG2	DALASHYGDEYINR	3	heavy	543.924819	y7	872.420401	17.95
P32352	ERG2	DALASHYGDEYINR	3	heavy	543.924819	y3	408.266072	17.95
P32352	ERG2	DALASHYGDEYINR	3	heavy	543.924819	y12	722.351562	17.95
P32352	ERG2	DALASHYGDEYINR	3	heavy	543.924819	y11	665.80953	17.95
P32352	ERG2	DALASHYGDEYINR	3	heavy	543.924819	y10	630.290973	17.95
P32352	ERG2	HNAAEGLSTEDLLQDV	3	light	623.309666	y7	858.467957	53.33
P32352	ERG2	HNAAEGLSTEDLLQDV	3	light	623.309666	y5	630.35695	53.33
P32352	ERG2	HNAAEGLSTEDLLQDV	3	light	623.309666	y4	517.272886	53.33
P32352	ERG2	HNAAEGLSTEDLLQDV	3	light	623.309666	y2	274.187366	53.33
P32352	ERG2	HNAAEGLSTEDLLQDV	3	light	623.309666	b6	580.2474	53.33
P32352	ERG2	HNAAEGLSTEDLLQDV	3	light	623.309666	b7	693.331464	53.33
P32352	ERG2	HNAAEGLSTEDLLQDV	3	light	623.309666	b11	1125.48071	53.33
P32352	ERG2	HNAAEGLSTEDLLQDV	3	heavy	625.316375	y7	864.488086	53.33
P32352	ERG2	HNAAEGLSTEDLLQDV	3	heavy	625.316375	y5	636.377079	53.33
P32352	ERG2	HNAAEGLSTEDLLQDV	3	heavy	625.316375	y4	523.293015	53.33
P32352	ERG2	HNAAEGLSTEDLLQDV	3	heavy	625.316375	y2	280.207495	53.33
P32352	ERG2	HNAAEGLSTEDLLQDV	3	heavy	625.316375	b6	580.2474	53.33
P32352	ERG2	HNAAEGLSTEDLLQDV	3	heavy	625.316375	b7	693.331464	53.33
P32352	ERG2	HNAAEGLSTEDLLQDV	3	heavy	625.316375	b11	1125.48071	53.33
P32352	ERG2	TLNEIC[+57]NSVISK	2	light	689.355759	y10	1163.5725	30.26
P32352	ERG2	TLNEIC[+57]NSVISK	2	light	689.355759	y9	1049.52957	30.26
P32352	ERG2	TLNEIC[+57]NSVISK	2	light	689.355759	y8	920.486979	30.26
P32352	ERG2	TLNEIC[+57]NSVISK	2	light	689.355759	y7	807.402915	30.26
P32352	ERG2	TLNEIC[+57]NSVISK	2	light	689.355759	y3	347.228896	30.26
P32352	ERG2	TLNEIC[+57]NSVISK	2	light	689.355759	y2	234.144832	30.26
P32352	ERG2	TLNEIC[+57]NSVISK	2	light	689.355759	b4	458.224539	30.26
P32352	ERG2	TLNEIC[+57]NSVISK	2	heavy	693.362858	y10	1171.5867	30.26
P32352	ERG2	TLNEIC[+57]NSVISK	2	heavy	693.362858	y9	1057.54377	30.26
P32352	ERG2	TLNEIC[+57]NSVISK	2	heavy	693.362858	y8	928.501178	30.26
P32352	ERG2	TLNEIC[+57]NSVISK	2	heavy	693.362858	y7	815.417114	30.26
P32352	ERG2	TLNEIC[+57]NSVISK	2	heavy	693.362858	y3	355.243095	30.26
P32352	ERG2	TLNEIC[+57]NSVISK	2	heavy	693.362858	y2	242.159031	30.26
P32352	ERG2	TLNEIC[+57]NSVISK	2	heavy	693.362858	b4	458.224539	30.26
P32353	ERG3	VLPASLAANIPVK	2	light	646.900462	y11	1080.64117	64.86
P32353	ERG3	VLPASLAANIPVK	2	light	646.900462	y10	983.588407	64.86
P32353	ERG3	VLPASLAANIPVK	2	light	646.900462	y9	912.551293	64.86
P32353	ERG3	VLPASLAANIPVK	2	light	646.900462	y7	712.435201	64.86
P32353	ERG3	VLPASLAANIPVK	2	light	646.900462	y6	641.398087	64.86
P32353	ERG3	VLPASLAANIPVK	2	heavy	650.907562	y11	1088.65537	64.86
P32353	ERG3	VLPASLAANIPVK	2	heavy	650.907562	y10	991.602606	64.86
P32353	ERG3	VLPASLAANIPVK	2	heavy	650.907562	y9	920.565492	64.86
P32353	ERG3	VLPASLAANIPVK	2	heavy	650.907562	y7	720.4494	64.86
P32353	ERG3	VLPASLAANIPVK	2	heavy	650.907562	y6	649.412286	64.86
P54781	ERG5	ENNYEPQVFFHEMR	3	light	613.942149	y7	965.466183	54.67
P54781	ERG5	ENNYEPQVFFHEMR	3	light	613.942149	y6	866.397769	54.67
P54781	ERG5	ENNYEPQVFFHEMR	3	light	613.942149	y5	719.329355	54.67
P54781	ERG5	ENNYEPQVFFHEMR	3	heavy	615.948858	y7	971.486312	54.67
P54781	ERG5	ENNYEPQVFFHEMR	3	heavy	615.948858	y6	872.417898	54.67
P54781	ERG5	ENNYEPQVFFHEMR	3	heavy	615.948858	y5	725.349484	54.67
P54781	ERG5	IFENC[+57]AQMAK	2	light	606.281008	y9	1098.47068	5.44
P54781	ERG5	IFENC[+57]AQMAK	2	light	606.281008	y8	951.402263	5.44
P54781	ERG5	IFENC[+57]AQMAK	2	light	606.281008	y7	822.35967	5.44
P54781	ERG5	IFENC[+57]AQMAK	2	light	606.281008	y5	548.286094	5.44
P54781	ERG5	IFENC[+57]AQMAK	2	light	606.281008	y3	349.190402	5.44
P54781	ERG5	IFENC[+57]AQMAK	2	heavy	610.288108	y9	1106.48488	5.44
P54781	ERG5	IFENC[+57]AQMAK	2	heavy	610.288108	y8	959.416462	5.44
P54781	ERG5	IFENC[+57]AQMAK	2	heavy	610.288108	y7	830.373869	5.44

P54781	ERG5	IFENC[+57]AQMAK	2	heavy	610.288108	y5	556.300293	5.44
P54781	ERG5	IFENC[+57]AQMAK	2	heavy	610.288108	y3	357.204601	5.44
P54781	ERG5	NFPVSPNYTAPK	2	light	667.840602	y10	1073.56259	28.01
P54781	ERG5	NFPVSPNYTAPK	2	light	667.840602	y9	976.509822	28.01
P54781	ERG5	NFPVSPNYTAPK	2	light	667.840602	y8	877.441408	28.01
P54781	ERG5	NFPVSPNYTAPK	2	light	667.840602	y7	790.40938	28.01
P54781	ERG5	NFPVSPNYTAPK	2	light	667.840602	y10	537.284931	28.01
P54781	ERG5	NFPVSPNYTAPK	2	light	667.840602	b3	359.171381	28.01
P54781	ERG5	NFPVSPNYTAPK	2	heavy	671.847701	y10	1081.57679	28.01
P54781	ERG5	NFPVSPNYTAPK	2	heavy	671.847701	y9	984.524021	28.01
P54781	ERG5	NFPVSPNYTAPK	2	heavy	671.847701	y8	885.455607	28.01
P54781	ERG5	NFPVSPNYTAPK	2	heavy	671.847701	y7	798.423579	28.01
P54781	ERG5	NFPVSPNYTAPK	2	heavy	671.847701	y10	541.292031	28.01
P54781	ERG5	NFPVSPNYTAPK	2	heavy	671.847701	b3	359.171381	28.01
P25340	ERG4	FPFLPYQILK	2	light	633.368267	y8	1021.60808	109.89
P25340	ERG4	FPFLPYQILK	2	light	633.368267	y7	874.539666	109.89
P25340	ERG4	FPFLPYQILK	2	light	633.368267	b2	245.128454	109.89
P25340	ERG4	FPFLPYQILK	2	heavy	637.375366	y8	1029.62228	109.89
P25340	ERG4	FPFLPYQILK	2	heavy	637.375366	y7	882.553865	109.89
P25340	ERG4	FPFLPYQILK	2	heavy	637.375366	b2	245.128454	109.89
P25340	ERG4	LQVQGEEK	2	light	465.748181	y6	689.346445	-24.02
P25340	ERG4	LQVQGEEK	2	light	465.748181	y5	590.278031	-24.02
P25340	ERG4	LQVQGEEK	2	light	465.748181	y4	462.219454	-24.02
P25340	ERG4	LQVQGEEK	2	light	465.748181	b2	242.149918	-24.02
P25340	ERG4	LQVQGEEK	2	heavy	469.755281	y6	697.360644	-24.02
P25340	ERG4	LQVQGEEK	2	heavy	469.755281	y5	598.29223	-24.02
P25340	ERG4	LQVQGEEK	2	heavy	469.755281	y4	470.233653	-24.02
P25340	ERG4	LQVQGEEK	2	heavy	469.755281	b2	242.149918	-24.02
P25340	ERG4	MTGNHLYDFFMGAPLN	3	light	694.329238	y8	855.450533	97.41
P25340	ERG4	MTGNHLYDFFMGAPLN	3	light	694.329238	y7	724.410049	97.41
P25340	ERG4	MTGNHLYDFFMGAPLN	3	light	694.329238	y5	596.351471	97.41
P25340	ERG4	MTGNHLYDFFMGAPLN	3	light	694.329238	y4	499.298707	97.41
P25340	ERG4	MTGNHLYDFFMGAPLN	3	light	694.329238	y2	272.171716	97.41
P25340	ERG4	MTGNHLYDFFMGAPLN	3	light	694.329238	y5	298.679373	97.41
P25340	ERG4	MTGNHLYDFFMGAPLN	3	light	694.329238	b10	1226.52991	97.41
P25340	ERG4	MTGNHLYDFFMGAPLN	3	heavy	696.335948	y8	861.470662	97.41
P25340	ERG4	MTGNHLYDFFMGAPLN	3	heavy	696.335948	y7	730.430178	97.41
P25340	ERG4	MTGNHLYDFFMGAPLN	3	heavy	696.335948	y5	602.3716	97.41
P25340	ERG4	MTGNHLYDFFMGAPLN	3	heavy	696.335948	y4	505.318836	97.41
P25340	ERG4	MTGNHLYDFFMGAPLN	3	heavy	696.335948	y2	278.191845	97.41
P25340	ERG4	MTGNHLYDFFMGAPLN	3	heavy	696.335948	y5	301.689438	97.41
P25340	ERG4	MTGNHLYDFFMGAPLN	3	heavy	696.335948	b10	1226.52991	97.41
P25340	ERG4	TFPFLPYQILK	2	light	683.892106	y9	1118.66084	114.08
P25340	ERG4	TFPFLPYQILK	2	light	683.892106	y8	1021.60808	114.08
P25340	ERG4	TFPFLPYQILK	2	light	683.892106	y7	874.539666	114.08
P25340	ERG4	TFPFLPYQILK	2	light	683.892106	y6	761.455602	114.08
P25340	ERG4	TFPFLPYQILK	2	light	683.892106	y2	260.196868	114.08
P25340	ERG4	TFPFLPYQILK	2	light	683.892106	y1	147.112804	114.08
P25340	ERG4	TFPFLPYQILK	2	light	683.892106	y9	559.83406	114.08
P25340	ERG4	TFPFLPYQILK	2	light	683.892106	b2	249.123368	114.08
P25340	ERG4	TFPFLPYQILK	2	heavy	687.899206	y9	1126.67504	114.08
P25340	ERG4	TFPFLPYQILK	2	heavy	687.899206	y8	1029.62228	114.08
P25340	ERG4	TFPFLPYQILK	2	heavy	687.899206	y7	882.553865	114.08
P25340	ERG4	TFPFLPYQILK	2	heavy	687.899206	y6	769.469801	114.08
P25340	ERG4	TFPFLPYQILK	2	heavy	687.899206	y2	268.211067	114.08
P25340	ERG4	TFPFLPYQILK	2	heavy	687.899206	y1	155.127003	114.08
P25340	ERG4	TFPFLPYQILK	2	heavy	687.899206	y9	563.841159	114.08
P25340	ERG4	TFPFLPYQILK	2	heavy	687.899206	b2	249.123368	114.08
P41338	ERG10	AIILGAQSIK	2	light	507.321317	y7	716.430115	32.04
P41338	ERG10	AIILGAQSIK	2	light	507.321317	y6	603.346051	32.04
P41338	ERG10	AIILGAQSIK	2	light	507.321317	y3	347.228896	32.04
P41338	ERG10	AIILGAQSIK	2	light	507.321317	b3	298.212518	32.04
P41338	ERG10	AIILGAQSIK	2	heavy	511.328416	y7	724.444314	32.04

P41338	ERG10	AIILGAQSIK	2	heavy	511.328416	y6	611.36025	32.04
P41338	ERG10	AIILGAQSIK	2	heavy	511.328416	y3	355.243095	32.04
P41338	ERG10	AIILGAQSIK	2	heavy	511.328416	b3	298.212518	32.04
P41338	ERG10	FGQTVLVDGVER	2	light	660.351334	y9	987.546936	37.11
P41338	ERG10	FGQTVLVDGVER	2	light	660.351334	y7	787.430844	37.11
P41338	ERG10	FGQTVLVDGVER	2	light	660.351334	y6	674.34678	37.11
P41338	ERG10	FGQTVLVDGVER	2	light	660.351334	y4	460.251423	37.11
P41338	ERG10	FGQTVLVDGVER	2	light	660.351334	b3	333.155731	37.11
P41338	ERG10	FGQTVLVDGVER	2	heavy	663.361398	y9	993.567065	37.11
P41338	ERG10	FGQTVLVDGVER	2	heavy	663.361398	y7	793.450973	37.11
P41338	ERG10	FGQTVLVDGVER	2	heavy	663.361398	y6	680.366909	37.11
P41338	ERG10	FGQTVLVDGVER	2	heavy	663.361398	y4	466.271552	37.11
P41338	ERG10	FGQTVLVDGVER	2	heavy	663.361398	b3	333.155731	37.11
P12683	HMG1	EVAALVIHGK	2	light	518.811116	y8	808.503949	6.49
P12683	HMG1	EVAALVIHGK	2	light	518.811116	y7	737.466835	6.49
P12683	HMG1	EVAALVIHGK	2	light	518.811116	y4	454.277243	6.49
P12683	HMG1	EVAALVIHGK	2	light	518.811116	y2	204.134267	6.49
P12683	HMG1	EVAALVIHGK	2	heavy	522.818216	y8	816.518148	6.49
P12683	HMG1	EVAALVIHGK	2	heavy	522.818216	y7	745.481034	6.49
P12683	HMG1	EVAALVIHGK	2	heavy	522.818216	y4	462.291442	6.49
P12683	HMG1	EVAALVIHGK	2	heavy	522.818216	y2	212.148466	6.49
P12684	HMG2	ALSTLAESPILVSEK	2	light	779.440346	y10	1072.58847	62.06
P12684	HMG2	ALSTLAESPILVSEK	2	light	779.440346	y9	1001.55135	62.06
P12684	HMG2	ALSTLAESPILVSEK	2	light	779.440346	y8	872.50876	62.06
P12684	HMG2	ALSTLAESPILVSEK	2	light	779.440346	y7	785.476731	62.06
P12684	HMG2	ALSTLAESPILVSEK	2	light	779.440346	y4	462.255839	62.06
P12684	HMG2	ALSTLAESPILVSEK	2	light	779.440346	y3	363.187425	62.06
P12684	HMG2	ALSTLAESPILVSEK	2	light	779.440346	b4	373.208161	62.06
P12684	HMG2	ALSTLAESPILVSEK	2	heavy	783.447445	y10	1080.60267	62.06
P12684	HMG2	ALSTLAESPILVSEK	2	heavy	783.447445	y9	1009.56555	62.06
P12684	HMG2	ALSTLAESPILVSEK	2	heavy	783.447445	y8	880.522959	62.06
P12684	HMG2	ALSTLAESPILVSEK	2	heavy	783.447445	y7	793.49093	62.06
P12684	HMG2	ALSTLAESPILVSEK	2	heavy	783.447445	y4	470.270038	62.06
P12684	HMG2	ALSTLAESPILVSEK	2	heavy	783.447445	y3	371.201624	62.06
P12684	HMG2	ALSTLAESPILVSEK	2	heavy	783.447445	b4	373.208161	62.06
P12684	HMG2	DIGNLSNQVIISVLPK	2	light	855.493444	y7	769.518202	95.32
P12684	HMG2	DIGNLSNQVIISVLPK	2	light	855.493444	y5	543.350074	95.32
P12684	HMG2	DIGNLSNQVIISVLPK	2	light	855.493444	y3	357.249632	95.32
P12684	HMG2	DIGNLSNQVIISVLPK	2	light	855.493444	y2	244.165568	95.32
P12684	HMG2	DIGNLSNQVIISVLPK	2	light	855.493444	b4	400.182674	95.32
P12684	HMG2	DIGNLSNQVIISVLPK	2	heavy	859.500543	y7	777.532401	95.32
P12684	HMG2	DIGNLSNQVIISVLPK	2	heavy	859.500543	y5	551.364273	95.32
P12684	HMG2	DIGNLSNQVIISVLPK	2	heavy	859.500543	y3	365.263831	95.32
P12684	HMG2	DIGNLSNQVIISVLPK	2	heavy	859.500543	y2	252.179767	95.32
P12684	HMG2	DIGNLSNQVIISVLPK	2	heavy	859.500543	b4	400.182674	95.32
P07277	ERG12	LTGAGGGGC[+57]SLTI	2	light	716.882475	y13	1218.62593	43.67
P07277	ERG12	LTGAGGGGC[+57]SLTI	2	light	716.882475	y10	1033.54589	43.67
P07277	ERG12	LTGAGGGGC[+57]SLTI	2	light	716.882475	y6	702.450851	43.67
P07277	ERG12	LTGAGGGGC[+57]SLTI	2	light	716.882475	y4	502.334758	43.67
P07277	ERG12	LTGAGGGGC[+57]SLTI	2	heavy	719.89254	y13	1224.64606	43.67
P07277	ERG12	LTGAGGGGC[+57]SLTI	2	heavy	719.89254	y10	1039.56602	43.67
P07277	ERG12	LTGAGGGGC[+57]SLTI	2	heavy	719.89254	y6	708.47098	43.67
P07277	ERG12	LTGAGGGGC[+57]SLTI	2	heavy	719.89254	y4	508.354887	43.67
P32377	ERG19	DASLPTLSQWK	2	light	623.327327	y7	859.467229	58.21
P32377	ERG19	DASLPTLSQWK	2	light	623.327327	y6	762.414465	58.21
P32377	ERG19	DASLPTLSQWK	2	light	623.327327	y4	548.282723	58.21
P32377	ERG19	DASLPTLSQWK	2	light	623.327327	y2	333.192117	58.21
P32377	ERG19	DASLPTLSQWK	2	light	623.327327	y7	430.237253	58.21
P32377	ERG19	DASLPTLSQWK	2	light	623.327327	b3	274.103361	58.21
P32377	ERG19	DASLPTLSQWK	2	light	623.327327	b4	387.187425	58.21
P32377	ERG19	DASLPTLSQWK	2	heavy	627.334427	y7	867.481428	58.21
P32377	ERG19	DASLPTLSQWK	2	heavy	627.334427	y6	770.428664	58.21
P32377	ERG19	DASLPTLSQWK	2	heavy	627.334427	y4	556.296922	58.21

P32377	ERG19	DASLPTLSQWK	2	heavy	627.334427	y2	341.206316	58.21
P32377	ERG19	DASLPTLSQWK	2	heavy	627.334427	y7	434.244352	58.21
P32377	ERG19	DASLPTLSQWK	2	heavy	627.334427	b3	274.103361	58.21
P32377	ERG19	DASLPTLSQWK	2	heavy	627.334427	b4	387.187425	58.21
P08524	ERG20	ADVLTAFLNK	2	light	546.308406	y7	806.477066	75.81
P08524	ERG20	ADVLTAFLNK	2	light	546.308406	y6	693.393001	75.81
P08524	ERG20	ADVLTAFLNK	2	light	546.308406	y5	592.345323	75.81
P08524	ERG20	ADVLTAFLNK	2	light	546.308406	y4	521.308209	75.81
P08524	ERG20	ADVLTAFLNK	2	light	546.308406	y2	261.155731	75.81
P08524	ERG20	ADVLTAFLNK	2	heavy	550.315506	y7	814.491265	75.81
P08524	ERG20	ADVLTAFLNK	2	heavy	550.315506	y6	701.4072	75.81
P08524	ERG20	ADVLTAFLNK	2	heavy	550.315506	y5	600.359522	75.81
P08524	ERG20	ADVLTAFLNK	2	heavy	550.315506	y4	529.322408	75.81
P08524	ERG20	ADVLTAFLNK	2	heavy	550.315506	y2	269.16993	75.81
P08524	ERG20	ALELASAEQR	2	light	544.290745	y7	774.410442	6.26
P08524	ERG20	ALELASAEQR	2	light	544.290745	y6	661.326378	6.26
P08524	ERG20	ALELASAEQR	2	light	544.290745	y5	590.289265	6.26
P08524	ERG20	ALELASAEQR	2	light	544.290745	y2	303.177529	6.26
P08524	ERG20	ALELASAEQR	2	light	544.290745	b3	314.171047	6.26
P08524	ERG20	ALELASAEQR	2	heavy	547.300809	y7	780.430571	6.26
P08524	ERG20	ALELASAEQR	2	heavy	547.300809	y6	667.346507	6.26
P08524	ERG20	ALELASAEQR	2	heavy	547.300809	y5	596.309394	6.26
P08524	ERG20	ALELASAEQR	2	heavy	547.300809	y2	309.197658	6.26
P08524	ERG20	ALELASAEQR	2	heavy	547.300809	b3	314.171047	6.26
P08524	ERG20	EAC[+57]DWYAHSLNY	3	light	694.970656	y10	1050.52145	38.11
P08524	ERG20	EAC[+57]DWYAHSLNY	3	light	694.970656	y7	736.36243	38.11
P08524	ERG20	EAC[+57]DWYAHSLNY	3	light	694.970656	y4	358.208495	38.11
P08524	ERG20	EAC[+57]DWYAHSLNY	3	light	694.970656	y3	261.155731	38.11
P08524	ERG20	EAC[+57]DWYAHSLNY	3	heavy	697.642055	y10	1058.53565	38.11
P08524	ERG20	EAC[+57]DWYAHSLNY	3	heavy	697.642055	y7	744.376629	38.11
P08524	ERG20	EAC[+57]DWYAHSLNY	3	heavy	697.642055	y4	366.222694	38.11
P08524	ERG20	EAC[+57]DWYAHSLNY	3	heavy	697.642055	y3	269.16993	38.11
P08524	ERG20	IEQLYHEYEESIAK	3	light	584.62107	y9	1105.51603	37.73
P08524	ERG20	IEQLYHEYEESIAK	3	light	584.62107	y8	968.457118	37.73
P08524	ERG20	IEQLYHEYEESIAK	3	light	584.62107	y13	819.885935	37.73
P08524	ERG20	IEQLYHEYEESIAK	3	light	584.62107	y11	691.335349	37.73
P08524	ERG20	IEQLYHEYEESIAK	3	light	584.62107	b3	371.192511	37.73
P08524	ERG20	IEQLYHEYEESIAK	3	heavy	587.292469	y9	1113.53023	37.73
P08524	ERG20	IEQLYHEYEESIAK	3	heavy	587.292469	y8	976.471317	37.73
P08524	ERG20	IEQLYHEYEESIAK	3	heavy	587.292469	y13	823.893034	37.73
P08524	ERG20	IEQLYHEYEESIAK	3	heavy	587.292469	y11	695.342449	37.73
P08524	ERG20	IEQLYHEYEESIAK	3	heavy	587.292469	b3	371.192511	37.73
P08524	ERG20	IGTDIQDNK	2	light	502.256371	y7	833.399937	-16.81
P08524	ERG20	IGTDIQDNK	2	light	502.256371	y6	732.352259	-16.81
P08524	ERG20	IGTDIQDNK	2	light	502.256371	y5	617.325316	-16.81
P08524	ERG20	IGTDIQDNK	2	light	502.256371	y4	504.241252	-16.81
P08524	ERG20	IGTDIQDNK	2	light	502.256371	y2	261.155731	-16.81
P08524	ERG20	IGTDIQDNK	2	heavy	506.26347	y7	841.414136	-16.81
P08524	ERG20	IGTDIQDNK	2	heavy	506.26347	y6	740.366458	-16.81
P08524	ERG20	IGTDIQDNK	2	heavy	506.26347	y5	625.339515	-16.81
P08524	ERG20	IGTDIQDNK	2	heavy	506.26347	y4	512.255451	-16.81
P08524	ERG20	IGTDIQDNK	2	heavy	506.26347	y2	269.16993	-16.81
P29704	ERG9	DYNEDLVDGR	2	light	598.264924	y8	917.4323	12.57
P29704	ERG9	DYNEDLVDGR	2	light	598.264924	y7	803.389373	12.57
P29704	ERG9	DYNEDLVDGR	2	light	598.264924	y6	674.34678	12.57
P29704	ERG9	DYNEDLVDGR	2	light	598.264924	y5	559.319837	12.57
P29704	ERG9	DYNEDLVDGR	2	light	598.264924	y4	446.235772	12.57
P29704	ERG9	DYNEDLVDGR	2	light	598.264924	y3	347.167359	12.57
P29704	ERG9	DYNEDLVDGR	2	light	598.264924	y2	232.140415	12.57
P29704	ERG9	DYNEDLVDGR	2	light	598.264924	b2	279.097548	12.57
P29704	ERG9	DYNEDLVDGR	2	heavy	601.274988	y8	923.452429	12.57
P29704	ERG9	DYNEDLVDGR	2	heavy	601.274988	y7	809.409502	12.57
P29704	ERG9	DYNEDLVDGR	2	heavy	601.274988	y6	680.366909	12.57

P29704	ERG9	DYNEDLVDGR	2	heavy	601.274988	y5	565.339966	12.57
P29704	ERG9	DYNEDLVDGR	2	heavy	601.274988	y4	452.255901	12.57
P29704	ERG9	DYNEDLVDGR	2	heavy	601.274988	y3	353.187488	12.57
P29704	ERG9	DYNEDLVDGR	2	heavy	601.274988	y2	238.160544	12.57
P29704	ERG9	DYNEDLVDGR	2	heavy	601.274988	b2	279.097548	12.57
P29704	ERG9	EIWSQYAPQLK	2	light	681.856252	y9	1120.57857	61.9
P29704	ERG9	EIWSQYAPQLK	2	light	681.856252	y8	934.499258	61.9
P29704	ERG9	EIWSQYAPQLK	2	light	681.856252	y7	847.467229	61.9
P29704	ERG9	EIWSQYAPQLK	2	light	681.856252	y6	719.408652	61.9
P29704	ERG9	EIWSQYAPQLK	2	light	681.856252	y5	556.345323	61.9
P29704	ERG9	EIWSQYAPQLK	2	light	681.856252	y4	485.308209	61.9
P29704	ERG9	EIWSQYAPQLK	2	light	681.856252	b3	215.110261	61.9
P29704	ERG9	EIWSQYAPQLK	2	heavy	685.863351	y9	1128.59277	61.9
P29704	ERG9	EIWSQYAPQLK	2	heavy	685.863351	y8	942.513457	61.9
P29704	ERG9	EIWSQYAPQLK	2	heavy	685.863351	y7	855.481428	61.9
P29704	ERG9	EIWSQYAPQLK	2	heavy	685.863351	y6	727.422851	61.9
P29704	ERG9	EIWSQYAPQLK	2	heavy	685.863351	y5	564.359522	61.9
P29704	ERG9	EIWSQYAPQLK	2	heavy	685.863351	y4	493.322408	61.9
P29704	ERG9	EIWSQYAPQLK	2	heavy	685.863351	b3	215.110261	61.9
P29704	ERG9	GC[+57]VEIFDYYLR	2	light	717.839745	y9	1217.6201	84.06
P29704	ERG9	GC[+57]VEIFDYYLR	2	light	717.839745	y8	1118.55169	84.06
P29704	ERG9	GC[+57]VEIFDYYLR	2	light	717.839745	y7	989.509094	84.06
P29704	ERG9	GC[+57]VEIFDYYLR	2	light	717.839745	y6	876.42503	84.06
P29704	ERG9	GC[+57]VEIFDYYLR	2	light	717.839745	y5	729.356616	84.06
P29704	ERG9	GC[+57]VEIFDYYLR	2	light	717.839745	y4	614.329673	84.06
P29704	ERG9	GC[+57]VEIFDYYLR	2	light	717.839745	b2	218.059388	84.06
P29704	ERG9	GC[+57]VEIFDYYLR	2	heavy	720.849809	y9	1223.64023	84.06
P29704	ERG9	GC[+57]VEIFDYYLR	2	heavy	720.849809	y8	1124.57182	84.06
P29704	ERG9	GC[+57]VEIFDYYLR	2	heavy	720.849809	y7	995.529223	84.06
P29704	ERG9	GC[+57]VEIFDYYLR	2	heavy	720.849809	y6	882.445159	84.06
P29704	ERG9	GC[+57]VEIFDYYLR	2	heavy	720.849809	y5	735.376745	84.06
P29704	ERG9	GC[+57]VEIFDYYLR	2	heavy	720.849809	y4	620.349802	84.06
P29704	ERG9	GC[+57]VEIFDYYLR	2	heavy	720.849809	b2	218.059388	84.06
P32476	ERG1	NITAQEPNVTR	2	light	621.825483	y9	1015.5167	-2.7
P32476	ERG1	NITAQEPNVTR	2	light	621.825483	y8	914.46902	-2.7
P32476	ERG1	NITAQEPNVTR	2	light	621.825483	y7	843.431906	-2.7
P32476	ERG1	NITAQEPNVTR	2	light	621.825483	y5	586.330736	-2.7
P32476	ERG1	NITAQEPNVTR	2	light	621.825483	b3	329.181946	-2.7
P32476	ERG1	NITAQEPNVTR	2	heavy	624.835548	y9	1021.53683	-2.7
P32476	ERG1	NITAQEPNVTR	2	heavy	624.835548	y8	920.489149	-2.7
P32476	ERG1	NITAQEPNVTR	2	heavy	624.835548	y7	849.452035	-2.7
P32476	ERG1	NITAQEPNVTR	2	heavy	624.835548	y5	592.350865	-2.7
P32476	ERG1	NITAQEPNVTR	2	heavy	624.835548	b3	329.181946	-2.7
P32476	ERG1	AHLTFIC[+57]DGIFSR	2	light	768.885018	y11	1328.66673	71.27
P32476	ERG1	AHLTFIC[+57]DGIFSR	2	light	768.885018	y10	1215.58267	71.27
P32476	ERG1	AHLTFIC[+57]DGIFSR	2	light	768.885018	y9	1114.53499	71.27
P32476	ERG1	AHLTFIC[+57]DGIFSR	2	light	768.885018	y5	579.324922	71.27
P32476	ERG1	AHLTFIC[+57]DGIFSR	2	light	768.885018	b2	209.103302	71.27
P32476	ERG1	AHLTFIC[+57]DGIFSR	2	light	768.885018	b3	322.187366	71.27
P32476	ERG1	AHLTFIC[+57]DGIFSR	2	heavy	771.895082	y11	1334.68686	71.27
P32476	ERG1	AHLTFIC[+57]DGIFSR	2	heavy	771.895082	y10	1221.6028	71.27
P32476	ERG1	AHLTFIC[+57]DGIFSR	2	heavy	771.895082	y9	1120.55512	71.27
P32476	ERG1	AHLTFIC[+57]DGIFSR	2	heavy	771.895082	y5	585.345051	71.27
P32476	ERG1	AHLTFIC[+57]DGIFSR	2	heavy	771.895082	b2	209.103302	71.27
P32476	ERG1	AHLTFIC[+57]DGIFSR	2	heavy	771.895082	b3	322.187366	71.27
P32476	ERG1	AHLTFIC[+57]DGIFSR	3	light	512.925771	y7	854.382513	71.27
P32476	ERG1	AHLTFIC[+57]DGIFSR	3	light	512.925771	y6	694.351865	71.27
P32476	ERG1	AHLTFIC[+57]DGIFSR	3	light	512.925771	y5	579.324922	71.27
P32476	ERG1	AHLTFIC[+57]DGIFSR	3	light	512.925771	y3	409.219394	71.27
P32476	ERG1	AHLTFIC[+57]DGIFSR	3	light	512.925771	b2	209.103302	71.27
P32476	ERG1	AHLTFIC[+57]DGIFSR	3	light	512.925771	b5	570.303458	71.27
P32476	ERG1	AHLTFIC[+57]DGIFSR	3	light	512.925771	b6	683.387522	71.27
P32476	ERG1	AHLTFIC[+57]DGIFSR	3	heavy	514.93248	y7	860.402642	71.27

P32476	ERG1	AHLTFIC[+57]DGIFSR	3	heavy	514.93248	y6	700.371994	71.27
P32476	ERG1	AHLTFIC[+57]DGIFSR	3	heavy	514.93248	y5	585.345051	71.27
P32476	ERG1	AHLTFIC[+57]DGIFSR	3	heavy	514.93248	y3	415.239523	71.27
P32476	ERG1	AHLTFIC[+57]DGIFSR	3	heavy	514.93248	b2	209.103302	71.27
P32476	ERG1	AHLTFIC[+57]DGIFSR	3	heavy	514.93248	b5	570.303458	71.27
P32476	ERG1	AHLTFIC[+57]DGIFSR	3	heavy	514.93248	b6	683.387522	71.27
P32476	ERG1	ILC[+57]AYNSPK	2	light	533.273509	y6	679.340966	-3.15
P32476	ERG1	ILC[+57]AYNSPK	2	light	533.273509	y5	608.303852	-3.15
P32476	ERG1	ILC[+57]AYNSPK	2	light	533.273509	y3	331.197596	-3.15
P32476	ERG1	ILC[+57]AYNSPK	2	heavy	537.280609	y6	687.355165	-3.15
P32476	ERG1	ILC[+57]AYNSPK	2	heavy	537.280609	y5	616.318051	-3.15
P32476	ERG1	ILC[+57]AYNSPK	2	heavy	537.280609	y3	339.211795	-3.15
P38604	ERG7	GVYIPVSYLSLVK	2	light	719.421228	y9	1005.59791	103.59
P38604	ERG7	GVYIPVSYLSLVK	2	light	719.421228	y7	809.476731	103.59
P38604	ERG7	GVYIPVSYLSLVK	2	light	719.421228	y4	446.29731	103.59
P38604	ERG7	GVYIPVSYLSLVK	2	light	719.421228	b3	320.160482	103.59
P38604	ERG7	GVYIPVSYLSLVK	2	heavy	723.428327	y9	1013.61211	103.59
P38604	ERG7	GVYIPVSYLSLVK	2	heavy	723.428327	y7	817.49093	103.59
P38604	ERG7	GVYIPVSYLSLVK	2	heavy	723.428327	y4	454.311509	103.59
P38604	ERG7	GVYIPVSYLSLVK	2	heavy	723.428327	b3	320.160482	103.59
P10614	ERG11	GHEFVFNAK	2	light	524.764166	y7	854.44068	8.02
P10614	ERG11	GHEFVFNAK	2	light	524.764166	y6	725.398087	8.02
P10614	ERG11	GHEFVFNAK	2	light	524.764166	y4	479.261259	8.02
P10614	ERG11	GHEFVFNAK	2	light	524.764166	b3	324.130245	8.02
P10614	ERG11	GHEFVFNAK	2	heavy	528.771265	y7	862.454879	8.02
P10614	ERG11	GHEFVFNAK	2	heavy	528.771265	y6	733.412286	8.02
P10614	ERG11	GHEFVFNAK	2	heavy	528.771265	y4	487.275458	8.02
P10614	ERG11	GHEFVFNAK	2	heavy	528.771265	b3	324.130245	8.02
P53045	ERG25	EQLYC[+57]LK	2	light	477.241678	y5	696.374909	10.95
P53045	ERG25	EQLYC[+57]LK	2	light	477.241678	y4	583.290845	10.95
P53045	ERG25	EQLYC[+57]LK	2	light	477.241678	y3	420.227516	10.95
P53045	ERG25	EQLYC[+57]LK	2	light	477.241678	y2	260.196868	10.95
P53045	ERG25	EQLYC[+57]LK	2	light	477.241678	b2	258.108447	10.95
P53045	ERG25	EQLYC[+57]LK	2	light	477.241678	b6	807.370552	10.95
P53045	ERG25	EQLYC[+57]LK	2	heavy	481.248777	y5	704.389108	10.95
P53045	ERG25	EQLYC[+57]LK	2	heavy	481.248777	y4	591.305044	10.95
P53045	ERG25	EQLYC[+57]LK	2	heavy	481.248777	y3	428.241715	10.95
P53045	ERG25	EQLYC[+57]LK	2	heavy	481.248777	b2	258.108447	10.95
P53045	ERG25	EQLYC[+57]LK	2	heavy	481.248777	b6	807.370552	10.95
P53045	ERG25	WWDYC[+57]LDTESGF	2	light	928.893434	y12	1369.59402	61.36
P53045	ERG25	WWDYC[+57]LDTESGF	2	light	928.893434	y11	1206.53069	61.36
P53045	ERG25	WWDYC[+57]LDTESGF	2	light	928.893434	y10	1046.50005	61.36
P53045	ERG25	WWDYC[+57]LDTESGF	2	light	928.893434	y9	933.415981	61.36
P53045	ERG25	WWDYC[+57]LDTESGF	2	light	928.893434	y8	818.389038	61.36
P53045	ERG25	WWDYC[+57]LDTESGF	2	light	928.893434	y6	588.298767	61.36
P53045	ERG25	WWDYC[+57]LDTESGF	2	light	928.893434	y5	501.266738	61.36
P53045	ERG25	WWDYC[+57]LDTESGF	2	heavy	932.900533	y12	1377.60822	61.36
P53045	ERG25	WWDYC[+57]LDTESGF	2	heavy	932.900533	y11	1214.54489	61.36
P53045	ERG25	WWDYC[+57]LDTESGF	2	heavy	932.900533	y10	1054.51424	61.36
P53045	ERG25	WWDYC[+57]LDTESGF	2	heavy	932.900533	y9	941.43018	61.36
P53045	ERG25	WWDYC[+57]LDTESGF	2	heavy	932.900533	y8	826.403237	61.36
P53045	ERG25	WWDYC[+57]LDTESGF	2	heavy	932.900533	y6	596.312966	61.36
P53045	ERG25	WWDYC[+57]LDTESGF	2	heavy	932.900533	y5	509.280937	61.36
P53199	ERG26	AIAEDMVLK	2	light	495.270435	y7	805.412416	27.32
P53199	ERG26	AIAEDMVLK	2	light	495.270435	y6	734.375303	27.32
P53199	ERG26	AIAEDMVLK	2	light	495.270435	y5	605.332709	27.32
P53199	ERG26	AIAEDMVLK	2	light	495.270435	y2	260.196868	27.32
P53199	ERG26	AIAEDMVLK	2	heavy	499.277535	y7	813.426615	27.32
P53199	ERG26	AIAEDMVLK	2	heavy	499.277535	y6	742.389502	27.32
P53199	ERG26	AIAEDMVLK	2	heavy	499.277535	y5	613.346908	27.32
P53199	ERG26	AIAEDMVLK	2	heavy	499.277535	y2	268.211067	27.32
P53199	ERG26	ANDPSSDFYTVALRPA	3	light	841.746943	y10	986.505406	95.1
P53199	ERG26	ANDPSSDFYTVALRPA	3	light	841.746943	y21	1112.06329	95.1

P53199	ERG26	ANDPSSDFYTVALRPA	3	light	841.746943	y20	1063.5369	95.1
P53199	ERG26	ANDPSSDFYTVALRPA	3	light	841.746943	y19	1020.02089	95.1
P53199	ERG26	ANDPSSDFYTVALRPA	3	light	841.746943	y17	918.991403	95.1
P53199	ERG26	ANDPSSDFYTVALRPA	3	light	841.746943	y16	845.457196	95.1
P53199	ERG26	ANDPSSDFYTVALRPA	3	light	841.746943	y15	763.925531	95.1
P53199	ERG26	ANDPSSDFYTVALRPA	3	light	841.746943	b3	301.11426	95.1
P53199	ERG26	ANDPSSDFYTVALRPA	3	heavy	845.760363	y10	992.525535	95.1
P53199	ERG26	ANDPSSDFYTVALRPA	3	heavy	845.760363	y21	1118.08341	95.1
P53199	ERG26	ANDPSSDFYTVALRPA	3	heavy	845.760363	y20	1069.55703	95.1
P53199	ERG26	ANDPSSDFYTVALRPA	3	heavy	845.760363	y19	1026.04102	95.1
P53199	ERG26	ANDPSSDFYTVALRPA	3	heavy	845.760363	y17	925.011532	95.1
P53199	ERG26	ANDPSSDFYTVALRPA	3	heavy	845.760363	y16	851.477325	95.1
P53199	ERG26	ANDPSSDFYTVALRPA	3	heavy	845.760363	y15	769.94566	95.1
P53199	ERG26	ANDPSSDFYTVALRPA	3	heavy	845.760363	b3	301.11426	95.1
P53199	ERG26	ANVVVHC[+57]ASPMH	4	light	695.092902	y7	850.466895	57.95
P53199	ERG26	ANVVVHC[+57]ASPMH	4	light	695.092902	y6	687.403566	57.95
P53199	ERG26	ANVVVHC[+57]ASPMH	4	light	695.092902	y5	572.376623	57.95
P53199	ERG26	ANVVVHC[+57]ASPMH	4	light	695.092902	y3	360.224145	57.95
P53199	ERG26	ANVVVHC[+57]ASPMH	4	light	695.092902	b2	186.087317	57.95
P53199	ERG26	ANVVVHC[+57]ASPMH	4	light	695.092902	b3	285.155731	57.95
P53199	ERG26	ANVVVHC[+57]ASPMH	4	heavy	697.096452	y7	858.481094	57.95
P53199	ERG26	ANVVVHC[+57]ASPMH	4	heavy	697.096452	y6	695.417765	57.95
P53199	ERG26	ANVVVHC[+57]ASPMH	4	heavy	697.096452	y5	580.390822	57.95
P53199	ERG26	ANVVVHC[+57]ASPMH	4	heavy	697.096452	y3	368.238344	57.95
P53199	ERG26	ANVVVHC[+57]ASPMH	4	heavy	697.096452	b2	186.087317	57.95
P53199	ERG26	ANVVVHC[+57]ASPMH	4	heavy	697.096452	b3	285.155731	57.95
P53199	ERG26	EPGLTPFR	2	light	458.747984	y6	690.393336	18.92
P53199	ERG26	EPGLTPFR	2	light	458.747984	y4	520.287808	18.92
P53199	ERG26	EPGLTPFR	2	light	458.747984	y3	419.24013	18.92
P53199	ERG26	EPGLTPFR	2	heavy	461.758049	y6	696.413465	18.92
P53199	ERG26	EPGLTPFR	2	heavy	461.758049	y4	526.307937	18.92
P53199	ERG26	EPGLTPFR	2	heavy	461.758049	y3	425.260259	18.92
Q12452	ERG27	AANAPVYVTR	2	light	531.290548	y8	919.499592	-1.32
Q12452	ERG27	AANAPVYVTR	2	light	531.290548	y7	805.456664	-1.32
Q12452	ERG27	AANAPVYVTR	2	light	531.290548	y6	734.419551	-1.32
Q12452	ERG27	AANAPVYVTR	2	light	531.290548	y4	538.298373	-1.32
Q12452	ERG27	AANAPVYVTR	2	light	531.290548	y6	367.713413	-1.32
Q12452	ERG27	AANAPVYVTR	2	light	531.290548	b3	257.124431	-1.32
Q12452	ERG27	AANAPVYVTR	2	light	531.290548	b4	328.161545	-1.32
Q12452	ERG27	AANAPVYVTR	2	heavy	534.300612	y8	925.519721	-1.32
Q12452	ERG27	AANAPVYVTR	2	heavy	534.300612	y7	811.476793	-1.32
Q12452	ERG27	AANAPVYVTR	2	heavy	534.300612	y6	740.43968	-1.32
Q12452	ERG27	AANAPVYVTR	2	heavy	534.300612	y4	544.318502	-1.32
Q12452	ERG27	AANAPVYVTR	2	heavy	534.300612	y6	370.723478	-1.32
Q12452	ERG27	AANAPVYVTR	2	heavy	534.300612	b3	257.124431	-1.32
Q12452	ERG27	AANAPVYVTR	2	heavy	534.300612	b4	328.161545	-1.32
Q12452	ERG27	EVFTNPLEAVTNPTYK	2	light	911.964716	y11	1232.65213	82.01
Q12452	ERG27	EVFTNPLEAVTNPTYK	2	light	911.964716	y9	1022.5153	82.01
Q12452	ERG27	EVFTNPLEAVTNPTYK	2	light	911.964716	y8	893.472708	82.01
Q12452	ERG27	EVFTNPLEAVTNPTYK	2	light	911.964716	y7	822.435595	82.01
Q12452	ERG27	EVFTNPLEAVTNPTYK	2	light	911.964716	y6	723.367181	82.01
Q12452	ERG27	EVFTNPLEAVTNPTYK	2	light	911.964716	y4	508.276575	82.01
Q12452	ERG27	EVFTNPLEAVTNPTYK	2	light	911.964716	y3	411.223811	82.01
Q12452	ERG27	EVFTNPLEAVTNPTYK	2	heavy	915.971816	y11	1240.66633	82.01
Q12452	ERG27	EVFTNPLEAVTNPTYK	2	heavy	915.971816	y9	1030.5295	82.01
Q12452	ERG27	EVFTNPLEAVTNPTYK	2	heavy	915.971816	y8	901.486907	82.01
Q12452	ERG27	EVFTNPLEAVTNPTYK	2	heavy	915.971816	y7	830.449794	82.01
Q12452	ERG27	EVFTNPLEAVTNPTYK	2	heavy	915.971816	y6	731.38138	82.01
Q12452	ERG27	EVFTNPLEAVTNPTYK	2	heavy	915.971816	y4	516.290774	82.01
Q12452	ERG27	EVFTNPLEAVTNPTYK	2	heavy	915.971816	y3	419.23801	82.01
Q12452	ERG27	LANPNFEK	2	light	466.745442	y7	819.399543	-5.86
Q12452	ERG27	LANPNFEK	2	light	466.745442	y6	748.36243	-5.86
Q12452	ERG27	LANPNFEK	2	light	466.745442	y5	634.319502	-5.86

Q12452	ERG27	LANPNFEK	2	heavy	470.752541	y7	827.413742	-5.86
Q12452	ERG27	LANPNFEK	2	heavy	470.752541	y6	756.376629	-5.86
Q12452	ERG27	LANPNFEK	2	heavy	470.752541	y5	642.333701	-5.86
Q12452	ERG27	LIETEDTNVR	2	light	595.306592	y8	963.43778	-2.95
Q12452	ERG27	LIETEDTNVR	2	light	595.306592	y7	834.395186	-2.95
Q12452	ERG27	LIETEDTNVR	2	light	595.306592	y6	733.347508	-2.95
Q12452	ERG27	LIETEDTNVR	2	light	595.306592	y5	604.304915	-2.95
Q12452	ERG27	LIETEDTNVR	2	light	595.306592	y4	489.277972	-2.95
Q12452	ERG27	LIETEDTNVR	2	heavy	598.316656	y8	969.457909	-2.95
Q12452	ERG27	LIETEDTNVR	2	heavy	598.316656	y7	840.415315	-2.95
Q12452	ERG27	LIETEDTNVR	2	heavy	598.316656	y6	739.367637	-2.95
Q12452	ERG27	LIETEDTNVR	2	heavy	598.316656	y5	610.325044	-2.95
Q12452	ERG27	LIETEDTNVR	2	heavy	598.316656	y4	495.298101	-2.95
P35196	RER2	SDFLIWQASSK	2	light	641.327327	y7	819.435929	62.91
P35196	RER2	SDFLIWQASSK	2	light	641.327327	y6	706.351865	62.91
P35196	RER2	SDFLIWQASSK	2	light	641.327327	y5	520.272552	62.91
P35196	RER2	SDFLIWQASSK	2	light	641.327327	y4	392.213974	62.91
P35196	RER2	SDFLIWQASSK	2	light	641.327327	b2	203.066248	62.91
P35196	RER2	SDFLIWQASSK	2	light	641.327327	b3	350.134661	62.91
P35196	RER2	SDFLIWQASSK	2	light	641.327327	b4	463.218725	62.91
P35196	RER2	SDFLIWQASSK	2	light	641.327327	b5	576.302789	62.91
P35196	RER2	SDFLIWQASSK	2	heavy	645.334427	y7	827.450128	62.91
P35196	RER2	SDFLIWQASSK	2	heavy	645.334427	y6	714.366064	62.91
P35196	RER2	SDFLIWQASSK	2	heavy	645.334427	y5	528.286751	62.91
P35196	RER2	SDFLIWQASSK	2	heavy	645.334427	y4	400.228173	62.91
P35196	RER2	SDFLIWQASSK	2	heavy	645.334427	b2	203.066248	62.91
P35196	RER2	SDFLIWQASSK	2	heavy	645.334427	b3	350.134661	62.91
P35196	RER2	SDFLIWQASSK	2	heavy	645.334427	b4	463.218725	62.91
P35196	RER2	SDFLIWQASSK	2	heavy	645.334427	b5	576.302789	62.91
Q12063	NUS1	HLMLYDYDGILQR	2	light	818.911232	y11	1386.67221	69.72
Q12063	NUS1	HLMLYDYDGILQR	2	light	818.911232	y10	1255.63173	69.72
Q12063	NUS1	HLMLYDYDGILQR	2	light	818.911232	y8	979.484336	69.72
Q12063	NUS1	HLMLYDYDGILQR	2	light	818.911232	y7	864.457393	69.72
Q12063	NUS1	HLMLYDYDGILQR	2	light	818.911232	y5	586.367121	69.72
Q12063	NUS1	HLMLYDYDGILQR	2	heavy	821.921297	y11	1392.69234	69.72
Q12063	NUS1	HLMLYDYDGILQR	2	heavy	821.921297	y10	1261.65186	69.72
Q12063	NUS1	HLMLYDYDGILQR	2	heavy	821.921297	y8	985.504465	69.72
Q12063	NUS1	HLMLYDYDGILQR	2	heavy	821.921297	y7	870.477522	69.72
Q12063	NUS1	HLMLYDYDGILQR	2	heavy	821.921297	y5	592.38725	69.72
Q12063	NUS1	HLMLYDYDGILQR	3	light	546.27658	y6	701.394064	69.72
Q12063	NUS1	HLMLYDYDGILQR	3	light	546.27658	y5	586.367121	69.72
Q12063	NUS1	HLMLYDYDGILQR	3	light	546.27658	y3	416.261593	69.72
Q12063	NUS1	HLMLYDYDGILQR	3	light	546.27658	b4	495.274801	69.72
Q12063	NUS1	HLMLYDYDGILQR	3	light	546.27658	b6	773.365072	69.72
Q12063	NUS1	HLMLYDYDGILQR	3	heavy	548.28329	y6	707.414193	69.72
Q12063	NUS1	HLMLYDYDGILQR	3	heavy	548.28329	y5	592.38725	69.72
Q12063	NUS1	HLMLYDYDGILQR	3	heavy	548.28329	y3	422.281722	69.72
Q12063	NUS1	HLMLYDYDGILQR	3	heavy	548.28329	b4	495.274801	69.72
Q12063	NUS1	HLMLYDYDGILQR	3	heavy	548.28329	b6	773.365072	69.72
Q12063	NUS1	YFGPAHVPNYAVK	2	light	731.877519	y7	790.445765	32.42
Q12063	NUS1	YFGPAHVPNYAVK	2	light	731.877519	y6	691.377351	32.42
Q12063	NUS1	YFGPAHVPNYAVK	2	light	731.877519	y11	576.811647	32.42
Q12063	NUS1	YFGPAHVPNYAVK	2	light	731.877519	b6	673.309272	32.42
Q12063	NUS1	YFGPAHVPNYAVK	2	heavy	735.884618	y7	798.459964	32.42
Q12063	NUS1	YFGPAHVPNYAVK	2	heavy	735.884618	y6	699.39155	32.42
Q12063	NUS1	YFGPAHVPNYAVK	2	heavy	735.884618	y11	580.818747	32.42
Q12063	NUS1	YFGPAHVPNYAVK	2	heavy	735.884618	b6	673.309272	32.42
Q12063	NUS1	YFGPAHVPNYAVK	3	light	488.254104	y7	790.445765	32.42
Q12063	NUS1	YFGPAHVPNYAVK	3	light	488.254104	y6	691.377351	32.42
Q12063	NUS1	YFGPAHVPNYAVK	3	light	488.254104	y10	548.300915	32.42
Q12063	NUS1	YFGPAHVPNYAVK	3	light	488.254104	y8	464.255977	32.42
Q12063	NUS1	YFGPAHVPNYAVK	3	light	488.254104	b2	311.139019	32.42
Q12063	NUS1	YFGPAHVPNYAVK	3	heavy	490.925504	y7	798.459964	32.42

Q12063	NUS1	YFGPAHVPNYAVK	3	heavy	490.925504	y6	699.39155	32.42
Q12063	NUS1	YFGPAHVPNYAVK	3	heavy	490.925504	y10	552.308015	32.42
Q12063	NUS1	YFGPAHVPNYAVK	3	heavy	490.925504	y8	468.263076	32.42
Q12063	NUS1	YFGPAHVPNYAVK	3	heavy	490.925504	b2	311.139019	32.42

Appendix Table 3. SRM MS assay for measuring SILAC steady-state levels of OST subunits.

Protein	SwissProt Name	Peptide	Charge	Ion	Mass Light	Mass Heavy	Retention time
Ost1p	OST1_YEAST	ANGNSFEFGPWEDIPR	2+	p	918.421	921.4311	51.2
Ost1p	OST1_YEAST	ANGNSFEFGPWEDIPR	1+	y9	1116.55	1122.567	
Ost1p	OST1_YEAST	ANGNSFEFGPWEDIPR	1+	y8	969.479	975.499	
Ost1p	OST1_YEAST	ANGNSFEFGPWEDIPR	1+	y7	912.457	918.4775	
Ost1p	OST1_YEAST	ANGNSFEFGPWEDIPR	1+	y4	500.283	506.3029	
Ost1p	OST1_YEAST	LSDFLHVSSGSDEK	3+	p	507.579	510.2505	36.4
Ost1p	OST1_YEAST	LSDFLHVSSGSDEK	1+	y9	945.427	953.4414	
Ost1p	OST1_YEAST	LSDFLHVSSGSDEK	1+	y8	808.368	816.3825	
Ost1p	OST1_YEAST	LSDFLHVSSGSDEK	1+	y7	709.3	717.3141	
Ost1p	OST1_YEAST	LSDFLHVSSGSDEK	2+	y13	704.323	708.3301	
Ost1p	OST1_YEAST	LSDFLHVSSGSDEK	2+	y12	660.807	664.8141	
Ost1p	OST1_YEAST	LSDFLHVSSGSDEK	2+	y11	603.294	607.3006	
Ost1p	OST1_YEAST	NLISQVANGQVLIK	2+	p	748.943	752.9505	48.5
Ost1p	OST1_YEAST	NLISQVANGQVLIK	1+	y11	1156.67	1164.683	
Ost1p	OST1_YEAST	NLISQVANGQVLIK	1+	y10	1069.64	1077.651	
Ost1p	OST1_YEAST	NLISQVANGQVLIK	1+	y9	941.578	949.592	
Ost1p	OST1_YEAST	NLISQVANGQVLIK	1+	y8	842.509	850.5236	
Ost1p	OST1_YEAST	NLISQVANGQVLIK	1+	y7	771.472	779.4865	
Ost1p	OST1_YEAST	NIASEPATEYFTAFESGIFSK	3+	p	770.371	773.042	59.5
Ost1p	OST1_YEAST	NIASEPATEYFTAFESGIFSK	1+	y9	985.499	993.5131	
Ost1p	OST1_YEAST	NIASEPATEYFTAFESGIFSK	1+	y8	914.462	922.476	
Ost1p	OST1_YEAST	NIASEPATEYFTAFESGIFSK	1+	y6	638.351	646.365	
Ost1p	OST1_YEAST	NIASEPATEYFTAFESGIFSK	1+	y5	551.319	559.333	
Ost1p	OST1_YEAST	LTFSYR	2+	p	393.711	396.7209	34.4
Ost1p	OST1_YEAST	LTFSYR	1+	y5	673.33	679.3505	
Ost1p	OST1_YEAST	LTFSYR	1+	y4	572.283	578.3029	
Ost1p	OST1_YEAST	LTFSYR	1+	y3	425.214	431.2344	
Ost1p	OST1_YEAST	LTFSYR	2+	y4	286.645	289.6551	
Ost2p	OST2_YEAST	VTSTSSAVLTDFQETFK	2+	p	930.965	934.972	50.3
Ost2p	OST2_YEAST	VTSTSSAVLTDFQETFK	1+	y10	1227.63	1235.64	
Ost2p	OST2_YEAST	VTSTSSAVLTDFQETFK	1+	y9	1128.56	1136.571	
Ost2p	OST2_YEAST	VTSTSSAVLTDFQETFK	1+	y8	1015.47	1023.487	
Ost2p	OST2_YEAST	VTSTSSAVLTDFQETFK	1+	y7	914.425	922.4396	
Ost2p	OST2_YEAST	VTSTSSAVLTDFQETFK	1+	y6	799.399	807.4127	
Ost2p	OST2_YEAST	RAYFAQIEK	2+	p	563.306	570.3234	31.5
Ost2p	OST2_YEAST	RAYFAQIEK	1+	b5	609.314	615.3345	
Ost2p	OST2_YEAST	RAYFAQIEK	1+	b6	737.373	743.3931	
Ost2p	OST2_YEAST	RAYFAQIEK	1+	b7	850.457	856.4771	
Ost2p	OST2_YEAST	RAYFAQIEK	1+	b8	979.5	985.5197	
Ost3p	OST3_YEAST	SPAYPFPLLR	2+	p	580.827	583.8368	49.2
Ost3p	OST3_YEAST	SPAYPFPLLR	1+	y8	976.562	982.5816	
Ost3p	OST3_YEAST	SPAYPFPLLR	1+	y7	905.524	911.5445	
Ost3p	OST3_YEAST	SPAYPFPLLR	1+	y6	742.461	748.4812	
Ost3p	OST3_YEAST	SPAYPFPLLR	1+	y5	645.408	651.4284	
Ost3p	OST3_YEAST	SPAYPFPLLR	1+	b4	419.193	419.1925	
Ost3p	OST3_YEAST	SSNSDTSIFFTK	2+	p	667.317	671.3243	39.1
Ost3p	OST3_YEAST	SSNSDTSIFFTK	1+	y10	1159.56	1167.577	
Ost3p	OST3_YEAST	SSNSDTSIFFTK	1+	y8	958.488	1053.534	
Ost3p	OST3_YEAST	SSNSDTSIFFTK	1+	y7	843.461	851.4753	
Ost3p	OST3_YEAST	SSNSDTSIFFTK	1+	y6	742.413	750.4276	
Ost3p	OST3_YEAST	SSNSDTSIFFTK	1+	y4	542.297	550.3115	
Ost3p	OST3_YEAST	QIIQAIK	2+	p	407.263	411.2704	31.3
Ost3p	OST3_YEAST	QIIQAIK	1+	y6	685.461	693.4749	

Ost3p	OST3_YEAST	QIIQAIK	1+	y5	572.377	580.3908	
Ost3p	OST3_YEAST	QIIQAIK	1+	y3	331.234	339.2482	
Ost3p	OST3_YEAST	QIIQAIK	2+	y5	286.692	290.699	
Ost5p	OST5_YEAST	TYEQLYK	2+	p	472.74	476.7469	29.7
Ost5p	OST5_YEAST	TYEQLYK	1+	y6	843.425	851.4389	
Ost5p	OST5_YEAST	TYEQLYK	1+	y5	680.361	688.3756	
Ost5p	OST5_YEAST	TYEQLYK	1+	y4	551.319	559.333	
Ost5p	OST5_YEAST	TYEQLYK	1+	y2	310.176	318.1903	
Ost5p	OST5_YEAST	TYEQLYK	2+	y6	422.216	426.2231	
Ost6p	OST6_YEAST	FVEMNAIPFIAR	2+	p	704.376	707.3864	52.2
Ost6p	OST6_YEAST	FVEMNAIPFIAR	1+	y10	1161.61	1167.629	
Ost6p	OST6_YEAST	FVEMNAIPFIAR	1+	y9	1032.57	1038.586	
Ost6p	OST6_YEAST	FVEMNAIPFIAR	1+	y8	901.525	907.5455	
Ost6p	OST6_YEAST	FVEMNAIPFIAR	1+	y7	787.483	793.5026	
Ost6p	OST6_YEAST	FVEMNAIPFIAR	1+	y5	603.361	609.3814	
Ost6p	OST6_YEAST	LQNVPHLVVYPPAESNK	3+	p	635.679	638.3505	40.9
Ost6p	OST6_YEAST	LQNVPHLVVYPPAESNK	1+	y10	1103.57	1111.587	
Ost6p	OST6_YEAST	LQNVPHLVVYPPAESNK	1+	y9	1004.5	1012.519	
Ost6p	OST6_YEAST	LQNVPHLVVYPPAESNK	1+	y8	905.436	913.4505	
Ost6p	OST6_YEAST	LQNVPHLVVYPPAESNK	1+	y7	742.373	750.3872	
Ost6p	OST6_YEAST	LQNVPHLVVYPPAESNK	1+	y6	645.32	653.3344	
Ost6p	OST6_YEAST	TYHAVADVIR	2+	p	572.809	575.8192	31.6
Ost6p	OST6_YEAST	TYHAVADVIR	1+	y8	880.5	886.5201	
Ost6p	OST6_YEAST	TYHAVADVIR	1+	y7	743.441	749.4611	
Ost6p	OST6_YEAST	TYHAVADVIR	1+	y6	672.404	678.424	
Ost6p	OST6_YEAST	TYHAVADVIR	1+	y3	387.271	393.2916	
Ost6p	OST6_YEAST	TYHAVADVIR	2+	y8	440.754	443.7637	
Swp1p	OSTD_YEAST	NLEMAFEPEIK	2+	p	660.829	664.8359	45.2
Swp1p	OSTD_YEAST	NLEMAFEPEIK	1+	y9	1093.52	1101.538	
Swp1p	OSTD_YEAST	NLEMAFEPEIK	1+	y8	964.481	972.495	
Swp1p	OSTD_YEAST	NLEMAFEPEIK	1+	y7	833.44	841.4545	
Swp1p	OSTD_YEAST	NLEMAFEPEIK	1+	y5	615.335	623.349	
Swp1p	OSTD_YEAST	NLEMAFEPEIK	1+	y4	486.292	494.3064	
Swp1p	OSTD_YEAST	YRIDLAK	2+	p	439.758	446.7755	30.7
Swp1p	OSTD_YEAST	YRIDLAK	1+	y3	331.234	339.2482	
Swp1p	OSTD_YEAST	YRIDLAK	1+	y2	218.15	226.1641	
Swp1p	OSTD_YEAST	YRIDLAK	1+	b4	548.283	554.3029	
Swp1p	OSTD_YEAST	YRIDLAK	1+	b5	661.367	667.3869	
Swp1p	OSTD_YEAST	YRIDLAK	1+	b6	732.404	738.424	
Wbp1p	OSTB_YEAST	LFDNIIVFPTK	2+	p	653.874	657.881	52.9
Wbp1p	OSTB_YEAST	LFDNIIVFPTK	1+	y9	1046.59	1054.602	
Wbp1p	OSTB_YEAST	LFDNIIVFPTK	1+	y8	931.561	939.5753	
Wbp1p	OSTB_YEAST	LFDNIIVFPTK	1+	y6	704.434	712.4483	
Wbp1p	OSTB_YEAST	LFDNIIVFPTK	1+	y5	591.35	599.3643	
Wbp1p	OSTB_YEAST	LFDNIIVFPTK	1+	y4	492.282	500.2959	
Wbp1p	OSTB_YEAST	LFLNELGIYPSPK	2+	p	745.916	749.9234	51.7
Wbp1p	OSTB_YEAST	LFLNELGIYPSPK	1+	y9	1003.55	1011.56	
Wbp1p	OSTB_YEAST	LFLNELGIYPSPK	1+	y8	874.503	882.5175	
Wbp1p	OSTB_YEAST	LFLNELGIYPSPK	1+	y7	761.419	769.4334	
Wbp1p	OSTB_YEAST	LFLNELGIYPSPK	1+	y5	591.314	599.3279	
Wbp1p	OSTB_YEAST	LFLNELGIYPSPK	1+	y4	428.25	436.2646	
Wbp1p	OSTB_YEAST	IGLSFTTDK	2+	p	491.266	495.2733	37.9
Wbp1p	OSTB_YEAST	IGLSFTTDK	1+	y8	868.441	876.4553	
Wbp1p	OSTB_YEAST	IGLSFTTDK	1+	y7	811.42	819.4338	
Wbp1p	OSTB_YEAST	IGLSFTTDK	1+	y6	698.336	706.3497	
Wbp1p	OSTB_YEAST	IGLSFTTDK	1+	y5	611.304	619.3177	
Wbp1p	OSTB_YEAST	IGLSFTTDK	1+	y4	464.235	472.2493	
Wbp1p	OSTB_YEAST	EQIVPILNAPR	2+	p	625.367	628.3769	43
Wbp1p	OSTB_YEAST	EQIVPILNAPR	1+	y9	992.625	998.6453	

Wbp1p	OSTB_YEAST	EQIVPILNAPR	1+	y8	879.541	885.5612	
Wbp1p	OSTB_YEAST	EQIVPILNAPR	1+	y7	780.473	786.4928	
Wbp1p	OSTB_YEAST	EQIVPILNAPR	1+	y6	683.42	689.44	
Wbp1p	OSTB_YEAST	EQIVPILNAPR	1+	y5	570.336	576.3559	
Stt3p	STT3_YEAST	TAYSSPSVVLPSQTPDGK	2+	p	917.465	921.4722	38.2
Stt3p	STT3_YEAST	TAYSSPSVVLPSQTPDGK	1+	y10	1041.56	1049.572	
Stt3p	STT3_YEAST	TAYSSPSVVLPSQTPDGK	1+	y9	942.489	950.5033	
Stt3p	STT3_YEAST	TAYSSPSVVLPSQTPDGK	1+	y8	829.405	837.4192	
Stt3p	STT3_YEAST	TAYSSPSVVLPSQTPDGK	1+	y5	517.262	525.2759	
Stt3p	STT3_YEAST	TAYSSPSVVLPSQTPDGK	2+	y16	831.423	835.4298	
Stt3p	STT3_YEAST	DFPQLFNGGQATDR	2+	p	783.371	786.3809	44.3
Stt3p	STT3_YEAST	DFPQLFNGGQATDR	1+	y10	1078.53	1084.548	
Stt3p	STT3_YEAST	DFPQLFNGGQATDR	1+	y9	965.444	971.4637	
Stt3p	STT3_YEAST	DFPQLFNGGQATDR	1+	y8	818.375	824.3952	
Stt3p	STT3_YEAST	DFPQLFNGGQATDR	1+	y7	704.332	710.3523	
Stt3p	STT3_YEAST	DFPQLFNGGQATDR	2+	y12	652.323	655.3332	
Stt3p	STT3_YEAST	ISEGIWPEEIK	2+	p	650.843	654.8499	43.3
Stt3p	STT3_YEAST	ISEGIWPEEIK	1+	y10	1187.59	1195.608	
Stt3p	STT3_YEAST	ISEGIWPEEIK	1+	y9	1100.56	1108.576	
Stt3p	STT3_YEAST	ISEGIWPEEIK	1+	y8	971.52	979.5339	
Stt3p	STT3_YEAST	ISEGIWPEEIK	1+	y6	801.414	809.4283	
Stt3p	STT3_YEAST	ISEGIWPEEIK	1+	y5	615.335	623.349	
Sec63p	SEC63_YEAST	AYESLTDELVR	2+	p	648.328	651.3376	41.1
Sec63p	SEC63_YEAST	AYESLTDELVR	1+	y8	932.505	938.5249	
Sec63p	SEC63_YEAST	AYESLTDELVR	1+	y7	845.473	851.4928	
Sec63p	SEC63_YEAST	AYESLTDELVR	1+	y6	732.389	738.4088	
Sec63p	SEC63_YEAST	AYESLTDELVR	1+	y4	516.314	522.3342	
Sec63p	SEC63_YEAST	QPLVPYSFAPFFPTK	2+	p	869.964	873.9709	57.8
Sec63p	SEC63_YEAST	QPLVPYSFAPFFPTK	1+	y9	1041.54	1049.555	
Sec63p	SEC63_YEAST	QPLVPYSFAPFFPTK	1+	y8	954.508	962.5226	
Sec63p	SEC63_YEAST	QPLVPYSFAPFFPTK	1+	y7	807.44	815.4542	
Sec63p	SEC63_YEAST	QPLVPYSFAPFFPTK	1+	y6	736.403	744.417	
Sec63p	SEC63_YEAST	IPLGQPAPETVGDFFFR	3+	p	630.996	633.0032	55.9
Sec63p	SEC63_YEAST	IPLGQPAPETVGDFFFR	1+	y8	988.489	994.5088	
Sec63p	SEC63_YEAST	IPLGQPAPETVGDFFFR	1+	y7	887.441	893.4611	
Sec63p	SEC63_YEAST	IPLGQPAPETVGDFFFR	1+	y5	731.351	737.3713	
Sec63p	SEC63_YEAST	IPLGQPAPETVGDFFFR	1+	b7	677.398	677.3981	
Sec63p	SEC63_YEAST	IPLGQPAPETVGDFFFR	1+	b9	903.493	903.4934	
Sec63p	SEC63_YEAST	NLNEEYTSDEIK	2+	p	727.836	731.843	32.7
Sec63p	SEC63_YEAST	NLNEEYTSDEIK	1+	y10	1227.54	1235.552	
Sec63p	SEC63_YEAST	NLNEEYTSDEIK	1+	y9	1113.49	1121.509	
Sec63p	SEC63_YEAST	NLNEEYTSDEIK	1+	y8	984.452	992.4662	
Sec63p	SEC63_YEAST	NLNEEYTSDEIK	1+	y7	855.409	863.4236	
Sec63p	SEC63_YEAST	NLNEEYTSDEIK	1+	y6	692.346	700.3603	
Sec63p	SEC63_YEAST	IGEVLGIK	2+	p	414.763	418.7702	36.6
Sec63p	SEC63_YEAST	IGEVLGIK	1+	y5	529.371	537.385	
Sec63p	SEC63_YEAST	IGEVLGIK	1+	y4	430.302	438.3166	
Sec63p	SEC63_YEAST	IGEVLGIK	1+	y3	317.218	325.2325	
Sec63p	SEC63_YEAST	IGEVLGIK	1+	b4	399.224	399.2238	
Sec63p	SEC63_YEAST	IGEVLGIK	1+	b6	569.329	569.3293	
Rps1ap	RS3A1_YEAST	EVQGSTLAQLTSK	2+	p	681.367	685.3743	36
Rps1ap	RS3A1_YEAST	EVQGSTLAQLTSK	1+	y10	1005.56	1013.572	
Rps1ap	RS3A1_YEAST	EVQGSTLAQLTSK	1+	y8	861.504	869.5182	
Rps1ap	RS3A1_YEAST	EVQGSTLAQLTSK	1+	y7	760.456	768.4705	
Rps1ap	RS3A1_YEAST	EVQGSTLAQLTSK	1+	y6	647.372	655.3865	
Rps1ap	RS3A1_YEAST	EVQGSTLAQLTSK	1+	y5	576.335	584.3494	
Rps1ap	RS3A1_YEAST	VISEILTK	2+	p	451.781	455.7886	34.7
Rps1ap	RS3A1_YEAST	VISEILTK	1+	y7	803.487	811.5015	
Rps1ap	RS3A1_YEAST	VISEILTK	1+	y6	690.403	698.4174	

Rps1ap	RS3A1_YEAST	VISEILTK	1+	y5	603.371	611.3854	
Rps1ap	RS3A1_YEAST	VISEILTK	1+	y4	474.329	482.3428	
Rps1ap	RS3A1_YEAST	VISEILTK	1+	y3	361.245	369.2587	
Rps1ap	RS3A1_YEAST	RVVDPFTR	3+	p	330.522	334.5358	32
Rps1ap	RS3A1_YEAST	RVVDPFTR	1+	y4	520.288	526.3079	
Rps1ap	RS3A1_YEAST	RVVDPFTR	1+	y3	423.235	429.2552	
Rps1ap	RS3A1_YEAST	RVVDPFTR	1+	b2	256.177	262.1969	
Rps1ap	RS3A1_YEAST	RVVDPFTR	1+	b4	470.272	476.2923	
Rps1ap	RS3A1_YEAST	RVVDPFTR	1+	b5	567.325	573.3451	
Rpl5p	RL5_YEAST	ADPAFKPTEK	2+	p	552.29	560.3044	25.4
Rpl5p	RL5_YEAST	ADPAFKPTEK	1+	y7	820.456	836.4847	
Rpl5p	RL5_YEAST	ADPAFKPTEK	1+	y6	749.419	765.4476	
Rpl5p	RL5_YEAST	ADPAFKPTEK	1+	y5	602.351	618.3792	
Rpl5p	RL5_YEAST	ADPAFKPTEK	1+	y4	474.256	482.27	
Rpl5p	RL5_YEAST	ADPAFKPTEK	2+	y8	459.258	467.2724	
Rpl5p	RL5_YEAST	YGITHGLTNWAAAYATGLLIAR	3+	p	778.418	780.4249	58.6
Rpl5p	RL5_YEAST	YGITHGLTNWAAAYATGLLIAR	1+	y11	1119.65	1125.672	
Rpl5p	RL5_YEAST	YGITHGLTNWAAAYATGLLIAR	1+	y9	977.578	983.598	
Rpl5p	RL5_YEAST	YGITHGLTNWAAAYATGLLIAR	1+	y8	814.515	820.5346	
Rpl5p	RL5_YEAST	YGITHGLTNWAAAYATGLLIAR	1+	y7	743.477	749.4975	
Rpl5p	RL5_YEAST	YGITHGLTNWAAAYATGLLIAR	1+	y6	642.43	648.4499	
Rpl5p	RL5_YEAST	GASDGGLYVPHSENR	2+	p	779.866	782.8759	30.3
Rpl5p	RL5_YEAST	GASDGGLYVPHSENR	1+	y9	1114.56	1120.584	
Rpl5p	RL5_YEAST	GASDGGLYVPHSENR	1+	y8	1001.48	1007.5	
Rpl5p	RL5_YEAST	GASDGGLYVPHSENR	1+	y6	739.348	745.3683	
Rpl5p	RL5_YEAST	GASDGGLYVPHSENR	1+	y4	505.237	511.2566	
Rpl5p	RL5_YEAST	GASDGGLYVPHSENR	2+	y11	614.807	617.8172	
Rpl5p	RL5_YEAST	GYLADDIDADSLEDIYTSAHEAI	3+	p	885.08	887.087	54
Rpl5p	RL5_YEAST	GYLADDIDADSLEDIYTSAHEAI	1+	y10	1160.61	1166.626	
Rpl5p	RL5_YEAST	GYLADDIDADSLEDIYTSAHEAI	1+	y9	1047.52	1053.542	
Rpl5p	RL5_YEAST	GYLADDIDADSLEDIYTSAHEAI	1+	y7	783.411	789.4309	
Rpl5p	RL5_YEAST	GYLADDIDADSLEDIYTSAHEAI	1+	y4	488.283	494.3029	
Rpl5p	RL5_YEAST	GYLADDIDADSLEDIYTSAHEAI	2+	y17	953.445	956.4549	
Rpl5p	RL5_YEAST	FPGWDFETEEIDPELLR	2+	p	1047	1050.007	57.7
Rpl5p	RL5_YEAST	FPGWDFETEEIDPELLR	1+	y10	1214.63	1220.646	
Rpl5p	RL5_YEAST	FPGWDFETEEIDPELLR	1+	y8	984.536	990.5562	
Rpl5p	RL5_YEAST	FPGWDFETEEIDPELLR	1+	y6	742.409	748.4295	
Rpl5p	RL5_YEAST	FPGWDFETEEIDPELLR	1+	y5	627.382	633.4026	
Rpl5p	RL5_YEAST	FPGWDFETEEIDPELLR	1+	y3	401.287	407.3072	
Rpl5p	RL5_YEAST	VFLDIGLQR	2+	p	530.811	533.8212	45.6
Rpl5p	RL5_YEAST	VFLDIGLQR	1+	y8	961.547	967.5667	
Rpl5p	RL5_YEAST	VFLDIGLQR	1+	y7	814.478	820.4983	
Rpl5p	RL5_YEAST	VFLDIGLQR	1+	y6	701.394	707.4142	
Rpl5p	RL5_YEAST	VFLDIGLQR	1+	y5	586.367	592.3873	
Rpl5p	RL5_YEAST	VFLDIGLQR	1+	y4	473.283	479.3032	

Curriculum vitae

Kristina Poljak

Personal information

Date of birth:	04.11.1987
Nationality:	Croatian
Current address:	Hohlstrasse 465, 8048 Zurich, Switzerland
E-mail:	poljakk@ethz.ch

Education

05/2012 – present **PhD thesis**
Institute of Microbiology, ETH Zürich, Zürich, Switzerland

09/2009 – 07/2011 **MSc in Molecular Biology**
Department of Molecular Biology, Faculty of Science, University of Zagreb, Zagreb, Croatia

09/2009 – 07/2011 **MSc in Bioindustrial Techniques**
Department of Biology, Faculty of Science, University of Orléans, France

09/2006 – 07/2009 **BSc in Molecular Biology**
Department of Molecular Biology, Faculty of Science, University of Zagreb, Croatia

Research Experience

5/2012 – present **PhD training**,
ETH Zürich, Institute of Microbiology, Zürich, Switzerland

11/2011 – 5/2012 **Research assistant**
ETH Zürich, Institute of Microbiology, Zürich, Switzerland

02/2011 – 07/2011 **Diploma thesis**
Centre de Biophysique Moléculaire (CBM) and Centre de Recherche sur la Matière Divisé (CRMD), Centre National de la Recherche Scientifique (CNRS), Orléans, France

10/2008 – 04/2010 **Research assistant**
Department for Biochemistry and Molecular Biology, Faculty of Pharmacy and Biochemistry, University of Zagreb, Croatia (awarded with Rector's Prize)

02/2011 – 09/2009 **Semester Project**
Department for Biochemistry, Faculty of Science, University of Zagreb

Scholarships, Honours and Awards

12/2015	Best Oral Presentation award at Targeted Proteomics Conference, *Mumbai, India*
02/2015	MIM Travel grant for participation at Gordon Research Workshop and Conference, *Braga, Italy*
07/2010	Rector's Prize (Best Research Project), *Zagreb, Croatia*
09/2009 – 09/2010	Croatian National Foundation Scholarship for Gifted Students, *Zagreb, Croatia*
09/2006 – 09/2009	National scholarship of the Croatian Ministry of Science, *Zagreb, Croatia*
09/2002 – 06/2006	Scholarship of the City of Sinj, *Sinj, Croatia*

Publications

1. Mueller S, Wahlander A, Selevsek N, Otto C, Ngwa E, **Poljak K**, Frey AD, Aebi M and Gauss R (2015) *Protein degradation corrects for imbalanced subunit stoichiometry in OST complex assembly*. Mol Biol Cell. 2015 Jul 15; 26 (14): 2596-608

2. Naegeli A, Neupert C, Fan YY, Lin CW, **Poljak K**, Papini AM, Schwarz F and Aebi M (2014) *Molecular analysis of an alternative N-glycosylation machinery by functional transfer from Actinobacillus pleuropneumoniae to Escherichia coli*. J Biol Chem. 2014 Jan 24: 284 (4):2170-9

Language Skills

Mother tongue: Croatian
Fluent: English (written, oral)
Intermediate: German (written, oral), Spanish (written, oral)
Basic: French (written, oral), Italian (written, oral)